



Water Technology and Sciences



Included in Thomson Reuters Science Citation Index® (ISI) • Expanded Thomson Reuters Research Alert® (ISI) • EBSCO • ProQuest • Elsevier • Redalyc



Water Technology and Sciences

Editorial Committee

Edit Board

M.I. Víctor J. Bourguett Ortiz
Director General
Instituto Mexicano de Tecnología del Agua

Editor in Chief
Dr. Nahún Hamed García Villanueva
Instituto Mexicano de Tecnología del Agua

Editor, Water and Energy
Dr. Humberto Marengo Mogollón
Comisión Federal de Electricidad

Editor, Water Quality
Dra. Blanca Elena Jiménez Cisneros
*Organización de las Naciones Unidas para la Educación,
la Ciencia y la Cultura*

Editor, Hydro-Agricultural Sciences
Dr. Oscar L. Palacios Vélez
Colegio de Postgraduados, México

Editor, Political and Social Sciences
Dra. Jacinta Palerm Viqueira
Colegio de Postgraduados, México

Editor, Water Management
Dr. Carlos Fernández-Jáuregui
*Water Assessment and Advisory-Global Network
(WASA-GN)*

Editor, Hydraulics
Dr. Felipe I. Arreguín Cortés
Comisión Nacional del Agua

Editor en Hidrología
Dr. Fco. Javier Aparicio Mijares
Consultor

Editor, Scientific and Technological Innovation
Dr. Polioptro F. Martínez Austria
Universidad de las Américas, Puebla

Technical Secretary
M.C. Jorge Arturo Hidalgo Toledo
Instituto Mexicano de Tecnología del Agua

Editorial coordination and careful editing: Helena Rivas- López •
Editorial assistance and editorial layout: Luisa Guadalupe
Ramírez-Martínez • **Figures design:** Luisa Guadalupe
Ramírez-Martínez and Rosario Castro-Rivera • **Coordination
arbitration:** Elizabeth Peña and Bibiana Bahena • **Proofreading
English:** Ellen Weiss • **Logo design and cover:** Oscar Alonso-Barrón
• **Design format:** Gema Alín Martínez-Ocampo • **Marketing:** Marco
Antonio Bonilla-Rincón.

• **Dr. Adrián Pedrozo Acuña**, Universidad Nacional Autónoma de México • **Dr. Alcides Juan León Méndez**, Centro de Investigaciones Hidráulicas, Cuba • **Dr. Aldo Iván Ramírez Orozco**, Centro del Agua para América Latina y el Caribe, México • **Dr. Alejandro López Alvarado**, Pontificia Universidad Católica de Valparaíso, Chile • **Dr. Álvaro A. Aldama Rodríguez**, consultor independiente • **Dr. Andrei S. Jouravlev**, Comisión Económica para América Latina y el Caribe, Chile • **Dr. Andrés Rodríguez**, Universidad Nacional de Córdoba, Argentina • **Dra. Anne Margrethe Hansen Hansen**, Instituto Mexicano de Tecnología del Agua • **Dr. Ariosto Aguilar Chávez**, Instituto Mexicano de Tecnología del Agua • **Dr. Arturo Marciano**, Asociación Internacional de Ingeniería e Investigaciones Hidráulicas, Venezuela • **Dra. Alma Chávez Mejía**, Universidad Nacional Autónoma de México • **Dr. Armando Guevara Gil**, Pontificia Universidad Católica, Perú • **Dra. Aziza Akhmouch**, Organización para la Cooperación y el Desarrollo Económico, Francia • **Dr. Carlos Díaz Delgado**, Universidad Autónoma del Estado de México • **Dr. Carlos Puente**, Universidad de California en Davis, Estados Unidos • **Dr. Cleverson Vitório Andreoli**, Andreoli Engenharia Associados, Brasil • **Dr. Carles Sanchis Ibor**, Universidad Politécnica de Valencia, España • **Dr. Carlos Chairez Araiza**, México, asesor • **Dr. Carlos Cruickshank Villanueva**, Universidad Nacional Autónoma de México • **Dr. Daene McKinney**, Universidad de Texas en Austin, Estados Unidos • **Dr. Daniel Murillo Licea**, Centro de Investigaciones y Estudios Superiores en Antropología Social • **Dr. Eduardo Varas Castellón**, Pontificia Universidad Católica de Chile • **Dr. Enrique Cabrera Marcet**, Universidad Politécnica de Valencia, España • **Dr. Enrique Playán Jubillar**, Consejo Superior de Investigaciones Científicas, España • **Dr. Ernesto José González Rivas**, Universidad Central de Venezuela • **Dr. Emmanuel Galindo Escamilla**, Universidad Autónoma del Estado de Hidalgo, México • **Dr. Eric Rendón Schneur**, Universidad Nacional Agraria La Molina, Perú • **Dr. Erick R. Bandala**, Universidad de las Américas Puebla, México • **Dr. Federico Estrada**, Centro de Estudios y Experimentación de Obras Públicas, España • **Dr. Fedro Zazueta**, Universidad de Florida, Estados Unidos • **Dra. Gabriela Eleonora Moeller Chávez**, Universidad Politécnica del Estado de Morelos • **Dr. Gerardo Buelna**, Dirección de Medio Ambiente y Centro de Investigación Industrial de Quebec, Canadá • **Dr. Gueorguiev Tzatchkov Velitchko**, Instituto Mexicano de Tecnología del Agua • **Ing. Héctor Garduño Velasco**, consultor internacional • **M.I. Horacio Rubio Gutiérrez**, Comisión Nacional del Agua, México • **Dr. Ismael Mariño Tapia**, Centro de Investigación y de Estudios Avanzados del Instituto Politécnico Nacional, México • **Dr. Ismael Piedra Cueva**, Universidad de la República, Uruguay • **Dr. Ismael Aguilar Barajas**, Instituto Tecnológico y de Estudios Superiores de Monterrey, México • **Dr. Iván Obando Camino**, Universidad de Talca, Chile • **Dr. Jaime Iván Ordóñez**, Universidad Nacional, Bogotá, Colombia • **Dr. Joaquín Rodríguez Chaparro**, Ministerio de Medio Ambiente, y Medio Rural y Marino, España • **Dr. José Ángel Raynal Villaseñor**, Universidad de Las Américas, Puebla, México • **Dr. José D. Salas**, Universidad de Colorado, Estados Unidos • **Dr. José Joel Carrillo Rivera**, Universidad Nacional Autónoma de México • **Dr. Juan Pedro Martín Vide**, Universidad Politécnica de Cataluña, España • **Dr. Julio Kuroiwa**, Universidad Nacional de Ingeniería, Perú • **Dr. José Luis Pimentel Equihua**, Colegio de Postgraduados, México • **M.C. Juan Andrés Martínez Álvarez**, Universidad Nacional Autónoma de México • **Dr. Juan B. Valdes**, The University of Arizona, Estados Unidos • **Dr. Karim Acuña Askar**, Universidad Autónoma de Nuevo León, México • **Dra. Luciana Coutinho**, Universidade Do Minho, Portugal • **Dr. Luis F. León**, Waterloo University, Canadá • **Dr. Luis Texeira**, Instituto de Mecánica de Fluidos e Ingeniería Ambiental, Uruguay • **Dra. Luisa Paré Ouellet**, Universidad Nacional Autónoma de México • **Ing. Manuel Contijoch Escontria**, Secretaría de Agricultura, Ganadería, Desarrollo Rural, Pesca y Alimentación, México • **Dr. Marcos Von Sperling**, Universidad Federal de Minas Gerais, Brasil • **Dra. María Claudia Campos Pinilla**, Universidad Javeriana, Colombia • **Dra. María Luisa Torregrosa**, Facultad Latinoamericana de Ciencias Sociales, México • **Dra. María Rafaela de Saldanha Matos**, Laboratorio Nacional de Ingeniería Civil, Portugal • **Dra. María Victoria Vélez Otlávaro**, Universidad Nacional de Colombia • **Dr. Michel Rosengaus Moshinsky**, Consultor independiente • **Dr. Moisés Berezowsky Verduzzo**, Universidad Nacional Autónoma de México • **Dra. María Teresa Oré**, Pontificia Universidad Católica del Perú • **M.I. Mercedes Esperanza Ramírez**, Camperos, Instituto Mexicano de Tecnología del Agua • **Dr. Miguel A. Medina**, Duke University, Estados Unidos • **Dra. Natalia Uribe Pando**, Water Lex, Suiza • **Dr. Óscar F. Ibáñez Hernández**, Consultor independiente • **Dr. Omar A. Miranda**, Instituto Nacional de Tecnología Agropecuaria, Argentina • **Dr. Paulo Salles Alfonso de Almeida**, Universidad Nacional Autónoma de México • **Dr. Rafael Pardo Gómez**, Instituto Superior Politécnico José Antonio Echeverría, Cuba • **Dr. Rafael Val Segura**, Instituto Mexicano de Tecnología del Agua • **Dr. Ramón Domínguez Mora**, Universidad Nacional Autónoma de México • **Dr. Ramón Fuentes Aguilar**, Instituto de Innovación en Minería y Metalurgia, Chile • **Dr. Ramón Ma. Gutiérrez Serret**, Centro de Estudios y Experimentación de Obras Públicas, España • **Ing. Raquel Duque**, Asociación Internacional de Ingeniería e Investigaciones Hidráulicas, Colombia • **Dr. Raúl Antonio Lopardo**, Instituto Nacional del Agua de Argentina • **Dr. Rodolfo Silva Casarín**, Universidad Nacional Autónoma de México • **Dr. Serge Léonard Tamari Wagner**, Instituto Mexicano de Tecnología del Agua • **Dr. Simón González**, Universidad Nacional Autónoma de México • **Dr. Tomás Martínez Saldaña**, Colegio de Postgraduados, México • **Dr. Víctor Hugo Alcocer Yamanaka**, Instituto Mexicano de Tecnología del Agua • **Dra. Ximena Vargas Mesa**, Universidad de Chile •

©*Water Technology and Sciences*. Vol. VI, No. 1, January-February, 2015, is a bimonthly publication edited by the Instituto Mexicano de Tecnología del Agua, Paseo Cuauhnáhuac 8532, Colonia Progreso, Jiutepec, Morelos, C.P. 62550, telephone +52 (777) 3 29 36 00, extension 474, www.imta.gob.mx/tyca, fsalinas@tlaloc.imta.mx. Responsible editor, Nahún Hamed García Villanueva; Copyright No. 04-2013-121014514100-203, granted by the Instituto Nacional de Derechos de Autor. ISSN pending. Responsible for the latest update of this issue: Sub-Department of Dissemination and Circulation, Francisco José Salinas Estrada, Paseo Cuauhnáhuac 8532, Colonia Progreso, Jiutepec, Morelos, C.P. 62550.

The contents of the articles are the exclusive responsibility of the authors and do not necessarily reflect the position of the editor of the publication.

The total or partial reproduction of the contents and images of the publication without prior authorization from the Instituto Mexicano de Tecnología del Agua are strictly prohibited.

Water Technology and Sciences is the translation of *Tecnología y Ciencias del Agua*, which is the continuation of the following journals: *Irrigación en México* (1930-1946); *Ingeniería hidráulica en México* (1947-1971); *Recursos hidráulicos* (1972-1978), and *Ingeniería hidráulica en México*, second period (1985-2009).



Water Technology^{and} Sciences

Vol. VI. No. 1, January-February 2015



Coordination for editorial comments,
[click here give](#)



For subscriptions, [click here](#)

Cover: Santa Catarina River, Monterrey, Mexico, July 2010.

Forensic flood analyses applies the methodology after a disaster occurs. It consists of the reconstruction of the event to determine how it happened, the contributing factors, what failed, and what were the causes of the damage. The next step in the analysis is the evaluation or study of the event with these points having been clarified. The final goal of the analysis is to recommend what is needed to help or improve the system and prevent this type of disaster in the future, to the extent possible. See article "Forensic Analysis of Floods: A Methodological Guide" by Aldo I. Ramírez and L. Alejandra Herrera-Lozano (pp. 25-49).

Photo: Conagua/OCRB.



Panoramic View of the 2007 Flood in Villahermosa, Tabasco, Mexico.

Photo: Conagua.

Technical articles

Flow Caused by Dam Breaks: Numerical Modeling Analysis

Ignacio Sabat
Oscar Link
Bernd Ettmer

Forensic Analysis of Floods: A Methodological Guide

Aldo I. Ramírez
L. Alejandra Herrera-Lozano

Growth Kinetics and Nutrient Uptake of Microalgae in Urban Wastewaters with Different Treatment Levels

César Carlos García-Gozalbes
Zouhayr Arbib
Aqualia, Españ
José Antonio Perales-Vargas-Machuca

Improvements in the Hydraulic Efficiency of Weirs with Free Outfalls in Dams

Mauro Iñiguez-Covarrubias
Waldo Ojeda-Bustamante
Carlos Díaz-Delgado

Development of the Balsas Hydrological Region by Modifying Prohibitions

Juan Carlos Valencia-Vargas

Prioritization of Needs to Replace Piping Using GIS and Multicriteria Evaluation

Vivian Verduzco
Jaime Garatuza
Salvador Díaz

Prioritization of Intervention Areas using a Morphometric Analysis and Vegetation Index

Adolfo López-Pérez
Mario R. Martínez-Menes
Demetrio S. Fernández-Reynoso

Numerical Hydrodynamic-Hydrological Modeling in Flood Zones Containing Infrastructure

Israel E. Herrera-Díaz
Clemente Rodríguez-Cuevas
Carlos Couder-Castañeda
José R. Gasca-Tirado

Artículos técnicos

Flujo inducido por el rompimiento de una presa: análisis mediante modelación numérica 5

Ignacio Sabat
Oscar Link
Bernd Ettmer

Análisis forense de inundaciones: una guía metodológica 25

Aldo I. Ramírez
L. Alejandra Herrera-Lozano

Cinéticas de crecimiento y consumo de nutrientes de microalgas en aguas residuales urbanas con diferentes niveles de tratamiento 49

César Carlos García-Gozalbes
Zouhayr Arbib
Aqualia, Españ
José Antonio Perales-Vargas-Machuca

Mejoras de eficiencia hidráulica en vertedores con canal de descarga libre en presas: propuesta metodológica 69

Mauro Iñiguez-Covarrubias
Waldo Ojeda-Bustamante
Carlos Díaz-Delgado

Desarrollo de la región hidrológica del Balsas mediante la modificación de su veda 81

Juan Carlos Valencia-Vargas

Priorización de necesidades de reemplazo de tuberías usando SIG y evaluación multicriterio 99

Vivian Verduzco
Jaime Garatuza
Salvador Díaz

Priorización de áreas de intervención mediante análisis morfométrico e índice de vegetación 121

Adolfo López-Pérez
Mario R. Martínez-Menes
Demetrio S. Fernández-Reynoso

Modelación numérica hidrodinámico-hidrológica en zonas de inundación con presencia de infraestructura 139

Israel E. Herrera-Díaz
Clemente Rodríguez-Cuevas
Carlos Couder-Castañeda
José R. Gasca-Tirado

Technical notes

Characterization of Meteorological Droughts in the Central Argentina

Leticia Vicario
Carlos M. García
Ingrid Teich
Juan Carlos Bertoni
Andrés Ravelo
Andrés Rodríguez

Water Usage in Northern Sinaloa: Allocating the Resource to Consumers

Jesús Torres-Sombra
José Alberto García-Salazar

Application of the ArcHydro Data Model to Calculate Surface Water Availability

María de los Ángeles Suárez-Medina
Carlos Patiño-Gómez
Jaime Velázquez-Álvarez
Jaime Rivera-Benites
Ernesto Aguilar-Garduño
Guillermo Bautista
Citlalli Astudillo-Enríquez

Comparison of PPD, SPI and RDI Indices to Classify Droughts: Zacatecas Weather Station, Mexico

Daniel Francisco Campos-Aranda

Discussion

Contributor's guide

Notas técnicas

Caracterización de las sequías meteorológicas en la región central de la Argentina 153

Leticia Vicario
Carlos M. García
Ingrid Teich
Juan Carlos Bertoni
Andrés Ravelo
Andrés Rodríguez

Uso del agua en el norte de Sinaloa: ¿a cuál consumidor asignar el recurso? 167

Jesús Torres-Sombra
José Alberto García-Salazar

Aplicación del modelo de datos ArcHydro en el cálculo de disponibilidad de agua superficial 175

María de los Ángeles Suárez-Medina
Carlos Patiño-Gómez
Jaime Velázquez-Álvarez
Jaime Rivera-Benites
Ernesto Aguilar-Garduño
Guillermo Bautista
Citlalli Astudillo-Enríquez

Contraste de los índices DPP, SPI y RDI para clasificación de sequías, en la estación climatológica Zacatecas, México 183

Daniel Francisco Campos-Aranda

Discusión 195

Guía para colaboradores 197

Flow Caused by Dam Breaks: Numerical Modeling Analysis

• Ignacio Sabat • Oscar Link* •
Universidad de Concepción, Chile

*Corresponding Author

• Bernd Ettmer •
Hochschule Magdeburg-Stendal, Alemania

Abstract

Sabat, I., Link, O., & Ettmer, B. (January-February, 2015). Flow Caused by Dam Breaks: Numerical Modeling Analysis. *Water Technology and Sciences* (in Spanish), 6(1), 5-23.

The finite volumes method is applied to solve 2D Saint Venant equations with source terms that determine runoff of shallow water, in order to calculate flows caused by dam breaks. The model is verified by calculating six cases with known solutions: (1) establishing normal flow based on a horizontal free surface; (2) establishing flow that is gradually varied in a channel with changes in roughness; (3) runoff over an obstacle; (4) formation of an oblique hydraulic jump; (5) damped oscillation of a free surface in a parabolic section; (6) runoff from the breaking of a circular dam and (7) runoff from the partial breaking of a dam. The model is applied to simulate the flow caused by the instantaneous breaking of dams in order to analyze the effect of the joint geometric configuration of the dam, reservoir, valley and channel on the outflow hydrograph. A total of 28 scenarios were simulated for a valley with a parabolic section and a channel with a trapezoidal section, in which the height and position of the dam wall were varied as well as the gap width, length of the slope and roughness of the channel downstream. The results obtained show that the height of the dam is the variable that has the largest effect on the peak flow of the outflow hydrograph and the gap width has a large effect on partial breaks. The roughness of the bed considerably mitigates the peak flow downstream and increases flood time. The position of the mural and the length of the slope have a smaller effect on floods caused by dam breaks. The model developed adequately predicts the complex behavior of the flow caused by the instant breaking of a dam and is therefore a simulation tool with predictive capabilities.

Keywords: Dam break, Saint Venant 2D equations, computational hydraulics, shock capturing conditions.

Received: 24/09/12
Accepted: 5/06/14

Resumen

Sabat, I., Link, O., & Ettmer, B. (enero-febrero, 2015). Flujo inducido por el rompimiento de una presa: análisis mediante modelación numérica. *Tecnología y Ciencias del Agua*, 6(1), 5-23.

Se aplica el método de los volúmenes finitos para dar solución a las ecuaciones de Saint Venant 2D con términos fuente que gobiernan el escurrimiento de aguas someras, a fin de calcular el flujo inducido por el rompimiento de una presa. El modelo se verifica mediante el cálculo de siete casos con solución conocida, que son: (1) establecimiento del flujo normal a partir de una superficie libre horizontal; (2) establecimiento del flujo gradualmente variado en un canal con cambio de rugosidad; (3) escurrimiento sobre un obstáculo; (4) formación del salto hidráulico oblicuo; (5) oscilación amortiguada de la superficie libre en un estanque parabólico; (6) escurrimiento inducido por el rompimiento de una presa circular, y (7) escurrimiento inducido por el rompimiento parcial de una presa. El modelo se aplica para simular el flujo inducido por el rompimiento instantáneo de presas, a fin de analizar el efecto de la configuración geométrica del conjunto presa, embalse, valle y cauce sobre el hidrograma de salida. Se simularon 28 escenarios, considerando un valle con sección parabólica y un cauce con sección trapezoidal, donde se varió la altura y orientación del muro de la presa, el ancho de la brecha, la pendiente longitudinal y la rugosidad del cauce aguas abajo. Los resultados obtenidos muestran que la altura de la presa es la variable más influyente en el caudal máximo del hidrograma de salida y que el ancho de la brecha tiene un efecto importante en rompimientos parciales. La rugosidad del lecho atenúa de forma considerable el caudal máximo hacia aguas abajo y aumenta el tiempo de crecida. La orientación del muro y la pendiente longitudinal tienen un efecto menor sobre las crecidas provocadas por rompimiento. El modelo desarrollado predice de manera adecuada el complejo comportamiento que exhibe el flujo inducido por el rompimiento instantáneo de una presa, constituyendo una herramienta de simulación con capacidad predictiva.

Palabras clave: rompimiento de presas, ecuaciones de Saint Venant 2D, hidráulica computacional, esquemas de shock.

Introduction

Dam breaks are important to hydraulic engineering because of the high likelihood that catastrophic consequences will occur from the flow induced downstream. Singh (1996) reported roughly 1 000 cases of dam breaks since the 12th century, around 200 of which were registered during the 20th century. Many breaks are well-documented in the specialized literature, such as the *Malpasset* (Hervouet & Petitjean, 1999), *St. Francis* (Begnudelli & Sanders, 2007), *Tous* (Alcrudo & Mulet, 2007) and *Gleno* (Pilotti, Maranzoni, Tomirotti, & Valerio, 2011). Singh (1996) and Vischer and Hager (1998) indicated that the main causes of dam breaks have been problems with the foundations (37%) and overtopping (30%). Given the importance of the problem, many countries currently require analyses of dam safety as part of dam projects, including the calculation of the flow produced by a possible rupture.

Earth and rock dams typically undergo gradual ruptures with the opening of a gap, taking hours to break and causing a gradual and changing flow downstream. Concrete dams undergo breaks instantaneously from the formation of a negative wave upstream dictated by the geometry of the valley, and a shock wave that propagates downstream (e.g., Vischer & Hager, 1998).

Rubio, Martínez and Meza (2012) estimated the peak flow caused by a gradual dam break by applying different empirical formulas. In order to determine the distance at which the passage of the flow no longer represents a danger to the population, they traced the flood downstream using the *HEC-RAS* software, considering a trapezoidal channel.

The most unfavorable condition is an instantaneous break, which can be modeled using Saint-Venant equations which include the source terms representing

the effect of the slope of the channel and the friction of the flow over the bed. The known analytical solutions describe a 1D case for a semi-infinite reservoir with a rectangular channel downstream from the dam. Dressler (1952, 1954) and Whitham (1955) proposed solutions for an instantaneous break with a dry channel and a horizontal slope while Hunt (1982, 1984) solved for an instant breakage with a dry channel and a longitudinal slope. Recently, Chanson (2009) proposed solutions by applying the method of characteristics to a semi-instantaneous break with a semi-infinite reservoir and an initially dry rectangular channel.

For real cases, flow resistance and the geometries of the valley and channel control the propagation of waves upstream and downstream. Therefore, in practice a 2D representation of the phenomenon is pertinent, which is obtained by applying numerical methods. The existence of shock waves requires implementing spatial discretization schemes with a very low numerical spread to ensure that the flows are kept at a local level and the solution is stabilized, especially in the vicinity of the shock. Most of these schemes have been proposed for the Riemann problem which does not consider source terms (e.g., Fraccarollo & Toro, 1995; Brufau & García-Navarro, 2003).

To solve the Saint-Venant equations with source terms when a shock wave is present, specific discretization schemes have been developed over recent years, called shock schemes. Combined with an appropriate drying-wetting strategy, these have an excellent capability to simulate idealized dam break flows. Gottardi and Venutelli (2004) extended the formulation of the Kurganov and Tadmor (2000) central scheme for the discretization of the source terms in the Saint Venant equations, obtaining favorable results from simulated dam

breaks. Zhu, Viser and Vrijling (2004) implemented a prediction-correction method using the MUSCLE-Hancock scheme (van Leer, 1985) to simulate case studies developed by the CADAM initiative (Morris, 2001). Soares-Frazao and Zech (2008) presented numerical simulations of the effects of dam break flows over an idealized city consisting of a 5 x 5 grid of square buildings positioned 45 and 90% with respect to the main direction of the flow. The calculations were compared to the experimental results and good agreement was obtained between the laboratory tests and the numerical results. Wang, Liang, Kesserwani y Hall (2011) extended the 1D formula proposed by Liang and Marche (2009) to simulate idealized breaks and the break of the *Malpasset* dam.

This article extends the numerical model developed by Link and Donoso (2008) to the 2D case with source terms and a drying-wetting strategy. The model is verified by calculating six cases with a known solution: 1) determining normal flow based on the free horizontal surface; 2) determining gradually changing flow in a channel with variations in roughness; 3) runoff over an obstacle; 4) formation of the oblique hydraulic jump; 5) damped oscillation of the free surface in a parabolic pond; 6) runoff caused by a break in a circular dam; and 7) runoff caused by the partial break of a dam. The model is applied to simulate the flow caused by the instantaneous break of a dam in order to analyze the effect of the combined geometry of the dam, reservoir, valley and channel on the outflow hydrograph.

Methodology

Governing Equations

The system of governing equations corresponding to the Saint-Venant equations with source terms, which in vector form is:

$$\frac{\partial W}{\partial t} + \nabla \cdot F = S \quad (1)$$

$$\frac{\partial W}{\partial t} + \frac{\partial F(W)}{\partial x} + \frac{\partial G(W)}{\partial y} = S \quad (2)$$

where W is the vector of flow variables; F and G are the flow vectors that comprise the flow matrix F in the x and y directions, respectively, and S is the vector of source terms corresponding to the slope of the bed and the friction of the channel bottom. The vectors W , F , G and S are given by:

$$W = \begin{bmatrix} h \\ u \cdot h \\ v \cdot h \end{bmatrix}, F = \begin{bmatrix} u \cdot h \\ u^2 \cdot h + \frac{g \cdot h^2}{2} \\ u \cdot v \cdot h \end{bmatrix},$$

$$G = \begin{bmatrix} v \cdot h \\ u \cdot v \cdot h \\ v^2 \cdot h + \frac{g \cdot h^2}{2} \end{bmatrix},$$

$$S = \begin{bmatrix} 0 \\ g \cdot h \cdot (S_{0x} - S_{fx}) \\ g \cdot h \cdot (S_{0y} - S_{fy}) \end{bmatrix} \quad (3)$$

where h (m) is the depth of the water column; u and v (m/s) the vertically integrated velocity in the directions of the Cartesian axes x , y ; t (s) is time; g (ms^{-2}) acceleration of gravity; x (m) the distance in the longitudinal direction; y (m) the distance in the transversal direction. The bottom slopes S_{0x} and S_{0y} are:

$$S_{0x} = -\frac{\partial z_0}{\partial x}, \quad S_{0y} = -\frac{\partial z_0}{\partial y} \quad (4)$$

where z_0 corresponds to the bathymetric height. The frictional slope S_{fx} and S_{fy} (m/m) is calculated using the Manning equation as:

$$S_{fx} = \frac{u \cdot n^2 \cdot \sqrt{u^2 + v^2}}{h^{\frac{4}{3}}},$$

$$S_{fy} = \frac{v \cdot n^2 \cdot \sqrt{u^2 + v^2}}{h^{\frac{4}{3}}} \quad (5)$$

where n ($m^{-1/3s}$) is the Manning roughness coefficient.

Discret Formulation of the Problem

The governing equations were transformed into their discret versions by applying the finite volumes method using a non-central scheme represented by the Q -schemes family, introduced by Harten, Lax and Van Leer (1983) and extended by Bermúdez and Vázquez (1994), and Bermúdez, Dervieux, Desiderii and Vázquez (1998) for surface water equations with source terms. Integrating the governing equation, we get:

$$\int_A \left(\frac{\partial W}{\partial t} \right) \partial A + \int_A (\nabla \cdot F(W)) \partial A = \int_A (S) \partial A \quad (6)$$

$$A \cdot \left(\frac{\partial W}{\partial t} \right) + \int_S \vec{F} \cdot \vec{n} \partial S = S \cdot A \quad (7)$$

$$\left(\frac{\partial W}{\partial t} \right) = -\frac{1}{A} \sum_S \vec{F} \cdot \vec{n} \partial S + S \quad (8)$$

where A is the area; S is the shape of the control volume and n is the normal vector to the shape. The flow term was estimated using the expression:

$$\int_{S_i} \vec{F} \cdot \vec{n} \partial S \approx \sum_{j=1}^{n_{\text{vecinos}}} \Gamma_{ij} \cdot \Phi(W_i^t, W_j^t, n_{ij}) \quad (9)$$

where Γ_{ij} (m) is the length of the face between volumes i and j and function Φ is defined as:

$$\Phi(U, V, n) = \frac{Z(U, n) + Z(V, n)}{2}$$

$$- \frac{1}{2} \cdot |Q(W_Q(U, V), n)| \cdot (V - U) \quad (10)$$

where:

$$Z(U, n) = A^*(U, n) \cdot U \quad (11)$$

$$W_Q(U, V) = \left(\frac{U + V}{2} \right) \quad (12)$$

$$Q(W, n) = A^*(W, n) \quad (13)$$

$$A^*(W, n) = X \cdot \Lambda \cdot X^{-1} \quad (14)$$

U and V are the vectors of the properties of finite volume flow; n is the normal vector to the face between U and V and A^* is the Jacobian matrix, according to Vijayasundaram (1986):

$$X = \begin{pmatrix} 0 & 1 & 1 \\ n_y & u + c \cdot n_x & u - c \cdot n_x \\ -n_x & v + c \cdot n_y & v - c \cdot n_y \end{pmatrix} \quad (15)$$

$$\Lambda = \begin{pmatrix} \lambda_1^* & 0 & 0 \\ 0 & \lambda_2^* & 0 \\ 0 & 0 & \lambda_3^* \end{pmatrix} \quad (16)$$

Note that λ_1^* , λ_2^* and λ_3^* (ms^{-1}) correspond to the eigenvalues of A^* . To avoid the indetermination of the problem in the discontinuities, the Harten entropy correction (1984) is introduced:

$$\lambda_i^* = \begin{cases} 0.5 \cdot \text{sign}(\lambda_i^*) \cdot \left(\frac{|\lambda_i^*|}{\epsilon} + \epsilon \right) & \text{si } |\lambda_i^*| \leq \epsilon \\ \lambda_i^* & \text{si } |\lambda_i^*| > \epsilon \end{cases} \left(\frac{\pi}{2} - \theta \right) \quad (17)$$

And e is considered to equal 10^{-5} (m s⁻¹).

Source Terms

The bottom slope was discretized as:

$$S_{0x} = -\frac{\partial z_0}{\partial x} = \sum_j^{n_{\text{vecinos}}} \frac{A_{ij}}{A_i} \cdot \frac{z_{0i} - z_{0j}}{d_{ij}} \cdot \cos(\theta_{ij}),$$

$$S_{0y} = -\frac{\partial z_0}{\partial y} = \sum_j^{n_{\text{vecinos}}} \frac{A_{ij}}{A_i} \cdot \frac{z_{0i} - z_{0j}}{d_{ij}} \cdot \sin(\theta_{ij}) \quad (18)$$

where z_{0i} and z_{0j} correspond to the bathymetric heights of volume i and its neighbor j , respectively; d_{ij} is the distance between the centers of the volumes; θ is the angle represented by the horizontal and the line that joins the centers of the volumes i and j , measured counterclockwise; A_{ij} is the area of the triangle represented by the center of the volume i and the shared vertices of volumes i and j ; and A_i is the surface area of volume i . The frictional slope is discretized using the Manning equation, as:

$$S_{fxi} = \frac{u_i \cdot n_i^2 \cdot \sqrt{u_i^2 + v_i^2}}{h_i^{\frac{4}{3}}},$$

$$S_{fyi} = \frac{v_i \cdot n_i^2 \cdot \sqrt{u_i^2 + v_i^2}}{h_i^{\frac{4}{3}}} \quad (19)$$

where u_i and v_i are the components of the velocity in the direction of the x and y axes, respectively; h_i is the depth of the water column and n_i corresponds to the Manning roughness coefficient at the center of volume i .

The temporal derivatives were estimated using the explicit Euler first-order method, such that the discrete solution is:

$$W_i^{t+\Delta t} = W_i^t - \Delta t \cdot \sum_{j=1}^{n_{\text{vecinos}}} \Gamma_{ij} \cdot \Phi(W_i^t, W_j^t, n_{ij})$$

$$+ g \cdot h_i \cdot \left(\begin{array}{c} 0 \\ \sum_j^{n_{\text{vecinos}}} \frac{A_{ij}}{A_i} \cdot \frac{z_{0i} - z_{0j}}{d_{ij}} \cdot \cos(\theta_{ij}) \\ \sum_j^{n_{\text{vecinos}}} \frac{A_{ij}}{A_i} \cdot \frac{z_{0i} - z_{0j}}{d_{ij}} \cdot \sin(\theta_{ij}) \end{array} \right) - \left(\begin{array}{c} 0 \\ \frac{u_i \cdot n_i^2 \cdot \sqrt{u_i^2 + v_i^2}}{h_i^{\frac{4}{3}}} \\ \frac{v_i \cdot n_i^2 \cdot \sqrt{u_i^2 + v_i^2}}{h_i^{\frac{4}{3}}} \end{array} \right) \quad (20)$$

Boundary Conditions

A transmissive contour was imposed for the open boundary case using a fictitious neighbor with flow properties identical to those of the volume located on the line (Toro, 2001):

$$W'_i = W_i \quad (21)$$

where W'_i corresponds to the fictitious elements and W_i to the volume in the domain boundary. For the closed boundary, a reflective contour was imposed, where the velocity perpendicular to the face is inverted (Toro, 2001):

$$\begin{bmatrix} u'_i \\ v'_i \end{bmatrix} = \begin{bmatrix} \cos(\theta_{ic}) & -\sin(\theta_{ic}) \\ \sin(\theta_{ic}) & \cos(\theta_{ic}) \end{bmatrix} \cdot \begin{bmatrix} u_i \\ v_i \end{bmatrix} \quad (22)$$

$$\begin{bmatrix} u''_i \\ v''_i \end{bmatrix} = \begin{bmatrix} \cos(\theta_{ic}) & \sin(\theta_{ic}) \\ -\sin(\theta_{ic}) & \cos(\theta_{ic}) \end{bmatrix} \cdot \begin{bmatrix} -u_i \\ v_i \end{bmatrix} \quad (23)$$

$$W'_i = \begin{bmatrix} h_i \\ h_i \cdot u''_i \\ h_i \cdot v''_i \end{bmatrix} \quad (24)$$

where h_i , u_i and v_i correspond to the properties of the volume on the boundary of the domain; θ_{ic} is the angle perpendicular to the face on the boundary and extending out from the volume; u'_i and v'_i are velocities rotated in θ_{ic} ; and u''_i and v''_i are the components of the velocity of the fictitious neighbor on the Cartesian axes.

Drying/Wetting Strategy

The drying/wetting strategy imposes the nullity of the Jacobians associated with a dry volume when two neighbors exist—one dry and one wet. In this case, the minimum depths are limited to values greater than or equal to zero, and a mass balance of wet neighbors is performed in order to guarantee continuity. Mathematically:

$$M_j = \begin{cases} 0, & \forall h_j \leq 0 \\ 1, & \forall h_j > 0 \end{cases} \quad (25)$$

$$\delta_i = \min(0, h_i) \quad (26)$$

$$h'_j = h_j + \frac{M_j \cdot A_{ij} \cdot \delta_i}{\sum_j M_j \cdot A_{ij}} \quad (27)$$

$$h'_j = h_i - \delta_i \quad (28)$$

$$W_i = \begin{bmatrix} h'_i \\ u_i \cdot h'_i \\ v_i \cdot h'_i \end{bmatrix} \quad (29)$$

where M_j indicates whether the volume j is dry or wet and δ_j is the amount of the mass to be balanced. Figure 1 shows the flow diagram for the proposed model.

Results

Verification of the Model

The capacity of the model developed was verified using a seven benchmark test: (1) determining normal flow based on a horizontal free surface; (2) determining gradually changing flow in a channel with variations in roughness; (3) runoff over an obstacle; (4) formation of an oblique hydraulic jump; (5) damped oscillation of a free surface in a parabolic section; (6) runoff from the breaking of a circular dam and (7) runoff from the partial breaking of a dam. These seven cases mentioned have a known solution and enable evaluating different aspects of the numerical model, such as convergence to equilibrium, conservation, the C-property introduced by Bermúdez and Vázquez (1994), simulation of flow discontinuities and modeling of the drying-wetting process. The numerical results were compared to analytical, semi-analytical and empirical solutions in graphic form and the maximum percentage difference was indicated.

Determining Normal Flow with a Horizontal Free Surface

A simulation was performed of runoff in a rectangular channel with a constant unit width of 100 m, a slope of 1/2 000 m/m and a Manning coefficient equal to 0.02 $\text{sm}^{-1/3}$. The initial and boundary conditions were:

$$h_{(x,y,0)} = 0.5 - 0.02 \cdot (100 - x) \quad q_{x(x,y,0)} = q_{y(x,y,0)} = 0$$

$$h_{(0,y,t)} = 0.5 \quad q_{x(L,y,t)} = 0.5 \cdot (q_{x(L,y,t-\Delta t)} + q_{x(L-\Delta x,y,t-\Delta t)})$$

The solution is given by the Manning equation and is equal to 0.22 $\text{m}^3/\text{s}/\text{m}$. A spatial discretization of $\Delta x = 0.25$ m and $\Delta y = 0.25$ m and a time step of $\Delta t = 0.05$ s were

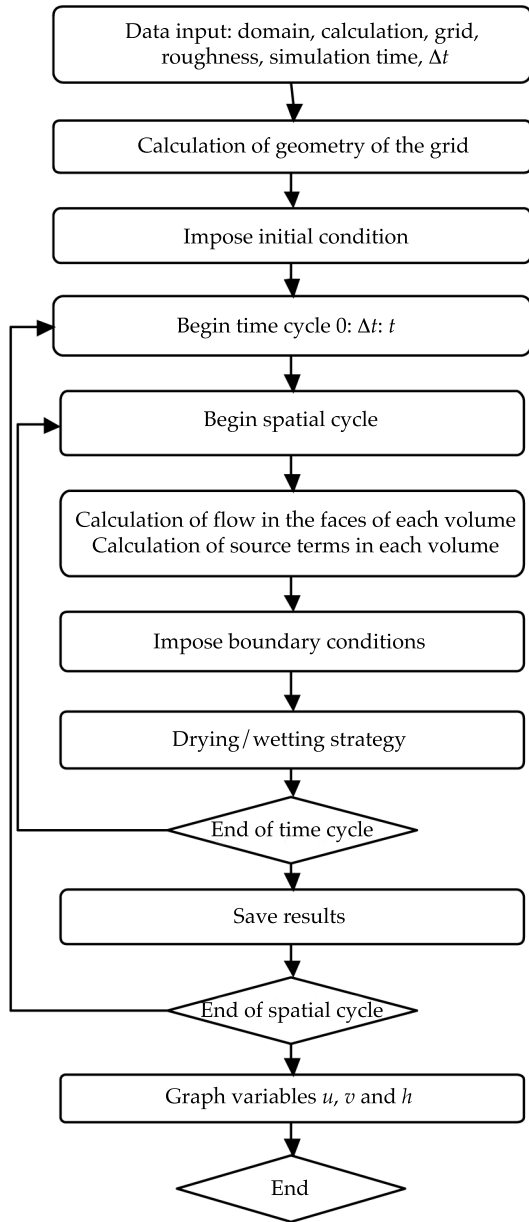


Figure 1. Flow Diagram.

used, with a Courant number of CFL = 0.15. Figure 2 shows the grid, initial condition and the calculated hydraulic axis.

Table 1 presents the maximum percentage difference between the depth and the flows calculated by the model and the Manning equation.

Determining Gradually Changing Flow in a Channel with Variations in Roughness

A simulation was performed of gradually varied runoff that causes changes in roughness in a rectangular channel with a constant unit width of 100 m and a slope of 2/ 1 000 m/m. The channel was divided into three 33.3 m sections, with Manning roughness values equal to 0.02, 0.04 and 0.02 sm^{-1/3}. The initial and boundary conditions were:

$$h_{(x,y,0)} = 0.92 - 0.002 \cdot (100 - x) \quad q_{x(x,y,0)} = q_{y(x,y,0)} = 0$$

$$q_{x(0,y,t)} = 3.21 \quad q_{x(L,y,t)} = 0.5 \cdot (q_{x(L,y,t-\Delta t)} + q_{x(L-\Delta x,y,t-\Delta t)})$$

$$h_{(L,y,t)} = 0.6$$

The numerical solution was compared to one calculated by the HEC-RAS software which solves the Bresse equations using the standard step method. A spatial discretization of Δx = 1 mand Δy = 0.4 m and a time step of Δt = 0.10 s were used, with a Courant number of CFL = 0.14. Figure 3 shows the grid, initial condition and calculated hydraulic axis.

The results of the simulation present a hydraulic axis similar to that obtained with HEC-RAS. Table 1 shows the maximum percentage difference between the depth and flows calculated by the model versus the HEC-RAS, which is under 0.5%.

Runoff over an Obstacle

A simulation was performed of runoff over an obstacle having a parabolic shape and located at the bottom of a rectangular channel with a unit width of 25 m, with no bottom slope or roughness. The geometry of the obstacle was:

$$z = \begin{cases} 0 \text{ m for } x < 7.5 \text{ m} \\ 0.2 - 0.2 \cdot \left(\frac{x-10}{2.5} \right)^2 \text{ m for } 7.5 \text{ m} < x < 12.5 \text{ m, } \forall y \\ 0 \text{ m for } x > 12.5 \text{ m} \end{cases}$$

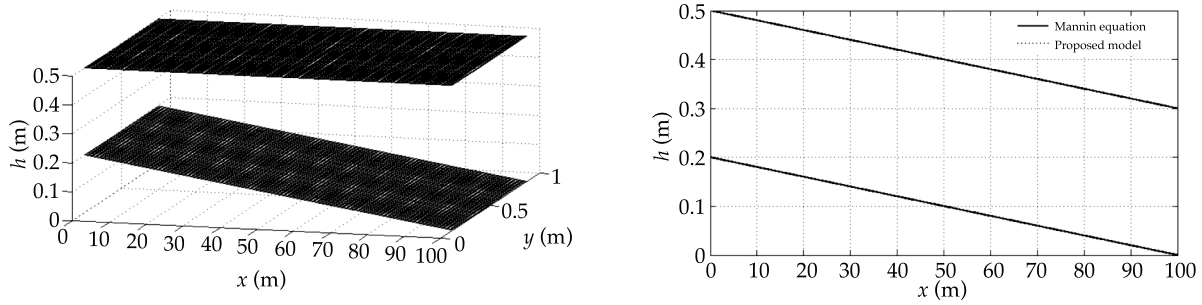


Figure 2. Grid and initial conditions (left) and hydraulic axis (right) calculated with the model and the Manning equation.

Table 1. Error of the results of the model in comparison to the known solutions for the calculation of depth and flow.

Test	Average error (%)		Maximum error (%)	
	<i>h</i>	<i>q</i>	<i>h</i>	<i>q</i>
Test 1	0.01	0.00	0.03	0.00
Test 2	0.36	0.02	0.76	0.04
Test 3a	0.05	0.04	0.33	0.19
Test 3b	1.98	0.03	10.07	0.27
Test 3c	2.54	0.03	8.80	0.35
Test 4	0.01	N/A	1.12	N/A
Test 5	1.18	1.37*	3.20	642.16*

* Error associated with the flow velocity.

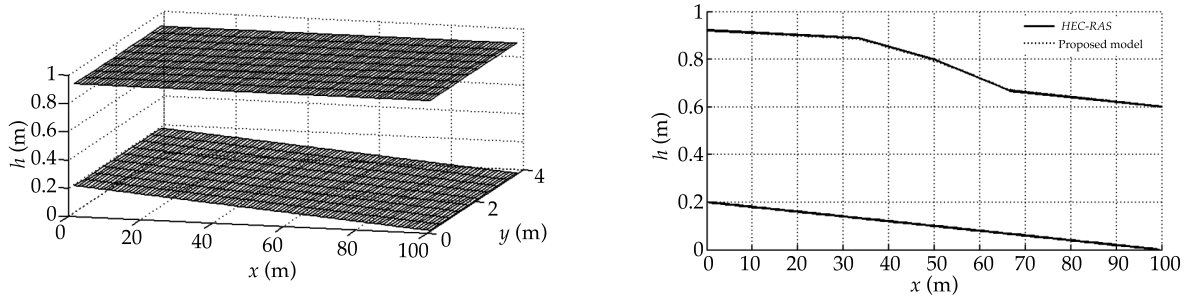


Figure 3. Grid and initial conditions (left) and hydraulic axis (right) calculated with the model and the HEC-RAS.

Three initial conditions and different boundary conditions were imposed: a) flow over an obstacle; b) regime change from subcritical to supercritical; and c) the formation of a hydraulic jump, shown in Table 2.

The numerical results were compared to the analytical solution published by

Alcrudo and Benkhaloun (2001). A spatial discretization of $\Delta x = 0.1$ m and $\Delta y = 0.1$ m and a time step of $\Delta t = 0.01$ s were used, with a Courant number of CFL = 0.26, 0.32 and 0.38 for cases a, b and c, respectively. Figure 4 shows the initial conditions and the hydraulic axes calculated.

Table 2. Initial and boundary conditions for tests 3a, 3b and 3c.

Test	Initial conditions	Boundary conditions
Test 3a	$h_{(x,y,0)} = 2.5$ $q_{x(x,y,0)} = q_{y(x,y,0)} = 0$	$q_{x(0,y,t)} = 4.42, \quad q_{y(0,y,t)} = 0$ $h_{(L,y,t)} = 2.0$
Test 3b	$h_{(x,y,0)} = 1.25$ $q_{x(x,y,0)} = q_{y(x,y,0)} = 0$	$q_{x(0,y,t)} = 1.53, \quad q_{y(0,y,t)} = 0$ $h_{(L,y,t)} = 0.5 \cdot (h_{(L,y,t-\Delta t)} + h_{(L-\Delta x,y,t-\Delta t)})$
Test 3c	$h_{(x,y,0)} = 0.45$ $q_{x(x,y,0)} = q_{y(x,y,0)} = 0$	$q_{x(0,y,t)} = 0.18, \quad q_{y(0,y,t)} = 0$ $h_{(L,y,t)} = 0.33$

The results of the simulation presented a hydraulic axis similar to that obtained by Alcrudo and Benkhaldoun (2001). Table 1 shows the maximum percentage difference between the depth and flows calculated by the model versus the solution by Alcrudo and Benkhaldoun(2001). In case a) the errors are very small, under 0.5%. In cases b) and c) the depth calculated presented errors as large as 10.87%, which is attributed to the dynamic pressures generated over an obstacle and which the model assumes to be hydrostatic.

Formation of the Oblique Hydraulic Jump

A simulation was performed of runoff in a rectangular channel 60 m long and 40 m wide, with no slope or friction, and a

narrowing beginning 20 m downstream from the inlet, with an angle of 8.95°. The initial and boundary conditions were:

Initial conditions

$$h_{(x,y,0)} = 1$$

$$q_{x(x,y,0)} = 8.57 \quad q_{y(x,y,0)} = 0$$

Boundary conditions

$$h_{(0,y,t)} = 1$$

$$q_{x(0,y,t)} = 8.57 \quad q_{y(0,y,t)} = 0$$

and ensures a supercritical runoff before the narrowing. The numerical solution was compared to the analytical solution published by Alcrudo and García-Na-

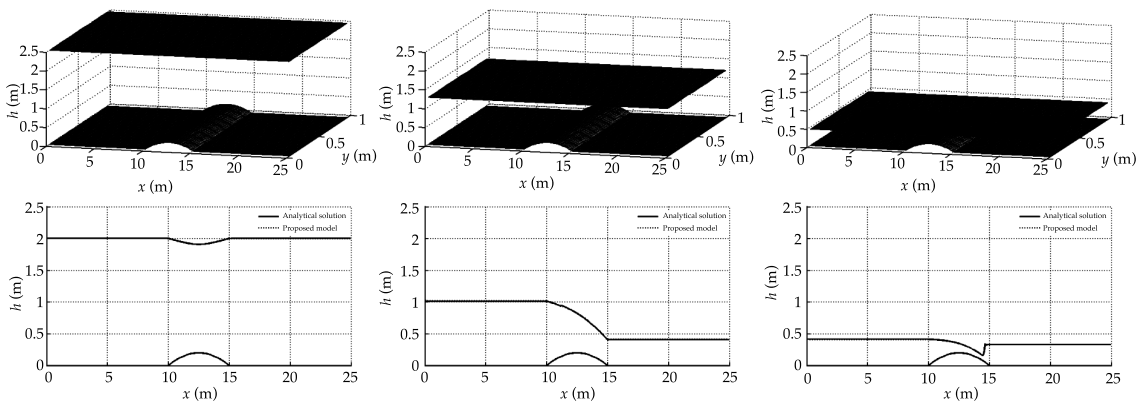


Figure 4. Initial conditions (above) and hydraulic axes calculated for test 3a (lower left), test 3b (lower center) and test 3c (lower right) with the model and the analytical solution introduced by Alcrudo and Benkhaldoun (2001).

varro (1993). A spatial discretization of $\Delta x = \Delta y = 0.5$ m and a time step of $\Delta t = 0.025$ s were used, with a Courant number of $CFL = 0.43$. A total of 150 s were simulated. Figure 5 shows the calculation grid, initial condition and the calculated free surface.

The analytical solution resulted in combined heights of 1.0 and 1.5 m, forming a 30° angle to the longitudinal axis. The results obtained with the proposed model are found to be in agreement with this solution. Table 1 shows the maximum percentage difference between the depth calculated by the model versus the Alcrudo and García-Navarro (1993) analytical solution. Flow is not compared since it is not determined by the analytical solution. The differences did not exceed 1.2%.

Oscillation of the Free Surface in a Parabolic Container

A simulation was performed of the oscillation of the free surface in a parabolic container with a surface radius of 4 500 m. An inclined free surface was initially imposed, according to Wang et al. (2011):

$$z_{(x,y)} = h_0 \cdot \frac{(x^2 + y^2)}{a^2}$$

$$h_{(x,y,t)} = h_0 - \frac{1}{2g} B^2 e^{-\tau t} - \frac{1}{g} B e^{-\tau t/2}$$

$$\cdot \left(\frac{\tau}{2} \sin(st) + s \cos(st) \right) \cdot x - \frac{1}{g} B e^{-\tau t/2}$$

$$\cdot \left(\frac{\tau}{2} \cos(st) - s \sin(st) \right) \cdot y$$

$$u_{(t)} = B e^{-\tau t/2} \cdot \sin(st) \quad v_{(t)} = -B e^{-\tau t/2} \cdot \cos(st)$$

where:

$$n = \sqrt{\frac{g \cdot \tau \cdot h^{\frac{4}{3}}}{\sqrt{u^2 + v^2}}} \quad s = \frac{\sqrt{p^2 - \tau^2}}{2} \quad p = \sqrt{\frac{8g \cdot h_0}{a^2}}$$

and $h_0 = 10$ m, $a = 3\,000$ m, $B = 5$ m/s and $\tau = 0.002$. The numerical solution was compared to the analytical solution published by Wang et al. (2011). A spatial discretization of $\Delta x = \Delta y = 50$ m and a time step of $\Delta t = 0.25$ s were used, with a Courant number of $CFL = 0.03$. A total of 3 600 s were simulated, which covers three oscillation periods. Figure 6 shows the calculation grid, initial condition, velocity graph at point $(x,y) = (1\,000,0)$ for both u and v components as well as the calculated free surface for $t = 900, 1\,800, 2\,700$ and $3\,600$ s.

The model was found to satisfactorily simulate the damped oscillations resulting from the effect of friction and these results agree very well with the analytical solution by Wang et al. (2011). The velocity graph calculated for the longitudinal component of the velocity agrees with the analytical solution while it differed from the transversal component, with a larger maximum error. Table 1 shows the maximum percentage difference between the depth and velocity calculated by the

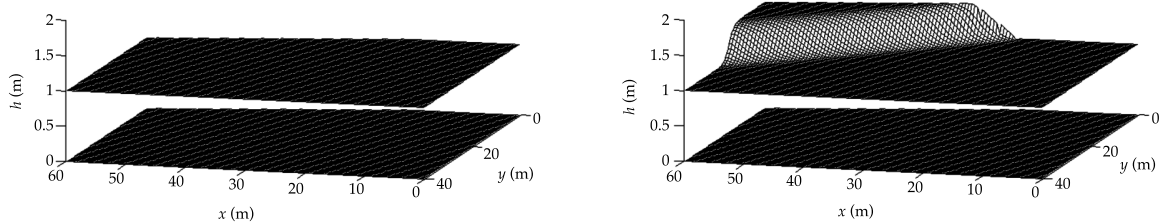


Figure 5. Grid and initial conditions (left) and free surface calculated (right) with the model.

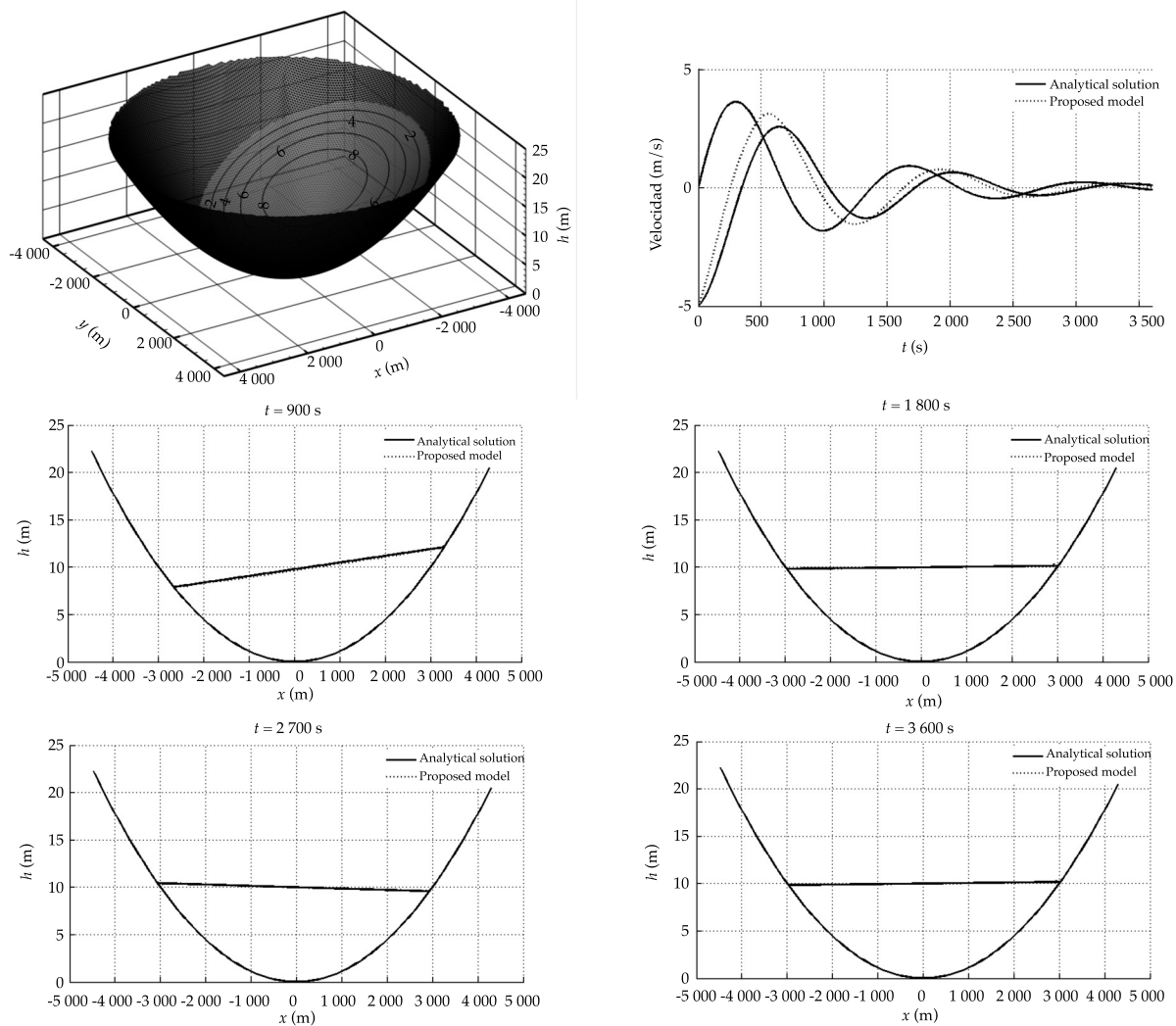


Figure 6. Grid and initial conditions (upper left), velogram at point $(x, y) = (1\ 000.0)$ (upper right) and free surface calculated for $t = 900, 1\ 800, 2\ 700$ and $3\ 600$ s with the proposed model and the analytical solution proposed by Wang et al. (2011).

model versus the analytical solution by Wang et al. (2011).

Runoff Caused by the Break of a Circular Dam

A simulation was performed of runoff caused by the instantaneous break of a dam measuring 10 m high and with a circular shape. A horizontal flood plain without friction and an initial depth of 1.0 m was considered in the area around the

dam. The initial and boundary conditions are shown in Table 3.

The numerical solution was graphically compared to the results from Mingham and Causon (1998). There is not enough history to compare point values or calculate the errors associated with the simulations. A spatial discretization of $\Delta x = \Delta y = 0.25$ m and a time step of $\Delta t = 0.01$ s were used. In all, 300 s were simulated. Figure 7 shows the calculation grid, initial condition and

Table 3. Initial and boundary conditions.

Initial conditions	Boundary conditions
$h_{(x,y,0)} = \begin{cases} 10, & \sqrt{x^2 + y^2} \leq 11 \\ 1, & \sqrt{x^2 + y^2} > 11 \end{cases}$ $q_{x(x,y,0)} = q_{y(x,y,0)} = 0$	$q_x(\text{Borde}_x,t) = -q_x(\text{Borde}_x,t)$ $q_y(\text{Borde}_y,t) = -q_y(\text{Borde}_y,t)$

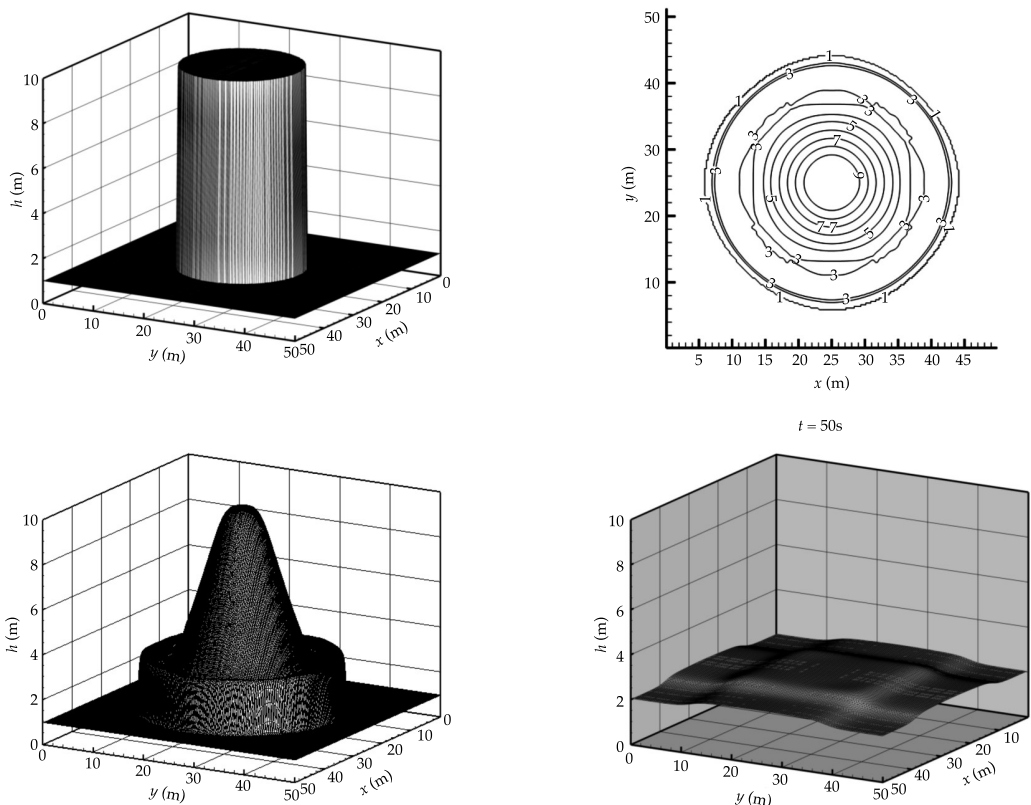


Figure 7. Grid and initial conditions (upper left), velocity fields (upper right) and free surface for $t = 0.69$ (lower left) and 300 s (lower right), calculated with the proposed model.

calculated free surface. The results of the simulation agree with the numerical solution by Mingham and Causon (1998).

Runoff Caused by a Partial Dam break

A simulation was performed of runoff caused by the instantaneous and asymmetrical break of a dam positioned perpendicular to the main axis of the

valley, measuring 200 m long, 10 m wide and 11 m high. The breakage zone was located between 95 and 170 m. A horizontal flood plain without friction downstream from the dam was modeled based on two situations: a) initially dry and b) with an initial water depth of 5 m. The initial and boundary conditions are shown in Table 4.

The numerical solution was graphically compared to results from Mingham and

Causon (1998). Not enough history exists to compare the point values or to calculate the error associated with the simulations. A spatial discretization of $\Delta x = 5$ m and $\Delta y = 5$ m and a time step of $\Delta t = 0.01$ s were used. A total of 150 s were simulated. Figure 8 shows the grid, initial condition, calculated free surface, isolines of the depth and velocity fields for scenarios a) and b). The results of the simulation agree with the numerical solution obtained by Mingham and Causon (1998).

Analysis of Flow Caused by a Dam break

Flow caused by the instantaneous break of a dam in an idealized hydraulic system was analyzed. The system was composed of a valley with a parabolic section and a channel with a trapezoidal section. In all cases, the channel downstream from the dam was considered to be initially dry. Figure 9 shows the geometry of the hydraulic system and the typical shape of the outflow hydrograph that caused the dam break.

Table 4. Initial and boundary conditions.

Initial dry condition	Initial wet condition
$h_{(x,y,0)} = \begin{cases} 10, & x < 100 \\ 0, & x > 100 \end{cases}$	$h_{(x,y,0)} = \begin{cases} 10, & x < 100 \\ 5, & x > 100 \end{cases}$
$q_{x(x,y,0)} = q_{y(x,y,0)} = 0$	$q_{x(x,y,0)} = q_{y(x,y,0)} = 0$

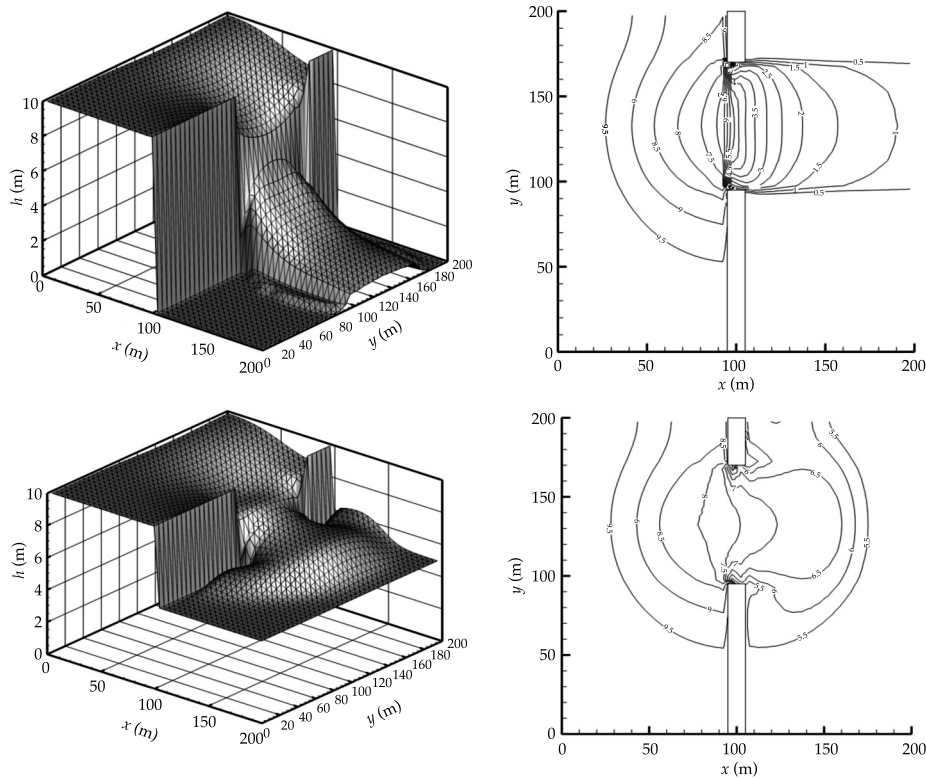


Figure 8. Grid and free surface calculated with the model (left) and isoline map of depths (right) for an initially dry (above) and wet (below) channel for $t = 7.2$ s.

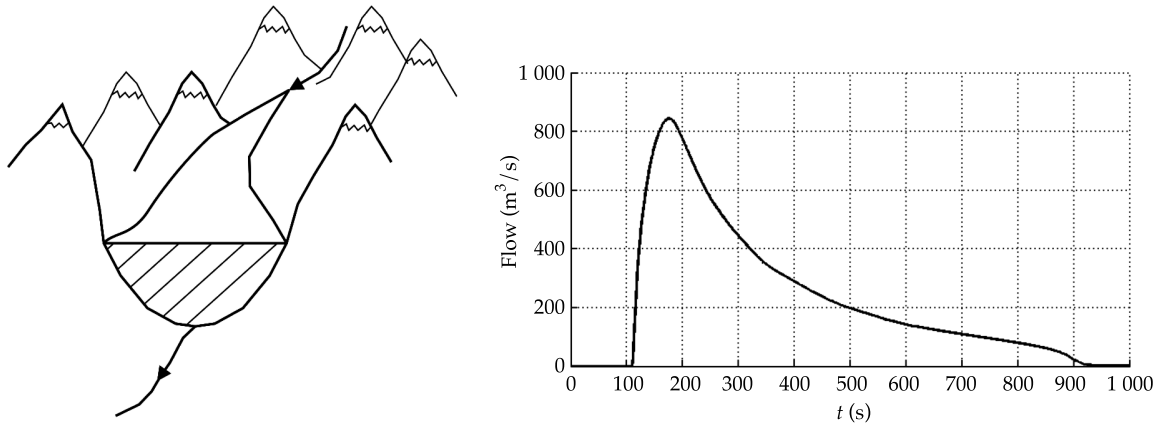


Figure 9. Hydraulic system (left) and outflow hydrograph (right).

Outflow Hydrograph

Figure 10 shows the peak flow of the outflow hydrograph in the section of the dam calculated with the model *versus* the flow corresponding to a gravity wave, calculated as:

$$Q = V \cdot A = \sqrt{\frac{2}{3} g \cdot h} \cdot A$$

where h is the depth of the dam and A is the cross-section of the gap. Calculations are shown for dam depths of 45,60, 75, 90, 105 and 120 m, and gap widths of 400, 450, 500, 550, 600 and 650 m.

A linear relationship is observed between the two flows, where the maximum flow at the outlet can be estimated to be $Q_{max} = 0.41 \cdot Q_{wave}$.

Effect of the Gap, Bottom Slope, Roughness and Orientation

Figure 11 shows the changes in the maximum outflow corresponding to the baseline scenario (gap = 400 m; $n = 0.02 \text{ sm}^{-1/3}$, orientation = 0°) with the gap, roughness

of the channel and orientation of the dam wall with respect to the longitudinal axis of the valley.

The roughness and orientation are observed to have a lesser effect on the peak flow of the outflow hydrograph. Meanwhile, peak flow increases rapidly as the gap widens until producing a complete breakage.

Attenuation of the Outflow Hydrograph

The attenuation of the outflow hydrograph downstream was studied by simulating 28 scenarios with different reservoir, dam orientations, gap widths and longitudinal slopes with respect to the longitudinal axis of the valley. This enabled analyzing the sensitivity of the hydraulic response to the geometric properties of the system. For each case, the baseline time and peak hydrograph flow were measured at a point located 2 km downstream from the dam. Table 5 shows the scenarios analyzed and Figure 12 shows the peak flow and flood time for the scenarios.

As in the outflow hydrograph for the dam section, the most sensitive variable

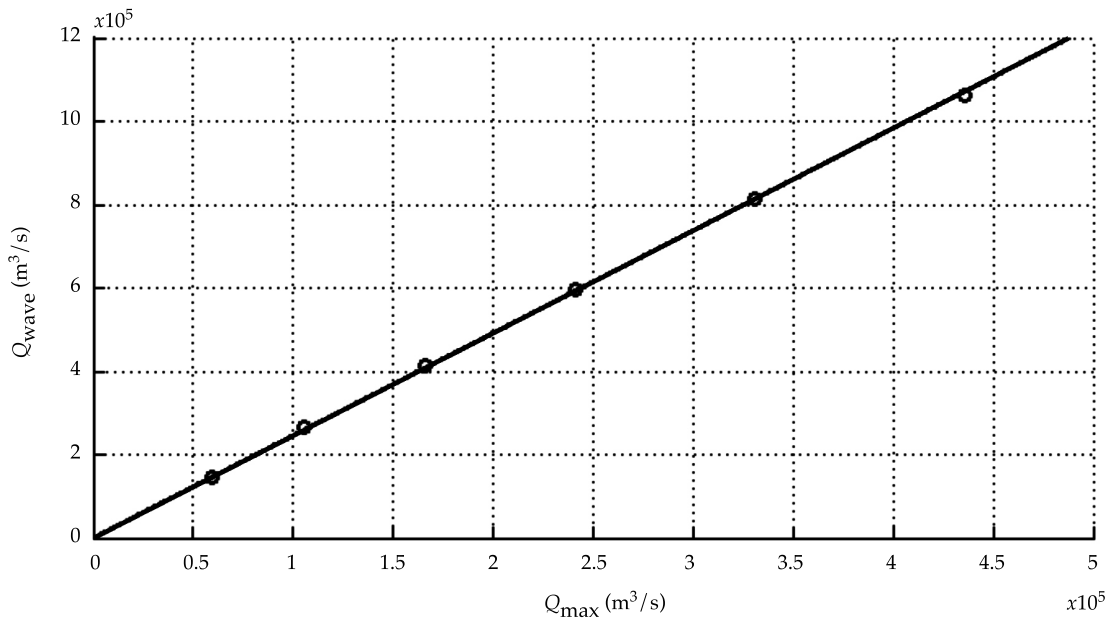


Figure 10. Maximum flow of the hydrograph and flow of a gravity wave.

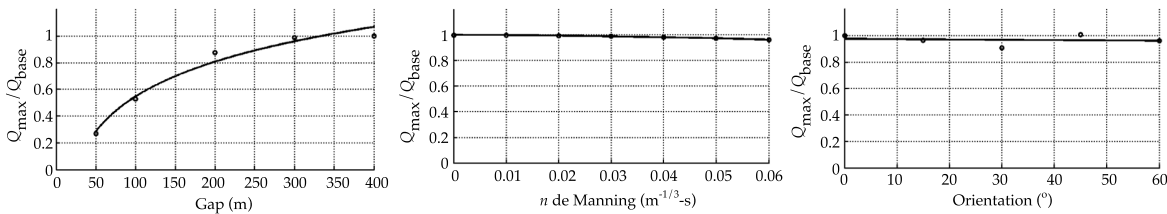


Figure 11. Effect of the gap (left), roughness (center) and orientation of the dam (right) on peak flow.

was the depth of the dam, which when increasing from 45 to 120 m produced changes in the maximum flow from 20 000 to 90 000 m^3/s . The next most sensitive variable was the gap, which in the case of partial breaks can cause the peak flow to change by a factor of 3. The roughness of the channel can cause a considerable decrease in the peak flow and an increase in flood time. The bottom slope and orientation have a smaller effect on the hydrograph and its attenuation downstream.

Conclusions

The finite volume methods was applied to solve 2D Saint-Venant equations with source terms in order to calculate the flow caused by a dam break.

The model was verified by calculating seven cases with known solutions which made it possible to determine the capacity to simulate runoffs with discontinuities as well as the drying/wetting process.

An analysis was conducted of the flow caused by an instantaneous dam

Table 5. Scenarios analyzed

Scenario	Depth	Slope	Gap	Orientation	Roughness
Scenario 01*	45	0.005	100	0	0.025
Scenario 02	45	0.005	100	15	0.025
Scenario 03	45	0.005	100	30	0.025
Scenario 04	45	0.005	100	45	0.025
Scenario 05	45	0.005	100	60	0.025
Scenario 06	45	0.000	100	0	0.025
Scenario 07	45	0.0025	100	0	0.025
Scenario 08	60	0.005	100	0	0.025
Scenario 09	75	0.005	100	0	0.025
Scenario 10	90	0.005	100	0	0.025
Scenario 11	105	0.005	100	0	0.025
Scenario 12	120	0.005	100	0	0.025
Scenario 13	45	0.005	50	0	0.025
Scenario 14	45	0.005	100	0	0.025
Scenario 15	45	0.005	200	0	0.025
Scenario 16	45	0.005	300	0	0.025
Scenario 17	45	0.005	400	0	0.025
Scenario 18	45	0.005	100	0	0.000
Scenario 19	45	0.005	100	0	0.010
Scenario 20	45	0.005	100	0	0.020
Scenario 21	45	0.005	100	0	0.030
Scenario 22	45	0.005	100	0	0.040
Scenario 23	45	0.005	100	0	0.050
Scenario 24	45	0.005	100	0	0.060
Scenario 25	45	0.001	100	0	0.025
Scenario 26	45	0.002	100	0	0.025
Scenario 27	45	0.003	100	0	0.025
Scenario 28	45	0.004	100	0	0.025

*Baseline case.

break with an idealized hydraulic system composed of a valley with a parabolic section and a channel with a trapezoidal section. Twenty-eight scenarios were simulated with different wall heights and orientations, gap widths, longitudinal slopes and channel roughness. The results show the dam height to be the variable that most affects the peak flow of the outflow hydrograph. Gap width has a significant effect on partial breaks. The

bed roughness considerably reduces the peak flow downstream and increases flood time. The orientation of the wall and the longitudinal slope have a smaller affect on floods caused by breaks.

The results obtained can be applied to planning dam projects and managing the risk of floods from breaks. The model developed satisfactorily calculated the complex behavior of flow caused by instantaneous dam breaks, and thus

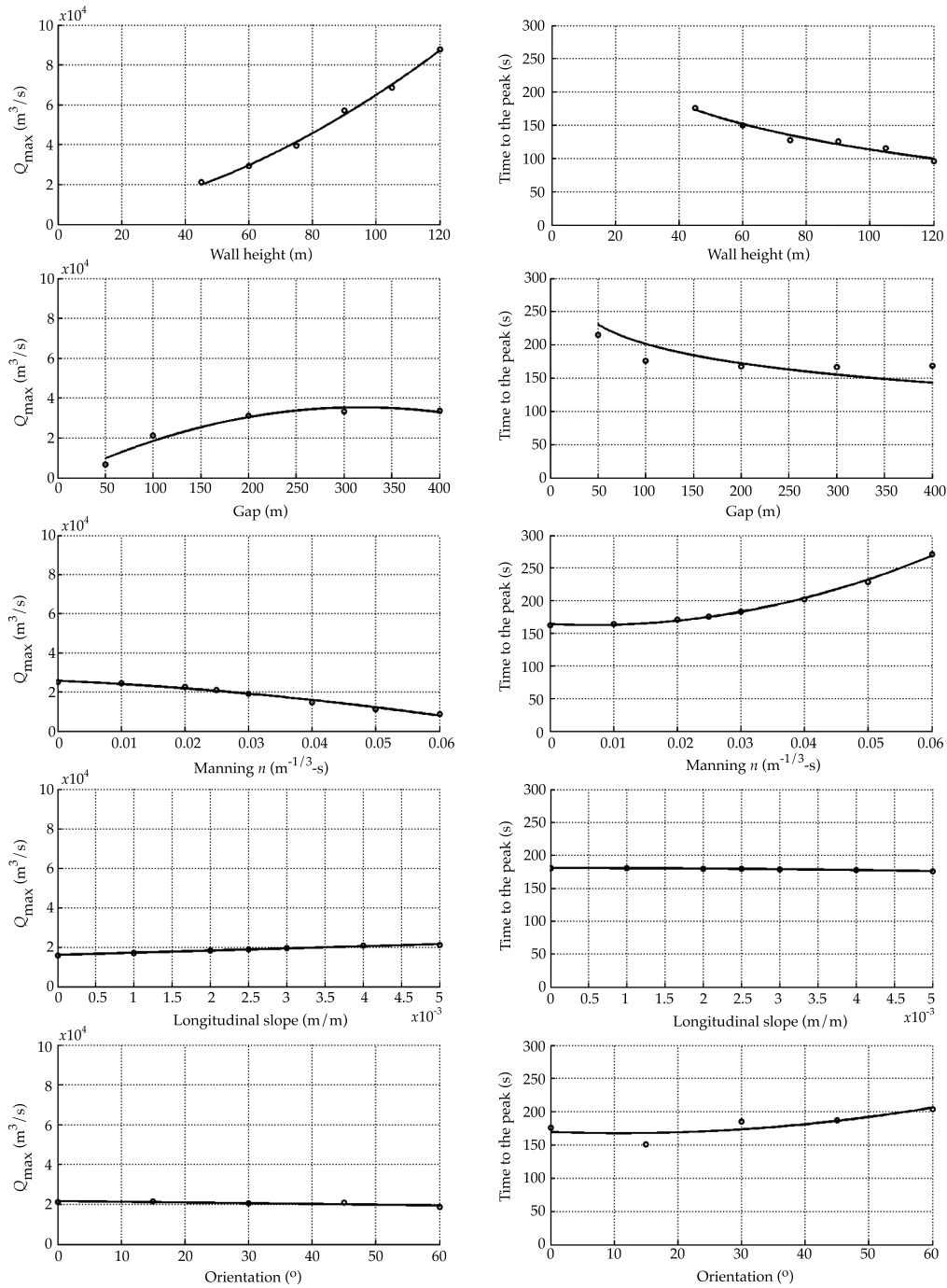


Figure 12. Peak flow (left) and flood time (right) for the scenarios analyzed.

is considered a simulation tool with predictive capacity. Input data for the model for particular study cases need to include the topography of the channel

and flood plains, the geometry of the wall and roughness. In the case of the gradual opening of gaps, it is necessary to know the shape of the gap in function of time.

Future developments will be aimed at extending the model to simulate runoff in conjunction with the evolution of the bed in order to include the effects of sediment transport.

Acknowledgements

The authors would like to thank the Chilean National Commission for Scientific and Technological Investigations (Nacional de Investigación Científica y Tecnológica de Chile (Conicyt)) and the German Academic Exchange Service (DAAD) for financing through project PCCI2012-027.

References

- Alcrudo, F., & Benkhaldoun, F. (2001). Exact Solutions to the Riemann Problem of the Shallow Water Equations with a Bottom Step. *Computers & Fluids*, 30(6), 643-671.
- Alcrudo, F., & García-Navarro, P. (1993). A High-Resolution Godunov-Type Scheme in Finite Volumes for the 2D Shallow-Water Equations. *International Journal for Numerical Methods in Fluids*, 16(6), 489-505.
- Alcrudo, F., & Mulet, J. (2007). Description of the Tous Dam Break Case Study (Spain). *Journal of Hydraulic Research*, 45, 45-57.
- Begnudelli, L., & Sanders, B. (2007). Conservative Wetting and Drying Methodology for Quadrilateral Grid Finite-Volume Models. *Journal of Hydraulic Engineering*, 133(3), 312-322.
- Bermúdez, A., & Vázquez, M. (1994). Upwind Methods for Hyperbolic Conservation Laws with Source Terms. *Computers & Fluids*, 23, 1049-1071.
- Bermúdez, A., Dervieux, A., Desiderii, J., & Vázquez, M. (1998). Upwind Schemes for the Two-Dimensional Shallow Water Equations with Variable Depth using Unstructured Meshes. *Computer Methods in Applied Mechanics and Engineering*, 155, 49-72.
- Brufau, P., & García-Navarro, P. (2000). Two-Dimensional Dam Break Flow Simulation. *International Journal for Numerical Methods in Fluids*, 33, 35-57.
- Chanson, H. (2009). Application of the Method of Characteristics to the Dam Break Problem. *Journal of Hydraulic Research*, 47(1), 41-47.
- Dressler, R. (1952). Hydraulic Resistance Effect upon the Dam-Break Functions. *Journal of Research of the National Bureau of Standards*, 49(3), 217-225.
- Dressler, R. (1954). Comparison of Theories and Experiments for the Hydraulic Dam Break Wave. *Proc. Int. Assoc. of Scientific Hydrology Assemblée Générale, Rome*, 3(38), 319-328.
- Gottardi, G., & Venutelli, M. (2004). Central Scheme for Two-Dimensional Dam-Break Flow Simulation. *Advances in Water Resources*, 27(3), 259-268.
- Fraccarollo, L., & Toro, E. (1995). Experimental and Numerical Assessment of the Shallow Water Model for Two-Dimensional Dam-Break Type Problems. *Journal of Hydraulic Research*, 33, 843-864.
- Harten, A. (1984). On a Class of High Resolution Total-Variation-Stable Finite-Difference Schemes. *SIAM. J. Numer. Anal.*, 21(1), 1-23.
- Harten, A., Lax, P., & Van Leer, A. (1983). On Upstream Differencing and Godunov-Type Schemes for Hyperbolic Conservation Laws. *SIAM Rev.*, 25, 35-61.
- Hervouet, J., & Petitjean, A. (1999). Malpasset Dam-Break Revisited with Two-Dimensional Computations. *Journal of Hydraulic Research*, 37(6), 777-788.
- Hunt, B. (1982). Asymptotic Solution for Dam-Break Problem. *Journal of the Hydraulics Division*, 108(1), 115-126.
- Hunt, B. (1984). Dam-Break Solution. *Journal of Hydraulic Engineering*, 110(6), 675-686.
- Kurganov, A., & Tadmor, E. (2000). New High-Resolution Central Schemes for Nonlinear Conservation Laws and Convection-Diffusion Equations. *Journal of Computational Physics*, 160, 241-282.
- Liang, Q., & Marche, F. (2009). Numerical Resolution of Well Balanced Shallow Water Equations with Complex Source Terms. *Advances in Water Resources*, 32(6), 873-884.
- Link, O., & Donoso, J. (2008). Development and Verification of a Numerical Model for Calculation of Flow in Open Channels using the Finite Volume Method. *Journal of Hydrology and Hydromechanics*, 56(3), 190-200.
- Mingham, C., & Causon, D. (1998). High-Resolution Finite-Volume Method for Shallow Water Flows. *Journal of Hydraulic Engineering*, 124(6), 605-614.
- Morris, M. (2001). *CADAM-EU Converted Action on Dam Break Modelling*. Recuperado de <http://www.hrwallingford.co.uk/projects/CADAM/>.
- Pilotti, M., Maranzoni, A., Tomirotti, M., & Valerio, G. (2011). 1923 Gleno Dam Break: Case Study and Numerical Modeling. *Journal of Hydraulic Engineering*, 137(4), 480-492.
- Rubio, H., Martínez, E., & Meza, A. (noviembre, 2012). *Evaluación de la longitud de peligro por rompimiento de bordos de almacenamiento con capacidad menor a 250.000 m³. Acapulco, Guerrero. XXII Congreso Nacional de Hidráulica.*
- Singh, V. (1996). *Dam Break Modelling Technology*. Dordrecht: Kluwer.
- Soares-Frazão, S., & Zech, Y. (2008). Dam-Break Flow through an Idealized City. *Journal of Hydraulic Research*, 46(5), 648-658.
- Toro, E. (2001). *Shock-Capturing Methods for Free-Surface Shallow Flows* (third edition). Chichester, UK: John Wiley and Sons Ltd.

- Van Leer, B. (1985). On the Relation between the Upwind-Differencing Schemes of Godunov, Enquist-Osher, and Roe. SIAM (Soc. Ind. Appl. Math.) *Journal on Scientific and Statistical Computing*, 5, 1-20.
- Vijayasundaram, G. (1986). Transonic Flow Simulations using an Upstream Centered Scheme of Godunov in Finite Elements. *Journal of Computational Physics*, 63, 416-433.
- Vischer, D., & Hager, W. (1998). *Dam Hydraulics*. Chichester, UK: John Wiley and Sons Ltd.
- Wang, Y., Liang, Q., Kesserwani, G., & Hall, J. (2011). A 2D Shallow Flow Model for Practical Dam-Break Simulations. *Journal of Hydraulic Research*, 49(3), 307-316.
- Whitham, G. (1955). The Effects of Hydraulic Resistance in the Dam Break Problem. *Proc. R. Soc. Lond.*, 227, 399-407.
- Zhu, Y., Visser, P., & Vrijling, J. (2004). Review on Embankment Dam Breach Modeling (pp. 1189-1196). In M. Wieland, Q. Ren, and J. S. Y. Tan (Eds.). *New Developments in Dam Engineering*. London: Taylor & Francis Group.

Institutional Address of the Authors

M.C. Ignacio Sabat

Departamento de Ingeniería Civil
Universidad de Concepción
Edmundo Larenas s/n
Concepción, CHILE
Teléfono: +56 (41) 2204 320
Fax: +56 (41) 2207 089
nacho.sabat@gmail.com

Dr. Oscar Link

Profesor asociado
Departamento de Ingeniería Civil
Universidad de Concepción
Edmundo Larenas s/n
Concepción, CHILE
Teléfono: +56 (41) 2204 320
Fax: +56 (41) 2207 089
olink@udec.cl

Dr. Bernd Ettmer

Professor
Fachbereich Wasser und Wasserwirtschaft
Hochschule Magdeburg-Stendal
Magdeburg-Stendal
Breitscheidstr. 2
39114 Magdeburg, GERMANY
Teléfono: +49 (0) (391) 886 4429
Fax: +49 (0) (391) 886 4430
bernd.ettmer@hs-magdeburg.de



SEO TABASCO

ENTRO C. P. 86000

CALLE
LEON ALFARO TORRES

COMP
ACCION
TELE
81 81

Flood in Villahermosa, Tabasco Mexico.

Photo: Conagua.

Forensic Analysis of Floods: A Methodological Guide

• Aldo I. Ramírez* •

Centro del Agua para América Latina y el Caribe, México

• L. Alejandra Herrera-Lozano •

Sistema de Agua Potable y Alcantarillado de San Miguel de Allende, México

*Corresponding Author

Abstract

Ramírez, A. I., & Herrera-Lozano, L. A. (January-February, 2015). Forensic Analysis of Floods: A Methodological Guide. *Water Technology and Sciences* (in Spanish), 6(1), 25-48.

A guide for the forensic analysis of floods is presented. It focuses on the search for effective strategies to increase knowledge about the subject without questioning previous concepts that have already been accepted by the scientific community while also establishing the participation of multidisciplinary teams. The guide is primarily based on the integration of hydrometeorological, hydrological and hydraulic processes, in addition to the analysis of political and social information. The systematic application of this guide in municipal, state and federal arenas will enable the standardization of information related to flood events and will facilitate the creation of reliable databases. These serve as the source of information for any investigation about this subject of importance to many countries.

Keywords: Forensic analysis, floods, methodological guide, ex-post analysis, extreme phenomena.

Resumen

Ramírez, A. I., & Herrera-Lozano, L. A. (enero-febrero, 2015). *Análisis forense de inundaciones: una guía metodológica*. *Tecnología y Ciencias del Agua*, 6(1), 25-48.

Se presenta una guía para el análisis forense de inundaciones, la cual se centra en la búsqueda de estrategias efectivas para incrementar el conocimiento del tema, sin cuestionar los conocimientos previos ya aceptados por la comunidad científica, pero sí estableciendo una participación de equipos multidisciplinarios. El sustento de la guía está basado principalmente en la integración de procesos hidrometeorológicos, hidrológicos e hidráulicos, incluyendo además el análisis de información tanto política como social. La aplicación sistemática de esta guía en los ámbitos municipal, estatal y federal permitiría estandarizar la información derivada de eventos inundantes y facilitaría la integración de bases de datos confiables, insumo de cualquier investigación, en este tema tan importante para muchos países.

Palabras clave: análisis forense, inundación, guía metodológica, análisis ex-post, fenómenos extremos.

Received: 12/01/12

Accepted: 26/09/14

Introduction and Conceptualization

Floods are not recent phenomena. And even the Great Flood has gone beyond religious meanings to be studied scientifically, resulting in several theories to explain it (Blick, 1991). Nevertheless, it is reasonable to think that information about floods has been more abundant and better documented over recent centuries. This type of event is considered among the disasters associated

with the most frequent and deadly natural phenomena, affecting an average of 520 million persons per year. Roughly half of the people who lose their lives in “natural disasters” have been victims of floods, and they are responsible for one-third of economic losses worldwide (UNESCO, 2008).

Numerous investigations have been conducted as part of the ongoing search to decrease the impact of floods in different

areas. Nevertheless, most of these are dispersed among different knowledge areas in the institutions conducting them. Furthermore, the reality is that the results are rarely brought together, making it difficult to obtain a solid and comprehensive tool to help perform objective evaluations. That is, a methodology with unified criteria has not been developed to objectively analyze what causes a flood event to become an unimaginable disaster.

The main objective of forensic engineering, and forensic hydrology in particular, is to determine the likely cause of an event and the human sources that contribute to increasing damages. Nevertheless, this field has rarely been used for phenomena of this type, missing out on the advantages it could provide investigations on this topic. Any forensic investigation has the predetermined objective to determine how an event occurred, and eventually what to do to prevent it from recurring. The first time the terms “forensic” and “hydrology” were applied to geoscience sub-disciplines was in the late 1970s when concerns about pollution of soil and water sources were popular. By the 1990s concerns had become directed towards the impact of human activities on the environment. And today, forensic investigations now include hydrology (Hurst, 2007).

Forensic hydrology is an environmental discipline. In addition to topics related to pollution, it could also appear in topics involving floods, drainage, water resources, pumping or any hydraulic structure. Forensic hydrology sometimes serves to prevent major damage, and at times to ration the use of water and its distribution.

Forensic analysis of floods is the application of a methodology after a disaster occurs. It consists of reconstructing the event to determine how it happened, what factors contributed to it, what failed and what were the factors involved in the

damage. The analysis will then be directed toward performing an evaluation or study of the event after the points mentioned have become clear. The final objective of the analysis is to suggest what is needed to aid or improve the system and thereby prevent this type of disaster in the future, to whatever extent possible. Flood analyses need to integrate hydrometeorological, hydrological, hydraulic, social and political principles with the help of technological modeling and simulation tools. The likely causes of damages due to floods in a basin can thereby be determined and the key factors involved in causing the damage can be documented.

The objective of the document herein is to provide a scientifically based methodological guide which makes it possible to analyze floods from the forensic perspective, unifying criteria and establishing methodological guidelines for analyses. This will make it possible to obtain results that are objective enough to plan strategies to mitigate their effects. The guide integrates geographic, hydrological, hydrological, social, political and economic factors, and includes how to identify which factors are primarily responsible for contributing to or aggravating a flood event. Therefore, from a forensic perspective, the emphasis of the guide is after the event. Nevertheless, in order to have baseline information for the analysis, some activities are described which could be conducted any time before the phenomena occurs.

Methodological Guide for Forensic Flood Analyses

This document establishes the desirable contents of a methodological guide for forensic flood analyses. Each section discusses different details, but always with the objective to organize the ideas and actions that arise through the evaluation

process. The most relevant part of the guide, and therefore its activities, relates to after the event causing the flood has already occurred. Nevertheless, recommendations for actions that are useful on a routine basis are established, not only those to be taken when an event occurs. The methodological guide is divided into three periods—before a flood event, during a flood event and after a flood event (when the impact has already been observed). The overall organization is composed of five phases, with a total of twenty stages. An ideal forensic flood analysis would contain all the stages presented in Table 1. Nevertheless, the analysis can be performed without one

of those, while always trying to meet the established requirements in order to obtain a complete and objective analysis.

Phase A. Compiling and Integrating the Information

A.1 Compiling the Information

The information that should be collected, in document form, for the stages before a flood event as well as during a disaster are described below. If a forensic evaluator can participate with the team responsible for the direct response during an emergency, highly valuable information could be

Table 1. Phases and Stages of a Forensic Flood Analysis.

Phase	Stage	Before	During	After
A. Collection and integration of information	1. Collection of geographic, hydrometeorological, hydraulic and political-social information			
	2. State and quality of hydrometeorological and hydrometric information			
	3. Geographic information system			
	4. Geomorphological characterization of basins			
B. Hydrometeorological and hydrological analysis	1. Genesis of storms			
	2. Temporal-spatial distributions			
	3. Time series analysis and determination of statistical parameters			
	4. Probabilistic analysis of frequencies			
	5. Estimation of excess rainfall (event)			
	6. Determination of return periods for rainfall and flow (event)			
	7. Modeling and simulation of rainfall-runoff process			
C. Hydraulic analysis	1. Modeling and simulation of river network, floodplains and urban zones			
	2. Review of hydraulic and protection works			
D. Integrative analysis	1. Review of action and development plans and programs			
	2. Analysis of emergency management			
	3. Integration of hydrological and hydraulic analysis with other factors			
	4. Generation of flood maps and determination of affects on human settlements			
E. Final diagnostic	1. Comparison with historical events			
	2. Summary of causes and effects			
	3. Lessons learned and actions proposed			

obtained since it would be first-hand information. In general, the compilation of information is not a simple task since it is often difficult to gain access to everything suggested herein, given that the information is dispersed throughout several institutions and agencies.

Geographic

To the extent possible, the following should be obtained before, during and after a flood event: geographic data, human factors, thematic maps, satellites images and aerial photography, as well as prior topographic surveys and images of the disaster zone at the basin, river and urban levels, among others.

Hydrometeorology

In terms of prognoses and records, the observation, interpretation and analysis of sufficient hydrometeorological data is vitally important. The climatological information is collected from conventional (manual) and automatic stations (usually digital). In addition, weather observatories exist which generate meteorological and climatological information nationally for national service institutions and international agencies. Observatories generally operate 24 hours per day 365 days per year without interruption and measurements of the elements pertaining to atmospheric time are taken every three hours. In the best of cases, the hydrometeorological data provide information about rainfall events in terms of their development, location, extension, magnitude, duration and intensity.

Hydraulics

This area includes hydrometric flow information as well as information about

the state of the hydraulic infrastructure. It contains:

- **Hydrometry.** The information from hydraulic records will be primarily focused on hydrometric data which refer to the collection of flows through a given section of a river or channel. Depending on the location, the records that could be obtained are flows in rivers, outflows from dams, flows captured and delivered to irrigation systems, or supply and levels. If the evaluator can participate in the surveys performed by the authorities in a disaster zone— by land, sea and air— it would be desirable to quantitatively document the water levels throughout critical sections and in the vicinity of structures in a river or on its banks, as well as the flow velocity and transport sediment, among other data.
- **Hydraulic works and protection infrastructure** existing at the site or basin. Information will be collected about hydraulic works present in the disaster zone and the supply basins. These works play a role in the hydrological and hydraulic dynamics of the study zone according to the purpose for which they were built. If information can be obtained at the exact moment when an event occurs, the evaluator should particularly develop a detailed record of the operating policies followed and any signs of possible structural damage. In terms of the inflows and outflows registered, it is important to verify that measurements are adequately taken and with sufficient frequency. A search for design data should be considered, including: date of construction, geographic location, use, dimensions and geometry, return period, expenses and works that are complementary to the infrastructure.

Design and real-time operating policies also need to be considered, as well as flow information related to the event. Flood protection works are critical to the completely simulate a system in which a disaster occurs.

Political-Social

The inclusion of this dimension is an important complement to the technical information, especially during the phase that evaluates the impacts of the event. The following are considered:

- Action and development plans and programs. Since the government is primarily responsible for responding to disasters caused by floods, actions plans and development programs are created at this level. These plans need to be collected for later analysis since they will provide a guide to verify the preventive and preparative measures implemented in a particular zone in the event of an emergency. Information about development programs also needs to be compiled in order to identify the series of actions established by governments to improve living conditions, and of course in this sense to prevent risk situations. Municipal planning documents should not be left out, since they are key to local land management, especially in terms of details regarding the occupation of vulnerable areas.
- Damage caused. Natural disasters cause a significant amount of fatalities and numerous material losses. Therefore, an overall perspective of the damages caused in an affected zone is useful in order to obtain a broad context of the repercussions of the particular disaster on the economy and society, as well as its impact on the national economy. Ideally, a complete analysis of the damages would be evaluated to quantify the economic losses, supported by a financial institution and an accepted methodology.
- Emergency Management. Natural as well as anthropogenic disasters are treated as an issue of humanitarian assistance, with actions directed at preparing to respond to emergencies and post-disaster reconstruction. The actions related to a latent risk and the emergency itself are important to prevent damages that can be avoided. It is therefore necessary to know the type of actions taken, which along with the technical information will enable identifying the failure in the system in the affected zone. Information is needed about warning and alert systems as well as about assisting the population during an emergency.
- Personal testimonies. Both direct and indirect testimonies from the population and people involved in the disaster are very important since they will provide information that is difficult to find in technical reports. In addition, they provide information about their experience of the disaster, with details that may be very valuable for forensic analyses. Interviews of those directly affected, observers and the authorities should be documented.
- Historical records. It is useful to have historical information about past flood events, including histories of flood events and destruction in the zone, records from communications media (radio, television and newspapers) and, of course, technical reports from each flood event, to whatever extent possible. This information enables comparing and contrasting the event analyzed with previous ones.

- Other factors that influence floods. Other factors exist that are not determinant of floods but can have a certain degree of influence on them. In this respect, information is sought about the correct comprehensive management for the zone, in terms that are closely linked to the development plan. Deforestation levels in the disaster zone should be investigated, as well as land use changes in supply basins. The sale of low-value high-risk land should also be investigated as well as the invasions into natural floodplains; that is, the non-observance of land management plans. In terms of the population and municipal services, it is desirable to have information about marginalization levels, garbage collection systems and the culture of handling of waste.

The compilation phase will be complemented by field investigations conducted after the event to update the information as required. The analysis of the information can help to determine critical sites for more detailed studies.

A.2 State and Quality of Hydrometeorological and Hydrometric Information

The records from climatological and hydrometric stations may be incomplete. In the event of a complete lack of climatological as well as hydrometric information, neighboring basins where similar events have occurred can be used. Nevertheless, with regard to precipitation records, indirect methods to generate information—such as interpolation or transposition of storms—will significantly reduce the reliability of the analysis and therefore should be avoided to the extent possible. For example, when precipitation information is lacking, using only hydrometric records is still an option.

With regard to the hydrometric stations, information may be lacking for periods when significant events occurred. In this case, alternative methods can be used to complete the information based on other nearby stations containing records. On the other hand, when only small gaps in the records exist the analysis can infer the information through some type of interpolation method. In general, if a flow registry exists in the basin of interest, this should be used directly.

A.3 Geographic Information System

The advantages of having a geographic information system (GIS) in the study zone are evident. The generation of a GIS is recommended at the moment of identifying a particular area with the potential of damage from floods. Geographic, geomorphological, climatological and hydrometric information would be inputted into the GIS as it is collected and thereby make it possible to comprehensively manage the entire cartography of the zone. This system can also be used to store social and economic layers of information which could provide important elements at some point during the evaluation. If a GIS exists when an event occurs, information could be inputted as it is collected in the field, thereby updating specific records in real-time, making this a highly useful and dynamic tool for later analyses. If a GIS does not exist when a disaster occurs, the use of one for that specific analysis should be seriously considered, in which all the information collected would be inputted as it is obtained. Baseline maps of the affected zones and supply basins should first be generated with the GIS. For example, Figure 1 presents the baseline map of the middle and lower Grijalva River basins, in southeast Mexico, where the delimitation of the supply area and the topography can be seen.

A.4 Geomorphological Characterization of the Basins

To understand the hydrological dynamics of the process that has occurred in a zone, the analysis conducted should include the comprehensive modeling of the hydrological systems in the affected basin and their supply basins. This would clearly identify the existing situation in the basin affected by a flood event.

Delimitation of the Zone and Characterization of the Basins

The delimitation of basins and sub-basins (those affected by the flood as well as supply basins) should be based on technical criteria

that take into account the topographic and hydrological characteristics of the site. Watersheds are delimited in order to define the basins on which the geomorphological characterization is based. A digital elevation model (DEM) is desirable, with a scale of at least 1:25 000 if resources allow, although for the upper basin a scale of 1:50 000 can be used and for the plains, 1:10 000. In addition to making it possible to graphically represent the shape and elevation of the study surface, a DEM is a powerful tool for subsequent analyses; for example, to obtain morphometric data to calculate hydrological parameters. From a hydrological perspective, the basins function as a large system which receives precipitations and transforms

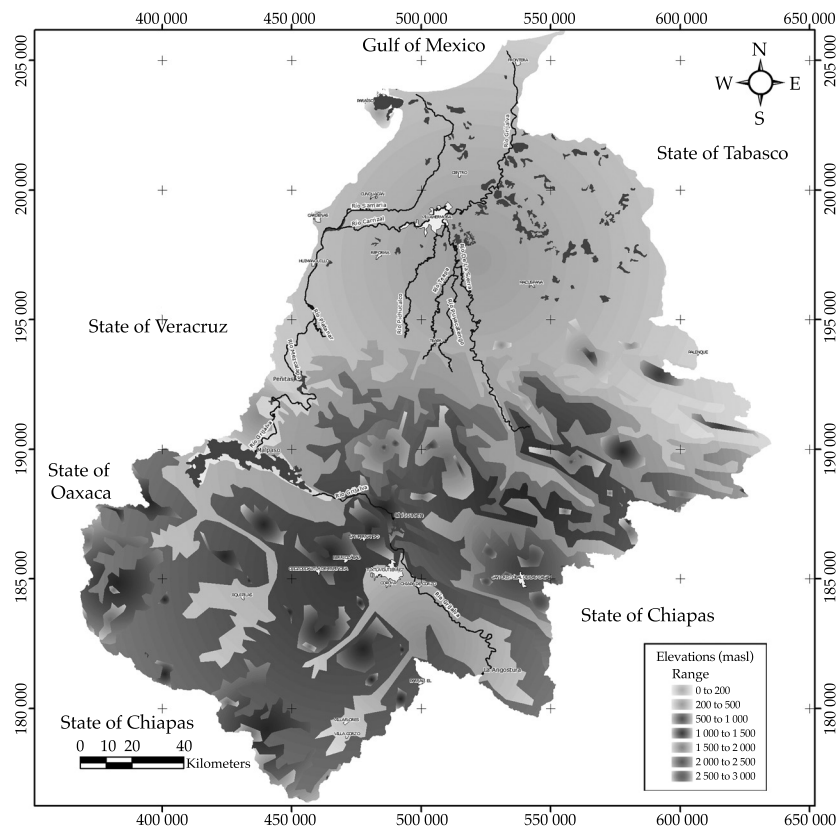


Figura 1. Cuenca media y baja del río Grijalva en un SIG.

them into runoff. This transformation depends on a large variety of parameters. Therefore, to identify the functioning of the basin, it should be geomorphologically characterized using physical parameters such as length and slope of the basin and river, as well as topographic parameters such as hypsometric curves, in addition to information about soil type, land use and vegetation cover. A GIS is an ideal analytical and imaging tool for all these elements.

Phase B. Hydrometeorological and Hydrological Analysis

This stage of analysis is undoubtedly one of the most critical to the methodology. Understanding the hydrometeorological and hydrological processes in a basin is the basis of the study and contributes to understanding the event that caused the flood problems.

B.1 The Genesis of Storms

The genesis of a storm that produces a flood event is key to forensic flood analyses. A storm is understood as a set of rainfalls with well-defined characteristics and that belong to the same meteorological disturbance. They may last a few minutes, several hours or even days and may have a spatial range from very small zones to very large regions. Two temporal and spatial scales are used to study a storm—mesoscale and synoptic (large-scale or cyclones). The mesoscale refers to systems with a horizontal scale ranging from several hundreds of meters to kilometers and with a duration of several hours, such as convective storms, circulation of breezes and mountain and valley winds. The synoptic scale extends several hundreds of kilometers and lasts several days or weeks,

such as cyclones at middle latitudes. Therefore, the information generated by synoptic reports and bulletins and forecasts emitted by authorities should be useful to establishing the genesis of the phenomenon and clearly determine whether it was one single phenomenon or a combination.

B.2 Spatial-Temporal Distributions

Spatial distribution is studied using isomaps which generally consist of isolines, or lines that join points of equal value. Software exists to construct these maps using very diverse interpolation methods, although when going beyond technical conventions they usually need to be refined with customized criteria. Isoline maps make it possible to visualize the distribution of the variables and obtain information about their spatial evolution. The temporal distribution is represented by temporal evolution graphs which represent the variation in any variable over time at a determined point. This information enables identifying trends and detecting seasonal variations. The amount of precipitation in a hydrological region is a climatic factor that varies greatly from year to year. This variability not only applies to time but also space, which means that rainfall depends on local conditions (Gutiérrez, Aparicio, & León, 2005). To represent rainfall in an affected basin and its supply basins, a monthly rainfall distribution can be obtained by including all the stations and all of the records, which will provide information for months when most of the precipitation falls. In addition, graphs can be generated to represent monthly accumulated precipitation for each station in order to perform partial evaluations for each one. All of this provides a background analysis and a reference framework.

In addition, mean mass curves can be constructed to determine the variation in mean precipitation over time in a basin. To reconstruct the field pertaining to rainfall which occurred before and during the flood, isohyet maps should be generated (Ramírez, 2012) to visualize the spatial distribution of the storm, with durations that can range from 5 minutes to over 96 hours, thereby identifying the center and evolution of the storms, as needed.

B.3 Time Series Analysis and Determination of Statistical Parameters

The time series analysis is useful to examine the evolution of past and present climates. According to Escalante and Reyes (2005), a time series is a set of observations performed sequentially, normally at equal intervals, and present statistical characteristics that show trends in behavior. A time series can be annual or periodic, the latter including seasonal, monthly, weekly, daily or hourly periods. A time series can be univariate or multivariate depending on whether one or several variables are involved. While this may be a basic analysis, it is key to every study. With these measurements, a set of observations pertaining to a variable is described using few indicators and certain group characteristics are defined. Comparing data with this method is more precise than with tables and graphs. In addition, these descriptive statistics will be useful to calculate the parameters of functions used in frequency analyses. If wanting to go more in-depth, stochastic hydrology methodologies can be used. The stochastic process is characterized by a general tendency or a deterministic component and a certain degree of uncertainty or randomness in the event. This analysis is performed using historical precipitation and runoff records in the study zone.

B.4 Frequency- Probability Analysis

A frequency analysis consists of assigning an exceedance frequency, or recurrence interval of events. The mathematical approach to the frequency analysis is based on a probability distribution. The parameters of a probability distribution are defined according to statistics obtained from observations (WMO, 1994) and define location, scale, shape and asymmetry, among other properties. Several techniques exist to estimate parameters, including methods of moments and maximum likelihood (Kite, 1988). The probabilistic analysis of frequencies is simply a procedure to estimate the exceedance probability of future or past events (Haan, 1986). For the purpose of this study, the exceedance probability of the flood event needs to be determined. Since the peak flow and its corresponding hydrograph are controlled by several climatic and physiographic factors, the most reliable estimation is obtained through the probabilistic processing of observed flood information (flows or levels). In addition, the probabilistic analysis of maximum rainfalls or extreme precipitation makes it possible to construct intensity-duration-return period curves which characterize storms in a study region. These curves are also an invaluable tool to determine runoff in basins without instruments. A frequency-probability analysis can be performed once the hydrometeorological and hydrometric information has been collected, its quality has been verified, and the sampling statistics and statistical parameters obtained. The minimum time period recommended by several authors ranges from 10 to 25 years (Esparza, 2005). Overall, to continue the hydrological analysis presented in this guide the procedure that should be followed for precipitation as well as flow registries is to

adjust the data to various functions using an analytical process. Following this, the distribution with the best fit is selected to thereby evaluate the magnitudes of the events for different probabilities of occurrence or return periods. Whichever analysis is used, it will be based on precipitation as well as runoff data (if the latter are available).

B.5 Estimation of Excess or Effective Rainfall from an Event

Excess rainfall is the difference between total registered rainfall and hydrological abstractions. Therefore, it refers to precipitation which is not intercepted, is not retained by the surface, does not infiltrate or evaporate. Thus, effective or excess precipitation is what generates direct runoff to the outlet of a basin. In the case of gauged basins, a simultaneous registry of precipitation and runoff from a storm will be available, and therefore excess rainfall will be calculated based on direct flow determined according to the flood hydrograph. This would be done by dividing the direct runoff volume by the area of the basin. On the other hand, if these abstractions are not known, such as in basins without instruments, specific methods are used, such as the curve number model developed by the *Natural Resources Conservation Service* (NRCS, 1986). The procedure to apply to the forensic flood analysis is chosen according to the information collected.

B.6 Determining Return Periods for Precipitation and Flow from an Event

The return period (T) is understood to be the time interval in which an event of a given magnitude can be equaled or exceeded, on average and over time (Aparicio, 2005). In

terms of probabilities, the return period is the inverse of the exceedance probability of an event, $T = 1 / P(X \geq x)$. Given that the rainfall-runoff relationship is non-linear, the return periods for rainfall and flows need to be differentiated. The return period for a particular rainfall is not the same as that for runoff generated by the same rainfall. Aldama, Ramírez, Aparicio, Mejía and Ortega(2006) have mathematically shown that the return period for a storm is different than the return period for the flow it produces, although little effort has been dedicated to determining the nature of this non-linearity. Eagleson (1972) was the first to address this topic and analyze it analytically. This is naturally a complicated process involving key variables, namely the soil moisture content at the moment of the precipitation as well as changes in vegetation, land use and anthropogenic activities in the basin. Therefore, a rainfall with a 100-year return period does not necessarily generate a flow having a 100-year return period. In a basin subject to increasing urbanization or deforestation, the same rainfall generates runoffs having increasingly longer return periods.

The estimate of the return period associated with a flood event is proposed as follows. Locate the flow associated with the flood event in the list of assigned probabilities using a plotting position formula such as that by Weibull (Kite,1988). This should consider that the registry did not include the value of the event in question but rather only historical values, that is, only registries up to the year prior to the flood event. If this flow falls within the magnitudes registered by the historical data, a return period for the event can easily be determined. Nevertheless, if the flow is located outside the magnitudes found in the registries then the return period T of the flood event can be calculated by fitting

the registries to an FDP one more time, considering that the fit does not include the value of the event in question. For this case, although the magnitude of the flow is larger than those in the historical registries, it can be associated with a return period through extrapolation. These two ways to assign T are intended to prevent the length of the registry or the magnitude of the event from influencing the value. The value of the flow associated with the flood event can later be incorporated into the historical records, which will result in a modification of the fit of the records to the FDP as well as a change in the recurrence interval values through the plotted position. Thus, the assigned value of T will also change. The above is intended to highlight the fact that the assignment of the occurrence probability is evolutionary and not static.

B.7 Modeling and Simulation of the Rainfall-Runoff Process

Flows of water caused by precipitation are estimated with rainfall-runoff models which can be included in a process to evaluate a response system in basins affected by a flood event. Simulation methods using software are more efficient and reliable to calculate runoff from rainfall since they enable performing a relatively detailed analysis using small time intervals. Nevertheless, if hydrometric records are not available or are too limited to obtain a reliable interpretation or extrapolation, then rainfall-runoff relationships can be very useful because of their ability to infer flow information based on precipitation records.

To model the rainfall-runoff process, initial moisture conditions in the basin when a storm begins are important, as is the amount, intensity and duration of the precipitation. Antecedent precipitation, a concept referring to rainfalls in the

immediate past, is the most important factor associated with moisture in the basin. In general, it is considered an exponential function, or the inverse of time, such that the most recent precipitations will most greatly affect antecedent moisture. To analyze complex storms with long durations, they need to be divided into as many intervals as possible. According to Linsley, Kohler and Paulhus (1990), in small basins under 250 km², the average intensity can be considered to be given by the duration and the total amount of precipitation, without losing much information. Regardless of the model used to simulate the rainfall-runoff process, a calibration stage must be included. The calibration makes it possible to determine the value of the errors in the results from a model or measurement with respect to a reference pattern, with sufficient precision and under specific conditions. It is crucial that these errors be sufficiently small and that they are determined with the highest precision possible. A helpful technique is the section-slope method using the Manning formula, especially to calibrate the model at a point. This method uses the history of the event, geometric characteristics and the roughness of the channel to obtain a good estimate of peak flow through ungauged basins.

In the best of cases, a rainfall-runoff model already developed for the study basin will be available. But if this is not the case the possibility of developing one should be considered. In the former case, the model can be run with rainfall data from the flood event and the resulting runoff can be estimated and compared to observed runoff. Regardless of the different rainfall-runoff models used, it is important to consider the limitations involved in applying each one to the zone, as well as the information that is available.

Phase C. Hydraulic Analysis

The purpose of a hydraulic analysis is to obtain good representations of the natural hydrodynamic behavior of systems and the hydraulic infrastructure, as well as the conditions involved in the event. Modeling will be used for a simplified representation of a real system.

C.1 Modeling and Hydraulic Simulation of the Network of Channels, Floodplains and Urban Zones

Modeling is required to simulate or reproduce the hydrodynamic behavior of a network of channels. An advanced hydraulic model is sought for the study basin. To this end, the geometry of the channels and the hydrodynamic variables of the system need to be known in order to compare the results from the model with those observed in reality, and to obtain a calibrated hydraulic model that enables performing a reliable analysis of what happens during a flood event.

For the initial development of the hydraulic model, certain geometric variables of the channel networks need to be known, such as the axis of the channel, characteristics of sections, elevations and depths. This information is generally obtained from the field, and therefore direct topographic surveys are ideal. Nevertheless, the use of a GIS can be useful to the processes and has been recommended. It will therefore be used in this case. When topographic information of the terrain is available at a scale of at least 1:5 000, details can be obtained after a DEM analysis. The topography of the channel must be taken into account in order to select a good scale and thereby generate sections that provide the characteristics mentioned above. Furthermore, some additional characteristics need to be

known, such as the type of material of the channel wall, which can be obtained through field investigations. Added to all of this is information about flow, which was generated with the hydrological analysis. Obstructions in the channels must also be considered, such as bridges, and the location of structures such as dams, pumping stations, etc. The type of flow must also be clearly identified in order to perform the modeling. In open channels, flow can be classified by many times and be described in many ways. It will be important to decide whether a modeling of impermanent flow is useful so as to include the transitory effect of flows. A modeling of mixed flows is always desirable. This provides the opportunity to include subcritical and supercritical flows. And spatially varied flow will in most cases need to be included. Likewise, the flow regime of the current will need to be determined for the modeling. This is classified according to the Froude number, a dimensionless ratio between inertial forces and gravitation forces in the critical state; subcritical when the flow velocity is low, and supercritical when it is high (Chow, 1994).

The roughness coefficient is an important characteristic of the channel. This is the value representing flow resistance due to friction, commonly handled with the Manning n . Chow (1994) mentions a guide to correctly determine the Manning roughness coefficient, which consists of four overall approaches: (1) Understand the factors that affect the value of n in order to obtain basic knowledge of the problem and decrease the degree of uncertainty; (2) Consult a table of common values of n for different types of channels; (3) Examine and become familiar with the appearance of some of the common channels; (4) Determine the value of n using an analytical procedure based on

theoretical velocity distributions in a cross-section of a channel, and on measured velocity or roughness data.

Modeling and simulation of a network's functioning should be done under normal conditions as well as in the event of a flood. The resulting levels will be highly important since they are the main variables used to generate flood maps. The hydraulic modeling of a network of channels will provide enough information to determine the overall behavior and that of the major event in the network. The information also enables determining the boundaries of floodplains during normal functioning and flood zones during major events. This information is important since once the floodplain is delimited and a determination is made as to whether human settlements are located there, a hydraulic analysis of the urban zone can be performed to establish the degree to which the dynamics of a city will be effected. To this end, the hydrodynamic functioning of streets can also be simulated.

In general, to evaluate the hydraulic analysis of an urban zone, parameters such as water depth, velocity, permanence of flow and supply of solids should be taken into account.

Erosive processes and sedimentation cause damages, including the reduction in the productivity of the soil, loss and degradation of soil and sedimentation in reservoirs, drainage ditches and channels, as well as damages to hydraulic infrastructure. For the study case, the damages of most interest are those caused by scouring around infrastructure near or in the river, as well as changes to the flow capacity of the river due to sedimentation.

Scouring is caused by an increase in flow velocity over a certain limit or by turbulence. Major flows can present a risk to infrastructures in rivers and can therefore be a decisive factor in aggravating an

emergency created by a major flow. Therefore, scouring is a factor to be taken into account in the present analysis. Erosion can completely destabilize a structure if scouring occurs near the foundation of the hydraulic work (Wang *et al.*, 2014). Likewise, a flood level can affect a river by causing scouring at the bottom, which would compromise the upper parts of the slope and could cause them to collapse. Therefore, the structural design of the foundation of the work should be reviewed, paying special attention to the date of construction and the repairs that have been made, as well as the foundation level and history of floods. The intention is to analyze how the structures and foundations have behaved in search of evidence of damage and to investigate the need for repairs.

Therefore, the scouring depth resulting the major event under study must be determined. Methods exist to accomplish this, such as the Lischtvan- Levediev (Maza, 1987). This will provide elements to analyze the behavior of structures and the river.

Changes in the hydraulic capacity of a river can be affected by the degree to which it and its respective floodplains are composed of unconsolidated sediments, which are quickly eroded by floods and high water levels. If the river transports fairly thick sediments during a flood, these will tend to be deposited along the bottom of the river and cause natural dykes to form. This could raise the bottom of the river, thereby increasing water levels. When this occurs there is a very high risk of flooding. Natural and induced landslides are also cases that can increase the risk of flooding, in which the amount of sediments transported by the river increases, causing the hydraulic capacity to decrease or, in the worst of circumstances blocking the river.

Another factor is the development of tides, where the overheight of the

sea level can worsen flooding inland, in areas relatively near the coast or cause coastal flooding. Historical sea levels and those associated with the phenomenon should be studied using either of the two approaches. There are three different types of sea overheight (in addition to the astronomical tide): breaking waves, wind drag and storm tides (USACE, 2008). These three types of overheight can occur in combination, although one will be predominant depending on the shape of the coast. To analyze this factor, information is needed about the phenomenon that causes the sea level to increase, as well as the sea level before and during the event and the extension and duration of the coastal flood. This will serve as a guide to analyze its combination with other factors. Coastal floods are primarily involved in obstructing natural runoff into the sea and blocking the flow of drainage systems, of course with their respective affects on the coastal area.

C.2 Review of Hydraulic and Protection Works

For this section, it is necessary to use the information collected about the works as well as the information generated from the hydrological analysis with and without the flood event. Reviewing hydraulic works usually focuses on comparing original design values with information generated from the hydrological analysis of a flood event under study. That is, values from the peak flows obtained from that analysis must be applied to the functioning of the works and compared to theoretical values for capacities and designs. It is therefore important to note that the failure of a structure could be caused by an event whose magnitude exceeds the design value as well as by a failure in the structural robustness of the works (Holický & Sýkora,

2009). Nevertheless, the information or procedures followed for the design of the works may not be available in some instances. In that case, current operating policies will need to be reviewed instead of design values. Based on the above, the general state and design of the works are analyzed to define whether they were key factors in the disaster. The works to be reviewed are described below.

Reservoirs and Dams

The conventional design process of a reservoir consists of determining a design flow using a frequency analysis, in which a level of risk is acceptable according to a determined return period. This design flow will be key to the analysis since it verifies the current conditions of the reservoir based on the design data, in order to later study normal flow volumes and the volume generated by a particular event under study. In general, two approaches to estimate flows through dams can be mentioned (Aldama *et al.*, 2006)—the hydrometeorological and the hydrometric approaches. In the hydrometeorological approach, precipitation records are analyzed and converted into runoff using rainfall-runoff models. A complete hydrograph of the flow can be obtained with this information. The hydrometric approach involves a frequency analysis of annual peak flows. Once the peak flow associated with a return period is estimated, the flow is usually increased, that is, assuming that the shape of the hydrograph is the same as that of the peak flood recorded. Including a bivariate approach is desirable, which refers to a joint frequency analysis. This makes it possible to assign a return period to the complete hydrograph of a flow, whereas the conventional hydrometric analysis only refers to the return period of the peak flow

and not that of the complete hydrograph (Ramírez & Aldama, 2000).

Pumping Stations

Generally, pumping stations are used to eliminate wastewater or rainwater from a zone which cannot be drained on its own by gravity, thereby preventing flooding. Pumping stations also directly protect against flooding. For example, they maintain the level of a canal or drain during peak flows by transporting water to a river with a large capacity. The location and functioning of pumping stations are the main factors to be reviewed. When verifying the functioning of the pumps, all the instrumentation is usually not available to test their complete behavior. Nevertheless, according to the manufacturer's information, such as the behavior curve, the equipment should fulfill particular operating conditions and can thereby be ensured to function adequately. Two parameters need to be determined—total load and flow. Since most of the installations have flow meters, only the total load will need to be determined. Having obtain this information, the test to verify the functioning is performed by locating the intersection of the two variables on the manufacturer's curve, which should be very close to the design point of the pump. For either of the two pumping station functions mentioned here, failure is an important factor to consider when evaluating the seriousness of a flood and its effects.

Canals and Drains

Here, only modified channels and artificially built canals are analyzed in order to improve the hydraulic system in the zone. The review will be primarily qualitative, verifying design data such

as slope, minimum and maximum flow velocities and the criteria used to estimate the free boundary, as well as the flood zone corresponding to the channel. The longitudinal slope is one of the most important hydraulic variables associated with the energy of a river. Because of this, channels need space for flow mobility, where the water overflows during floods and the energy dissipates. Therefore, the design characteristics of the channel need to be reviewed, as well as its historical evolution and the current characteristics before a flood. This will enable identifying whether a factor in the evolution of the channel or drain could have been decisive and have worsened the flood problem. It is important to identify relationships with degradation or improvements, and to describe the deficiencies in the structures in the channel as well as their functioning. Finally, a qualitative review of the channels and drains is implicit in the analysis of the results of the hydraulic modeling.

Drinking Water Supply Systems

Drinking water supply systems can fail during flood events and leave the population without service, which can primarily create public health problems. Therefore, the study of these systems is a factor in the forensic approach to floods. To analyze this type of hydraulic work, the most important factors are location (specifically the conduction line coming from the source) and supply type and medium. The flood problem is related to the supply source. If the source is a dam or reservoir, the main problem could be a failure in the dam wall and thus in the intake. When the water is pumped from a well to a tank, the supply may be interrupted if the flood level reaches the pumps. After reviewing the supply source and verifying whether a failure occurred,

problems with the conduction line should be investigated. There are different types of lines—buried, ground level or elevated. If any of these types of lines are located in the floodplain of a river, they could break from the force of the water. Therefore, the topography of the area in which the system is located should be reviewed, as well as the piping materials, junctions and any special parts. The drinking water supply system could also fail due to floods in the headworks. Considering what has been presented, the flow of the flood and design flows play a secondary role in these cases.

Drainage Systems

The main function of a drainage system is to transport wastewater and rainwater from human settlements to sites where it will not cause damage or inconvenience the inhabitants (Conagua, 2007). The most important factor in the failure of drainage systems—whether they are sanitary, pluvial or a combination thereof—is the exceedance of their capacity. Therefore, more attention needs to be given to the design characteristics of piping, that is, design flow, diameter and material. It is also important to review design velocities, current functioning and functioning during flood events, as well as the pressure in conduits that operate under pressure. In addition, the transport of materials or garbage into the system can be a consideration, which obviously generates problems for eliminating excess water from streets as well as for the flow inside the pipes. Although it is difficult to obtain evidence right before an event, this information makes it possible to infer trends in the overall behavior of those actions. This will help to identify whether the system failed due to design parameters or because of external causes. The rational method has been most commonly used

to review and design drainage systems. Nevertheless, an instantaneous unit hydrograph could also be used when there are simultaneous measurements of flow at the outlet of the urban basin and of rainfall at some of the points within the basin. If the hydrometry is lacking, a synthetic unit hydrograph can be used (Ramírez, 2012).

Protection Infrastructure

The main parameter in the design flood protection works is the return period of the design flood. Return periods are related to the characteristics of the area to be protected. If a protection work such as those mentioned previously or another one in the study area fails during an emergency, its functioning will be reviewed to find the cause of the failure.

Phase D. Integrative Analysis

D.1 Review of Action and Development Plans and Programs

When a development plan is used as a management tool to promote the social development of a particular region, it attempts to improve the quality of life of the people and address unsatisfied basic needs. Even though civil organizations work towards the development of the society, the concept of a development plan is usually associated with the role of the State and its policies and strategies. The policies and strategies involved in these development plans should be reviewed for clarity and accuracy, and of course they should be evaluated as to whether they have been implemented or are in the process of being implemented. The follow-up of these actions should be reviewed since they are strategic visions for the future and the solutions they offer need to be maintained over time, making

them crucial to the population, its safety and well-being. The designs of the plans need to be reviewed to verify that they are sustainable and contain improvements that will remain in the society after the plan has been completed. Thus, a development plan should be aimed at teaching the population to manage latent risks and not only be directed towards restoration actions. Even though this measure is secondary to the main action, it promotes self-sufficiency. The implementation of a development plan involves political commitment and, of course, a financial investment to carry out the projects. The amounts invested should be reviewed without having to conduct audits. And some type of cost-benefit analysis should be performed up to the date of the disaster to evaluate the application of these resources and the benefits obtained. Development plans should not neglect issues such as reforestation, protected zones that are directly related with levels of felling and deforestation in the disaster zone, as well as other changes in land use in supply basins which can be analyzed with historical vegetation and land use maps to see the evolution in the zone. Land planning should also be investigated to identify the location of high-risk lands sold at low values. The concentration of vulnerable human settlements should be determined as well as invasion into natural floodplains by urban settlements, commercial zones and other land uses. In particular, the legality of settlements in connection with the plan itself should be evaluated. It is also important to identify marginalization levels in high-risk settlements, as well as factors that influence the settlement of populations in these locations. Furthermore, the government's sensitivity to the risk situation should be identified, as well as any actions that it may have taken in this respect. Finally, but no

less important, is the analysis of garbage collection systems and culture regarding wastes, including the specification of points where wastes are concentrated, collection days and destination. In general, it is important to review municipal responsibilities and the common culture related to wastes together, checking that this has not been a factor in increasing the impact of the disaster, primarily because of the decreased capacity of drainage in urban zones.

D.2 Emergency Management

The management of an emergency involves actions to be taken before it occurs and the immediate response to the population and infrastructure during the disaster (DGPC,2006). Preparation and warnings can be summarized by programs at different levels and in different areas. These include social programs as well as institutional programs that disseminate information and educate the population about the risks to which they are exposed. These are primarily programs belonging to federal and local governments since these entities are responsible for civil protection at the state and municipal levels. In addition, the value of programs that provide real-time monitoring of events representing risks to the population should be recognized, known as early warning systems; or the absence of this type of tool. Actions to respond to the population during an emergency could form the basis of all the procedures to be implemented in the event of an emergency, since everything that is done should be based on the protection and safety of the population and not only on economic losses. Since the actions taken are the result of planning and the projections generated by programs, adequate preparation should

be ensured to reduce the impact during a disaster. A review of programs in the study zone should include their specific progress, efficiency and legitimate implementation, since the objectives proposed by each of the programs depend on their correct application. If programs are not executed as planned, then the reason for this should be identified since it can become a determining factor in increasing the magnitude of a disaster.

D.3 Integration of Hydrological and Hydraulic Analyses with other Factors

This section involves integrating all the technical factors involved in the flood into one joint analysis and adding the social and economic factors that can be obtained (land planning and development plans, degree of marginalization of the population and waste handling, among many others). It would be ideal to think that all of the elements involved are considered. Therefore the analyst should consider adding all elements not mentioned here that are believed to have an influence on a particular case, in order to identify which ones were key determinants in the event or in aggravating it. In addition, it is useful to organize them hierarchically in order to more efficiently and objectively determine the causes and effects of floods, and to propose actions that help to minimize the risk of a similar event in the future. It is important to take into account the static nature of all of the analyses, due to which the dynamic aspect of the external factors involved will be difficult to evaluate. It is important to remember that systems do not exist in isolation but rather a dynamic relationship exists with other elements in the surrounding environment. Therefore, if the relationships of each of the factors analyzed are adequately connected, it will be possible to come close to the reality of an event and to minimize uncertainty.

D.4 Generation of Flood Maps and Determination of Effects

A flood map marks the intersection between the land surface and water levels corresponding to a flow of interest. Thus, areas having different risk levels can be identified and the settlement or use of lands related with high risk levels can be prohibited or restricted. To generate flood maps with automated procedures, software that jointly performs hydrological and hydraulic modeling at the street level can be used. A semi-automated procedure can generate flood maps using separate hydrological and hydraulic modeling and perform external integration using GIS software. Modeling that is performed separately are known to increase errors due to the manipulation and transfer of information, and the ability of coupled modeling to forecast flood levels is limited. But if each of the models is adequately applied the errors will surely be minimized. Therefore, flood maps are generated as follows. First, a DEM is generated and a map of the basins obtained. The DEM is used again and with the detailed topography the alignment of rivers and the characteristics of the banks and cross-sections are alternately obtained. The hydrological model is used to obtain flows, which serve as input for the hydraulic model. After performing the hydraulic simulation, flood levels are obtained from the cross sections. Finally, these levels are processed and the geographic and hydraulic information is combined to generate the flood maps. For example, Figure 2 shows the extension of the 2007 flood in the Tabasco plains.

After generating the theoretical flood maps based on the modeling, they can be compared to the actual flood area by analyzing the differences between them, attempting to locate zones that are more

problematic and finding their associations with all the factors analyzed previously. The relationships between these factors and the flood zones can thereby be established. Theoretical flood maps delimit the risk zones in a general way and the map of the flood under study delimits the effects that have occurred. This enables objectively determining the main reasons why the event reached a particular magnitude.

After using the hydraulic modeling to determine the levels occurring in the urban zones, the percentage of damage can be identified according to type: direct (housing, educational buildings, health infrastructure, public facilities, etc.), indirect (supply of goods, interruption in services and communication systems, loss of work hours, among others) and

intangible economic loss (those affected, the injured and loss of human life). For example, in the case of direct costs the analysis of the effect on human settlements includes the determination of economic loss related to housing and businesses, infrastructure, crop areas, means of communication and economic activities. The methodology used for this is divided into two steps— quantification of goods affected (for example, housing and schools affected, area of damaged pavement, loss of crops, etc.) and the quantification of the costs of these effects. For the latter, unit costs for each category should be assigned according to values established by the authorities responsible for each area. For example, in Mexico criteria can be obtained from the National Disaster

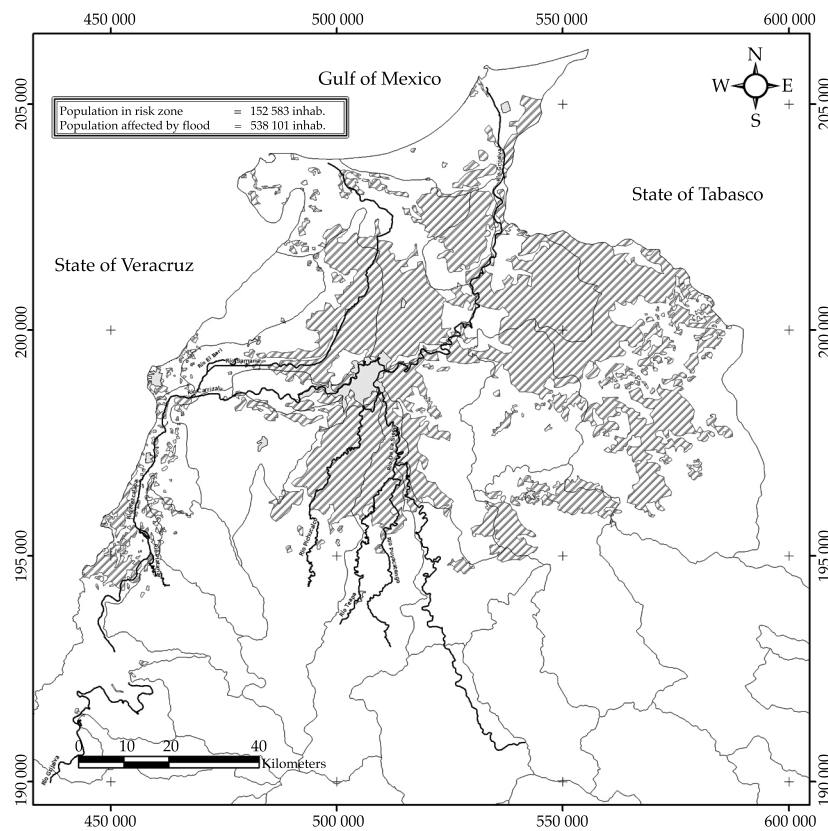


Figura 2. Extensión de la inundación de 2007 en Tabasco, México (Herrera, 2010).

Prevention Center (Centro Nacional de Prevención de Desastres (Cenapred, 2006a) for tangible damage and from Iturre (2007) for intangible damage. A catalogue or system of unit costs related to repairs or new constructions can also be consulted, such as the one maintained by Conagua (Conagua, 2004).

Phase E. Final Diagnostic

With the final diagnostic, an objective identification is sought of the factors that functioned differently than normal or than what was expected, with which a hierarchy can be created and weights can be assigned according to the degree to which each one failed. By creating a matrix of the factors and assigning a value to each one according to their causes, the factors involved in the failure can be objectively determined and actions can be identified that will decrease the impact of future events.

E.1 Comparison with Historic Events

Based on the history of flood events and the destruction caused in the study area, records from communications media and personal testimony from those affected, observers and authorities should be gathered into a document to perform a general analysis. Nevertheless, if a complete analyses of previous events are available one of those should undoubtedly be used. Thus it will be possible to compare these events to the one that is currently occurring in order to identify recurring factors that influence floods in the study zone, with similar magnitudes or within a range of association. This will serve as a guide to discover whether the structural and non-structural actions have been adequately applied over the history of the study zone or if other actions not previously considered need to be taken.

E.2. Objective Evaluation of Causes and Effects

An integrated analysis of technical factors (hydrometeorological, hydrological and hydraulic) along with the social and economic dimensions explained previously enable producing an objective evaluation of the causes and effects. The result will provide documented evidence of how major was the event from the probabilistic point of view and to what degree other external factors contributed to magnifying the impact of the flood. Thus, for example, it should be clear the degree to which damage was caused by the deficient operation of infrastructure, or by illegal settlements in high-risk zones or rainfalls and runoff with high return periods. It is important to note that a combination of all the factors may be the best explanation possible in most cases. In that case a weighting of the causes is recommended, assuring of course that this is done based on objective findings from the analysis.

E.3 Lessons Learned and Actions Proposed

Without a doubt, one of the best ways to use the findings and results from a forensic analysis of a flood event is the opportunity to learn and potentially plan actions oriented towards preventing or at least decreasing possible damages from similar events (Aparicio, Martínez-Austria, Güitrón, & Ramírez, 2009). The following questions can be answered based from the lessons from a forensic study:

How major was the event which caused the flood? What exceedance probability can be assigned to rainfalls and runoffs? To what degree may the damage have been reduced by the early warning of the magnitude of the event? Did most of the damage occur in floodable zones and invaded plains? What role did the hydraulic infrastructure play

in both the positive management of the event as well as the magnification of the impacts? If operable infrastructure exists, was the operating policy for major floods predetermined? Was the hydraulic design of the infrastructure adequate? Have urban development plans been respected? Have they been adapted for the case of floods? If these exist, do they need to be adapted for high flood risks? To what extent is the conservation of supply basins related to the damage caused by the event? How adequate was the emergency response? Was there sufficient coordination among institutions?

The forensic analysis would be expected to provide the elements needed for authorities and decision-makers to establish programs to address and control these phenomena in the future. Although this has already occurred to a certain extent, it would be desirable for the process to be based on objective technical reports. For example, after the damage from the battering of Hurricane Gilbert in the city of Monterrey in 1988, a flood control dam was built in one of the main basins supplying the Santa Catarina River, which passes through the urban zone. Thanks to that infrastructure, damages from floods generated by Tropical Storm Alex in 2010 were mitigated to some extent (Ramírez, 2011).

Another result of the forensic analysis is undoubtedly the proposal for actions aimed at decreasing the damage generated by future floods. Of course, while general ideas always exist, the concrete relationship of possible courses of action will depend on the particular case. Nevertheless, the following could be considered, just to name a few:

- Strengthening the hydrometeorological and hydrological monitoring network.
- Implementing an early warning system (hydrological)
- Reviewing and adapting operating policies related to infrastructure.
- Reviewing the hydraulic capacity on bridges and other drainage works.
- Reviewing the vulnerability of urban infrastructure (roads, supply, drainage, treatment, etc.)
- Determining the degree to which regular and irregular settlements are vulnerable to floods.
- Verifying the state of streams and rivers in terms of possible obstructions and invasions.
- Developing an atlas of risks of floods.
- Projects for works and actions to control floods.
- Incorporating hydrological criteria into urban development plans.
- Proposing reforestation and soil control in upper basins.
- In urban areas, encouraging the use of control measures based on good practices at the source of floods, such as those known as “sustainable urban drainage systems.”
- Reviewing plans for coordination among the different levels of government.

Suggested Time frame for the Phases

Based on the scope of each phase and the experience in developing and supervising flood management projects, the time frame required to develop a forensic flood analysis has been established as a guide. Table 2 shows the phases and stages, and the benefit of their being completed during the three time periods— before, during and after a flood event.

Order of Magnitude of Damages from Floods

The damages associated with floods vary greatly and generally depend on the severity of the event and the vulnerability

of the systems. For example, Table 3 presents the most recent significant damages caused by floods in Mexico.

As can be seen, the financial costs of the damages from the floods have been large, most of which has been covered by the Natural Disasters Fund (Fondo de Desastres Naturales (Fonden)) or the Fund for the Rural Population Affected by Weather Emergencies (Fondo para Atender a la Población Rural

Afectada por Contingencias Climáticas (FAPRACC)). Instead of using these funds, a desirable vision is that which addresses the problems contributing to floods with programs such as the Fund to Prevent Natural Disasters (Fondo para la Prevención de Desastres Naturales (Fopreden)) which is more oriented towards prevention than emergency response.

Conclusions

The problems caused by floods can be permanently solved only in a very few cases. Some of the most significant reasons why they cannot be solved are the cost of the works, regions undergoing socioeconomic conflicts involving land use and the economic infeasibility of these types of projects. Therefore, terms such as flood “control” and “mitigation” of the effects of floods are used to indicate that these projects attempt to prevent major damage and offer protection up to a certain level of risk. The control and mitigation of the effects of floods inevitably need to be preceded by a comprehensive analysis of past events in the zone. This will serve as a guide to guide the actions needed and achieve the projected results. To reduce the factors that

Table 2. Suggested time frame for completing the stages and phases of a forensic flood analysis.

Phase	Stage	Before	During	After			
				One week	One month	3 to 6 months	1 year
A. Collection and integration of information	A.1	✓	✓	✓	✓		
	A.2	✓					
	A.3	✓	✓	✓	✓	✓	✓
	A.4	✓					
B. Hydrological analysis	B.1			✓			
	B.2	✓			✓		
	B.3	✓					
	B.4	✓			✓		
	B.5				✓		
	B.6				✓		
	B.7	✓			✓		
C. Hydraulic analysis	C.1	✓			✓	✓	
	C.2			✓	✓		
D. Integrator analysis	D.1	✓					
	D.2			✓			
	D.3					✓	
	D.4					✓	
E. Final diagnostic	E.1					✓	
	E.2					✓	
	E.3					✓	✓

Table 3. Some of the damages associated with floods in Mexico.

Event	Year	Amount of damage (million of pesos)	Reference
Hurricanes <i>Wilma</i> and <i>Stan</i>	2005	39 832	Cenapred (2006b)
Hurricane <i>Emily</i>	2005	8 872	Cenapred (2006c)
Floods in Tabasco and Chiapas	2007	31 871	CEPAL (2008)
Tropical storm <i>Alex</i> in Nuevo Leon	2010	16 249	CERNL (2014a) CERNL (2014b)

influence the magnitude of the impact of floods, local and regional levels must be coordinated. Causes and effects related to the vulnerability of a zone reach beyond the local level. Likewise, corrective and prospective actions must be applied at the basin level. Coordination among government levels involves coordinated actions and consistency in carrying out the projects. To implement approaches to mitigate the impact of disasters caused by floods, there must be consistency among municipal, state and regional plans to proceed with a comprehensive view of the territory. It is important to consider applying structural and non-structural measures. Structural measures can include strengthening existing infrastructure and relocating housing, infrastructure or business centers located in risk zones. Non-structural measures may be active or passive. Active measures are those which encourage direct interaction with persons, such as organizing emergency responses, developing and strengthening institutions, formal education and training, communications campaigns, community participation and management at the local level. Passive measures are more closely related to legislation and planning, such as construction regulations, construction codes, land use regulations, financial stimuli and promoting insurance. These measures do not require significant economic resources and, therefore, are very favorable to creating processes that mitigate the effects of

floods. In conclusion, the actions resulting from the analysis must be consistent with the factors that influence the magnitude of the disaster analyzed. Regardless of the factors involved in the flood, a culture of insurance use is highly recommended. Actually, obtaining insurance is nothing other than the need to be covered for a possible event or catastrophe, that is, what may eventually or possibly happen. While 90% of the population has auto insurance, the percentage of people with homeowners insurance is not nearly as high.

This article presents a methodological guide to conduct a completely objective forensic flood analysis for the general purpose of contributing to planning actions aimed at preventing or at least decreasing damages caused by these natural phenomena.

References

- Aldama, A., Ramírez, A., Aparicio, J., Mejía, R., & Ortega, G. (2006). *Seguridad hidrológica de las presas en México*. Jiutepec, México: Instituto Mexicano de Tecnología del Agua.
- Aparicio, J. (2005). *Fundamentos de hidrología de superficie*. México, DF: Editorial Limusa.
- Aparicio, J., Martínez-Austria, P., Güitrón, A., & Ramírez A. (2009). Floods in Tabasco, Mexico: A Diagnosis and Proposal for Courses of Action. *Journal of Flood Risk Management*, 2(2), 132-138.
- Blick, E. F (1991). *A Scientific Analysis of Genesis*. Oklahoma City: Hearthstone Publishing.
- Cenapred (2006a). *Guía básica para la elaboración de atlas municipales de peligros y riesgos. Fenómenos Hidrometeorológicos*. México, DF: UNAM.

- Cenapred (2006b). *Características e impacto socioeconómico de los huracanes "Stan" y "Wilma" en la república mexicana en el 2005*. Documento LC/MEX/L.751. México, DF: Centro Nacional de Prevención de Desastres. Comisión Económica para América Latina y el Caribe de las Naciones Unidas.
- Cenapred (2006c). *Características e impacto socioeconómico del huracán "Emily" en Quintana Roo, Yucatán, Tamaulipas y Nuevo León en julio de 2005*. Documento LC/MEX/L.693. México, DF: Centro Nacional de Prevención de Desastres. Comisión Económica para América Latina y el Caribe de las Naciones Unidas.
- CEPAL (2008). *Tabasco: características e impacto socioeconómico de las inundaciones provocadas a finales de octubre y a comienzos de noviembre de 2007 por el frente frío número 4*. Documento LC/MEX/L.864. México, DF: Comisión Económica para América Latina y el Caribe de las Naciones Unidas, Secretaría de Gobernación México, Gobierno del Estado de Tabasco, Centro Nacional de Prevención de Desastres.
- CERNL (2014a). *Consejo Estatal para la Reconstrucción de Nuevo León*. Gobierno del Estado de Nuevo León. Recuperado de <http://www.reconstruccionnl.org.mx>.
- CERNL (2014b). *Juntos reconstruyendo Nuevo León*. En *Memorias del Consejo Estatal para la Reconstrucción de Nuevo León*. Gobierno del Estado de Nuevo León. Recuperado de www.conl.mx.
- Chow, V. (1994). *Open Chanel Hydraulics*. Singapore: McGraw-Hill International Editions.
- Conagua (2004). *Sistema de Consulta del Manual de Costos Estimados para Proyectos de Infraestructura Hidráulica 2004. Versión 2*. México, DF: Gerencia de Evaluación y Programación, Subdirección General de Programación, Comisión Nacional del Agua.
- Conagua (2007). *Manual de Agua Potable y Alcantarillado Sanitario. Alcantarillado Sanitario*. México, DF: Comisión Nacional del Agua.
- DGPC (2006). *Manual de Organización y Operación del Sistema Nacional de Protección Civil*. México, DF: Dirección General de Protección Civil, Secretaría de Gobernación.
- Eagleson, P. (1972). Dynamics of Flood Frequency. *Water Resources Research*, 8(4), 878-898.
- Escalante, C., & Reyes, L. (2005). *Técnicas estadísticas en hidrología*. México, DF: Facultad de Ingeniería de la UNAM.
- Esparza, J. (2005). *La influencia de la longitud del registro en las estimaciones de gastos de diseño en México*. Tesis de maestría. México, DF: UNAM.
- Gutiérrez, A., Aparicio, J., & León, J. (2005). Modelación del régimen pluviométrico en la ciudad de Morelia. Cap. 2. En A. Gutiérrez, A. Ramírez, & F. Sánchez (Eds.). *Las ciencias del agua en Morelia. Aplicaciones frente a los retos del siglo XXI*. México, DF: IMTA-UMSNH.
- Haan, C. (1986). *Statistical Methods in Hydrology*. Iowa: The Iowa State University Press.
- Herrera, A. (2010). *Guía metodológica para el análisis forense de inundaciones*. Tesis de maestría. Facultad de Ingeniería. México, DF: UNAM.
- Holický, M., & Sýkora, M. (2009). Forensic Investigation for Fluvial Flood Damage in the Czech Republic. In *Proceedings of ICE-Civil Engineering*, 162(5), Institution of Civil Engineers, UK.
- Hurst, R. (2007). An Overview of Forensic Hydrology. *Southwest hydrology*, 6(4), 16-17.
- Iturre, H. (2007). *Valor social del tiempo*. México, DF: CEPEP.
- Kite, G. W. (1988). *Flood and Risk Analyses in Hydrology*. Littleton, USA: Water Resources Publications.
- Linsley, R., Kohler, M., & Paulhus, J. (1990). *Hidrología para Ingenieros*. México, DF: McGraw-Hill.
- Maza, J. (1987). *Introduction to River Engineering*. México, DF: UNAM, División de Estudios de Posgrado. Facultad de Ingeniería.
- NRCS (1986). *Urban Hydrology for Small Watersheds*. Technical Release 55. Washington, DC: Natural Resources Conservation Service, USDA.
- Ramírez, A. (2011). *Evaluación del funcionamiento de la presa Rompe Picos*. Reporte técnico que forma parte integral del Informe del Proyecto "Reconstrucción del río Santa Catarina después del huracán Alex", contratado por la Comisión Nacional del Agua. México, DF: ITESM.
- Ramírez, A. (2012). *Hidrología esencial*. México, DF: Editorial Digital, ITESM.
- Ramírez, A., & Aldama, A. (2000). *Análisis de frecuencias conjunto para la estimación de avenidas de diseño*. México, DF: AMH, IMTA.
- UNESCO (2008). *Floods*. Recuperado del sitio de Internet de la UNESCO, http://portal.unesco.org/science/en/ev.phpURL_ID=6012&URL_DO=DO_TOPIC&URL_SECTION=201.html.

Institutional Address of the Authors

Dr. Aldo I. Ramírez

Centro del Agua para América Latina y el Caribe, México
 Instituto Tecnológico y de Estudios Superiores de
 Monterrey
 Av. Eugenio Garza Sada 2501 Sur
 Colonia Tecnológico Edificio CEDES
 64849 Monterrey, Nuevo León, México
 Teléfono: +52 (818) 3582 000, extensión 5560
 aldo.ramirez@itesm.mx

M.I. Lucía Alejandra Herrera Lozano

Sistema de Agua Potable y Alcantarillado de San Miguel
 de Allende
 Prolongación Alcocer núm. 2
 Fracc. La Conspiración
 37740 San Miguel de Allende, Guanajuato, México
 Teléfono: +52 (415) 1524 429, extensión 108
 alexa.hidraulica@gmail.com

Growth Kinetics and Nutrient Uptake of Microalgae in Urban Wastewaters with Different Treatment Levels

• César Carlos García-Gozalbes* •
Universidad de Cádiz, España

*Corresponding Author

• Zouhayr Arbib •
Aqualia, España

• José Antonio Perales-Vargas-Machuca •
Universidad de Cádiz, España

Abstract

García-Gozalbes, C.C., Arbib, Z. & Perales-Vargas-Machuca, J. A. (January-February, 2015). Growth Kinetics and Nutrient Uptake of Microalgae in Urban Wastewaters with Different Treatment Levels. *Water Technology and Sciences* (in Spanish), 6(1), 49-68.

The main objective of this work was to study the speed of growth and nitrogen and phosphorus uptake in a bloom of cultured microalgae in urban wastewater receiving different levels and types of treatment. To this end, microalgae were cultured in duplicate with discontinuity under controlled temperature, light and aeration conditions. Four test media were used consisting of four wastewater effluents: (1) pretreatment, (2) secondary clarifier, (3) UASB bioreactor (Upflow Anaerobic Sludge Blanket) and (4) mixture of UASB and secondary wastewater. All were obtained from the same urban wastewater treatment station. Verhulst and Photobiotreatment models were used to analyze the results. The study found different temporal evolutions of the biomass concentration and total dissolved N and P with the different media tested. Productivity was greater in tests with water from the UASB reactor ($0.094 \text{ g SS l}^{-1} \text{ d}^{-1}$). In this culture medium, the speed at which nitrogen was removed was similar to the rest of the wastewater tested while phosphorus removal was slower than the other media studied.

Keywords: Urban wastewater, nutrient removal, microalgae, photo-bioreactor, kinetic model.

Resumen

García-Gozalbes, C.C., Arbib, Z. & Perales-Vargas-Machuca, J. A. (enero-febrero, 2015). Cinéticas de crecimiento y consumo de nutrientes de microalgas en aguas residuales urbanas con diferentes niveles de tratamiento. *Tecnología y Ciencias del Agua*, 6(1), 49-68.

El objetivo principal de este trabajo ha sido el estudio de la velocidad de crecimiento y de consumo de nitrógeno y fósforo de un bloom de microalgas cultivadas en aguas residuales urbanas con diferente nivel y tipología de tratamiento. Para ello se han cultivado las microalgas por duplicado en discontinuo bajo condiciones controladas de temperatura, luz y aireación, en cuatro medios de ensayo, consistentes en cuatro aguas residuales: (1) salida de pretratamiento; (2) efluente de decantación secundaria; (3) efluente de un reactor anaerobio de flujo ascendente denominado UASB (Upflow Anaerobic Sludge Blanket), y finalmente, (4) mezcla de efluente del UASB y agua de secundario, todas de la misma estación depuradora de aguas residuales urbanas. La modelización cinética para el análisis de resultados con los modelos de Verhulst y el Photobiotreatment model indica una evolución temporal diferente de la concentración de biomasa, N y P total disuelto, respectivamente, en los diferentes medios de ensayo. La productividad es mayor en los ensayos con agua procedente del biorreactor UASB ($0.094 \text{ g SS l}^{-1} \text{ d}^{-1}$). En este medio de cultivo, la velocidad de eliminación del nitrógeno no presenta diferencia con el resto de aguas residuales utilizadas en el ensayo, mientras que en el caso del fósforo, la eliminación es la menor de entre todos los medios estudiados.

Palabras clave: aguas residuales urbanas, eliminación de nutrientes, microalgas, fotobiorreactor, modelo cinético.

Received: 15/01/14
Accepted: 26/08/14

Introduction

The ongoing deterioration in the environment due to pollution from anthropogenic activities, and specifically in aquatic systems, has a direct negative impact on water quality. Urban wastewater is one of the main sources of water pollution. The growth in urbanization and in the urban population has increased the amount of municipal wastewater generated.

The composition of wastewater reflects the lifestyles of societies and technologies used for production (Gray, 1989). It contains undesirable substances such as organic matter, suspended solids, inorganic compounds (primarily nitrogen and phosphorus) and/or xenobiotic compounds. An estimated 80% of the water used worldwide is not collected or treated (UNEP, 2010). Therefore, there is a need for investments and improvements in processes to collect, treat and eliminate wastewater.

State-of-art water treatment technologies have been positively influenced by scientific support and public interest. Conventional processes to treat urban wastewater consist primarily of four stages: pretreatment (roughing, desanding and degreasing); primary treatment; secondary treatment (in most conventional treatment systems this stage consists of an aerobic biological process called active sludge, although some countries such as Brazil are using anaerobic treatments more widely, such as UASB reactors (Upflow Anaerobic Sludge Blanket)); and finally, treatment of sludge generated, which usually includes concentration, another stabilization (biological or chemical) and dehydration. Conventional urban wastewater treatment systems were not designed to remove inorganic compounds such as nitrogen and

phosphorus. The removal of these compounds using advanced biological (AO: anaerobic aerobic, A2O; anaerobic-anoxic-aerobic; Bardenpho, etc.) and chemical (chemical precipitation of phosphorus) methods is needed to attain acceptable discharge levels. The 91/271/CEE Directive establishes very strict discharge levels of nitrogen and phosphorus for sensitive regions, primarily because these compounds are the main causes of eutrophication processes. The concept of eutrophication is defined by the European Commission in its 91/271/CEE (European Commission Directive, 1998) as “the enrichment of water by nutrients, especially compounds of nitrogen and phosphorus, causing an accelerated growth of algae and higher forms of plant life to produce an undesirable disturbance to the balance of organisms and the quality of the water concerned.” Today, eutrophication is one of the primary problems in the management of surface water (Kennish & De Jonge, 2012) and presents a serious long-term threat to health and the functioning of hydric ecosystems worldwide. Measures to stop the eutrophication of aquatic systems worldwide include reducing the use of nitrogen and phosphorus compounds, when possible, followed by decreasing concentrations of these nutrients in effluents from wastewater treatment systems through adequate treatment. Microalgae technology to eliminate N and P is a possible alternative to conventional biological technologies (Ruiz *et al.*, 2011).

The use of microalgae has practical short-term applications because it efficiently removes nutrients (nitrogen and phosphorus) and thus can play an important role in the tertiary treatment of wastewater (Arbib *et al.*, 2013). In practice, the use of a photobioreactor with microalgae has obtained nitrogen and/or phosphorus removal efficiencies of over

90% (De Pauw, Bruggeman, & Persoone, 1978; Shelef, Azov, Moraine, & Oron, 1980; Martin, Picard, & De la Noüe, 1985; Arbib *et al.*, 2013). Compared to current conventional processes, microalgae generates biomass which can be used as prime material for the production of a large variety of biological fuels, such as biogas (Brune, Lundquist, & Benemann, 2009), biodiesel (Gouveia & Oliveira, 2009) and biohydrogen (Rashid *et al.*, 2013). In addition, water from treatment system effluents is oxygenated and the greenhouse gases released into the atmosphere are reduced (Velan & Saravanane, 2013). This technology also makes it possible to recycle the nutrients as fertilizers (Dawson & Hilton, 2011), providing significant environmental and economic benefits. Nevertheless, this technology still requires considerable investigation, development and innovation to make scientific and technological progress so that it can move from the pilot stages to a commercial scale (Benemann, 2009).

La diferente bibliografía revisada en estThe different literature reviewed by this study reflects a lack of agreement about the best place to locate a microalgae photobioreactor in the flow of a wastewater treatment system. Some authors (Cabanelas *et al.*, 2013) have proposed an anaerobic process to reduce organic matter in wastewater followed by a microalgae photobioreactor to reduce nutrients. Some (Arbib *et al.*, 2013) propose the use of photobioreactors as “end-of-the-line” treatment after the secondary treatment of wastewater, and yet other authors (Liang, Sarkany, & Cui, 2009) propose the use of mixotrophic cultures of bacteria-microalgae located after primary treatment.

Kinetic models are an indispensable tool for the study of microalgae productivity.

These models not only provide a basis to design the reactor but also to improve processes by facilitating the exploration of different environmental conditions and functioning (Ruiz *et al.*, 2012). The use of the Verhulst model (Verhulst, 1838) in studies with photobioreactors has been increasing recently (Ruiz *et al.*, 2013) because of its mathematical simplicity and its simple biological definition.

The objective of the present work is to study the kinetic growth and nutrient uptake of a natural bloom of cultured microalgae in urban wastewater subject to different types of treatment. This is based on the initial hypothesis that microalgae can be cultured in urban wastewater and that the volumetric productivity of algae biomass may depend on the degree to which the water is treated (which in turn affects the nutrient content and turbidity of the medium). This study is aimed at contributing data to support the decision regarding the best location of this type of biotechnology in the flow of conventional urban wastewater treatment system.

Material and Methods

Microalgae used

As inoculate for the tests, microalgae bloom (95% dominance of *Coelastrum* sp.) from a 9.6 m³ pilot Raceway photobioreactor was used, with continuous feed of effluent from a 20 m³ pilot UASB anaerobic reactor, fed with wastewater from pretreatment effluent from the El Torno wastewater system (Chiclana de la Frontera, Cádiz; 36° 25'38.15" N, 6° 9' 23.9" W). This system is part of the infrastructure pertaining to the European Union's 7th Framework Programme, called the “ALL-gas project” (<http://www.all-gas.eu/Pages/default.aspx>).

Test Conditions

To perform the experiments, 2 000 ml capacity PYREX® borosilicate jars were used as photobioreactors with a volume of 2 l of culture medium. This was inoculated by centrifugation with enough pre-concentrated inoculate (3 000 g for 1 minute) to supply all of the experiments with a similar concentration of biomass (roughly 350 mg SS l⁻¹). The operating conditions were as follows: constant aeration of 2 l min⁻¹ (provided by a compressor with a Phoenix MKC-510V membrane); photoperiod of 14:10 hours of light:darkness; light intensity of 175 μmol m⁻² s⁻¹ (provided by two FSL T8 6W/865 fluorescent lamps) and a temperature of 24 ± 1°C. Figure 1 shows the experimental equipment.

Culture media and experimental design

Three effluent samples from the El Torno treatment plant were taken: one at a point located between pretreatment and primary treatment, one at the secondary treatment outlet and another at the UASB reactor outlet. The samples were conserved at 4° C until used.

These wastewater samples were used to prepare the four culture media used in the experiments. Each medium corresponded

to a reactor and its repetition ('). The first (Medium 1, M1 – reactor TPM1 and TPM1') was prepared after letting the water pour out from the pretreatment for 16 hours. This was done instead of using water directly from the outlet of the primary decanter since the El Torno treatment system doses the wastewater with ferric sulfate before primary treatment and the presence of this coagulant could interfere with the results of the test. The second culture medium (Medium 2, M2 – reactor TSM2 and TSM2') was prepared with water discharged from the secondary decanter. The third medium (Medium 3, M3 – reactor UASB and UASB') used water discharged from the UASB unit. Lastly, a fourth culture medium was prepared (Medium 4, M4 – reactors TSM2 + UASB and TSM2 + UASB') with a mixture of water from the UASB effluent and from the secondary decanter, in a 1:1 proportion. The UASB effluent was diluted because it could have an excess concentration of ammonium which inhibits the growth of microalgae (Wang, Wang, Chen, & Ruan, 2010).

Analytical Methods

Temperature and pH

Samples were taken daily and pH values were measured electrochemically (pH-metro GLP 32, CRISON®). Temperatures were recorded outside the culture chamber as well as inside the reactors (using an HI 98509 digital probe thermometer). In addition, the evolution of the microalgae bloom was monitored microscopically on a daily basis.

Biomass

The concentration of biomass was determined daily— indirectly using optical density (680 nm) and directly with



Figure 1. Photograph of the eight photobioreactors.

gravimetric measurements of suspended solids. For optical density measurements, the samples were diluted in the proportions needed to ensure the values measured fell within the detection range of the spectrophotometry. The standard APHA-2540 D (APHA-AWWA-WEF, 1992) method was used to measure suspended solids, and dry weight was determined using gravimetry with fiberglass filters ((GF/F CAT no. 1825-047, Whatman™).

To determine the elemental composition of the inoculate, the volume required to obtain approximately 1 g of biomass pellet was centrifuged (3 000 g for 1 minute) and dried by lyophilization. After digestion with a Speedwave® microwave system (Berghof, 2008), an elemental analysis was performed of carbon, nitrogen, hydrogen and sulfur using a CHNS-932 Leco® (Anon, 1991) analyzer. Phosphorus was analyzed with ICP-AES (EPA, 2008) atomic emission spectrometry. Each of the elements were analyzed in triplicate, except for phosphorus which was analyzed in duplicate.

Determination of COD, total nitrogen and phosphorus

Filtered samples were used to determine organic matter and nutrient contents (GF/F CAT no. 1825-047, Whatman™). The COD₅ was determined at the beginning and end of the tests using hot acid oxidation with dichromate, according to the standard method APHA-5220 D (APHA-AWWA-WEF, 1992). Nitrogen concentration in the form of nitrates (N-NO₃), ammonium (N-NH₄) and nitrites (N-NO₂) was measured at the beginning and end of the tests with colorimetry according to the methods by Muller and Weidemann (1955), APHA 4500-NH₃ D and APHA 4500-NO₂B (APHA-AWWA-WEF, 1992), respectively. The concentration of phosphorus in the form of phosphates (P-PO₄) was measured with colorimetry at the beginning and end of each

test according to the standard method APHA 4500-P-E (APHA-AWWA-WEF, 1992). Lastly, total phosphorus and nitrogen contents were measured daily with oxidation after filtration of the sample with Oxysolve® (Köthe & Bitsch, 1992), followed by an analysis of phosphates and nitrates.

Statistical Analysis

The data from the temporal evolution of biomass, nitrogen and phosphorus concentrations were used to model the kinetic growth of the biomass and nutrient uptake with Verhulst (1838) models according to Ruiz *et al.* (2013) and the *Photobiotreatment model* (PhBT) developed by Ruiz *et al.* (2012). This was based on non-linear regression techniques using *Microsoft Excel Solver* (version 7.0 Microsoft®) (Walsh & Diamond, 1995), with the non-linear GRG optimization code proposed by Ragsdell (1975), and Fallahi, Hall and Ragsdell (1981), which was later used by Mariappan and Krishnamurthy (1996) in some applications.

Results and Discussion

Physiochemical Characterization of Culture Media

Table 1 presents the main physiochemical characteristics of the culture media before beginning the experiment, that is, before inoculation with microalgae.

Evolution of pH

As seen in Figure 2, the initial average pH in the eight reactors was 7.4 ± 0.2 . After 24 hours, the pH increased markedly in all the reactors, most notably in the tests conducted in TSM2' and TSM2 + UASB', where the pH reached 10. Meanwhile, a decrease in pH was observed at the end of

Table 1. Mean characteristics of the four culture media.

Parameters	M1	M2	M3	M4
pH	7.45	7.23	7.47	7.43
Suspended solids, SS (mg l ⁻¹)	130	39	41	42
Volatile suspended solids, SSV (mg l ⁻¹)	98	35.5	39	40
N-NO ₃ (mg l ⁻¹)	1.12	15.34	0.83	8.56
N-NH ₄ (mg l ⁻¹)	21.30	4.15	18.91	13.59
N-NO ₂ (mg l ⁻¹)	0.09	1.38	0.01	0.92
Total dissolve nitrogen, N (mg l ⁻¹)	24.75	19.01	23.63	13.24
P-PO ₄ (mg l ⁻¹)	5.34	0.17	5.32	2.40
Total dissolved phosphorus, P (mg l ⁻¹)	5.02	0.23	4.80	2.43
N/P	5.0	82.65	4.9	5.5
COD _s (mg l ⁻¹)	158	104.5	170	186

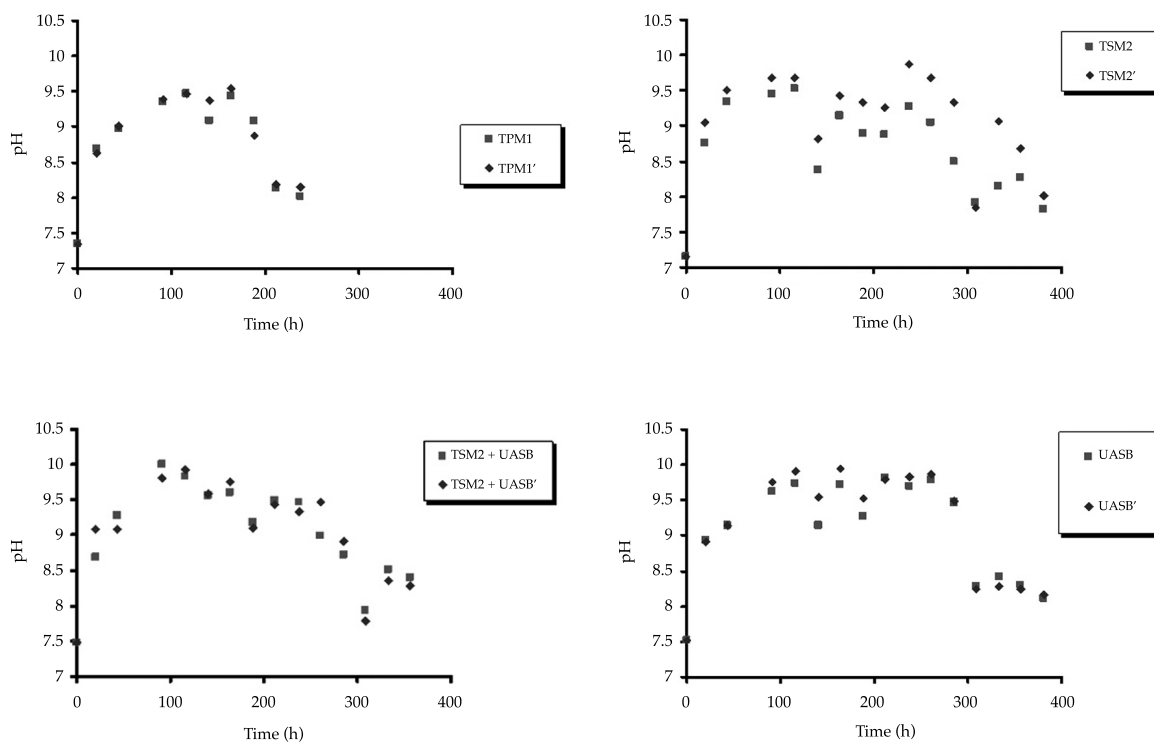
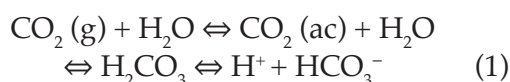


Figure 2. Evolution of pH in the different culture media.

the tests, dropping to values of around 8, which were reached after approximately 200 hours into the test in reactors TPM1 and TPM1' and after 300 hours in the rest of the reactors. The decrease in pH indicates the cessation of photosynthetic activity.

Some works, such as Tang, Han, Li, Miao and Zhong (2011), report the same behavior in pH as the experiment herein, in which the photosynthetic activity of the microalgae in a wastewater culture results in a gradual increase in pH due to the effect

on the equilibrium of carbonated species in the water. During the light phase of photosynthesis, the microalgae assimilate CO_2 . When the CO_2 dissolves in water it forms carbonic acid molecules (H_2CO_3). This acid is found in a fraction that is 10^3 times less than dissolved CO_2 (ac) since it easily disassociates in water to form H^+ protons and HCO_3^- bicarbonate ions, as shown in equation (1):



In turn, the bicarbonate ion disassociates in water to form H^+ ions and CO_3^{2-} carbonate ions (equation (2)):



Thus, when a microalgae culture is in the exponential growth phase, dissolved inorganic carbon (DIC) uptake (in the form CO_2 , H_2CO_3 , HCO_3^- or CO_3^{2-}) displaces the equilibriums, as indicated in equations (1) and (2), towards a reduction in the concentration of H^+ protons, thereby increasing the pH (Tang *et al.*, 2011). The optimal pH for most of the microalgae species is around neutral. Nevertheless, species such as *C. littorale* (Schnackenberg, Ikemoto, & Miyachi, 1996) grow most quickly in acidic conditions (pH around 4). The optimal value for other species is around 9, such as *Spirulina platensis* (Qiang, Zarmi, & Richmond, 1998).

Biomass Growth

In a batch culture, the most common growth curve for microorganisms is logistic, as obtained in several studies, including Peleg, Corradini and Normand (2007). This also occurred in our study. Figure 3 shows the evolution of microalgae bloom in the different cultures. Each curve

presents two of the four phases that are typical of batch cultures: exponential growth and the stationary phase. The adaptation phase is virtually non-existent since the inoculate was obtained from a culture containing wastewater from the same treatment systems as the medium. The test was considered to be completed once the stationary state was reached, that is, when the concentration values obtained over consecutive days were similar. As can be seen in the experimental data represented by the symbols in Figure 3, the test ended after 240 h in reactors TPM1 and TPM1', and after 400 h in the rest of the reactors.

When comparing Figures 2 and 3, we can see that the periods during which the pH remained at high levels coincided with periods during which the cultures were undergoing the exponential growth phase. In all the reactors, this period began after 100 h of testing, lasting up to 190 h in the TPM1 and TPM1' reactors and up to 270 h in UASB and UASB'. This seems to confirm the hypothesis that pH increases due to CO_2 uptake by microalgae.

To quantify the growth, the experimental data were fitted to the Verhulst logistic model (1838). The Verhulst model is a kinetic growth model based on the time it takes for microorganism generation (exponential growth phase and stationary phase). This is a non-mechanistic model which is widely used by other authors (Peleg *et al.*, 2007; Ruiz *et al.*, 2012; Ruiz *et al.*, 2013, Arbib *et al.*, 2013).

The Verhulst model (1838) is mathematically expressed as shown in equation (3):

$$\frac{\delta X(t)}{\delta t} = \mu X(t) \left[1 - \frac{X(t)}{X(m)} \right] \quad (3)$$

where $\delta X(t)/\delta t$ is the rate of change in the concentration of microorganisms, X_m is the

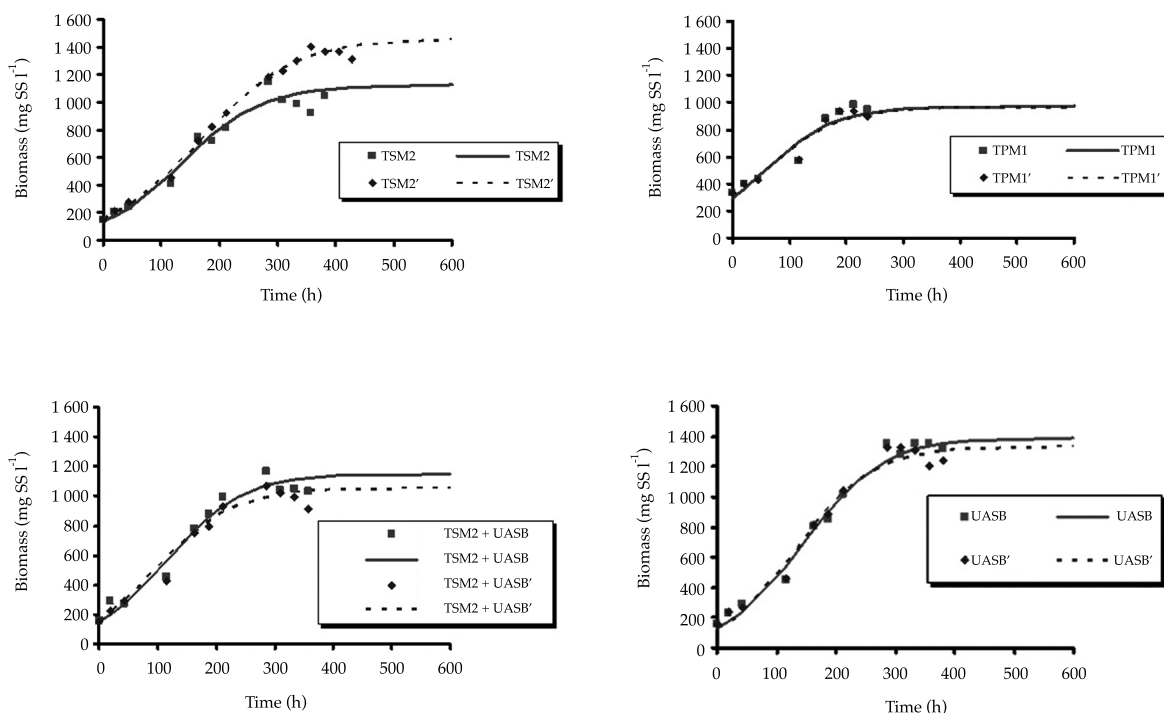


Figure 3. Evolution of biomass of microalgae bloom in the different culture media. The symbols are experimental data and lines represent predictions by the model.

maximum cell concentration that a system can reach in batch, and μ is the maximum specific growth rate.

The integrated form of the equation subject to the initial value $X_0 = X(t = 0)$ (equation (3)) was used to describe the experimental data (equation (4)):

$$X = \frac{X_0 X_m e^{\mu t}}{X_m - X_0 + X_0 e^{\mu t}} \quad (4)$$

where X is the momentary concentration of microalgae and X_0 is the initial concentration of the biomass.

The kinetic parameters obtained from the model are shown in Table 2. Figure 3 and Table 2 indicate a very good fit of the experimental data to the model (regression coefficient values R^2 over 0.9), which suggests a reliable prediction with the experimental data.

Table 2 shows very similar values of X_m , X_0 and μ among the test repetitions, except in the case of TSM2 and TSM2'. There were no differences in the experimental conditions of the reactors that would explain this difference.

The values of X_0 were between 130 and 160 mg SS l⁻¹, except in TPM1 and SPM1', where they reached nearly 300 mg SS l⁻¹. Table 1 shows that culture M1 contains roughly 130 mg SS l⁻¹, while M2, M3 and M4 have around 40. That is, the cultures in TPM1 and TPM1' have higher initial concentrations of suspended solids than the other reactors.

Furthermore, Table 2 shows that X_m varies more widely than μ , with variation coefficients of 0.16 and 0.09, respectively. The average value of μ was 0.015 h⁻¹, the same order of magnitude found by other authors. For example, Samorì, Samorì,

Table 2. Kinetic parameters of the growth of microalgae bloom using the Verhulst model.

Nomenclature	TPM1	TPM1'	TSM2	TSM2'	TSM2 + UASB	TSM2 + UASB'	UASB	UASB'
X_0 (mg SS l ⁻¹)	295.3	297.4	137.2	158.7	154.4	166.6	135.9	129
X_m (mg SS l ⁻¹)	971.6	967.4	1 126.3	1 469.3	1 150.8	1 054	1 392.5	1 332.1
μ (h ⁻¹)	0.016	0.016	0.014	0.012	0.016	0.016	0.015	0.016
R^2	0.95	0.96	0.96	0.99	0.97	0.95	0.99	0.98

Guerrini and Pistocchi (2013) obtained values of μ of 0.015 h⁻¹ for *Desmodesmus communis* using wastewater effluent from primary treatment which was ammonium rich (around 30 mg N-NH₄ l⁻¹). Some of the conditions of the cultures in that study were very similar to our tests, except for light intensity which was lower (88 $\mu\text{mol m}^{-2} \text{s}^{-1}$) and the controlled addition of CO₂ (2%). Other authors, such as Ruiz *et al.* (2012), obtained μ values around 0.035 h⁻¹ for *Chlorella vulgaris* in wastewater, while when using an ammonium rich synthetic medium a μ value of 0.06 h⁻¹ was obtained. In the review by Griffiths and Harrison (2009), growth rate data were collected for 55 microalgae species, including *Chlorophytas*, cyanobacteria and other taxons. They obtained μ values between 0.028 h⁻¹ and 0.04 h⁻¹, in a wide range of reactor configurations, designs and scales and under diverse nutrient supply conditions.

The values obtained for X_m were between 967 and 1 469 mg SS l⁻¹ (Table 2). Other authors, such as Ruiz *et al.* (2012), obtained results between 700 and 1 300 mg SS l⁻¹ in experiments with *Chlorella vulgaris* in wastewater. Tang *et al.* (2011) obtained X_m values between 700 and 1 800 mg SS l⁻¹ with *Scenedesmus obliquus* and *Chlorella pyrenoidosa* when experimenting with different cultures and applying different CO₂ doses. Meanwhile, Patel, Barrington and Lefsrud (2012) obtained results between 200 and 600 mg SS l⁻¹

when experimenting with synthetic cultures and different initial phosphorous concentrations in both freshwater species (*Chlorella* sp., *Monoraphidium minutum* sp., and *Scenedesmus* sp.) and sea species (*Nannochloropsis* sp., *N. limnetica* sp. and *Tetraselmis suecica* sp.). If we compare the mean values of X_m among the repetitions in our study, the lowest is 969.5 mg SS l⁻¹, corresponding to reactor TPM1, followed by TSM2 + UASB (1 102 mg SS l⁻¹). The UASB reactor had the highest biomass concentration, with a mean value among repetitions of 1 362.3 mg SS l⁻¹.

Temperature (T^{a}) is one of the factors that has been found to influence the growth of a microalgae culture, as shown by Shelef, Moraine and Oron (1978), Heussler (1985) and Talbot, Thébault, Dauta and De la Noüe (1991). Nevertheless we discard this factor given that T^{a} was kept constant throughout the tests. Light intensity is another factor (Talbot *et al.*, 1991; Barbosa, Hoogakker, & Wijffels, 2003), which we can also discard because all the experiments were run with the same light intensity. Another influential factor could be that the available light for the microalgae depends on the light path. This was the same in all reactors since they had the same diameter. Lastly, the turbidity of the culture could affect the growth. For instance, data from the suspended solid contents in cultures (Table 1) suggest that the turbidity of the media could be a determinant of the maximum growth of the batch microalgae

cultures. To prove this, the correlation between suspended solids concentrations at the beginning of the tests (experimental data) and the X_m values (Table 2) were evaluated for all the reactors, resulting in a correlation probability of around 95% ($r = -0.69$, $p < 0.06$). Likewise, the correlation between X_0 and X_m parameters were also evaluated (both calculated by the Verhulst model), finding a significant and inverse correlation ($r = -0.71$, $p < 0.05$). Therefore it is possible to state that a correlation exists between the turbidity of the culture in the reactors and the maximum batch concentration.

Another influential factor is the presence of nutrients such as phosphorus and nitrogen. Both nutrients are needed for most growth scenarios because of a strong and direct correlation between nutrient concentrations and kinetic growth parameters. As with X_0 , possible correlations between initial total nitrogen and phosphorus concentrations with X_m were studied (experimental data), and no significant correlations were found with nitrogen ($r = -0.19$, $p < 0.66$) or with phosphorus ($r = -0.15$, $p < 0.73$). The presence of trace elements is another factor that can limit growth and affect X_m (Hecky & Kilham, 1988), but since wastewater is a much more complex matrix than synthetic cultures, we conclude that all the micronutrient concentrations in all the cultures were low enough that they did not limit growth.

In order to compare the different reactors used in our tests based on a single parameter, batch productivity was calculated. According to Ruiz *et al.* (2012), the kinetic parameters from the Verhulst growth model during the exponential growth phase can be used to calculate the batch productivity (P) of the reactors. This is defined as the time between the moment at which a biomass concentration of 10%

over the initial concentration is reached and the time it takes to reach 90% of the maximum biomass concentration in the reactor (equation (5)):

$$P = \frac{\mu(0.9X_m - X_0)}{\ln\left(\frac{9(X_m - 1.1X_0)}{1.1X_0}\right)} \quad (5)$$

where P is the volumetric productivity of the biomass.

Figure 4 shows the mean values of P for the repetitions (*). We can see that the lowest mean value occurred in the TPM1* reactor ($0.071 \text{ g SS l}^{-1} \text{ d}^{-1}$) and the highest in the UASB* ($0.094 \text{ g SS l}^{-1} \text{ d}^{-1}$). We can also graphically see that reactors TPM1*, TSM2* and TSM2 + UASB* all have similar productivities, around $0.077 \text{ g SS l}^{-1} \text{ d}^{-1}$, while the productivity in UASB* is 10% higher than all the others.

Other authors, such as Ruiz *et al.* (2012), obtained productivity values of $0.01 \text{ g SS l}^{-1} \text{ d}^{-1}$ for *Chlorella vulgaris* in wastewater and $0.15 \text{ g SS l}^{-1} \text{ d}^{-1}$ in wastewater enriched with nitrogen, phosphorus and micronutrients. This difference in productivity with respect to the values obtained by our study could be due to injection of combustion gases in the

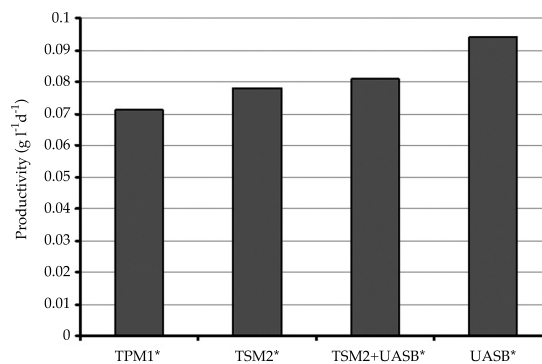


Figure 4. Representation of biomass productivity means ($\text{g SS l}^{-1} \text{ d}^{-1}$), according to the culture medium in the different reactors.

Ruiz *et al.* (2012) study, at a proportion of 5% CO₂ to ensure the availability of dissolved carbon. In addition, the microalgae grew with an irradiance 40% higher than that used in our study. In other works, such as Samorì *et al.* (2013), productivities similar to those found by our study were obtained, the lowest of which was 0.018 g SS l⁻¹ d⁻¹ in a *Desmodesmus communis* culture from primary effluent, with an irradiance of 88 μmol m⁻²s⁻¹, while the highest was 0.227 g SS l⁻¹ d⁻¹ but with a high irradiance (440 μmol m⁻²s⁻¹) and an ammoniacal nitrogen content over 80 mg N-NH₄ l⁻¹. In this case, the addition of 2% of CO₂ and the different light intensities used can explain the differences in productivity values. Other authors, such as Cabanelas *et al.* (2013), worked with *Chlorella vulgaris* cultured in effluents from different treatment processes and with an irradiance similar to the one used in our study, without adding CO₂. This work also obtained productivities similar to ours, where the lowest value was 0.039 g SS l⁻¹ d⁻¹ in the effluent from the primary decanter, which contained an initial suspended solids concentration of 300 mg l⁻¹, and the highest was 0.195 g SS l⁻¹ d⁻¹ in an effluent with 140 mg l⁻¹ initial suspended solids, 125 mg l⁻¹ ammonia nitrogen and around 60 mg l⁻¹ total phosphorus concentration.

Nutrient Removal

Nutrient removal in microalgae culture in wastewater and synthetic media is directly and indirectly due to the activity of microalgae (Ruiz *et al.*, 2012). It occurs directly through the assimilation of nutrients by cells for use in the metabolic processes. Indirectly, nutrients are removed by abiotic processes, such as an increase in pH over 9 as a consequence of the metabolizing of CO₂ by microalgae. If we compare Figure 3 with Figures 5 and 6, we can see that the

periods during which the algal biomass grew exponentially coincided with periods with greater nutrient removal. This seems to confirm that biological processes associated with microalgae play an important role in nutrient removal.

Nitrogen

Figure 5 shows the removal curve for total dissolved nitrogen for the different culture media. The experimental data represented by symbols show a reduction in the concentrations of these nutrients in all reactors over the course of the test.

As seen in Figure 5, the experimental data show a reduction in total dissolved nitrogen to under 10 ppm in all the reactors due to the rapid assimilation of the algae 3 to 5 days after the culture was prepared. In addition, with a very similar initial concentration in all the reactors (29 ± 1 mg N l⁻¹) the mean removal percentage for the repetitions was 74% for reactors TSM2, TSM2 + UASB and UASB, while TPM1 had a percentage of 81%. Since the slope of the removal of N in TPM1 and TPM1' is steeper and the highest removal percentages also occurred in these reactors, this suggests that N removal did not occur as a result of assimilation but rather because of volatilization, and the cessation of growth may have been caused by other factors, such as a higher initial concentration of suspended solids in these reactors, with a lower X_{max} and a higher increase in pH.

To quantify nutrient removal, the experimental data were fitted to the PhBT (*Photobiotreatment*) model (Ruiz *et al.*, 2012). This is a simple and useful tool to describe nutrient removal experiments in batch with microalgae. The model has been experimentally validated with *Chlorella vulgaris* culture in wastewater and in different synthetic cultures (Ruiz *et al.*, 2012).

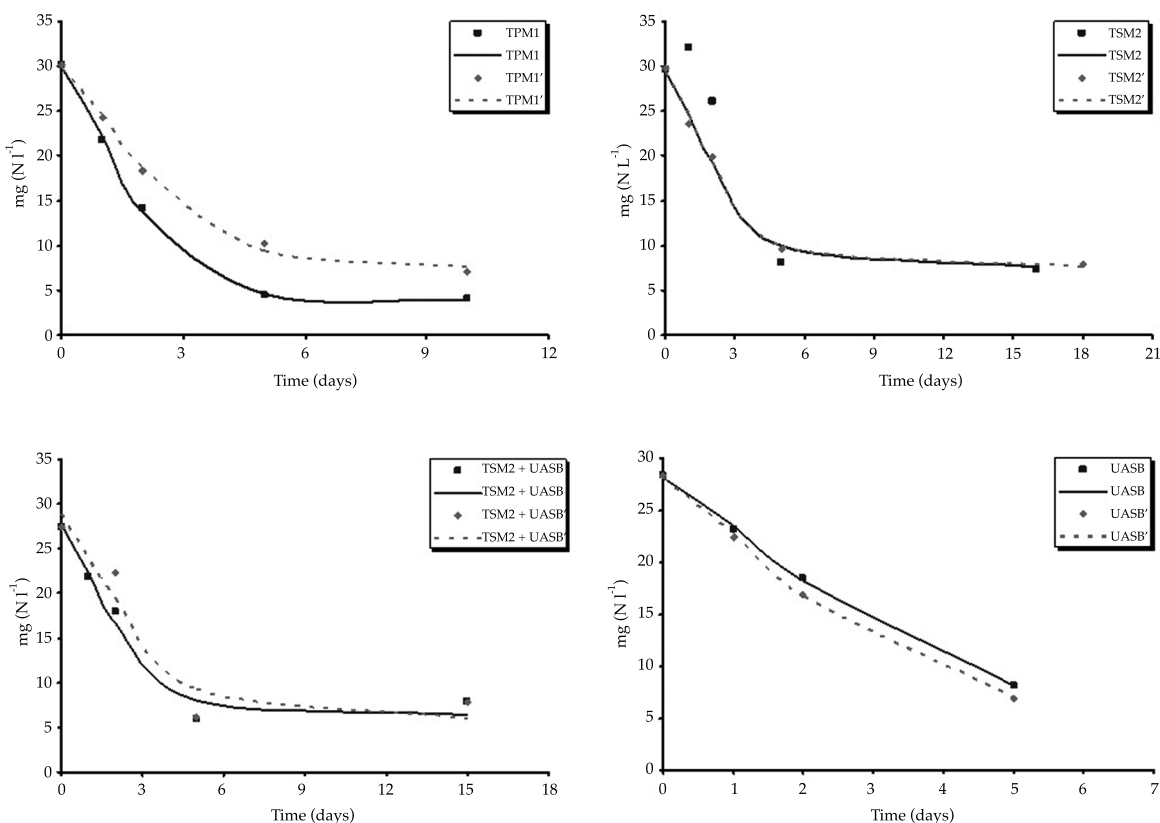


Figure 5. Total dissolved nitrogen removal with different culture media using microalgae bloom. The symbols represent experimental data and lines represent the nutrient concentrations predicted by the model.

Equation (6) expresses the kinetics of the substrate uptake by microorganisms (Quiroga, Perales, Romero, & Sales, 1999):

$$\frac{-\delta S}{\delta t} = kY \left[-S^2 + (S_{T0} + S_{na})S - S_{T0}S_{na} \right] \quad (6)$$

where $\delta S(t)/\delta t$ is the speed of substrate assimilation; k is the kinetic constant; Y is the ratio of the amount of biomass produced to the amount of substrate consumed; S_{T0} is the total initial amount of the substrate (dissolved nutrients in the culture medium along with nutrients present in the inoculate) and S_{na} is the concentration of the unassimilated substrate.

When integrating the above equation, considering that $(A_0/Y) + S_0 = S_{TV}$ the mathematical expression of the PhBT can be described as:

$$S = \frac{\left(\frac{A_0}{Y} + S_0\right)(S_0 - S_{na}) - S_{na}\left(S_0 - \left(\frac{A_0}{Y} + S_0\right)\right)e^{kt}}{(S_0 - S_{na}) - \left(S_0 - \left(\frac{A_0}{Y} + S_0\right)\right)e^{kt}} \quad (7)$$

where S_0 is the initial amount of the culture substrate; A_0 is the amount of the initial biomass and $1/Y_0$ is the content of the inoculate in the substrate, therefore A_0/Y is the amount of the substrate incorporated in the inoculate.

To quantify nitrogen removal, the experimental data corresponding to nutrient concentrations were used for S . The value of $1/Y_0$ was obtained by analyzing the composition of the inoculate, which resulted in a nitrogen content of 6.2% ($0.062 \text{ mg N mg}^{-1} \text{ SS}^{-1}$). The value of A_0 was calculated according to the difference between the concentration of suspended solids when beginning the experiment and the concentration in the culture medium before inoculation. Thus, two values were obtained (Table 3), one based on experimental values ($A_{0\text{exp}}$) and the other on the values predicted by the Verhulst model, $X_0(A_{0V})$.

Table 3 shows initial biomass values $A_{0\text{exp}}$ between 113 and 198 mg l^{-1} in TSM2 and TPM1, respectively, with a mean of the reactors of 136.5 mg l^{-1} . The values of A_{0V} were between 88 and 167.4 mg l^{-1} in reactors UASB' and TPM1', respectively, with a mean of 121.8 mg l^{-1} . As seen in Table 4, the values of the kinetic parameters are very similar, regardless of the value of A_0 used. In addition, the middle value of the means of $A_{0\text{exp}}$ and A_{0V} for the different reactors was chosen (129.2 mg l^{-1}), which along with $1/Y_0$ defines the now fixed factor S_{T0} without affecting the modeling. In addition, when applying the model we had one less fit parameter (S_{T0}) which simplifies the calculation and results in a better fit for the rest of the parameters. In fact, the fit was very good, as can be seen in Figure 5, with a determination coefficient over 92% for all the experiments (Table 5). In addition, all the kinetic parameters are

physically significant (Table 5).

We can see from Table 5 that at the end of testing none of the values of S_{na} in any of the reactors exceeded the limits (10-15 ppm) established by European norms for treatment material in urban wastewater (Directiva 98/15/CEE). The lowest value was 3.92 mg N l^{-1} , in reactor TPM1, and the highest was 7.65 mg N l^{-1} , in TSM2'. Reduction percentages of around 80% were obtained with all the cultures. Ruiz et al. (2012) obtained removal efficiencies of 100% in *Chlorella vulgaris* cultures, with unassimilated substrate (S_{na}) concentrations below detection limits in all their experiments, except for synthetic culture rich in ammoniacal nitrogen, in which the inhibition of pH stops nutrient uptake, resulting in a higher value ($14.9 \pm 1.1 \text{ mg N l}^{-1}$) and in a reduction percentage of only 50%. In conditions very similar to ours, other authors, such as Ruiz-Marin, Mendoza-Espinosa and Stephenson (2010), have obtained nitrogen removal efficiencies between 80 and 100% using *Scenedesmus obliquus*, with initial concentrations of 27 mg N l^{-1} .

In order to compare the nutrient removal obtained in the different reactors in our study based on a single parameter, the kinetic parameters of the PhBT model were used to calculate the speed of nutrient uptake ($-dS/dt$), for which the following equation is used:

$$-\frac{dS}{dt} = \frac{\Delta S}{\Delta t} = \frac{S_{90} - S_f}{t_{90} - t_f} \quad (8)$$

Table 3. Initial biomass values calculated based on experimental data ($A_{0\text{exp}}$) and those obtained by the Verhulst model (A_{0V}), and mean values for each series.

Nomenclature	TPM1	TPM1'	TSM2	TSM2'	TSM2 + UASB	TSM2 + UASB'	UASB	UASB'	Media
$A_{0\text{exp}}$ (mg l^{-1})	198	198	113	113	118	118	117	117	136.5
A_{0V} (mg l^{-1})	165.3	167.4	98.2	119.7	114.4	126.6	94.9	88	121.8

Table 4. Kinetic parameters with the PhBT model, according to the A_0 value used.

Nomenclature	TPM1		TPM1'		TSM2		TSM2'		TSM2 + UASB		TSM2 + UASB'		UASB		UASB'	
	A_{0exp}	A_{0V}	A_{0exp}	A_{0V}	A_{0exp}	A_{0V}	A_{0exp}	A_{0V}	A_{0exp}	A_{0V}	A_{0exp}	A_{0V}	A_{0exp}	A_{0V}	A_{0exp}	A_{0V}
S_{70} (mg N l ⁻¹)	42.8	40.9	42.8	40.9	56.1	55.2	37.2	37.6	35.7	35.5	36.0	36.8	35.6	34.2	35.63	33.8
S_0 (mg N l ⁻¹)	30.6	30.6	30.5	30.5	49.1	49.1	30.2	30.2	28.4	28.4	28.7	28.7	28.3	28.3	28.4	28.4
S_{min} (mg N l ⁻¹)	2.8	2.8	5.9	5.9	6.2	6.2	7.1	7.1	6.2	6.2	5.9	5.9	-14.5	-14.4	-7.3	-7.3
μ (h ⁻¹)	0.018	0.018	0.014	0.014	0.019	0.019	0.014	0.014	0.016	0.016	0.013	0.013	0.005	0.005	0.008	0.008

where t_{90} is the time it takes from the beginning of the test to the moment at which 10% substrate removal is reached ($S_{90} = 0.9 \cdot S_0$) (to avoid the differences in latency periods), while t_f is the time it takes to reach 10% of the minimum substrate concentration in the reactor ($S_f = 1.1 \cdot S_{na}$). Table 5 shows a similar nitrogen uptake speed ($-dN/dt$) for all the reactors. The uptake was slower in reactor TSM2 + UASB' (2.82 mg N l⁻¹ d⁻¹) and faster in reactor TPM1 (4.49 mg N l⁻¹ d⁻¹). When taking into account the mean values of the repetitions, nitrogen uptake, from slower to faster, was: TSM2 + UASB (3.04 mg N l⁻¹ d⁻¹), which was very similar to TSM2 (3.05 mg N l⁻¹ d⁻¹) and to UASB (3.06 mg N l⁻¹ d⁻¹); and lastly, TPM1 (3.96 mg N l⁻¹ d⁻¹), where nitrogen uptake was fastest. This suggests the largest amount of nitrogen will be removed in a batch microalgae culture, in a culture medium such as that used in reactor TPM1 with a particular volume and time, with a difference of 20 to 30% compared to the other cultures studied.

Phosphorus

Figure 6 shows the removal curve for total dissolved phosphorus for the different culture media. As can be seen, the initial total dissolved phosphorus concentration was not the same for each reactor, except for reactors TPM1 and UASB, and their repetitions, which were very similar (roughly 4 mg P l⁻¹). A rapid uptake of phosphorus was also seen over the first two days, which is directly related to the increase in biomass. Over 60% of the phosphorus was removed after 20 to 30 h, except in reactors UASB and UASB', where this percentage was not reached until 50 h.

To quantify the removal of total dissolved phosphorus, the same analytical process used for nitrogen was applied. Therefore, the

Table 5. Kinetic parameters for nitrogen removal using microalgae bloom with the PhBT model and speed of nitrogen uptake using mean A_0 .

Nomenclature	TPM1	TPM1'	TSM2	TSM2'	TSM2 + UASB	TSM2 + UASB'	UASB	UASB'
S_0 (mg N l ⁻¹)	29.89	29.81	33.51	29.32	27.66	28.9	28.12	28.14
S_{na} (mg N l ⁻¹)	3.92	7.63	5.87	7.65	6.46	6.05	5.23	5.02
μ_N (h ⁻¹)	0.043	0.033	0.026	0.03	0.033	0.028	0.029	0.033
R^2	0.999	0.997	0.928	0.996	0.975	0.929	0.999	0.999
$-dN/dt$ (mg N l ⁻¹ d ⁻¹)	4.49	3.43	3.01	3.1	3.27	2.82	2.86	3.27

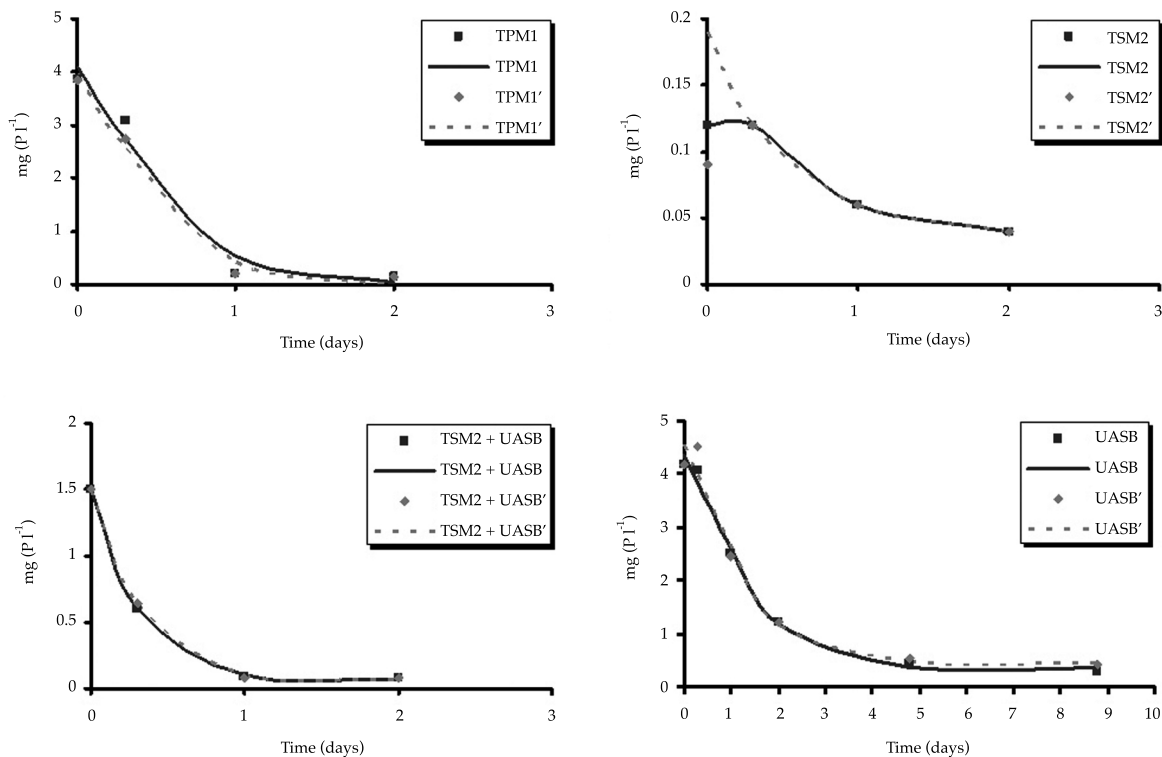


Figure 6. Total dissolved phosphorus removal in the different culture media using microalgae bloom. Symbols are experimental data and lines represent nutrient concentrations predicted by the kinetic model.

experimental data were also fit to the PhBT model, but with a variation in the amount of substrate incorporated in the inoculate (A_0/Y) from equation (7) which, in this case, is determined by the phosphorus content in the inoculate biomass ($1/Y_0 = = 0.0097$ mg P mg⁻¹ SS⁻¹). Table 6 shows the kinetic parameters calculated for phosphorus removal for all the tests, including the data obtained from cases

TSM2 and TSM2', which were difficult to fit to the PhBT model since the phosphorus concentration was not precisely detected. This was due to a low initial concentration of the culture medium used in these reactors (0.04-0.12 mg P l⁻¹).

Table 6 shows that none of the values of S_{na} corresponding to any of the reactors exceeded the limits for total dissolved phosphorus (1

Table 6. Kinetic parameters for phosphorous removal using microalgae bloom with the PhBT model and speed of phosphorus uptake using the mean of A_0 .

Nomenclature	TPM1	TPM1'	TSM2	TSM2'	TSM2 + UASB	TSM2 + UASB'	UASB	UASB'
S_0 (mg P l ⁻¹)	4.09	3.96	0.19	0.19	1.5	1.5	4.34	4.54
S_{na} (mg P l ⁻¹)	0.02	0.02	0.04	0.04	0.07	0.06	0.35	0.46
μ_p (h ⁻¹)	0.142	0.149	0.082	0.082	0.193	0.181	0.059	0.064
R ²	0.974	0.989	0.999	0.999	0.999	0.999	0.990	0.970
-dP/dt (mg P l ⁻¹ d ⁻¹)	1.04	1.08	0.06	0.06	0.98	0.91	0.86	0.99

ppm) established by Directive 98/15/CEE (European Commission Directive, 1998). The lowest value was 0.02 mg P l⁻¹, in reactors TPM1 and TPM1', and the highest was 0.46 mg P l⁻¹, in UASB'. The reduction percentages were over 80% in all cases, reaching 100% removal of phosphorus in reactors TPM1 and TPM1'. Ruiz *et al.* (2012) obtained removal efficiencies over 80% in *Chlorella vulgaris* cultures using different culture media with wastewater and synthetic media, except in the case of synthetic medium rich in ammoniacal nitrogen, where the inhibition of pH stops nutrient uptake and the reduction percentage is 50%. Other authors, such as Ruiz-Marín *et al.* (2010) obtained phosphorus removal efficiencies between 50 to 100% with *Scenedesmus obliquus* and an initial concentration of 12 mg P l⁻¹, in conditions very similar to our study.

Table 5 shows the values for the maximum specific phosphorus removal rate, μ_p , which are generally higher than the nitrogen values. This suggests that phosphorus absorption is higher than nitrogen, in proportion to the biomass demand (Ruiz *et al.*, 2012). Considering the mean of the repetitions, μ_p is 95% greater in reactor TSM2 + UASB than in UASB and 25% greater than in TPM1.

As was done with nitrogen, to compare the reactors using a single parameter, the phosphorus uptake speed ($-dP/dt$) was calculated. Table 6 shows this to have values between 0.86 and 1.08 mg P l⁻¹ d⁻¹ in reactors UASB and TPM1', respectively. The mean value of the repetitions (TPM1 (1.06 mg P l⁻¹

d⁻¹), TSM2 + UASB (0.94 mg P l⁻¹ d⁻¹), UASB (0.92 mg P l⁻¹ d⁻¹)) shows that the phosphorus uptake is 10% faster in medium M1 than in media M3 and M4 and 100% faster than in M2. This phosphorous uptake is much slower than the nitrogen uptake, roughly 3 times slower, with a ratio of 3:1 nitrogen uptake speed to phosphorus, respectively. This ratio is very similar to that obtained with the samples of water used in this test, with a N:P ration of 5:1 for media M1 and M3, and 2:1 for medium M4 (Table 1); while M2 had a ratio of 82:1 because of the low initial phosphorus concentration in this culture.

Evaluation of the Importance of Abiotic Processes in Dissolved Nitrogen and Phosphorus Removal with the Culture Media Studied

Considering that the pH reached values over 8 during the test (Figure 2), abiotic processes such as the stripping of ammonium (Trussel, 1972) or precipitation of phosphates (Larsdotter, Jansen, & Dalhammar, 2007) may have occurred, in addition to biological assimilation of nitrogen and phosphorus by microalgae.

To evaluate the amount of nitrogen removal caused by stripping, the theoretical nitrogen content ($N_{\text{theoretical}}$) in the final biomass was calculated for the 8 reactors (Table 7) based on the following equation and using the kinetic parameters in Table 2 (X_0 , X_m) and Table 5 (S_0 , S_{na}):

$$N_{\text{teórico}} = \frac{1}{Y_m} = \frac{S_0 - S_{na}}{X_m - X_0} \quad (9)$$

This value can be used to calculate the nitrogen removed by stripping ($N_{\text{stripping}}$) through the following balance of matter:

$$N_{\text{stripping}} = (N_{d,t=0} + N_{p,t=0}) - (N_{d,t=m} + N_{p,t=m}) \quad (10)$$

where $N_{d,t=0}$ is the initial dissolved nitrogen or S_0 ; $N_{p,t=0}$ is the initial particulate nitrogen or X_0/Y_0 ; $N_{d,t=m}$ is the final dissolved nitrogen or S_{na} , and $N_{p,t=m}$ is the final particulate nitrogen or X_m/Y_m . The percentage of this nutrient lost by stripping is $\%N_{\text{stripping}} = N_{\text{stripping}} / (S_0 + (X_0/Y_0))$. According to the calculations, it can be stated that 11 to 18% of nitrogen is removed by stripping (Table 7).

In the case of phosphorus, and considering that this component does not have an aerial phase, Table 7 shows the calculations of the phosphorus content in the biomass at the end of the test ($P_{\text{theoretical}}$) for each reactor according to equation (9). This was determined previously for nitrogen but using the kinetic parameters in Table 2 (X_0, X_m) and Table 6 (S_0, S_m). The results obtained show that $P_{\text{theoretical}}$ falls between the

values 0.1 and 0.6% (Table 7), which are typical values for this nutrient in microalgae (Kaplan, Richmond, Dubinsky, & Aaronson, 1986). Therefore, it can be stated that it is plausible that the amount of removal by the precipitation of phosphorus was not highly significant.

Conclusions

Microalgae can be cultured in urban wastewater using several treatment levels.

Wastewater from a UASB effluent is the culture medium with the highest volumetric productivity of biomass, when using microalgae bloom under controlled laboratory conditions.

For all the wastewater studied, nitrogen and phosphorus removal by microalgae resulted in concentration levels below the discharge limits established by Directiva 98/15/CEE for urban wastewater treatment stations.

Nutrient uptake speed did not differ greatly among the different culture media tested.

Kinetic models such as the Verhulst and PhBT models with experimental data are reliable prediction tools.

Abiotic N and P removal processes contributed no more than XX and XX%, respectively, to the removal of these

Table 7. Parameters for nitrogen and phosphorus contents to evaluate nutrient removal by abiotic processes.

Nomenclature	TPM1	TPM1'	TSM2	TSM2'	TSM2 + UASB	TSM2 + UASB'	UASB	UASB'
$N_{d,t=0}$ (mg l ⁻¹)	29.89	29.81	33.51	29.32	27.66	28.9	28.12	28.14
$N_{p,t=0}$ (mg l ⁻¹)	18.29	18.41	8.49	9.79	9.54	10.29	8.34	7.99
$N_{d,t=m}$ (mg l ⁻¹)	3.92	7.63	5.87	7.65	6.46	6.05	5.23	5.02
$N_{p,t=m}$ (mg l ⁻¹)	37.31	32.03	31.47	24.29	24.49	27.14	25.37	25.60
$N_{\text{theoretical}}$ (mg l ⁻¹)	0.04	0.03	0.03	0.02	0.02	0.03	0.02	0.02
$N_{\text{stripping}}$ (mg l ⁻¹)	6.97	8.59	4.67	7.22	6.29	6.04	5.95	5.52
$\%N_{\text{stripping}}$ (%)	14.46	17.81	11.12	18.43	16.89	15.40	16.28	15.27
$P_{d,t=0}$ (mg l ⁻¹)	4.09	3.96	0.19	0.19	1.5	1.5	4.34	4.54
$P_{d,t=m}$ (mg l ⁻¹)	0.02	0.02	0.04	0.04	0.07	0.06	0.35	0.46
$P_{\text{theoretical}}$ (%)	0.60	0.59	0.02	0.01	0.14	0.16	0.32	0.34

nutrients in all the tests, and biological assimilation was the process that contributed the most to removal.

The results obtained indicate several options for where to place microalgae biotechnology in the flow diagram of a conventional urban wastewater treatment system, for the removal of nitrogen and phosphorus. Nevertheless, the results from the volumetric productivity of biomass indicate that the best option would be to use microalgae photobioreactors in tertiary treatment, after the process to remove organic matter with a UASB anaerobic reactor.

References

- Anonymous (1991). CHN-900/CHNS-932 *Elemental Analysers for Carbon, Hydrogen, Nitrogen, Sulfur and Oxygen*. Available at: <http://richmondscientific.com/manuals/tm262manual.pdf>.
- Anonymous (2008). *Berghof Application Report: Speedwave Four Microwave Pressure Digestion, Food, Pharma, Cosmetics*. Germany. Available at: http://www.berghof.com/fileadmin/Dateien-Einpflege/Seitenbaum/Home-Downloads/Produkte/Laborgeraete/Aufschlusstechnik/speedwave four/Berghof_Laborgeraete_PR_Mikrowellendruckaufschluss_SpeedwaveFour_EN.pdf.
- APHA-AWWA-WEF (1992). *Standard Methods for the Examination of Water and Wastewater* (1). Available at: <http://www.umass.edu/tei/mwwp/acrobat/sm9010-40intro.PDF>.
- Arbib, Z., Ruiz, J., Álvarez-Díaz, P., Garrido-Pérez, C., Barragan, J., & Perales, J. A. (2013). Long Term Outdoor Operation of a Tubular Airlift Pilot Photobioreactor and a High Rate Algal Pond as Tertiary Treatment of Urban Wastewater. *Ecological Engineering*, 52, 143-153. Accessed October 28, 2013. Available at: <http://linkinghub.elsevier.com/retrieve/pii/S092585741200451X>.
- Barbosa, M. J., Hoogakker, J., & Wijffels, R. H. (2003). Optimisation of Cultivation Parameters in Photobioreactors for Microalgae Cultivation Using the A-Stat Technique. *Biomolecular Engineering*, 20(4-6), 115-123. Accessed October 24, 2013. Available at: <http://linkinghub.elsevier.com/retrieve/pii/S1389-034403000339>
- Benemann, J. R. (2009). *Microalgal Biofuels: A Brief Introduction*. Available at: <http://advancedbiofuelsusa.info/wp-content/uploads/2009/03/microalgae-biofuels-an-intro-duction-july23-2009-benemann.pdf>.
- Brune, D. E. J., Lundquist, T., & Benemann, J. R. (2009). *Microalgal Biomass for Greenhouse Gas Reductions; Potential for Replacement of Fossil-Fuels and Animal Feeds*, Available at: http://digitalcommons.calpoly.edu/cgi/viewcontent.cgi?article=1171&context=cenv_fac.
- Cabanelas, I. T. D., Ruiz, J., Arbib, Z., Alexandre Chinalia, F., Garrido Pérez, C., Rogalla, F., Andrade Nascimento, I., & Perales, J. A. (2013). Comparing the Use of Different Domestic Wastewaters for Coupling Microalgal Production and nutrient Removal. *Bioresource Technology* 131, 429-436.
- Dawson, C. J., & Hilton, J. (2011). Fertiliser Availability in a Resource-Limited World: Production and Recycling of Nitrogen and Phosphorus. *Food Policy*, 36, S14-S22. Accessed November 9, 2013. Available at: <http://linkinghub.elsevier.com/retrieve/pii/S0306-919210001260>.
- De Pauw, N., Bruggeman, E., & Persoone, G. (1978). Research on the Tertiary Treatment of Swine Manure by Mass Culturing of Algae. *Mitt. Internat. Verin. Limnol*, 21, 490-506.
- EPA (2008). *EPA Method 6010c (2000): Inductively coupled plasma-atomic emission spectrometry*. Washington, DC: E. and A. D. (4304) Office of Science and Technology.
- European Commission Directive (1998). Amending Council Directive 91/271/EEC with Respect to Certain Requirements Established in Annex I. *Official Journal of the European Communities*, 98/15/EC, 29-30.
- Fallahi, B., Hall, A. S., & Ragsdell, K. M. (1981). Application of the Generalized Reduced Gradient Method to Selected Mechanisms Synthesis Problems (49-56 pp.). In *International Conference on Software Engineering*. San Diego, California, USA.
- Gouveia, L., & Oliveira, A. C. (2009). Microalgae as a Raw Material for Biofuels Production. *J. Ind. Microbiol. Biot.*, 36(2), 269-274.
- Gray, N. F. (1989). *Biology of Wastewater Treatment*. Oxford: Oxford University Press.
- Griffiths, M. J., & Harrison, S.T.L. (2009). Lipid Productivity as a Key Characteristic for Choosing Algal Species for Biodiesel Production. *Journal of Applied Phycology*, 21(5), 493-507. Accessed October 19, 2013. Available at: <http://link.springer.com/10.1007/s10811-008-9392-7>.
- Hecky, R. E., & Kilham, P. (1988). Nutrient Limitation of Phytoplankton in Freshwater and Marine Environments: A Review of Recent Evidence on the Effects of Enrichment. *Limnology and Oceanography*, 33, 796-822.
- Heussler, P. (1985). Development and Results of Peruvian-German Microalgae Project. *Ergebn. Limnol.*, 20, 1-8.
- Kaplan, D., Richmond, A. E., Dubinsky, Z., & Aaronson, S. (1986). Algal Nutrition. In *Crc Handbook of Microalgal Mass Culture, Richmond*. Boca Raton: CRC Press.

- Kennish, M. J., & De Jonge, V. N. (2012). Chemical Introductions to the Systems Diffuse and Nonpoint Source Pollution from Chemicals Nutrients Eutrophication (p. 315). In E. McLusky, & D. Wolanski (Eds.). *Treatise on Estuarine and Coastal Science Human-induced Problems (Uses and Abuses)*. Oxford: Elsevier.
- Köthe, J., & Bitsch, R. (1992). Oxysolv® Plus Microwave – A New Way for Sample Preparation. *Fresenius' Journal of Analytical Chemistry*, 343(9-10), 717-718.
- Larsdotter, K., Jansen, J. L. C., & Dalhammar, G. (2007). Biologically Mediated Phosphorus Precipitation in Wastewater Treatment with Microalgae. *Environ. Technol.*, 28(9), 953-960.
- Liang, Y. N., Sarkany, N., & Cui, Y. (2009). Biomass and Lipid Productivities of *Chlorella vulgaris* under Autotrophic, Heterotrophic and Mixotrophic Growth Conditions. *Biotechnol Lett.*, 31(7), 1043e9.
- Mariappan, J., & Krishnamurthy, S. (1996). A Generalized Exact Gradient Method for Mechanism Synthesis. *Mechanism and Machine Theory*, 31(4), 413-421.
- Martin, C., Picard, G., & De la Noüe, J. (1985). Epuration Biologique du Lisier de Porc par Production de Biomasses D'algues Unicellulaires. *Mircen J. Appl. Microbiol. Biotechnol.*, 11, 173-184.
- Müller, R., & Weidemann, F. (1955). Die Bestimmung des Nitrats in Wasser. *Jahrb. Wasserchem. Wasserreinigungstechnik*. Verlag Chemie 12, 247-271.
- Patel, A., Barrington, S., & Lefsrud, M. (2012). Microalgae for Phosphorus Removal and Biomass Production: A Six Species Screen for Dual-Purpose Organisms. *GCB Bioenergy*, 4(5), 485-495. Accessed October 28, 2013. Available at: <http://doi.wiley.com/10.1111/j.1757-1707.2012.01159.x>.
- Peleg, M., Corradini, M. G., & Normand, M. D. (2007). The Logistic (Verhulst) Model for Sigmoid Microbial Growth Curves Revisited. *Food Research International*, 40, 808-818.
- Qiang, H., Zarmi, Y., & Richmond, A. (1998). Combined Effects of Light Intensity, Light-Path and Culture Density on Output Rate of *Spirulina Platensis* (Cyanobacteria). *European Journal of Phycology*, 33, 165-171.
- Quiroga, J. M., Perales, J. A., Romero, L. I., & Sales, D. (1999). Biodegradation Kinetics of Surfactants in Seawater. *Chemosphere*, 39, 1957-1969.
- Ragsdell, K. M. (1975). On the Application of the Generalized Reduced Gradient Method to Mechanism Synthesis (pp. 405-410). *World Congress on the Theory of Mach. and Mech. 4th*. Avtomaticheskaya Svaraka.
- Rashid, N., Ur Rehman, M. S., Memon, S., Ur-Rahman, Z., Lee, K., & Han, J. (2013). Current Status, Barriers and Developments in Biohydrogen Production by Microalgae. *Renewable and Sustainable Energy Reviews*, 22, 571-579.
- Ruiz, J., Álvarez-Díaz, P. D., Arbib, Z., Garrido-Pérez, C., Barragán, J., & Perales, J. A. (2011). Effect of Nitrogen and Phosphorus Concentration on their Removal Kinetic in Treated Urban Wastewater by *Chlorella vulgaris*. *Int. J. Phytoremediation*, 13(9), 884-896.
- Ruiz, J., Álvarez-Díaz, P. D., Arbib, Z., Garrido-Pérez, C., Barragán, J., & Perales, J. A. (2013). Performance of a Flat Panel Reactor in the Continuous Culture of Microalgae in urban Wastewater: Prediction from a Batch Experiment. *Bioresource Technology*, 127, 456-463. Accessed October 28, 2013. Available at: <http://www.ncbi.nlm.nih.gov/pubmed/23138070>.
- Ruiz, J., Arbib, Z., Álvarez-Díaz, P. D., Garrido-Pérez, C., Barragán, J., & Perales, J. A. (2012). Photobiotreatment Model (Phbt): A Kinetic Model for Microalgae Biomass Growth and Nutrient Removal in Wastewater. *Environmental Technology*, 34(8), 979-991. Accessed October 28, 2013. Available at: <http://www.tandfonline.com/doi/abs/10.1080/09593330.2012.724451>.
- Ruiz-Marin, A., Mendoza-Espinosa, L. G., & Stephenson, T. (2010). Growth and Nutrient Removal in Free and Immobilized Green Algae in Batch and Semi-Continuous Cultures Treating Real Wastewater. *Bioresource Technology*, 101, 58-64.
- Samorì, G., Samori, C., Guerrini, F., & Pistocchi, R. (2013). Growth and Nitrogen Removal Capacity of *Desmodesmus Communis* and of a Natural Microalgae Consortium in a Batch Culture System in View of Urban Wastewater Treatment: Part I. *Water Research*, 47(2), 791-801. Accessed October 27, 2013. Available at: <http://www.ncbi.nlm.nih.gov/pubmed/23211134>.
- Schnackenberg, J., Ikemoto, H., & Miyachi, S. (1996). Photosynthesis and Hydrogen Evolution under Stress Conditions in a CO₂-Tolerant Marine Green Alga *Chlorococcum littorale*. *Journal of Photochemistry and Photobiology B: Biology*, 62, 34-59.
- Shelef, G., Azov, Y., Moraine, R., & Oron, G. (1980). Algal Mass Production as an integral Part of a Wastewater Treatment and Reclamation System. In *Algae Biomass*. Amsterdam: Shelef&Soeder, Ed., Elsevier/North-Holland Biomedical Press.
- Shelef, G., Moraine, R., & Oron, G. (1978). Photosynthetic Biomass Production from Sewage. *Ergebn. Limnol.*, 11, 3-14.
- Smith, V. H., & Schindler, D. W. (2009). Eutrophication Science: Where do We Go from Here? *Trends Ecol. Evol.*, 24, 201-207.
- Talbot, P., Thébault, J. M., Dauta, A., & De La Noüe, J. (1991). A Comparative Study and Mathematical Modeling of temperature, Light and Growth of Three Microalgae Potentially Useful for Wastewater Treatment. *Water Research*, 25(4), 465-472. Accessed October 29, 2013. Available at: <http://www.sciencedirect.com/science/article/pii/0043135491900833>.
- Tang, D., Han, W., Li, P., Miao, X., & Zhong, J. (2011). CO₂ Biofixation and Fatty Acid Composition of *Scenedesmus obliquus* and *Chlorella pyrenoidosa* in Response to Different

- CO₂ Levels. *Bioresource technology*, 102(3), 3071-3076. Accessed October 24, 2013. Available at: <http://www.ncbi.nlm.nih.gov/pubmed/21041075>.
- Trussel, R. P. (1972). The Percent of Un-Ionized Ammonia in Aqueous Ammonia Solutions at Different pH Levels and Temperatures. *J. Fish. Res. Bd. Can.*, 29, 1505-1507.
- UNEP (2010). *Sick Water? The Central Role of Wastewater Management in Sustainable Development. A Rapid Response Assessment*. E. Corcoran et al. (Eds.). Available at: http://www.unep.org/pdf/SickWater_screen.pdf.
- Velan, M., & Saravanane, R. (2013). CO₂ Sequestration and Treatment of Municipal Sewage by Microalgae, *International Journal of Innovative Technology and Exploring Engineering*. 2(5), 307-310.
- Verhulst, P. F. (1838). Notice Sur la Loi que la Population Suit dans son Accroissement. *Corres. Math. Phys.*, 10, 113-121.
- Walsh, S., & Diamond, D. (1995). Non-Linear Curve Fitting Using Microsoft Excel Solver. *Talanta*, 42, 561-572.
- Wang, L., Wang, Y. K., Chen, P., & Ruan, R. (2010). Semi-Continuous cultivation of *Chlorella vulgaris* for Treating Undigested and Digested Dairy Manures. *Applied Bio-Chemistry and Biotechnology*, 162, 2324-2332.

Institutional Address of the Authors

Lic. César Carlos García Gozalbes

Licenciado en Ciencias Ambientales por la Universidad de Cádiz
Centro Andaluz de Ciencia y Tecnología Marinas (Cacytmar)
Campus Universitario Polígono Río San Pedro
11510, Puerto Real, Cádiz, ESPAÑA
Teléfono: +34 (67) 5307 607
carlos.garciago@alum.uca.es

Dr. Zouhayr Arbib

Investigador de Aqualia, Gestión Integral del Agua S.A.
EDAR de El Torno, Chiclana de la Frontera, España
Campus Universitario Polígono Río San Pedro
11510, Puerto Real, Cádiz, ESPAÑA
Teléfono: +34 (95) 6016 747
zouhayr.arbib@fcc.es

Lic. José Antonio Perales Vargas-Machuca

Profesor del Departamento de Tecnologías del Medio Ambiente
Universidad de Cádiz
Centro Andaluz de Ciencia y Tecnología Marinas (Cacytmar)
Campus Universitario Polígono Río San Pedro
11510, Puerto Real, Cádiz, ESPAÑA
Teléfono: +34 (95) 6016 747
joseantonio.perales@uca.es

Improvements in the Hydraulic Efficiency of Weirs with Free Outfalls in Dams

• Mauro Iñiguez-Covarrubias • Waldo Ojeda-Bustamante* •
Instituto Mexicano de Tecnología del Agua

*Corresponding Author

• Carlos Díaz-Delgado •
Universidad Autónoma del Estado de México, Estado de México

Abstract

Iñiguez-Covarrubias, M., Ojeda-Bustamante, W., & Díaz-Delgado, C. (January-February, 2015). Improvements in the Hydraulic Efficiency of Weirs with Free Outfalls in Dams. *Water Technology and Sciences* (in Spanish), 6(1), 69-79.

Hydraulic infrastructure in Mexico is aging and in many cases there is an urgent need for rehabilitation. This task requires the application of new hydraulic as well as hydrological design methods that are consistent with current technological developments, to the extent possible. Free weirs are hydraulic infrastructures used in reservoirs and are generally located in very wide channels or those with high hydraulic loads, characteristics which are vitally important to determine the height of a dam wall. A proposal is presented for an alternative design and to improve hydraulic efficiency by substituting the free weir with a labyrinth weir. This proposal is based on the duckbill weir design. A case study was conducted in the "El Ejidatario" dam located in Sombrerete, Zacatecas, Mexico. The results show that with the installation of a labyrinth weir the length increased to 5.67 times that of the free weir. In addition, with a change in load from 80 to 30 cm the weir load decreased 62.5% and the capacity of the reservoir increased 12% with the same mean elevation. The hydraulic efficiency of the duckbill weir was compared to that of the piano key weir for the same weir length and installation conditions, resulting in a 208% improvement. It is recommended to install the new weir in the same site as the free weir, only adapting the entrance to the stilling basin while using the same outlet to the discharge channel. A labyrinth weir is recommended when physical or study conditions require it, since in this case by increasing the hydraulic efficiency of the weir the capacity of the reservoir will increase and, thus, the service life.

Keywords: Labyrinth weir, duckbill weir, free outflow weirs, dam safety.

Resumen

Iñiguez-Covarrubias, M., Ojeda-Bustamante, W., & Díaz-Delgado, C. (enero-febrero, 2015). Mejoras de eficiencia hidráulica en vertedores con canal de descarga libre en presas: propuesta metodológica. *Tecnología y Ciencias del Agua*, 6(1), 69-79.

En México, la infraestructura hidráulica está avejentada y en muchos casos urge rehabilitarla. Esta tarea requiere la aplicación de nuevos métodos de rediseño tanto hidráulico como hidrológico y en lo posible acorde con los desarrollos tecnológicos actuales. Una obra de infraestructura hidráulica utilizada en embalses son los vertedores con canal de descarga libre, generalmente ubicada en canales muy anchos o con cargas hidráulicas altas, características de importancia vital al determinar la altura de la cortina. Se presenta una propuesta de alternativa de diseño y de mejoras de la eficiencia hidráulica, al sustituir la estructura del cimacio por un vertedor tipo laberinto. Esta propuesta adopta las bases del diseño de vertedores de "pico de pato". Como caso de estudio, se aplicó para el vertedor de la presa "El Ejidatario", ubicada en Sombrerete, Zacatecas, México. Los resultados muestran que con la instalación del vertedor "pico de pato" se aumentó la longitud de vertido 5.67 veces en relación con la proporcionada con el cimacio; asimismo, se reduce la carga vertedora en 62.5%, al pasar de una carga de 80 a 30 cm y se incrementa en un 12% la capacidad del embalse con la misma altura del NAME. Además, se comparó la eficiencia hidráulica del "pico de pato" respecto al vertedor "tecla de piano" para la misma longitud de vertido y condiciones de instalación, siendo mayor en 208%. Se recomienda en la instalación del nuevo vertedor utilizar el mismo sitio del cimacio, sólo adecuando la entrada al tanque amortiguador y conservando la salida del canal de descarga. Se concluye recomendar un vertedor "pico de pato" en donde las condiciones físicas o de estudio se requiera, ya que al aumentar la eficiencia hidráulica del vertedor para este caso, aumenta la capacidad del embalse y, por lo tanto, la vida de servicio.

Palabras clave: vertedor "pico de pato", vertedores de descarga libre, seguridad en presas.

Received: 06/02/13
Accepted: 11/09/14

Introduction

The hydraulic infrastructure in Mexico is aging and rehabilitation is urgently needed in many cases. This task requires applying new hydraulic and hydrological design methods, and to the extent possible in accordance with current technological developments. Currently, the hydraulic infrastructure in irrigation districts and units in Mexico is maintained, operated and administered by users and the National Water Commission (Conagua, Spanish acronym). Most of the economic resources invested in these tasks is spent on administrative areas, with little resources assigned to maintaining the infrastructure (IMTA, 2007). The hydrological infrastructure includes reservoirs, large and small networks, roads and drainage networks, and the unfortunately forgotten flood works, and particularly weirs.

One type of hydraulic infrastructure used in reservoirs are weirs with free outfall channels, generally located in channels that are very wide or that have high hydraulic loads, characteristics which are crucially important to determining the height of a dam wall (SARH, 1973; Arreguín, 2000; CFE, 1981). The method proposed by USDI (1979) is used to design weirs with free outfall channels based on fluid mechanics theories by Chow (1959), Henderson (1966), Levi (1567) and Levi and Aldama (1979), among others. These structures have been installed in a significant number of reservoirs in Mexico, especially in dams with mixed materials, and have become costly because of the ratio of the weir length to the hydraulic load over the weir in very large channels with low or high water depths and short weir lengths, requiring a taller dam wall. Nevertheless, they are known for ease in operations since they do not require equipment or manual labor.

Modern infrastructure designs in irrigation districts and units in Mexico include methods to control the flow of water and operations. To this end, level control structures are used in order to prevent variations in the discharge of flow in intakes. The design methodology applied is based primarily on works by Hay and Taylor (1970). These authors present a general design methodology using experiments involving the hydraulic functioning of labyrinth weirs. The functioning of long-crested weirs consists of increasing the discharge per the structure's unit width to obtain a fixed operating level over the weir crest. Figure 1 shows the overview and cross-section of a portion of a channel containing a long-crested weir. In this figure, L_n is the distance from the water mirror to the height of the crest, H is the hydraulic load over the weir and W_h is the height of the weir.

The design of the long-crested weir consists of determining the length of the weir crest that allows for maintaining the water level over the weir within a maximum operating range. Hay and Taylor (1970) defined a method which requires estimating a parameter called W_r . The authors reported the values of W_r (Table 1) which they obtained experimentally by varying the ratio H/W_h against the ratio Q_n/Q_d , where Q_n is the design flow of the labyrinth weir and Q_d is the flow that passes through the normal weir $Q_d = C_d * L * H^{(3/2)}$, $L = L_n - 0.2H$ and C_d = discharge coefficient for the normal weir. In addition, W_r is the variable in the ratio to determine the length of the weir crest (L_e), which is determined with equation (1):

$$L_e = L_n \left(\frac{C_s}{C_d} \right) W_r \quad (1)$$

where L_e = effective length; C_s = discharge coefficient of the long-crested weir, the

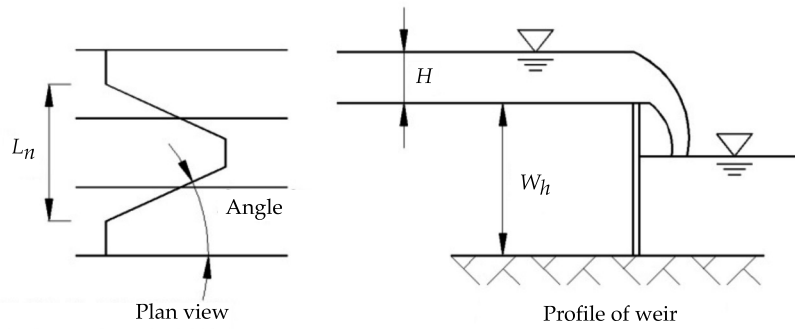


Figure 1. Plan view and profile of long-crested weir.

Table 1. Values of W_r (Hay & Taylor, 1970).

Ratio of Q_u/Q_d	Ratio of H/W_h				
	0.1	0.2	0.3	0.4	0.5
1	1.00	1.00	1.00	1.00	1.00
2	2.00	2.00	2.00	2.10	2.20
3	3.00	3.05	3.15	3.33	3.50
4	4.00	4.10	4.33	4.65	5.90
5	5.05	5.26	5.77	7.99	-
6	6.09	6.71	8.20	-	-
7	7.22	8.10	-	-	-
8	8.30	-	-	-	-

angle α of the weir is the inclination of the weir with respect to the longitudinal axis of the channel (Figure 1) and is determined by $\alpha = 0.75 \arcsin(L_n/L_e)$.

The number of cycles of the weir is determined using the models shown in Figure 2. For the representative model, the following ratios are used: L_e/L_n indicated with an asterisk; L_n/W_h indicated with two asterisks; and the angle α indicated with three asterisks. In addition, each model is indicated by the number located at the top. Hay and Taylor (1970) more extensively present the individual steps used to develop their proposal, based on Walker (1987), among others.

Ribeiro *et al.* (2012) have proposed a type of free outfall weir structure for storage dams, called “piano key.” The shape of this type of weir is similar to that

of a rectangular section of the duckbill weir, as shown in Figure 3. Ribeiro *et al.* (2012) mentioned that to design the weir, they did not take into account the studies by Hay and Taylor (1970).

Figure 3 shows the plan view and cross-section of the “piano key” weir. In this type of weir, the inside section “B” is not a free outfall and section “A” of the outlet is not a vertical wall. Table 2 presents the general characteristics of the “piano key” weir but with three parts $\frac{3}{4}$ inflow to valve, lateral flow through the valve and outflow from valve.

Table 2 includes the equations for separate flow calculations for three types of weirs which are joined to make the “piano key” weir. According to Sotelo-Ávila (1979) the discharge coefficient is higher for a weir with fewer obstacles to

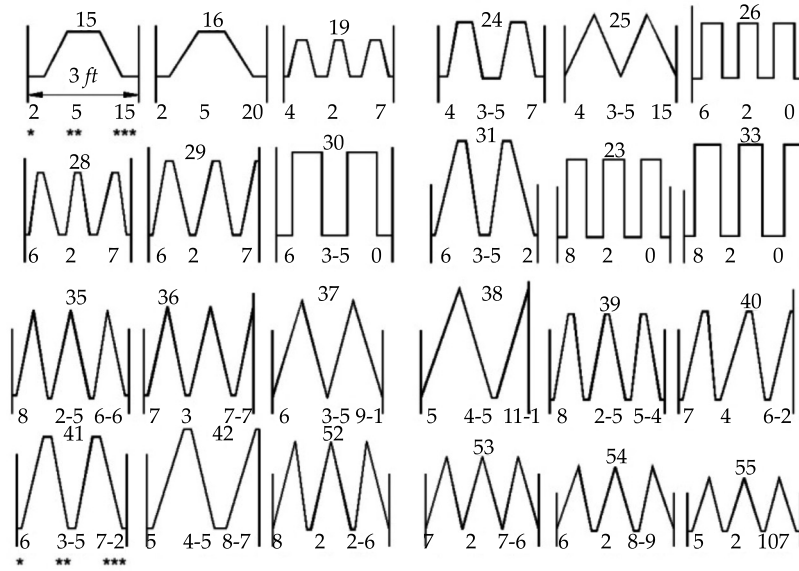


Figure 2. Models of long-crested weirs reported by Hay and Tayler (1970).

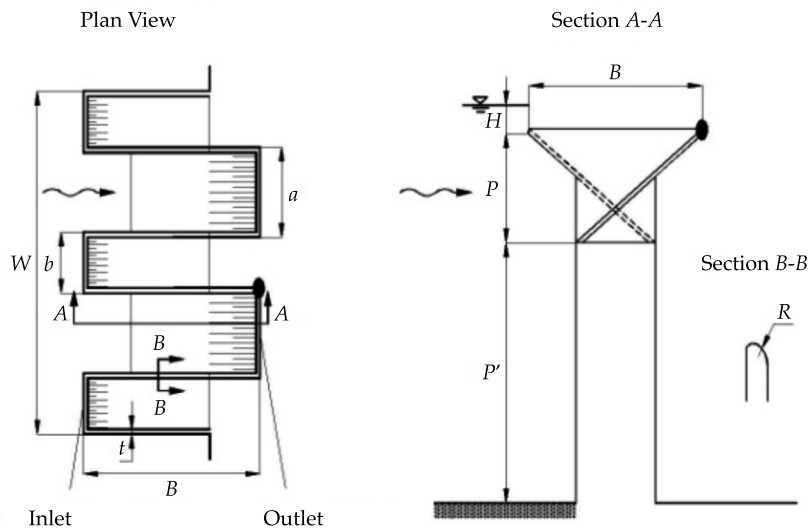


Figure 3. Plan and profile views of the “piano key” weir (Ribeiro *et al.*, 2012).

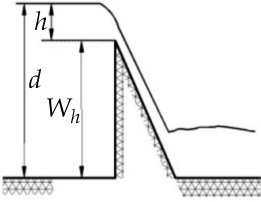
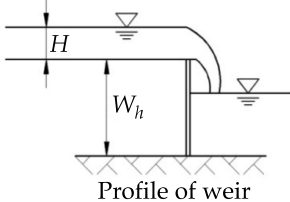
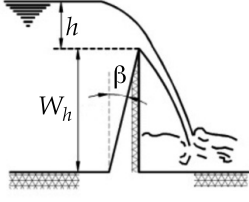
overcome. This means that the highest discharge coefficient occurs when there is free outfall and no lateral contractions.

According to Ribeiro *et al.* (2012) flow with the “piano key” weir is a function of the parameters in equation (2):

$$Q_{PWK} = f(\rho, g, \nu, \sigma, H, L, P, P', W, a, b, s_{inlet}, s_{outlet}, \alpha, t, R) \quad (2)$$

where ρ = density of the water; g = acceleration of gravity; ν = dynamic viscosity; s = surface tension; H = hydraulic load

Table 2. Values of Q for three types of weirs.

Flow entering the inlet	Lateral flow in the inlet	Outflow from the inlet
		
$Q = CLh^{2/3} \left(1 + 0.787C^2 \frac{h^2}{d^2} \right)$	$Q = \frac{2}{3} C \sqrt{2g} LH^{3/2}$	$Q = \frac{2}{3} C \alpha \sqrt{2g} LH^{3/2}$

over the weir; L = length of the weir; P = height of the “piano key” weir; P' = height from the floor to the beginning of the weir; W = width of the weir crest; a = outer width of the key; b = inner width of the key; S_{inlet} = slope of the inlet; S_{outlet} = slope of the outlet; α = angle between the inlet and outlet; t = thickness of the weir wall; R = radius of the weir crest.

The methodology reported by Ribeiro *et al.* (2012) for the design of the weir is based on results from investigations performed at a model scale. Based on the experimental results, the ratios H/a vs. r and H/P vs. r were determined for different values of L/W .

Given what has been presented thus far, the challenge for researchers who are designing hydraulic infrastructure is to develop new and more efficient design methods and, to the extent possible, in accordance with the most current technological developments. Therefore, the work herein presents an original alternative proposal for the design of weirs. Specifically, it proposes substituting weirs with free outfalls in storage dams using a labyrinth control weir in order to improve the hydraulic efficiency of weirs with free outfall channels in dams, while also increasing storage capacity without changing the mean elevation and increasing the useful life of the reservoir.

Materials and Methods

“El Ejidatario” reservoir was used for the case study, located on the common land named Felipe Angeles, in the municipality of Sombrerete, state of Zacatecas, Mexico (Figure 4). The geographic coordinates are $23^\circ 34' 30''$ north latitude and $103^\circ 33' 30''$ west longitude, with an elevation of 2 217.97 masl (Colegio de Postgraduados, 1977).

The area of the basin is 50 km², mean annual precipitation is 500 mm and mean annual runoff is estimated at 4.5 hm³. The reservoir has a useful storage capacity of

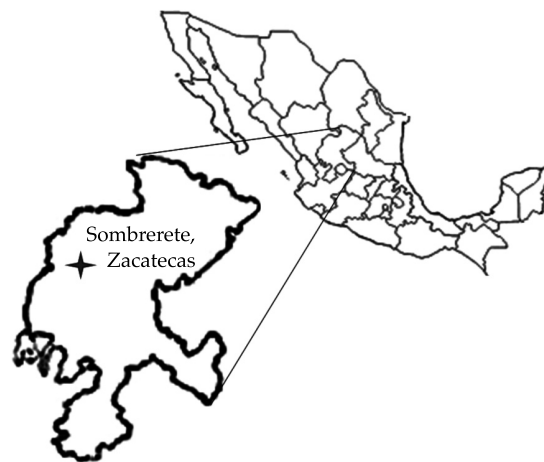


Figure 4. Map of location, state of Zacatecas, Mexico.

1.25 hm³ and supplies an irrigation area of 150 hectares (Colegio de Postgraduados, 1977). An excess free outfall weir is located on the left bank, with a maximum spill capacity of 35 m³/s. The intake channel and the discharge channel are not revetted since they are located on top of rhyolite rock (Colegio de Postgraduados, 1977).

The weir structure is described as a weir with a free outfall channel (Arreguín & Alcocer, 2011) which contains an access channel, weir crest, stilling basin or energy dissipater, and a discharge channel. The weir crest is composed of a free outfall weir which adopts the shape of the flow of the water as it falls, known as a Creager profile. The access channel has an base intake channel and an outlet measuring 25.0 m wide. The slopes of the channel are $k = 0:1$ and are located at the beginning in the access channel at a grade line level of 2 212.70 masl. Figure 5 shows the access channel to the weir, the location of the free outfall weir and the weir outfall with level curves.

The proposal begins with the methodology performed by Hay and Taylor (1970) for the design of duckbill weirs. Since this methodology does not allow for

designs involving more than three cycles, separating the crest width and the flow into units is proposed for the purpose of the present case study since it contains very large sections. This is done by dividing by the same denominator and thereby obtaining designs for the separate units as independent bodies. After the designs are developed the parts are joined in the resulting integral. This structure needs to be applied to the intake channel, weir structure, energy dissipater and discharge channel.

Three steps are used to design and locate duckbill-type long-crested weirs. Step one: the width of the channel and flow is divided by seven structures, with the units: Q_n = design flow = 5 m³/s; (b) base = 3.57 m; (k) slope = 0:1; (m) slope = 0.0008; (n) Manning = 0.017; (Y_n) normal water depth = 1.091 m; (Y_c) critical water depth = 0.585 m. It is important to mention that the real load over the weir is considered to be 0.30 m, which is the maximum tolerant load for the height of the weir.

Step 2: design of the duckbill weir. The weir is designed using the method proposed by Hay and Taylor (1970).

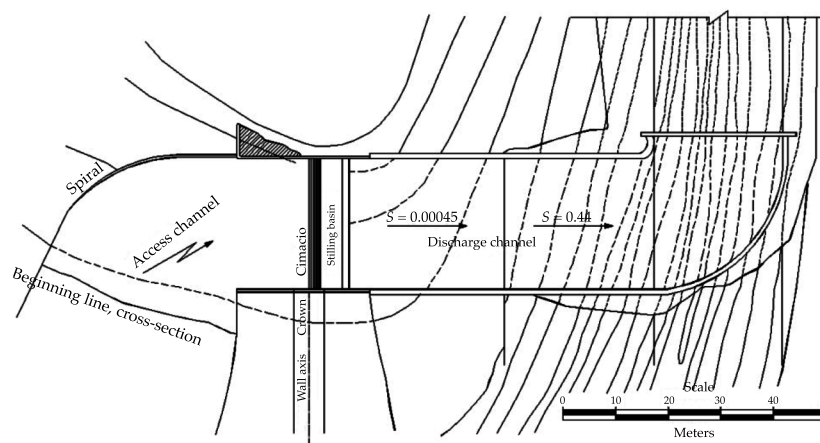


Figure 5. Plan view of the weir structure.

The input data are (W_h) height of the weir = 1.0 m and (h) load over the weir = 0.3 m. The dimensions obtained for the duckbill weir are effective length of the weir = 20.21 m; angle (alfa) = 7.63° ; (Wr) efficiency coefficient = 4.58; L_e = effective length = $L_n - 0.2H = 3.57 - 0.2 * 0.3 = 3.51$; $Cd = 1.778 + (H/Wh) = 1.778 + (0.3/1.0) = 2.078$; $Qd = Cd * L * H^{(3/2)} = 2.078 * 3.51 * (0.3)^{(3/2)} = 1.19 \text{ m}^3/\text{s}$; flow ratio $Q_{pp}/Q_d = 5.0/1.19 = 4.17$; and (a) width of the peaks = 0.13 m. The result is the selection of model 31 with two cycles (Figure 2); it is shown in Figure 6.

Step 3: once the design of the structure is obtained, the individual weir designs are joined. Figure 7 shows the general characteristics of the long-crested weirs proposed for the right banks of the main channel, with base = 25 m, total length = 141.47 m and 14 cycles throughout the

weir structure (seven units with two cycles each). The weir is installed, fitted to the energy dissipater structure and the plans are developed.

The proposal continues with the methodology performed by Ribeiro *et al.* (2012) to design “piano key” weirs. Separating the crest width and flow units is again proposed by dividing by the same denominator to obtain separate unit designs, as independent bodies. Once the individual units are designed they are joined in the resulting integral. This structure needs to be applied to the intake water channel, weir structure, energy dissipater and discharge channel.

The design and location of long-crested “piano key” weirs were determined using three steps. Step one: the channel width and flow are divided by seven structures, with the units: $Qn = \text{design flow} = 5 \text{ m}^3/\text{s}$ and (b) base = 3.57 m. It is important to mention that the actual load over the weir is considered to be 0.30 m, which is the maximum load tolerated given the dimensions of the duckbill weir. The effective length of the weir is 20.21 m.

Step 2: This step involves a revision of the “piano key” weir design based on the methodology proposed by Ribeiro *et al.* (2012). According to the authors, the design takes into account a height (H) of the hydraulic load over the weir of 0.3 m; inside weir length (for this case a and b are the same) $a = 0.89$, $b = 0.89$ m; and

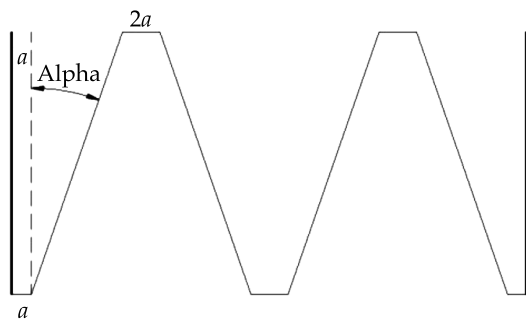


Figure 6. Plan view of “duckbill” weir, from Hay and Taylor (1970).

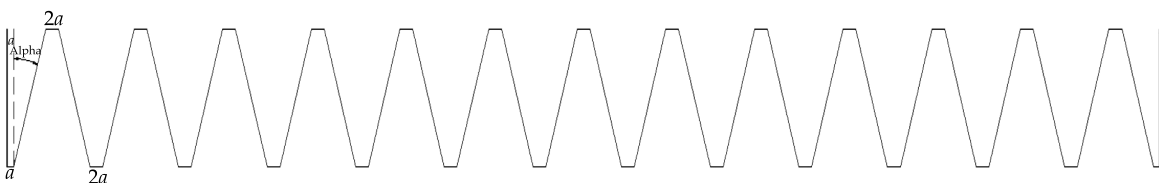


Figure 7. Union of all partial weir designs into one single “duckbill” structure.

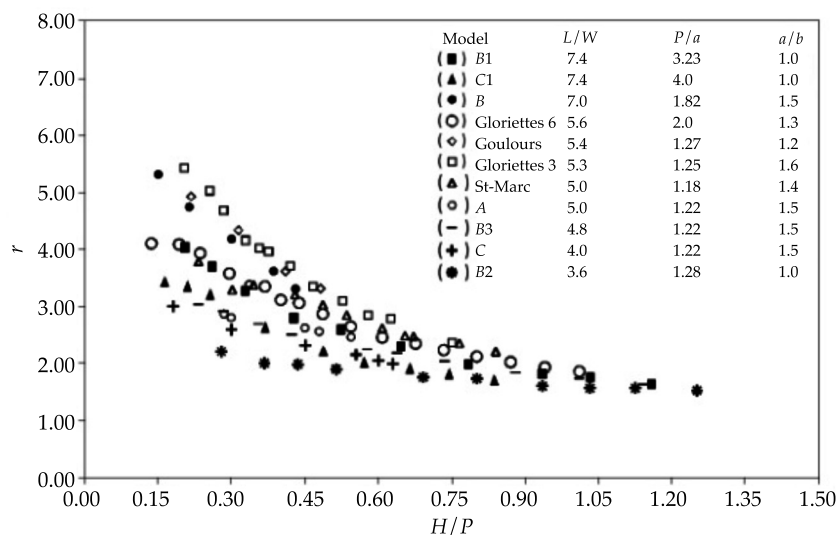


Figure 8. Ratio of H/P vs. r .

weir height $P = 1.0$. The ratio $a/b = 1.0$ and $P/a = 1.0/0.89 = 1.12$ are always greater than one. With the help of Figure 8 and $H/P = 0.3/1.0 = 0.3$, along with the ratio L/W , the ratio r between flows is obtained— $r = Q_{TP}/Q_d = 2.0$ (Figure 8) with model B2.

In terms of the dimensions presented ($a = 0.89$ m, $b = 0.89$ and the ratio $a/b = 1.0$) and given the “piano key” shape, model

30 is chosen from Figure 2, which in total corresponds to a length of 20.21. This result is represented in Figure 9.

Step 3: This step consists of joining all the peaks into one single structure; that is, the individual designs of the “piano key” weir are joined. Figure 10 presents the general characteristics of the long-crested weirs proposed for the right bank of the main channel, with base = 25 m; total length $L = 141.47$ m and seven units containing two cycles each, resulting in 14 keys. The weir is installed with the energy dissipater structure and the plans are developed.

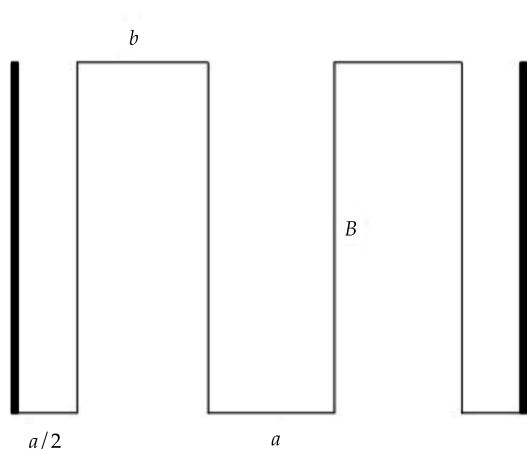


Figure 9. Plan view of “duckbill” weir, model 30.

Results and Discussion

The results obtained show that the two designs have the same base, $b = 25$ meters. The length of the nine weir crest is 5.67 times longer than the weir with the free outfall, increasing from 25 meters to 141.47 meters, with 14 cycles throughout the weir structure.

The results obtained demonstrate that for “piano key” weirs, when the length of the weir crest and channel width ratio L/W

increase, a/b will be greater than 1. The weir resembles a duckbill weir. The increase in the value of r only depends on elevation P . For this exercise, $P = 1.0$ meters.

The flow relation for the “piano key” weir is $r = 2.0$, and therefore can only permit a flow of $Q_{TP} = 2 * 1.19 \text{ m}^3/\text{s} = 2.38 \text{ m}^3/\text{s}$. This is due to increased loss in hydraulic load at the inlet and outlet of the keys since they are not considered free outfall. This demonstrates that the weir with the higher discharge coefficient is the free outfall weir (Anderson & Tullis, 2012), indicating an increase in the efficiency of the weir, which is achieved by increasing the height P , as seen in the models in Figure 8, with the same weir crest length. It is interesting to note how the efficiency of the “piano key” weir increases when increasing the height of the free outfall weir, which in this case

cannot be increased.

With the duckbill weir, the flow efficiency ratio is $Q_n/Q_d = 5.0 / 1.19 = 4.17$; that is, 208% greater than that of the “piano key.” It is important to mention that it was necessary to divide the width in the duckbill design, since to apply the methodologies proposed herein the design recommendations only allow for a structure with no more than three peaks.

The results obtained show that the design alternatives analyzed provide a reduction of 62.5% in the weir load when the hydraulic load decreased from 80 to 30 cm, when the elevation of the weir crest increased from 2 213.20 masl to the new elevation of 2.213.70 masl, respecting the mean elevation level of 2 214.0 while also having increased the storage capacity by 12%. Figure 11 shows a graphic of the

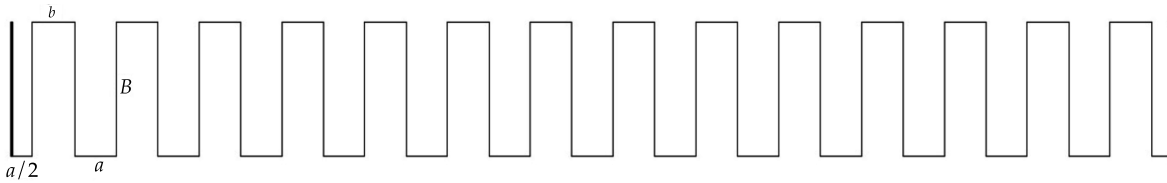


Figure 10. Union of all peaks into one single “piano key” structure.

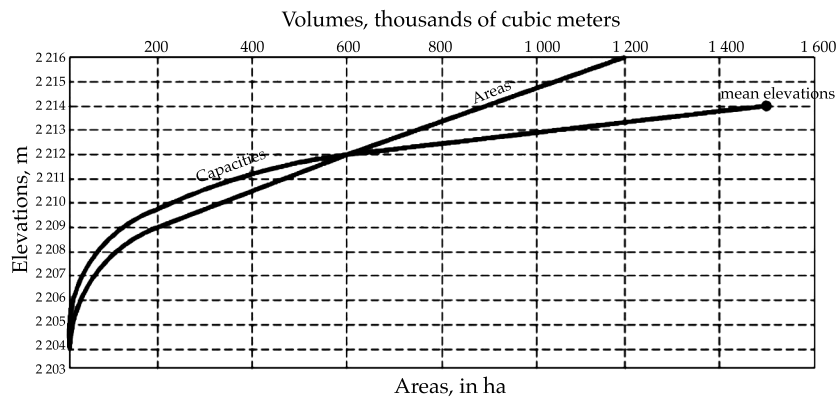


Figure 11. Elevations-areas-capacities curve.

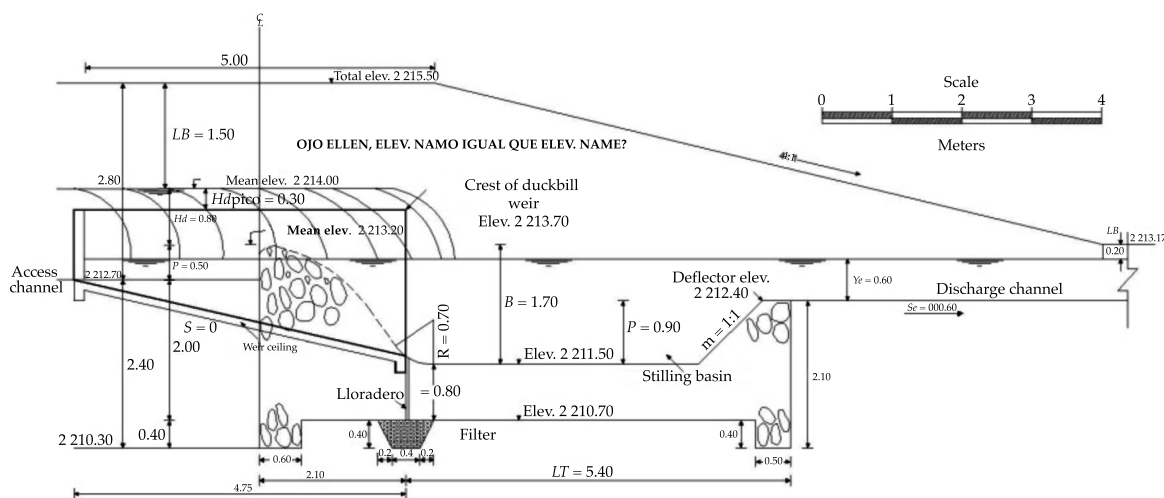


Figure 12. Lengthwise profile of the adapted weir structure.

elevations-areas-capacities of the reservoir.

Figure 12 shows the longitudinal profile of the duckbill weir structure installed with adaptations by eliminating the free outfall weir while retaining the same energy dissipater structure, respecting the outlet levels of the discharge channel. Since it is recommended to use the same site as the weir the additional cost is very low; the dyke elevation is shown to be 2 215.5 masl, among others.

Conclusions and Recommendations

Based on the methodological presented herein, the recommendation can be made to substitute the free outfall weir of a free outfall weir with a duckbill weir in storage dams when necessary and when physical conditions permit. In effect, this new configuration of the excess weir structure, reduces the hydraulic load over the weir for the design flow, significantly increases storage capacity, therefore, in this case extends the useful life of the reservoir.

Likewise, the use of the alternative design proposals presented herein is

recommended, first with the methodology proposed by Hay and Taylor (1970); the efficiency increased by 200% for this case. It is important to mention that the two design methods analyzed are applicable as long as the conditions in which they were tested are respected. Nevertheless, the method by Ribeiro *et al.* (2012) for the same weir crest length as the duckbill requires the height of the variable P to be taller, a requirement which is difficult to meet with the present case. The alternative methodology presented herein facilitates the design and reengineering of weirs with free outfall channels in dams with existing infrastructure, as well as the design of new weirs in storage dams, but with greater hydraulic efficiency. Finally, it is noteworthy that the designs obtained with the application of this methodology retain the characteristics of being easy to operate without the need for equipment or manual labor.

References

Anderson, R. M., & Tullis, B. P. (April 1, 2012). Comparison of

- Piano Key and Rectangular Labyrinth Weir Hydraulics. *Journal of Hydraulic Engineering*, 138(4), 358-361.
- Arreguín, F. (2000). *Obras de excedencia* (262 pp.). Jiutepec, México: Instituto Mexicano de Tecnología del Agua.
- Arreguín, F., & Alcocer, V. (2011). *Diseño hidráulico de vertedores* (244 pp.). Jiutepec, México: Instituto Mexicano de Tecnología del Agua.
- CFE (1981). *Obras de excedencia* (134 pp.). Colección Manual de Diseño de Obras Civiles. México, DF: Comisión Federal de Electricidad.
- Chow, V. T. (1959). *Open Channel Hydraulics* (680 pp.). New York: McGraw-Hill.
- Colegio de Postgraduados (1977). *Manual para proyectos de pequeñas obras hidráulicas para riego y abrevadero* (247 pp.). México, DF: SARH.
- Henderson, F. M. (1966). *Open Channel Flow* (522 pp.). New York: MacMillan.
- IMTA (2007). *Plan director DR 087 Rosario Mezquite, Yurécuaro Michoacán* (456 pp.). Proyecto CNA-IMTA, enero-diciembre. Jiutepec, México: Instituto Mexicano de Tecnología del Agua.
- Levi, E. (1957). *Mecánica de los fluidos* (p. 266). México, DF: UNAM, Instituto de Ingeniería.
- Levi, E. & Aldama, A. A. (1979). *Diseño hidrodinámico y automatización fluídica en obras hidráulicas* (170 pp.). México, DF: UNAM, Instituto de Ingeniería.
- Hay, N., & Taylor, G. (November, 1970). Performance and Design of Labyrinth Weir. *Journal of the Hydraulics Division*, 96, No HY11, 2337-2357.
- Ribeiro, L., Bieri, M., Boillat, L., Schleiss, J., Singhal, G., & Sharma, N. (February 1, 2012). Discharge Capacity of Piano Key Weirs. *Journal of Hydraulic Engineering*, 138(2), 199-203.
- SARH (1973). *Proyecto de zonas de riego* (567 pp.). México, DF: Dirección de Proyectos de Irrigación, Departamento de Canales,
- Sotelo-Ávila, G. (1979). *Hidráulica general* (560 pp.). México, DF: Limusa.
- USDI (1979) *Diseño de presas pequeñas* (639 pp.). México, DF: CECSA, U.S. Department of Interior.
- Walker, R. E. (1987). Long Crested Weirs. Planning, Operation, Rehabilitation and Automation of Irrigation Water Delivery Systems (344 pp.). *Symposium Proceedings*, New York, ASCE.

Institutional Address of the Authors

Dr. Mauro Iñiguez-Covarrubias

Dr. Waldo Ojeda-Bustamante

Instituto Mexicano de Tecnología del Agua
 Paseo Cuauhnáhuac 8535 Colonia Progreso
 62550 Jiutepec, Morelos, México
 mic@tlaloc.imta.mx
 wojeda@tlaloc.imta.mx

Dr. Carlos Díaz-Delgado

Centro Interamericano de Recursos del Agua
 Facultad de Ingeniería
 Universidad Autónoma del Estado de México
 Cerro de Coatepec s/n
 50130 Toluca, Estado de México, México
 Teléfono: +52 (722) 2965 550
 Fax: +52 (722) 2965 551
 cdiazd@uaemex.mx



Villita Dam, Michoacan, Mexico.

Photo provided by Magnolia Velázquez Olivares and Valverde.

Development of the Balsas Hydrological Region by Modifying Prohibitions

• Juan Carlos Valencia-Vargas* •
Comisión Estatal del Agua, Morelos, México
*Corresponding Author

Abstract

Valencia-Vargas, J. C. (January-February, 2015). Development of the Balsas Hydrological Region by Modifying Prohibitions. *Water Technology and Sciences* (in Spanish), 6(1), 81-97.

Balsas Hydrological Region No. 18 consists of 8 states and 420 municipalities in Mexico, with an area corresponding to 6% of the national territory. Over 10% of the country's population lives there and it generates 10% of the electricity and 25% of the hydroelectric power consumed in the country. In 1937, only 38% of the population had electricity. Therefore, the federal government created the Federal Electric Commission (FEC) which began to build the first hydroelectric plants, taking advantage of runoffs in upper portions of basins-- from small water flows to large falls. Given the topography of the Balsas River basin, it is a natural generator of electricity, which is why the use of its waters for activities not related to energy generation was prohibited. The resulting inability to provide the population water to meet its basic needs produced economic and social marginalization in the region. To correct this situation, the Balsas River Basin Council decided to modify the prohibition and allocate water for human use and consumption. On March 22, 2011, the presidential decree was published which permitted allocating 219 645 221.83 m³/year (until 2030), with a reserve of 113 001 678.17 m³/year, benefiting 340 municipalities and 4 245 115 inhabitants.

Keywords: water, prohibitions, development.

Resumen

Valencia-Vargas, J. C. (enero-febrero, 2015). Desarrollo de la Región Hidrológica del Balsas mediante la modificación de su veda. *Tecnología y Ciencias del Agua*, 6(1), 81-97.

La Región Hidrológica núm. 18 Balsas está constituida por ocho estados y 420 municipios, con una superficie correspondiente a 6% del territorio nacional, concentrando en él mismo más de 10% de la población nacional. Es generadora de 10% de la energía eléctrica que se consume en el país y de 25% de la energía hidroeléctrica de México. En 1937, solamente 38% de la población contaba con energía eléctrica; por ello, el gobierno federal creó la Comisión Federal de Electricidad (CFE) y ésta inició la construcción de las primeras plantas hidroeléctricas, aprovechando los escurrimientos de las partes altas de las cuencas, con gastos de agua pequeños y caídas grandes. La topografía de la cuenca del río Balsas es útil de forma natural para la generación de energía eléctrica; por ello se vedó el aprovechamiento de sus aguas, afluentes y subafluentes para otra cosa que no fuera la generación de energía. Esto, sin embargo, generó marginación y rezago social en la región, al no poder dotar de agua a la población para que pudiera satisfacer sus necesidades básicas. A fin de corregir esta situación, en el Consejo de Cuenca del Río Balsas se decidió modificar la veda, con el objetivo de poder asignar volúmenes para uso y consumo humano. El 22 de marzo de 2011 se publicó el Decreto Presidencial que permitió asignar 219 645 221.83 m³/año, con una reserva de 113 001 678.17 m³/año, beneficiando a 340 municipios y 4 245 115 habitantes hasta el año 2030.

Palabras clave: agua, veda, desarrollo.

Received: 14/03/13
Accepted: 07/05/14

Background

In Mexico, water is administered by basins. The country has been divided into 13 hydrological regions whose boundaries were adjusted to include whole municipalities

and to facilitate the administrative management of programs. One of these regions, the one we will analyze, is Balsas Hydrological-Administrative Region IV located in southern Mexico.

Balsas Hydrological-Administrative Region IV is composed of Balsas Hydrological Region No. 18 (Figure 1), with an area of 117 305 km² (Conagua, 2010) representing 6% of the national territory. It is bordered to the north by Lerma-Santiago Hydrological Region no. 12, Rio Panuco No. 26 and No. 27, northern Veracruz; to the west by Armeria-Coahuayana Hydrological Region No. 16 and Michoacan Coast No. 17; to the south by the Pacific Ocean and hydrological regions Costa Grande de Guerrero No. 19 and Costa Chica de Guerrero No. 20; and to the east by Papaloapan Hydrological Region No. 28.

Balsas Hydrological Region no. 18 covers 8 of the 32 states in the country,

including the entire state of Morelos (100%) and portions of the states of Tlaxcala (75%), Guerrero (63%), Michoacán (62%), Puebla (55%), Mexico State (36%), Oaxaca (9%) and Jalisco (4%), with a total of 420 municipalities, according to the latest version of the “Agreement for the determination of the territorial boundaries of Conagua basin entities” (*Diario Oficial de la Federación, DOF*), April 1, 2010.

Hydrological Region No. 18 is bounded by the Southern Sierras Madre and the Juarez mountains as well as the neo-volcanic belt. It forms a very elongated depression with very narrow valleys. Most of the region has steep slopes and a geological makeup that is not very favorable to the control and storage of the

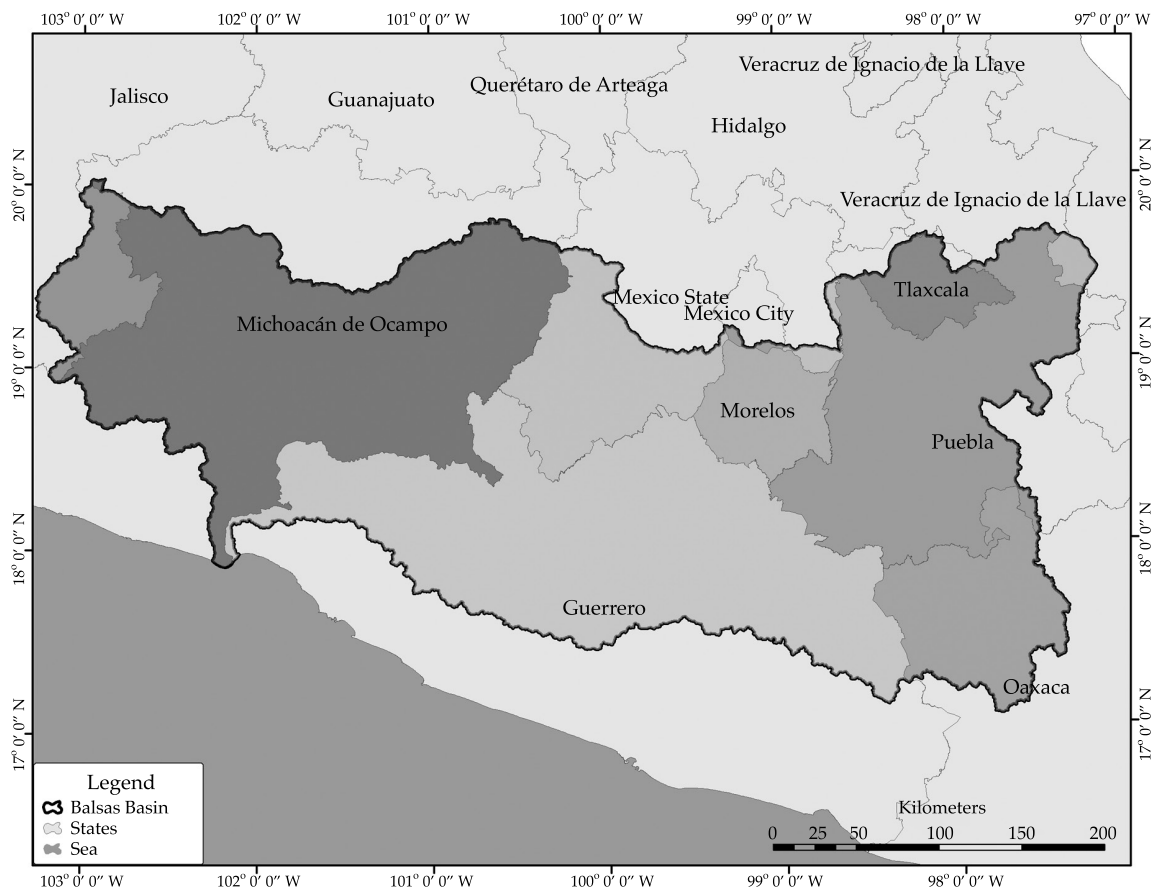


Figure 1. Location of Balsas Hydrological Region No. 18.

large runoffs which are generated in the hydrological regions, with a significant potential runoff of 991 millimeters per year.

Hydrology

Runoff in Balsas Hydrological Region No. 18 has been analyzed in 15 hydrological basins, as shown in Figure 2. They were divided according to physical conditions, that is, the watersheds that define them and the existing control structures (dams and hydrometric stations). The closed basins were defined solely by their physical boundaries. In addition, Balsas Hydrological Region No. 18 has been divided into hydrological sub-regions—Upper Balsas, Middle Balsas and Lower Balsas.

Mean annual precipitation in the region is 991 millimeters. This was determined with data obtained from records from 587 weather stations in the region belonging to Conagua. Generally, precipitation mainly occurs from May to October. Because of the torrential nature in most of the cases, it is difficult to make use of the precipitation.

Most occurs between July and September (80% of the annual total), with less in the month of August. The most severe droughts in the basin occur in March, particularly because of low precipitation beginning in November.

Steep slopes and torrential rainfall create large floods in very short periods of time. Along with severe deforestation in the upper portions, processes of erosion and significant sediment transport have been generated. The erosion has environmental impacts such as altering the regulation of the hydrological cycle, reducing crop yields and fishing production, degrading the vegetation cover, decreasing biodiversity, shortening the useful life of hydraulic works, contributing to sediments in river beds and destabilizing hillsides, which creates risks for persons, housing and infrastructure, as shown by a study of 37 hydrological regions in the country (Horrillo, Pedrozo, & Onandia, 2011). These physical characteristics explain why, in the 1940s, the water in this basin was used to generate electricity instead of for consumptive uses.

There is little potential to develop

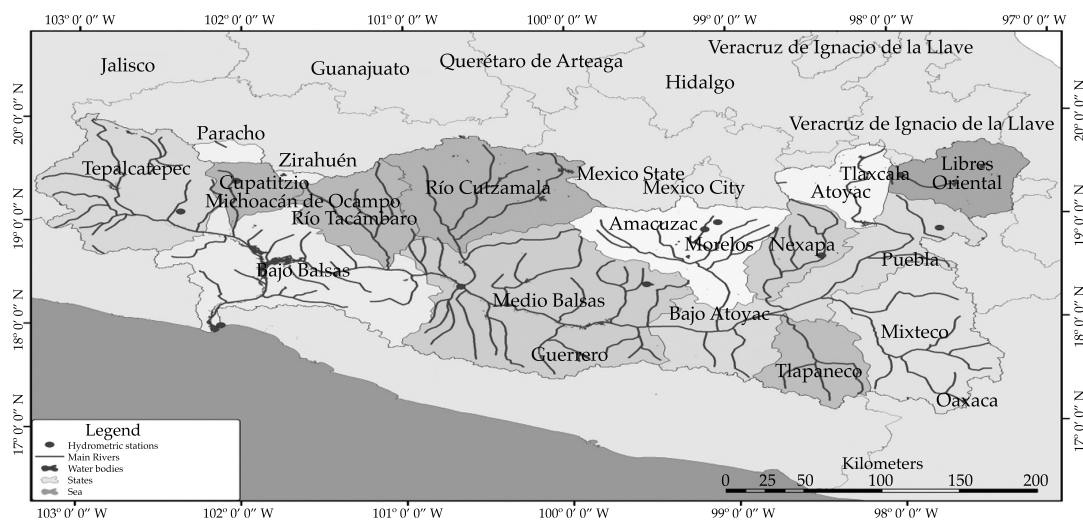


Figure 2. Sub-regions and hydrological basins in Balsas Hydrological Region No. 18.

agriculture since most of the basin consists of mountainous regions with small valleys containing poor soil and low productivity because of the steep slopes. Although these characteristics are not suitable to agricultural production they do provide great energy potential and natural conditions for generating electricity, since the Balsas River's narrow passes and steep slopes make damming very attractive and inexpensive.

Population

According to historical data (INEGI historical series for several years) the population has grown more than 300% over the past five decades.

There are currently 10 990 154 inhabitants, representing a little over 10% of the total population of the country (INEGI, 2010). Of the 420 municipalities in the region, 45 have a population over 50 000 inhabitants, which represents 56% of the total population of the region. There are 17 urban centers with a population over 100 000, representing 37.4% of the population in the region.

Decrees Related to Restrictions or Reserves

In 1937, only 38% of the population had electricity. Therefore, the federal

government created the Federal Electricity Commission (CFE, Spanish acronym) which began to build the first hydroelectric power plants, thereby utilizing the runoffs in the upper parts of the basins, with small water flows and large falls.

Since the natural conditions in the Balsas River basin favor the generation of electricity, the use of its water and tributaries for anything other than the generation of electricity was restricted by the following judicial instruments:

- The National Hydraulic Energy Reserve, in the section 50 kilometers upstream from the Balsas train overpass, in the municipality of Arcelia, Guerrero to its mouth at the Pacific Ocean in the municipality of Union, Guerrero, with 200 000 liters per second up to an annual volume of 6 307 200 000 cubic meters (DOF, June 18, 1940).
- The National Hydraulic Energy Reserve established for the benefit of the Tepalcatepec Commission for the generation of energy in the section between the Churumuco Canyon and the upper vertex of the Balsas River delta, which represents the border between the states of Guerrero and Michoacan, with a flow of 400 cubic meters per second, continuously throughout the year, up to a maximum annual volume of 12 614 400 000 m³ (DOF, October 30, 1956).

Table 1. Population of Balsas Hydrological Region, by state.

States	Population in 2010 (inhab)	Municipalities
Guerrero	1 175 379	45
Jalisco	20 753	3
México	980 608	33
Michoacán	1 818 314	45
Morelos	1 777 227	33
Oaxaca	295 155	78
Puebla	3 828 390	127
Tlaxcala	1 094 328	56
Total	10 990 154	420

- The National Hydraulic Energy Reserve in the section between the confluence of the Mixteco and Atoyac Rivers up to 35 kilometers downstream from the confluence of the Tacambaro River with the Balsas River, and in the rapids and calm waters of the Amacuzac River from Cacahuamilpa to its confluence with the Balsas River, in the state of Morelos, with a volume of 13 610 320 000 (DOF, August 25, 1958).
- The water rights restriction for an undefined period of time pertaining to the Balsas River and all its tributaries that constitute its tributary basin from the beginning of the state of Puebla to its mouth at the Pacific Ocean (DOF, February 2, 1966).

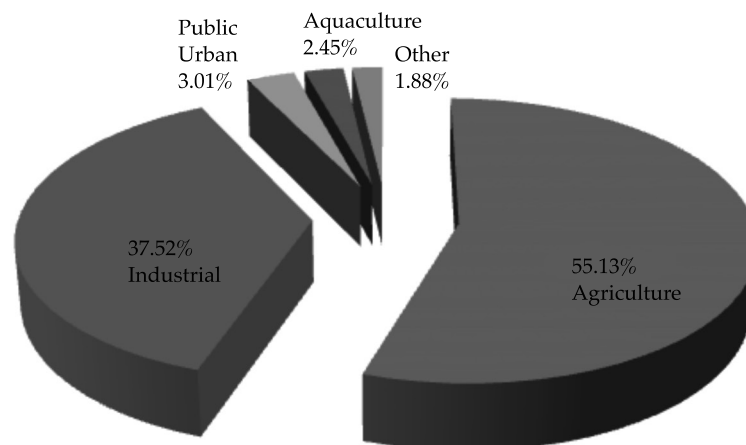
The Result: Marginalization and Social Lag

The surface water reserves allocated to generate electricity resulted in the inability to provide the population with water or a supply for their productive activities, restricting development in the various states

in which the basin is located (Figure 3).

This fact is reflected in the high to very high degree of marginalization in the different municipalities located in the upper basin (Figure 4), kilometers away from the electric plant, primarily in the sub-regions of Tepalcatepec (Middle Balsas) and the Lower Balsas where the water's main productive activity is hydrogenation.

Marginalization is none other than a measurement-summary by state and/or municipality which enables us to observe the overall impact of the unmet needs of the population, such as lack of access to education, inadequate housing, the perception of insufficient income and relationships with residences in small localities. Table 2 shows two states in the basin (Guerrero and Oaxaca) with a very high degree of marginalization and another two (Puebla and Michoacan de Ocampo) with a high degree of marginalization. Another aspect presented in the table worth highlighting is that the marginalization indices for Guerrero, Oaxaca and Puebla are ranked 1, 3 and 5 in the nation, respectively.



Usage of surface water in the region.

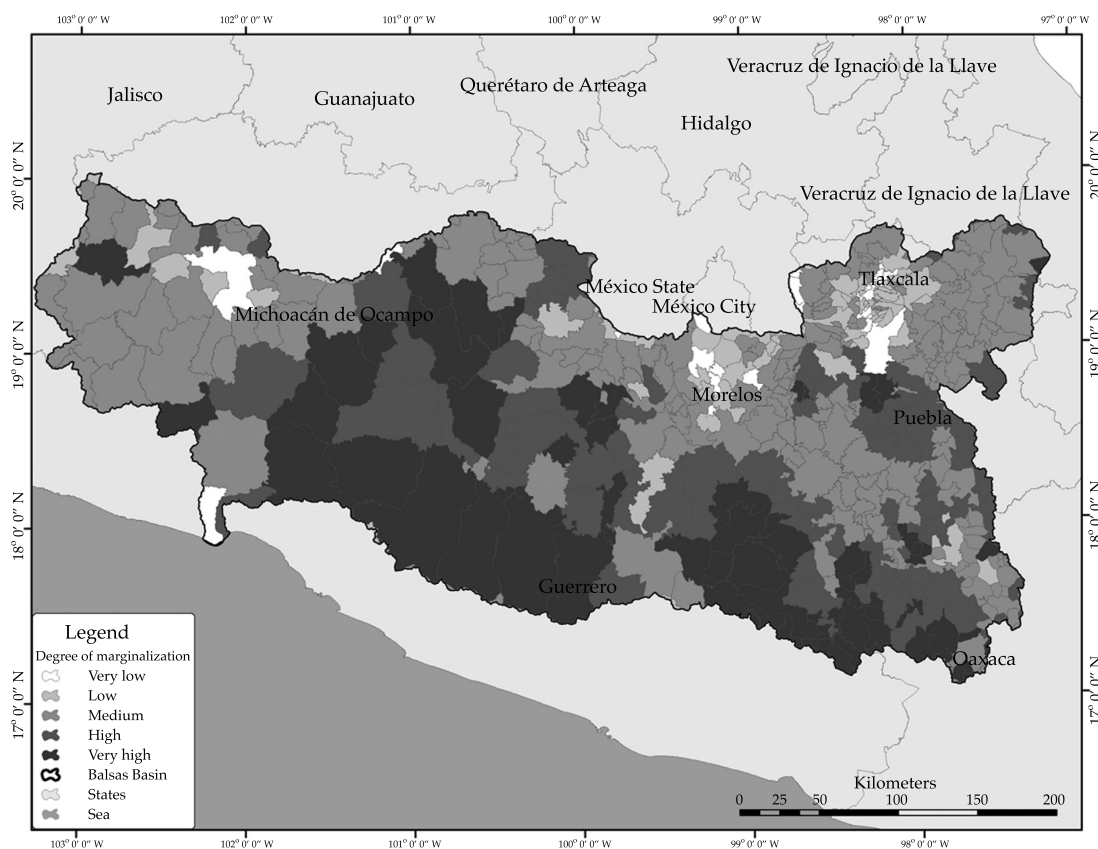


Figure 4. Degree of marginalization in the hydrological region (Conapo, 2010).

Another way to measure, define and identify poverty is using the social lag index, which enables us to see the overall impact of the unmet needs of the population resulting from a lack of education, health services, adequate housing and quality basic services. Table 3 shows the results from this index for the basin.

Prospective Analysis

Productive activities need to grow and intensify in order to achieve a series of strategic objectives, such as combating poverty, economic growth, food security and improving our international competitiveness. But in our country, this development is found to be limited by the availability of water, which results

in different degrees of overexploitation and scarcity. If this trend continues, the unsustainable use of water resources undoubtedly will impose limits on economic and social development.

This is one of the greatest problems not only in our country but worldwide. Therefore, the foundations are being sought today for Mexico to secure the supply of water required for development— using it efficiently, recognizing its strategic and economic value, protecting water bodies and conserving the environment for future generations.

The trends indicate that urban development will take several forms, often with informal housing on the outskirts of urban areas, which are difficult to access and therefore difficult to provide potable

Table 2. Marginalization index (MI) and degree of marginalization (DM) in the zone (estimates from Conapo based on INEGI, Population and Housing Census).

State	% of pop. 15 years or older who are illiterate	% of pop. 15 years or older with incomplete elementary educ.	% household occup. without drainage or toilet	% household occup. without electricity	% of household occup. without plumbed water	% households with some level of overcrowding	% household occup. with dirt floor	% pop. in localities with under 5 000 inhab.	% of pop. with 2 minim. salaries	MI	DM	National ranking
Guerrero	16.82	31.60	19.58	4.38	29.79	50.18	19.61	49.68	54.94	2.53	Very high	1
Jalisco	4.39	18.02	1.50	0.78	3.86	30.10	3.19	17.50	27.15	-0.82	Low	27
Mexico State	4.41	14.29	3.18	0.79	5.67	37.93	3.94	19.10	35.34	-0.55	Low	22
Michoacán	10.25	29.19	3.81	1.70	8.06	36.17	10.98	40.58	43.69	0.52	High	8
Morelos	6.46	17.88	1.98	0.81	8.25	34.17	7.80	24.65	38.23	-0.27	Medium	19
Oaxaca	16.38	33.85	4.01	4.93	23.66	46.53	19.33	61.51	57.77	2.14	Very high	3
Puebla	10.44	25.13	3.09	1.67	12.40	44.59	9.86	38.50	52.45	0.71	High	5
Tlaxcala	5.22	15.52	2.69	1.00	1.47	42.96	3.73	36.40	52.99	-0.14	Medium	16

Table 3. Social lag index (SLI) and degree of social lag (DSL) in the basin (Coneval, 2010).

States	% of pop. 15 years and older who are illiterate	% pop. 6-14 years not attending school	% pop. 15 years and older with incomplete elementary educ.	% pop. without health care	% households with dirt floor	% households without toilet or bathroom	% of households without plumbed water from the public network	% of households without drainage	% of households without electricity	% viviendas que no disponen de lavadora	% of households with a washing machine	SLI	DSL	National ranking
Guerrero	16.68	6.49	53.75	45.75	18.35	19.52	37.74	22.55	4.18	60.57	26.81	2.52	Very high	1
Jalisco	4.36	5.27	41.19	34.51	3.02	2.37	5.34	2.06	0.83	19.20	7.35	-0.66	Very low	25
Mexico State	4.38	3.84	34.76	40.39	3.76	4.02	7.81	5.26	0.81	34.29	20.60	-0.37	Low	19
Michoacán	10.18	7.13	53.71	44.36	10.25	4.96	11.82	10.76	1.75	34.76	18.16	0.75	High	6
Morelos	6.42	5.15	37.19	35.28	7.21	3.17	12.39	4.43	0.97	38.11	14.25	-0.13	Medium	16
Oaxaca	16.27	5.64	57.80	43.08	18.74	5.41	30.10	28.35	5.23	62.70	40.04	2.42	Very high	2
Puebla	10.38	5.78	49.09	49.28	9.46	4.60	16.17	12.31	1.86	52.06	36.31	1.07	High	5
Tlaxcala	5.19	3.28	38.97	37.77	3.85	4.57	4.36	5.36	1.20	51.47	33.68	-0.05	Medium	13

water and treatment services. Meanwhile, in urban zones where extreme poverty is more prevalent, a larger percentage of persons do not have access to water services and their dispersion makes it difficult to provide services. We could say there is a polarization and concentration of development and economic, human and technological resources in regions and areas with fewer natural resources, and this concentration makes them highly vulnerable to overexploitation and pollution.

The Balsas River Basin Committee

The Balsas River Basin Committee (CCRB, Spanish acronym) was created March 26, 1999. The National Waters Law, article 3 section XV, defines the basin committees as mixed member groups to provide coordination and negotiation, support, consultation and advising to Conagua, as well as the corresponding basin organizations, states, municipal and federal entities, and representatives of water users and the civil organizations

related to the respective hydrological basin or region.

The CCRB promotes water management systems using social participation as a key element in the feasibility of plans, programs, norms and regulations to address basic water supply needs and the treatment of water in rivers and streams, as well as to regulate the exploitation and use of surface water, groundwater and wastewater in the basin, in accordance with its availability.

Prospective Technical Analysis

The prospective technical analysis mentioned earlier was developed in order to define the strategic guidelines and criteria for sustainable use of water by different water users as well as to ensure a water supply at the lowest possible cost and with the maximum benefits. This analysis was divided into four areas, which are included in the “2030 Water Agenda.”

The result of this technical study is a description of the supply deficit and sustainability of water for different uses.

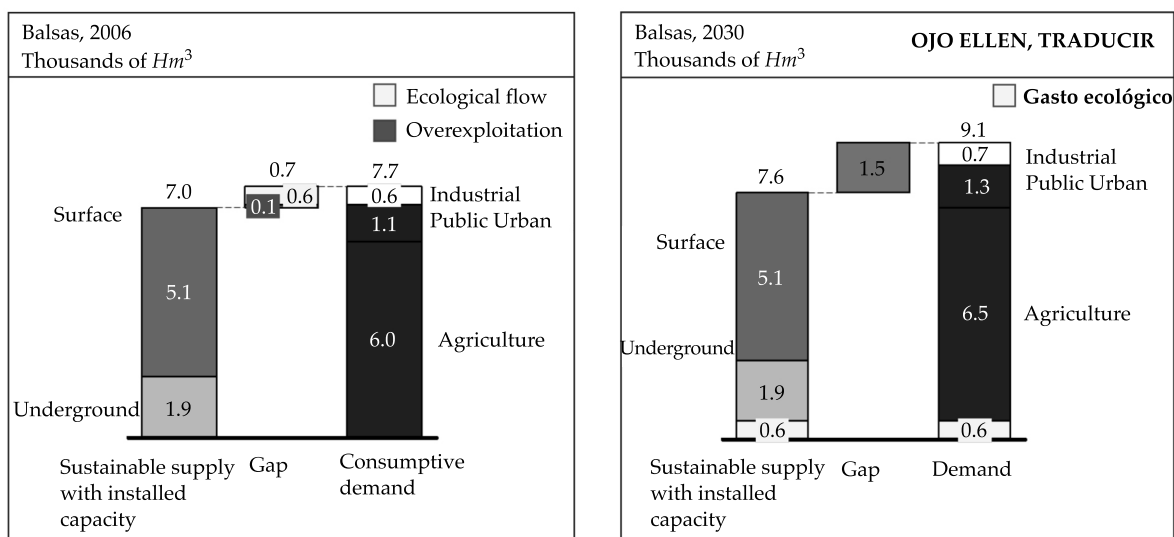


Figure 5. Current “gap” and projected “gap” for 2030.

This is called the “gap” (difference between the accessible sustainable supply per installed capacity and total demand). The study also resulted in a projection of this gap for the year 2030. The study of Balsas Hydrological-Administrative Region IV resulted as follows.

As of the date of the study, the Balsas Hydrological-Administrative Region was able to provide a supply (volume of water that can be delivered to the final user) per installed capacity of 7.0 thousand Hm^3 — 5.1 thousand Hm^3 in surface water and 1.9 thousand Hm^3 in groundwater. Meanwhile, the water consumption demand (volume to satisfy the water required by productive sectors and the society) was 7.7 thousand Hm^3 — 6.0 thousand Hm^3 for farming, 1.1 for public urban use and 0.6 thousand Hm^3 for industrial use.

Based on the above, 0.7 thousand Hm^3 represents unsustainable use in the Balsas Hydrological-Administrative Region, that is, it causes the overexploitation of the aquifers and low ecological flow. The problem worsens considerably when adding a required demand of 12 thousand Hm^3 for non-consumptive use by hydroelectric and thermoelectric plants in the region.

A current projection for 2030, considering the current infrastructure and a growth in demand by the sectors, indicates a gap of 1.5 thousand Hm^3 ; that is, total water demand would be 9.1 thousand Hm^3 while the supply would be 7.6 thousand Hm^3 .

The regions with the largest problem with the sustainability of the resource (the widest gap) are: Upper Balsas, Puebla, 27%; Tepalcatepec, Michoacan, 26%; Middle Balsas, Guerrero, 15%, and Upper Balsas, Morelos, 9%, together representing 76% of the problem in the region.

Evidence of this overexploitation is clearly seen in the aquifers in the basin. The region is divided into 46 aquifers, or hydrological units, to manage and administer groundwater (DOF, 2001), 5 of which are overexploited— Tepalcingo-Axochiapan, in the state of Morelos; Valle de Tecamachalco, Atlixco-Izúcar de Matamoros, Libres Oriental, in the state of Puebla, and Ciudad Hidalgo-Tuxpan, in the state of Michoacan (Figure 6).

And while the number of overexploited aquifers in the region already represents 10.87% of the total, the concern is even greater when observing, for example, that extraction already equals the recharge in the Quitupan aquifer (1439) located in the Lower Balsas sub-region, or the Zacatepec (1703) and Valley of Puebla (2104) aquifers located in the Upper Balsas, with extraction volumes of 95 and 90% of recharge, respectively (Estadísticas del Agua en la Cuenca del Río Balsas, 2010). This reflects the high probability that these aquifers will soon be overexploited.

The importance of groundwater in the Balsas basin is demonstrated by the amount of volume used by the primary users. Of the total groundwater volume

Table 4. Cells with the most problems with water sustainability.

Planning cell	Sustainable offer (Hm^3)	Demand (Hm^3)	Gap (Hm^3)	Percentage of the total in the region
Alto Balsas, Puebla	1 570	1 981	411	27
Tepalcatepec, Michoacán	2 506	2 912	406	26
Medio Balsas, Guerrero	516	739	222	15
Alto Balsas, Morelos	853	983	130	9

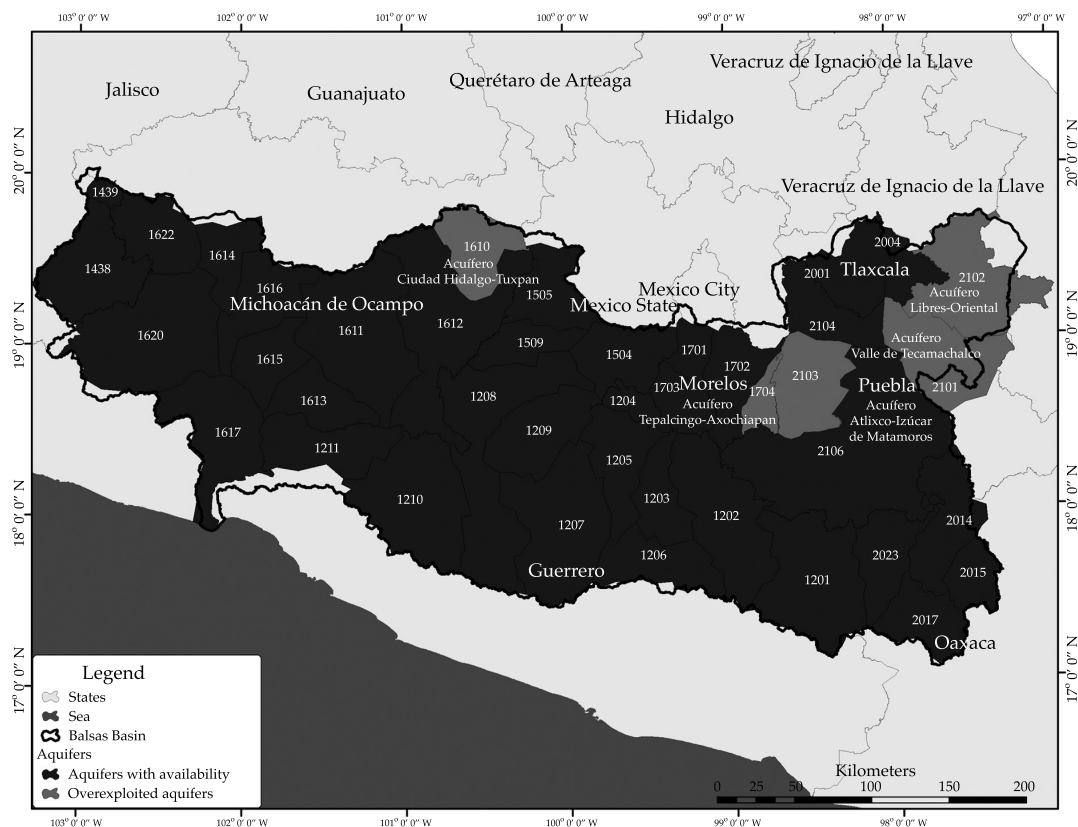


Figure 6. Aquifers in Balsas Hydrological Region No. 18.

permitted for consumption, 56% is for agricultural use, 32% for public-urban use and 12% for consumption. This indicates an increase in the number of overexploited aquifers (Conagua, 2010).

When adding the pollution of surface water, the problem becomes even more serious. This is again shown by the prospective technical analysis conducted in the region. This study shows that 620 Hm³ of municipal wastewater are generated in the basin, only 85 Hm³ of which is treated according to law with the existing infrastructure. This represents less than 15% of the volume generated. The projection for 2030 with the existing infrastructure shows an increased volume of a little over 27%, with a untreated water gap of 791 Hm³.

The regions that this study found to be most affected by water quality problems are: Upper Balsas, Puebla with 44%; Upper Balsas, Morelos with 17%; Upper Balsas, Tlaxcala with 10%; and Tepalcatepec, Michoacan with 7%.

Without considering use by the generation of electricity, agriculture uses a little over 55.13% of the surface water in the hydrological region, industry uses 37.52% and the rest is used for public-urban (3.01%), aquaculture (2.45%) and other (1.88%) purposes.

Even though agriculture represents the largest consumptive use of water in the hydrological region, only 4.9% of the total surface of the hydrological region is irrigated, representing 19% of the total crop area; that is, 81.0% of the agricultural area is seasonal.

In addition, increasing food production to achieve food security for a growing population will increase water scarcity in some regions as well as competition among users. This presents a complex challenge that directly involves water policy as well as agricultural, rural development and economic policies.

At the same time, and to be expected, more scarcity and competition for the use of water resources increases the risk of social conflicts over its use and places pressure on the environmental use of water, compromising social stability and environmental sustainability.

Based on these results, in the Fourth Ordinary Session of the CCRB held March 27th, 2008, the committee agreed that the Conagua would lift the restriction in the Balsas River Basin in order to allocate and reserve volumes for human use and consumption.

This rather extensive process consisted of specific planning of actions to be conducted, the search, integration and analysis of data, and several meetings of specialized groups, as well as performing various calculations to estimate the possibility of modifying the restrictions. To this end, technical studies were performed of national surface water in Balsas Hydrological Region No. 18, according to the NOM-011-CONAGUA-2000.

During the 30th session of the Balsas River Basin Committee's Follow-up and Evaluation Group, held May 30th, 2007, the Specialized Planning Group was created on September 27, 2007 with the main objective of creating mechanisms to enable revising the Agreement for the Restriction of the Balsas Hydrological Region No.18 and identify options to increase the availability of water for different uses while revising the restrictions.

The Specialized Planning Group was composed of representatives from the three levels of government, as well as users and organized civil groups who discussed the surface water problem in the basin. This workgroup established the criteria to determine the additional volumes of surface water from the Balsas River that will eventually be allocated to supply potable water to communities with no other supply options.

The proposed municipalities in each state and their respective volumes are shown in Table 5.

A volume of 332 646 793 m³ of surface water is projected for 2030 to supply 340 municipalities in the 8 states in Balsas Hydrological Region No. 18, which is feasible to obtain from the dams that supply the hydroelectric plants. Table 6 shows the potential reductions corresponding to these plants.

Table 5. Surface water requirement, by state.

State	Municipalities	Requirement (l/s)	Requirement (m ³ /year)
Mexico State	34	2 169.06	68 403 497.35
Guerrero	39	2 749.59	86 711 143.44
Jalisco	3	17.89	564 314.97
Michoacán	29	1 831.49	57 757 732.25
Morelos	21	1 702.26	53 682 542.61
Oaxaca	78	686.6	21 652 597.53
Tlaxcala	6	66.59	2 100 000.00
Puebla	130	1 324.68	41 774 965.25
Total	340	10 548.16	332 646 793.39

Table 6. Potential volumes of surface water required by hydroelectric plants.

Hydroelectric plant	Federal Elec. Commission License No. m ³ /year	% reduction in volume	National water requirement for domestic, public and urban use	
			(l/s)	m ³ /year
Portezuelo I (Echeverría)	56 581 000	42.06	754.63	23 797 969
Portezuelo II	61 043 000	38.80	751.04	23 684 684
Bartolina	15 444 000	0.00	0.00	0.00
Cóbano	330 599 000	4.64	486.42	15 339 794
Cupatitzio	427 032 000	3.59	486.13	15 330 449
El Caracol	4 453 787 000	4.15	5 860.99	184 832 161
El Durazno	290 950 000	3.00	276.78	8 728 500
Itzícuaró	18 720 000	12.75	75.68	2 386 800
Ixtapantongo	536 098 000	1.63	277.09	8 738 397
San Pedro Porúa	18 142 000	0.00	0.00	0.00
Santa Bárbara	546 198 000	1.68	290.97	9 176 126
Tamazulapam	23 661 000	3.58	26.86	847 064
Tingambato	625 601 000	1.60	317.40	10 009 616
Zumpimito	277 862 000	5.52	486.36	15 337 982
Infiernillo	12 699 153 000	2.09	8 416.17	265 412 298
La Villita	12 699 153 000	2.09	8 416.17	265 412 298
Total	33 080 024 000	2.57		849 034 137

On October 21, 2010, the 5th Ordinary Session of the Basin Committee was held, in which the technical studies of the national surface waters in Balsas Hydrological Region No. 18 were approved. This established the volumes required to supply national surface water to public urban and domestic users in the municipalities in the basin up to the year 2030. Its publication in the *Official Journal of the Federation* (DOF, Spanish acronym) was authorized.

The proposal was submitted for consideration by the Presidency of the Republic's Judicial Board after meeting all the judicial and administrative requirements by Conagua and the Ministry of the Environment and Natural Resources, and after review by the Federal Commission for Regulatory Improvements. The Judicial Committee approved it on January 26th, 2011, and the agreement was published in the DOF, thereby making public the technical studies of the national surface waters in the Balsas Hydrological Region

No. 18. This is one of the most important steps towards the modification of the decree restricting the use of the water in the basin.

The Official Mexican Norm (NOM, Spanish acronym) NOM-011-CONAGUA-2000, Conservation of Water Resources, establishes the specifications and the method to determine the annual mean availability of national waters in a hydrological regions based on the main channel and the discharge in the region. This is determined and calculated using the expression:

$$D = Ab - R_{xy}$$

where:

D = annual mean availability of surface water in the basin.

Ab = annual mean volume of runoff downstream from the basin.

R_{xy} = current annual volume usage committed downstream.

The basin's annual mean downstream runoff volume is determined by the expression:

$$Ab = Ar + Cp + R + Im - Ex - Uc$$

where:

Ar = annual mean runoff upstream from the basin.

Cp = annual mean natural runoff.

R = annual return volume.

Im = annual importation volume.

Ex = annual exportation volume.

Uc = annual volume of surface water extraction.

Table 7 presents the application of the equation to calculate Ab in each basin, as well as the relationships between them to determine the annual mean runoff upstream from the basin (Ar) into the sequential basins.

Runoff downstream (Ab) from this basin is represented by the remaining resources from basin X (Cp and R) and the resources supplied by the other basins (Ar and Im) after satisfying demand (Uc , Ex). This runoff obviously becomes term Ar in basin Y and, depending on its own supply, some or all of this supply (R_{xy}) will be needed to satisfy its own demands. Thus, the non-committed (D) availability in basin X is given by:

$$D = Ab - R_{xy}$$

If Ab is less than the amount committed downstream (R_{xy}), mathematically D would be negative, but in real terms it can be said that there is no availability downstream from the study basin.

The condition of whether a basin may provide new water resources for use depends on whether the availability D is greater than or equal to zero.

Results

After thoroughly evaluating the conditions in the basin and the availability of the water resource, and after conducting the different work sessions (with participation from society, the Federal Electric Commission, state and federal governments), the modification of the degree was signed on March 19, 2011 in the city of Huetamo, state of Michoacan, and published in the DOF on March 22, 2011 as "DECREE to modify the diverse instruments that constitute national water reserves and establish restrictions in Balsas Hydrological Region No. 18," the same day of the "World Water Day." This decree took effect on March 23, 2011 and directly benefits 340 municipalities and 4 245 115 inhabitants until the year 2030.

In addition, at this same meeting the Follow-up and Evaluation Group was instructed to analyze the feasibility of making surface water available for uses other than human consumption, beginning with non-consumption uses, and if applicable propose the corresponding strategies. This initiated a new planning process with new goals and objectives.

The aim of this new decree was to administer the use of national waters in this hydrological region in order to give priority to addressing the existing problems in the basins in this region and to solve the conflicts associated with the problems described. The primary goal is to solve the water supply problem in the region and primarily to regulate domestic and public urban uses in the riverside municipalities in the basin, as well as increase the coverage of potable water services.

The Decree stipulates the following:

The reserved water may be used, in the volume required, for domestic and public

Table 7. Annual mean runoff volume in the basin downstream, millions of cubic meters.

Hydrological Basin	Ar	Cp	R	Im	Ex	Uc	Ab	R _{xy}	D	Availability
Alto Atoyac River	0	448.9	244.2	0	316.9	403	-26.8	0.0	-26.8	Deficit
Amacuzac River	0	2 102.40	189.1	0	6	1 053.40	1 232.1	1 537.8	-305.7	Deficit
Tlapaneco River	0	1 040.90	4.5	0	0	18	1 027.4	1 282.4	-255.0	Deficit
Nexapa River	0	497.1	193.5	97.9	0	744.7	43.8	54.6	-10.8	Deficit
Mixteco River	0	874.3	36.7	0	3.7	93.1	814.2	1 016.4	-202.2	Deficit
Bajo Atoyac River	3 117.60	423.8	33.7	219	0	301.3	3 492.80	4 434.4	-941.6	Deficit
Cutzamala River	0	2 246.50	3 392.20	0	59.2	3 595.50	1 984	1 919.5	64.5	Deficit
Medio Balsas River	5 004.90	3 921.30	4 528.10	6	86	4 937.50	8 436.80	12 076.7	-3 639.9	Deficit
Cupatitzio River	0	1 118.60	1 148.60	0	0	1 834.50	432.7	618.4	-185.7	Deficit
Tacámbaro River	0	917.9	67.1	0	0	223.5	761.5	1 088.4	-3 26.9	Deficit
Tepalcatepec River	0	1 734.00	731.9	0	19.6	1 646.80	799.5	1 142.8	-343.3	Deficit
Bajo Balsas River	10 442.30	1 261.10	15 885.10	0	647.3	16 122.10	10 819.10	0.0	10 819.1	Availability
Paracho-Nahuatzen River	0	83.2	0	0	0	0	83.2	85.0	-1.8	Deficit
Zirahuén River	0	40.2	1.5	0	0	3	38.7	55.0	-16.3	Deficit
Libres-Oriental River	0	346.3	2.4	0	0	6.6	342.1	350.0	-7.9	Deficit
Total		17 056.50	26 458.60	322.9	1138.7	30 983.00				

urban purposes...and with no limits on flow diversion or annual volume for the operation of hydraulic works under the responsibility of the National Waters

Commission. Persons or corporations requiring the use of national waters according to the terms of the Reserves, as modified by the Decree herein, shall submit a request to the National Water Commission for rights or allocation, as long as no case exceeds the volumes determined for each State.

This decree extends the restrictions to the 15 tributary basins currently in the region for 80 years in order to re-establish ecological balance and promote a new distribution of the water runoff without compromising the stability of the hydrological region, while applying the existing water reserves to usage requiring priority attention.

In the short-term, the modification of the reserve agreements has permitted legally allocating volumes to the municipalities benefited by the decree, thereby supplying communities that have historically lacked this valuable resource (Figure 7).

Having quality water in sufficient quantities enables the population to have access to levels of social and economic wellbeing that will decrease poverty and marginalization.

This modification of the restricted volumes in the basin does not increase the amount of water rights granted but rather reduces the volume allocated to generating electricity, which represents a little over 1% of the volume granted to the Federal Electric Commission for the 17 existing hydroelectric plants and the three thermoelectric plants in the basin. As a result of this technical study and the

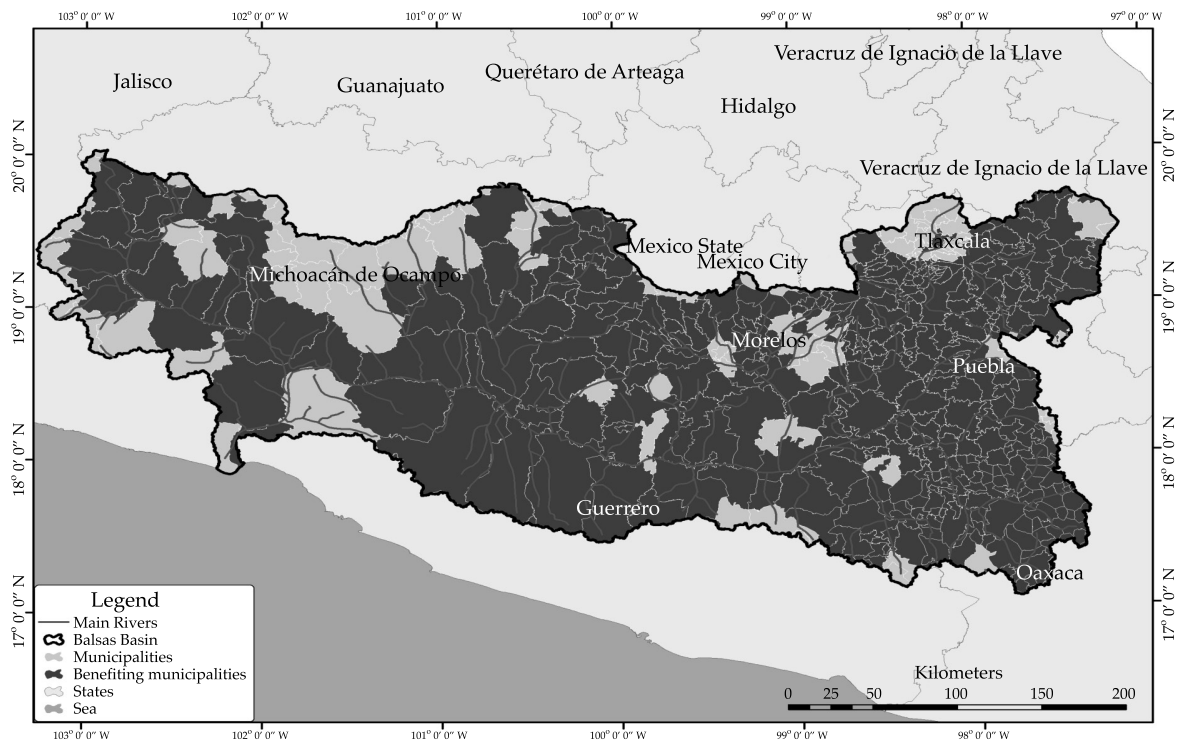


Figure 7. Municipalities benefited by the modifications of the restrictions.

specific calculations were performed, it was determined that the corresponding volume does not affect the production of the plants mentioned. Thus, Conagua modified the volume allocated in accordance with its authority granted by the National Waters Law.

After gaining this important achievement for the region, work was carried out to deliver the water rights titles to these municipalities, beginning with the publication in the Federal Official Journal on June 24, 2011 of guidelines for granting licenses and allocating national surface water in the Balsas Hydrological region.

As a result of this modification and after an application process for allocations and rights, on October 5, 2011 (Conagua, 2011) the president of the Mexican Republic delivered 340 licenses corresponding to or a volume of 219 645 221.83 m³/year and reserved a volume of 113 001 678.17 m³/year for future allocations (Table 8). This occurred at an event by Conagua at the facilities of the Commission in the presence of municipal presidents, governors, ministers and other authorities involved in water resources, as well as those receiving the benefits and civil society.

Conclusions

The modification of the decree for the restriction and reserves related to the Balsas brought about an end to a 70-year prohibition on the use of surface water in the region.

The modification of the decree benefitted 340 municipalities, representing 80% of the total municipalities in the basin. A total of 4 245 115 inhabitants will be benefitted up to the year 2030, which is 38.6% of the total population of the basin.

The volume allocated was 219 645 221.83 m³/year, and a volume of 113 001 678.17 m³/year was reserved for future allocations.

The total volume required by the municipalities in the basin— 332 646 793.39 m³/year ³/₄represented only 1% of the total volume granted to the Federal Electric Commission (33 080 024 000 m³/year), which will not affect the functioning of the hydroelectric and thermoelectric plants installed in the region.

By having quality water in sufficient quantities, the population will have access to levels of social and economic wellbeing which will decrease poverty and marginalization.

Table 8. Volume designated and reserved in the region, by state.

State	No. of municipalities	Volume designated (m ³ /year)	Volume reserved (m ³ /year)
Mexico	34	45 959 262.12	22 444 237.88
Jalisco	3	112 279.36	452 070.64
Morelos	21	18 117 579.58	35 564 970.42
Tlaxcala	6	422 349.62	1 677 650.38
Guerrero	39	77 710 199.30	9 000 950.70
Michoacán	29	29 616 736.84	28 141 013.16
Oaxaca	78	12 509 975.01	9142 624.99
Puebla	130	35 196 840.00	6 578 160.00
Total	340	219 645 221.83	113 001 678.17

References

- Conagua (2010). *Estadísticas del agua en la cuenca del río Balsas, 2010*. México, DF: Organismo de Cuenca Balsas.
- Conagua (2011). *Estudios técnicos de aguas nacionales superficiales de la Región Hidrológica número 18 Balsas*. México, DF: Organismo de Cuenca Balsas.
- Conagua (2010). *Análisis técnicos prospectivos de la Región Hidrológica número 18 Balsas*. Cuernavaca, México: Organismo de Cuenca Balsas.
- Conapo (2010). *Índices de marginación 2010*. México, DF: Consejo Nacional de Población.
- Coneval (2010). *Índices de rezago social 2010*. México, DF: Consejo Nacional de Evolución de la Política de Desarrollo Social.
- DOF (varios años). Acuerdo por el que se determina la circunscripción territorial de los Organismos de Cuenca de la Comisión Nacional del Agua (abril, 2010); Nacionalización de la industria eléctrica (diciembre, 1960); Declaratoria de constitución de las reservas nacionales de energía eléctrica en las aguas del río Balsas (junio, 1940; octubre, 1956; agosto, 1958; febrero, 1966); Acuerdo por el que se dan a conocer los estudios técnicos de aguas nacionales superficiales de la Región Hidrológica núm. 18 Balsas (enero, 2011); Decreto por el que se modifican los diversos por los que se constituyen reservas de aguas nacionales y se establece la veda en la Región Hidrológica núm. 18 Balsas (marzo, 2011). *Diario Oficial de la Federación*.
- Horrillo, J. M., Pedrozo, A., & Onandía, B. (enero-marzo 2011). Mapa Nacional de Erosión Potencial. *Tecnología y Ciencias del Agua*, 2(1), 5-19.
- INEGI (varios años). *Series Históricas; 1960-2005; VIII Censo General de Población 1960; IX Censo General de Población y Vivienda 1970; X Censo General de Población y Vivienda 1980; XI Censo General de Población y Vivienda 1990; Censo de Población y Vivienda 1995; XIII Censo General de Población y Vivienda 2000; II Censo de Población y Vivienda 2005; Censo y Censo de Población y Vivienda 2010*. México, DF: Instituto Nacional de Estadística y Geografía.

Institutional address of the author

Ing. Juan Carlos Valencia-Vargas

Comisión Estatal del Agua, Morelos
Avenida Plan de Ayala 825, cuarto piso
Plaza Cristal, Col. Teopanzolco
62350 Cuernavaca, Morelos, MÉXICO
Teléfono: +52 (777) 1008 370, extensión 1503
juancarlos.valencia@morelos.gob.mx



Conservation Works, Patzcuaro, Michoacan, Mexico.

Photo: Roberto Menéndez.

Prioritization of Needs to Replace Piping Using GIS and Multicriteria Evaluation

• Vivian Verduzco* • Jaime Garatuza • Salvador Díaz •
Instituto Tecnológico de Sonora, México

*Corresponding Author

Abstract

Verduzco, V., Garatuza, J., & Díaz, S. (January-February, 2015). Prioritization of Needs to Replace Piping Using GIS and Multicriteria Evaluation. *Water Technology and Sciences* (in Spanish), 6(1), 99-120.

Although the deterioration of infrastructure directly affects the physical efficiency of systems, it is financially impossible to renovate entire systems. This situation requires prioritizing actions to increase the efficiency of potable water networks. One of the primary components affecting the physical efficiency of water supply systems are pipes, which are affected by a series of parameters related to the hydraulic behavior of the system (age of piping, material, roughness, pressure, demand and diameter, among others). The development of a hydraulic simulation model using the Pipelinet system in ArcGis provides real-time information about conditions and risks associated with potable water, considering the spatial component, which determines the importance of each element in the network according to its location. This facilitates a multicriteria analysis of factors that are endogenous and exogenous to piping, for consideration by authorities of operations entities in order to prioritize activities to rehabilitate, replace and expand the system. The present work is intended to integrate the advantages of a geographic information system (GIS) into a multi-attribute analysis of the urban potable water distribution system of Providencia, Sonora, Mexico, and to propose a decision-making method to support the planning and control of the potable water network.

Keywords: Hydraulic model, planning, water distribution systems, rehabilitation, decision making.

Resumen

Verduzco, V., Garatuza, J., & Díaz, S. (enero-febrero, 2015). *Priorización de necesidades de reemplazo de tuberías usando SIG y evaluación multicriterio*. *Tecnología y Ciencias del Agua*, 6(1), 99-120.

El deterioro de infraestructura afecta directamente la eficiencia física del sistema, sin embargo, debido al factor económico es imposible renovar el sistema en su totalidad. Tal situación demanda el establecimiento de prioridades en acciones para el incremento de eficiencias en la red de agua potable. Uno de los principales componentes que afectan la eficiencia física de los sistemas de abastecimiento de agua son las tuberías, las cuales son afectadas por una serie de parámetros que condicionan el comportamiento hidráulico del sistema (edad de la tubería, material, rugosidad, presión, demanda y diámetro, entre otros). La integración del modelo de simulación hidráulica, mediante el sistema Pipelinet basado en ArcGis, brinda información en tiempo real acerca de las condiciones y riesgos de la red de agua potable, considerando la componente espacial, la cual condiciona la importancia de cada elemento de la red de acuerdo con su ubicación. Esto facilita un análisis multicriterio, considerando factores endógenos y exógenos de las tuberías, tomados en cuenta por las autoridades participantes en un organismo operador en la tarea de jerarquizar actividades de rehabilitación, reemplazo y crecimiento del sistema. En el presente trabajo se pretende integrar las bondades que ofrecen los sistemas de información geográfica (SIG) en un análisis multiatributo del sistema de distribución de agua potable urbano en Providencia, Sonora, México, y proponer un método de toma de decisiones que apoye la planeación y el control de la red de agua potable.

Palabras clave: modelo hidráulico, planeación, red de agua potable, rehabilitación, toma de decisiones.

Received: 09/12/13

Accepted: 11/09/14

Introduction

Deterioration of infrastructure threatens the quality of water provided to users and directly affects the efficiency of systems.

Nevertheless, it is financially impossible to rehabilitate or renovate entire systems (Castelán, 2001; Tortajada, 2006; Yamijala, 2007). When prioritizing the needs of a potable water distribution system, it is

necessary to consider factors that are endogenous and exogenous to the system (Alonso-Guzmán, 2010). The evaluation of these factors will enable prioritizing rehabilitation and replacement activities.

Deficiencies in the use of water for urban services and poor management of the resource have been identified as international problems (Garduño, 1994). The National Water Commission (NWC) has performed several analyses and in reports on the program to modernize water operations entities indicated an average overall efficiency of operating entities (OE) in the country of 36%. This is the result of physical and commercial efficiency, which are 52.1% and 69.5%, respectively (CNA, 2008). If the trends over recent years continue it will be difficult to provide continuous water service to cities with a high growth rate that are using systems with poor physical efficiency, since increasing the coverage involves increasing the infrastructure and the amount of water supplied to the network, which would increase losses (CEA, 2004).

The municipality of Cajeme is located in the southern portion of the state of Sonora, Mexico (Figure 1). It is the second largest in the state, with an operating entity which can supply over 95% of the urban area and 93% of the rural area (Ayuntamiento de Cajeme, 2000). Because of ongoing deterioration in the potable water pipes installed in the early 20th century (period of high economic growth in the municipality), leaks from fissures and ruptures in the piping present a constant problem. The lack of a plan by the OOMAPASC (Spanish acronym; Cajeme potable water operations, sewage and treatment entity) to replace the piping has led to improvised responses to failures in the distribution networks, which involve high costs and low benefits for the system.

Addressing this serious situation is a significant challenge for society and par-

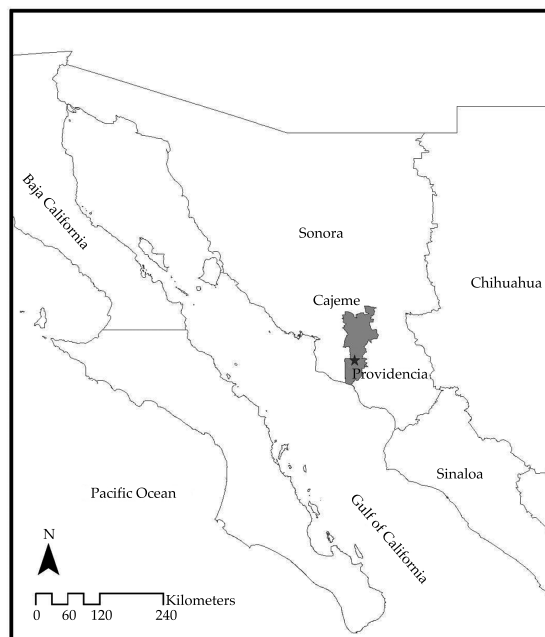


Figure 1. Location of Providencia Sonora, Mexico.

ticularly for the planners and administrators of potable water supplies. It involves developing new ways to address the problem, increasing the use of new technologies and improving communications among decision-makers—efforts which have become increasingly necessary (Kallis & Coccossis, 2001). Given this context, the article herein proposes a methodology to aid planning and decision-making by establishing priorities for the rehabilitation of potable water systems. This methodology is based on a multicriteria evaluation of factors that are endogenous and exogenous to the distribution network that are relevant to prioritizing rehabilitation needs, using calculations by a hydraulic simulation model and the use of a Geographic Information System (GIS).

Material y Materials and Methods

To perform this study, a series of procedures was followed to facilitate

making decisions about the rehabilitation of a potable water distribution system based on the case study of the current system in Providencia, Sonora, located in the municipality of Cajeme (Figure 1). The objective of describing the methodology is to highlight how the use of GIS can improve planning actions related to a potable water distribution system.

*TD*Decision-making

Decision-making has become a mathematical science which formalizes the human reasoning and thinking used to choose a solution to a problem. In the overall process proposed by Eastman (2006), the first step in decision-making is to establish the objective of the decision. Given the context presented herein, the objective of this work is to prioritize and select the piping that most needs to be rehabilitated in the potable water distribution system in Providencia,

Sonora. Figure 2 presents the decision-making methodology proposed, which was applied to the current conditions of the case study distribution network.

Identification and Establishment of Decision Factors

In the analysis of the functioning of the potable water network, endogenous and exogenous factors that describe the deterioration of the piping and the aging process are identified (Alonso-Guzmán, 2010; Alonso-Guzmán, Pérez-García, Izquierdo-Sebastian, & Herrera-Fernández, 2013). Information was analyzed to establish the selection criteria, considering quantifiable elements or evidence that can be used to make decisions related to the objective mentioned previously.

The decision factors that influence the prioritization of the rehabilitation of the infrastructure were established based on the

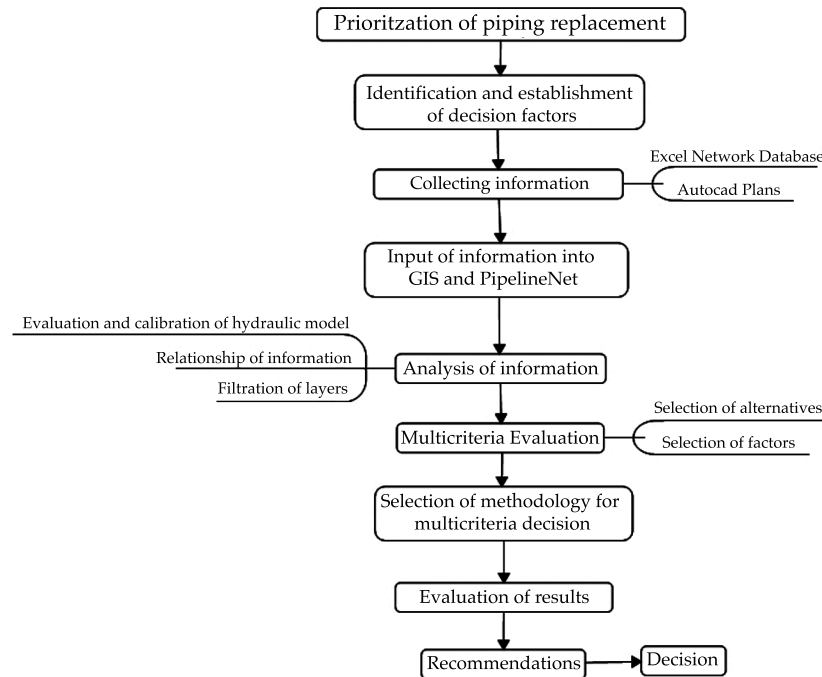


Figure 2. Decision-making steps adapted from Morais and Almeida (2006).

experience of the operating entity. Options were thereby proposed by identifying not only traditionally technical criteria but also spatial, economic and social criteria that are key to selecting piping to be replaced. This involves considering endogenous and exogenous factors that can provide information about problems and the state of the distribution network. To accomplish the objective mentioned, the factors presented in Figure 3 were determined based on the information available for the case study.

Table 1 shows the factors included and the criteria applied to determine the priority states.

The leaks index was calculated according to reports by OOMAPASC, which was based on the number of leaks for each pipe divided by the length of the pipe and the years with a history of leaks:

$$LI = \text{no. of leaks} / \text{length} / \text{years}$$

The number of years included those for which the OOMAPASC reported leaks. Whether the pipe had been recently replaced was also taken into account, and the year of replacement was used to

prevent calculating a high index for a pipe that had a large number of leaks in the past but had been replaced.

The significance index proposed by Arulraj and Rao (1995) was used, which is calculated for each pipe as follows:

$$SI = LQ / (CD)$$

Where L = length of the pipe (m); Q = flow in the pipe (m^3/s); D = diameter of the pipe (m); C = Hazen-William coefficient. Based on this index, the relative importance of each one of the pipes in the network was calculated.

Collecting the Information Needed for Decision-Making

Location and Characteristics of the Study Zone

The project is located in the town of Providencia, municipality of Cajeme, state of Sonora, Mexico. Providencia has a population of 4 510 inhabitants and is located at $109^\circ 59' 36''$ longitude and $27^\circ 30' 37''$ latitude, at an average altitude of 30 meters (INEGI, 2005). It is bordered on the

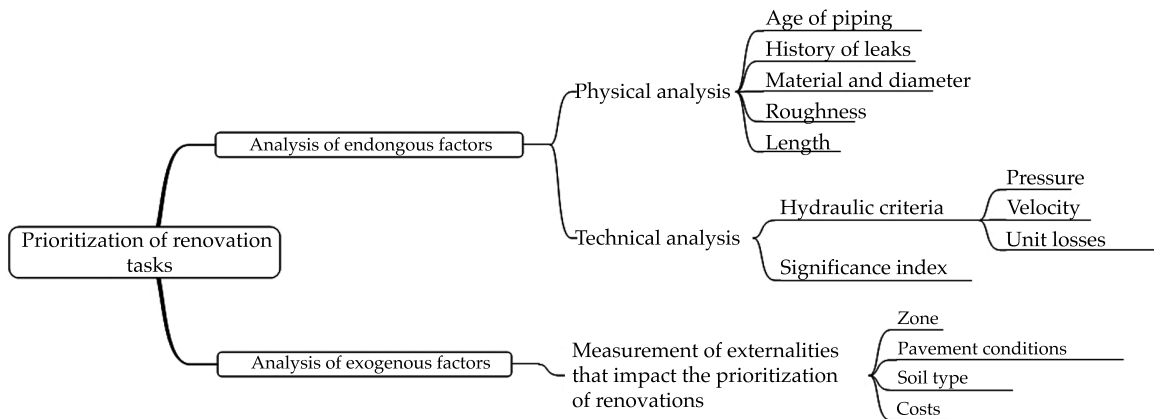


Figure 3. Classification of factors that influence the prioritization of renovation tasks.

Table 1. List of factors or attributes of the distribution system.

Factor, F	Decision Factors	Criteria
F1	Zone	Vulnerable zones, that is, areas near hospitals, shelters, schools, sports centers, commercial zones, etc. which are more important to rehabilitate.
F2	Material and diameter	Order in relation to material and diameter of piping. According to the literature reviewed, a smaller diameter represents more risk of failure. Importance according to whether it is a main or secondary distribution line.
F3	Roughness coefficient	To create the model, predetermined values from the manufacturer's tables are used. Then, these coefficients are determined and used to calibrate the model. The criteria will be to give a higher priority to a high roughness coefficient. Value ranges for each material are established.
F4	Paved zone	According to the criteria by the OE, priority is given to the zone containing pavement since it directly impacts repair costs.
F5	Leak index	Lines with a high leak index, calculated according to reports and supervisor experience (see equation (1)). A high index received higher replacement priority (Bourguett, 2001).
F6	Importance	According to the significance index (see equation (2)). The higher significance index the higher its importance to the system (Arulraj & Rao, 1995).
F7	Repair cost	Based on the average unit value for the repair of each type of piping.
F8	Length	Based on information from the network. Criteria established by the analysis of the literature, the longer the length the greater the risk of a leak.
F9	Velocity	Pipes should have a maximum velocity of 5.0 m/s and minimum of 0.3 m/s (CNA, 2009).
F10	Unit loss in load	Losses in load due to friction between sections should not exceed 5 km (CNA, 2009). Over 5 m /km represents low efficiency, therefore poor functioning.
F11	Pressure	Pressures should be between 1.5 and 5 kg/cm ² . For small urban localities a minimum of 1.0 kg/cm ² is acceptable (CNA, 2009). According to the literature review, higher pressure represents higher risk of failure.
F12	Age	For primary distribution networks, 20 to 30 years of useful life is expected. For secondary distribution networks, 15 to 30 years (CNA, 2009), Old piping represent a higher risk.

east by the municipal capital which is the City of Obregon.

The collection and integration of information constitutes the key part of the

proposed methodology. Table 2 presents the information that was collected and the computing package used for incorporating it into the GIS.

Table 2. Information Integrated into a GIS and Analyzed.

Original format	Information
Autocad Plans	Piping diameter
	Piping connections
	Trazo y ubicación de tuberías
	Level curves
	Lotification
	Location of new intakes
	Property information
Excel Database	ID
	Location
	Age of piping
	Diameter
	Material
	Roughness
	Significance index
	Flow
	Leaks
	Unit price
	Nodes

Integration and Analysis of GIS Information

The information about the study area was integrated. The methodology used was as follows:

1. Physical assembly, transfer of existing water network plans from AutoCAD to GIS format using *Arcview*.
2. Information from AutoCAD plans was integrated into the GIS, including information about the town, such as division of lots, blocks, location of piping, etc. To this end, a detailed inspection needed to be performed of the information contained in each layer of AutoCAD, verifying that each element contained its identifier and corresponding layer.
3. The information in each layer was then filtered and extracted for use in “shapes” according to their attributes (Table

3). Table 4 specifies the information obtained from the municipal records.

The ID data corresponding to the piping, location, age, length, diameter, material, roughness, significance index, leaks, unit price and nodes previously entered into a database (*MS-Excel*) were input into the GIS. This was done after classifying the information contained in the GIS file, that is, the ID was assigned to each of the data (pipes, nodes and other elements) in the GIS for later correlation with the data collected in the *MS-Excel* database, joining the information with the “join” command.

Pipelinenet

After collecting the data pertaining to the distribution network, a simulation model of the hydraulic behavior of the potable water network was developed and calibrated using *Pipelinenet*. This

Table 3. Fields composed of information from the AutoCAD plans.

Layer Name	Type	Information
ProvPipes	Polyline	Location of piping in the AP distribution system according to field data and information from OE.
ProvNodes	Point	Location of nodes in the distribution system from field data and information from the OE.
Current Lotification	Polyline	Community lots. Information obtained from the AutoCAD plans of the photographic restitution of Providencia. Municipal Property Department.
Level Curves	Polyline	Elevation lines of the natural terrain based on information from the municipal archives.
New Intakes	Point	Intakes installed from 2006-2010 obtained from the potable water operating entity (OOMAPASC).
Vulnerable Zones	Polygon	Areas with hospitals, shelters, schools, sports centers, parks, commercial zones, etc. (information obtained in the field and from municipal records).

Table 4. Fields based on information from the Municipal Property Department, Cajeme.

Layer Name	Type	Information
Neighborhoods	Polygon	Locations of the neighborhoods in the community.
Blocks	Polygon	Boundaries and locations of blocks in the town.
Providencia Streets	Polyline	Location, length and pavement conditions of streets and roads in the town according to information from the municipal records and obtained in the field.
OBR106,OBR107,OBR108, OBR95,OBR96,OBR97, OBR84,OBR85,OBRE86.tif	"raster"	Very high quality photographs in *.tif format, georeferenced in *.tfw files.

is an *ArcGIS*-based system designed for hydraulic and water quality modeling. The steps used in the analysis, evaluation and calibration of the hydraulic model in *Pipelinenet* will be described next.

Hydraulic Simulation Model

Analysis

Information obtained from the operating entity and in the field was input into the hydraulic model in *Pipelinenet*. This included diameter, material, age of the pipes, roughness, topography of the terrain,

location of the pump, flow provided by the pump, elevation of the pump, functioning of the network and tank.

The hydraulic simulation model was developed using static and dynamic simulations. The Darcy-Weisbach equation was used for head loss.

Calibration

Calibrations were performed for different scenarios. The model was primarily calibrated by comparing and analyzing field data obtained from the assembly of a measurement system with the data

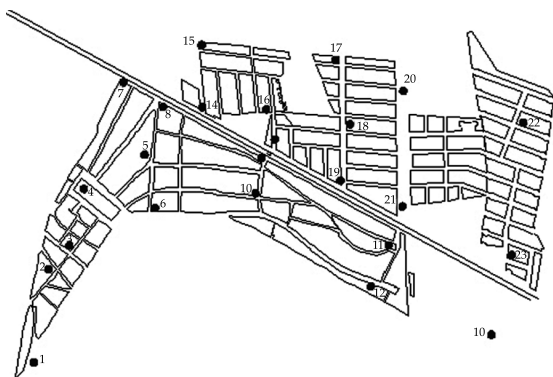


Figure 4. Location of calibration points coordinates.

predicted by the model. To this end, pressure data was obtained at 23 points in the distribution network for two days during two time periods (peak hour in the morning and in the afternoon). The locations of the calibration points are shown in Figure 4 and their coordinates are presented in Table 5. This is an iterative process in which successive and appropriate adjustments were made to the model so it would respond to reality with the degree of precision desired. To calibrate the model, the following parameters were

modified in *Pipelinenet*: 1) consumption scenarios (changes in flows assigned to nodes) assuming possible leaks due to the deterioration of the network; 2) roughness values, assuming mineral incrustations which can reduce the inside diameter of the piping; 3) pumping capacities, assuming poor pumping efficiency. The model was calibrated until the results were satisfactory according to recommendations by the National Water Commission (CAN, 2009).

Five manometric pressure sensors with data-loggers were installed at 5 points in the town, thereby obtaining a registry of changes in pressure in the network over the day. These were monitored from Monday through Sunday for one week. Table 6 presents the coordinates of the location of the data-loggers. These data were used to calibrate the dynamic model.

Demand Curve

Information obtained from the NWC (CNA, 2007) related to changes in hourly flow for small towns was used to analyze the model in dynamic mode. Figure 5 shows the values of the variations in

Table 5. Location of calibration points coordinates.

Point	Coordinates		Point	Coordinates	
	N	W		N	W
1	27° 30' 42.1"	109° 59' 79.0"	13	27° 30' 29.8"	109° 58' 56.2"
2	27° 30' 57.0"	109° 59' 74.0"	14	27° 30' 80.4"	109° 59' 44.7"
3	27° 30' 60.6"	109° 59' 69.5"	15	27° 30' 89.7"	109° 59' 39.3"
4	27° 30' 66.4"	109° 59' 69.0"	16	27° 30' 86.5"	109° 59' 36.4"
5	27° 30' 64.8"	109° 59' 57.6"	17	27° 30' 89.2"	109° 59' 22.1"
6	27° 30' 75.8"	109° 59' 57.1"	18	27° 30' 81.5"	109° 59' 20.2"
7	27° 30' 87.8"	109° 59' 63.1"	19	27° 30' 70.4"	109° 59' 20.9"
8	27° 30' 82.5"	109° 59' 55.1"	20	27° 30' 82.7"	109° 59' 10.8"
9	27° 30' 72.3"	109° 59' 38.6"	21	27° 30' 69.4"	109° 59' 11.1"
10	27° 30' 68.2"	109° 59' 39.4"	22	27° 30' 74.7"	109° 58' 91.8"
11	27° 30' 60.2"	109° 59' 11.3"	23	27° 30' 59.6"	109° 58' 89.2"
12	27° 30' 54.0"	109° 59' 15.8"			

Table 6. Coordinates of points where pressure was measured for calibration.

Point	North	West
1	27° 30.808'	109° 59.447'
2	27° 30.836'	109° 59.610'
3	27° 30.757'	109° 59.510'
4	27° 30.641'	109° 59.739'
5	27° 30.890'	109° 59.211'

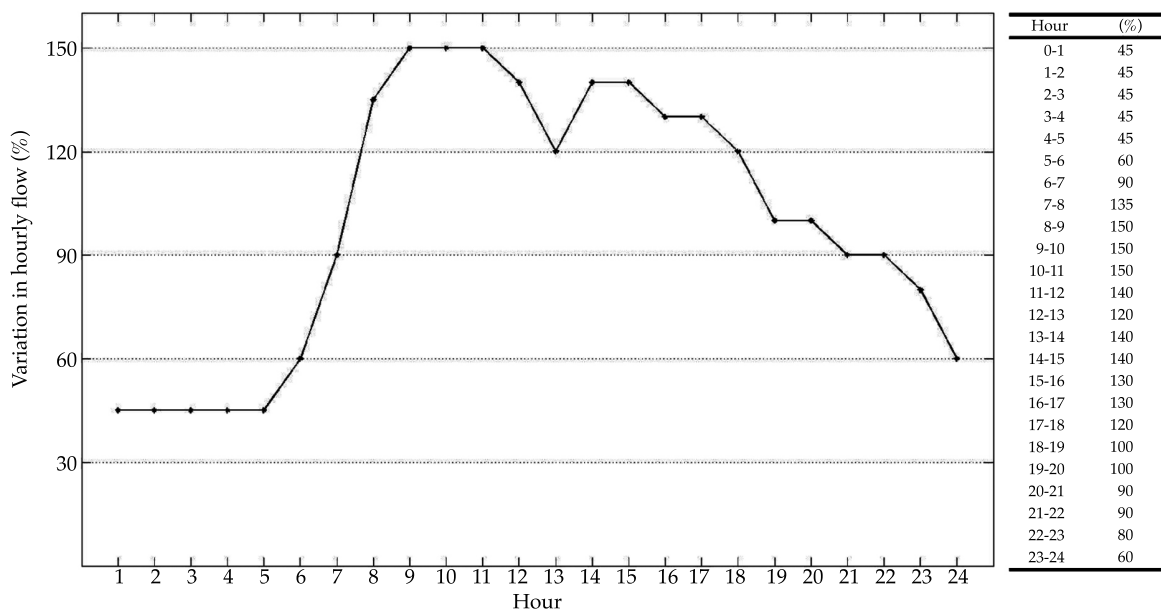


Figure 5. Demand curve (CNA, 2007).

average consumption expressed as hourly percentages of daily maximum flow.

Pipelinenet was used to integrate the demand curve, running the hydraulic simulation model with hourly variations.

Results from the Model

The results from the calibrated model provided information related to the operating behavior of the system, such as pressures in the distribution network, unit loss in load in the lines, flow in the network, velocity in each of the pipes, roughness coefficient (calibrated) and leaks index estimated for each line, among others.

When running the hydraulic model in GIS using *Pipelinenet* the results are automatically classified, with divisions into sub-layers as shown in Table 7.

Multicriteria Evaluation

Once GIS contained the information needed, it was analyzed. The multicriteria evaluation handles problems related to decision-making by considering various criteria to establish priorities among the options under consideration (Zeleny & Cochrane, 1982). The proposed methodology is essentially based on applying selection criteria according to

Table 7. Information managed and presented by *Pipelinenet*.

Field name	Description	Parameters
Junctions Reservoirs Tanks	Node	Elevation
		Base demand
		Initial quality
		Demand
		Height
		Pressure
		Quality
Pipes Pumps Valves	Links	Length
		Diameter
		Roughness
		Bulkcoeff
		Walkcoeff
		Initial state
		Flow
		Friction factor
		Unit loss in load
		Reaction rate
		Velocity
Quality		

parameters, such as nearness to elements of interest or the operating characteristics of lines (pipes) and each point (node), all of which pertains to analyzing the information associated with each element studied.

First, the options that could be used to analyze the information according to the established priorities were defined. To make a decision about which lines have a high or low rehabilitation priority, three evaluation options were established by determining the priority factors according to the criteria and the needs of the entity. The factors for each decision variable were weighted according to the evaluation by the managers and technicians in the potable water operating entity.

Evaluation Options

The proposed evaluation scenarios involve integrating different decision factors in the analysis, as shown later. These factors are:

- Probability of failure.
- Operating conditions.
- Cost.

As will be seen later, these criteria are difficult to apply using traditional methods, while they are relatively simple to determine using GIS.

Heuristic Selection of Factors

After collecting and analyzing the information, the criteria that influence the prioritization were selected based on the weighting. The GIS was used to build filters for the spatial data in order to eliminate information that did not need to be displayed. Table 8 presents the criteria included for each decision variable.

To analyze the information in the GIS, the raster format first had to be reclassified. This was composed of each decision variable for each of the proposed evaluation scenarios. As mentioned previously, the weight used

Table 8. Prioritization criteria according to the attribute.

Factor, F	Decision factors	Criteria
F1	Zone	Vulnerable zones, that is, areas near hospitals, shelters, schools, sports centers, commercial zones, etc. which are more important to rehabilitate.
F2	Material and diameter	Order in relation to material and diameter of piping. According to the literature reviewed, a smaller diameter represents more risk of failure. Importance according to whether it is a main or secondary distribution line.
F3	Roughness	The criteria is to give a higher priority to a high roughness coefficient. These absolute roughness coefficients are determined and taken from the calibration of the model. Units are in millimeters (mm).
F4	Paved zone	According to the criteria by the OE, priority is given to the zone containing pavement since it directly impacts repair costs.
F5	Leak index	Lines with a high leak index calculated according to reports and the supervisors' experience have a high priority.
F6	Importance	According to the significance index. The higher the significance index the higher the importance in the system. A mayor índice de significancia, mayor importancia en el sistema.
F7	Repair price	According to the average unit value for the reparation of each type of piping.
F8	Length	Based on information from the network. Criteria established by the literature, the greater the length the higher the risk of leaks.
F9	Velocity	Pipes should have a maximum velocity of 5.0 m/s and minimum of 0.3 m/s (CNA).
F10	Unit loss in load	Losses in load due to friction between sections should not exceed 5 km (CNA). Over 5 m / km represents low efficiency, therefore poor functioning.
F11	Pressure	Pressures should be between 1.5 and 5 kg/cm ² . For small urban localities a minimum of 1.0 kg/cm ² is acceptable (CNA). According to the literature review, higher pressure represents higher risk of failure.
F12	Age	For primary distribution networks, 20 to 30 years of useful life is expected. For secondary distribution networks, 15 to 30 years (CNA), Old piping represent a higher risk.

in the reclassification of each attribute was assigned according to experience acquired over time or knowledge about similar cases in other companies responsible for the operations of the municipality's potable water networks.

With the tools provided by the geographic information system, different operators were applied based on the information needed to analyze and assign weights to the scenarios. The raster calculator was used for the multicriteria evaluation method known as "weighted linear

combination", or WLC. This procedure makes it possible to retain the variability of the continuous decision factors while also combining and exchanging factors. It also enables assigning a weight to the decision factors to indicate the relative importance of each variable. This analysis provides a panorama which avoids extreme risks, positioning the analysis in medium risks and facilitating a total combination among factors (Eastman, 2006) (see Figure 6).

As shown in Figure 6, in the WLC multicriteria evaluation the risk is moderate

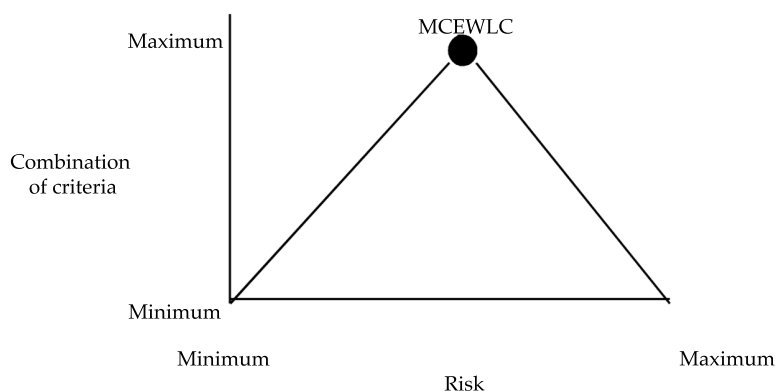


Figure 6. Exchange of criteria versus Risk (adapted from Eastman, 2006).
Multicriteria evaluation with weighted linear combination (MCEWLC).

when the combination of factors is highest (maximum combination of criteria). This is because this type of evaluation weights the relative importance of the decision factors, facilitating the maximum inclusion of decision factors and thereby obtaining a total score distant from the extreme risk for each scenario.

The evaluation for each one of the scenarios was:

$$\text{Rehabilitation priority} = \frac{\sum \text{Decision factors}}{\text{Number of factors}}$$

The numerator represents the sum of the values obtained according to the scale presented in Table 10 for each of the decision factors included in the evaluation scenario. The denominator represents the number of decision factors included in the evaluation scenario. Next, the evaluation scenarios considered and the decision factors related to each one will be discussed.

- *Evaluation scenario 1. Probability of a failure*

The likelihood of a failure in a pipe may be related to the structural deterioration of the pipe itself, which decreases its

structural elasticity/strength and the ability to support the different types of forces acting on it. Deterioration may also be caused by the internal surface of the pipe which would directly decrease hydraulic capacity, degrade the water quality and, on occasion, affect the structural capacity in cases of extreme corrosion.

With respect to determining the priority for replacing a pipe and the cost-effectiveness of doing so, it is critical to replace pipes with a high probability of failure. While most new pipes made of PVC (polyvinyl chloride) and PE (polyethylene) have little probability of failure, finding those with a higher probability is more complicated because several factors are involved.

Geographic data such as soil type, load characteristics (demographic development, vehicular traffic), historical installation practices and fluctuations in groundwater can also help to explain the incidence of and variations in the probability of failure (Kleiner, Rajani, & Wang, 2007).

The analysis to determine the pipes with highest probability of failure was based on what has been mentioned above as well as the literature review and the available information, as described below.

Table 9. Summary of characteristics of the piping in the distribution system, Providencia, Sonora.

	Characteristic	Number of pipes	Length (m)	% length
Diameter	<= 75 mm	70	8 389.1	58.3
	100 mm	25	2 176.2	15.1
	150 mm	39	3 395.8	23.6
	200 mm	4	428.0	3.0
	Total	138	14 389.2	100.0
Age	<=5	45	5 816.3	40.4
	5 a 10	58	5 483.8	38.1
	15	8	947.6	6.6
	20	4	178.4	1.2
	30	23	1 963.1	13.6
	Total	138	14 389.2	100.0
Material	PVC	131	13 868.6	96.4
	AC	7	520.6	3.6
	Total	138	14 389.2	100.00
Community	Providencia	82	9 565.67	66.48
	Severo Girón	44	4 118.4	28.62
	A. López Nogales	12	705.1	4.90
	Total	138	14 389.2	100.00

Decision factors: age, leak index, pressure, length, roughness coefficient, zone, repair cost.

- *Evaluation scenario 2. Operating conditions*

The hydraulic behavior provides a reliable indicator of the hydraulic capacity of the distribution network when the pipes are reaching their maximum hydraulic capacity to provide the flows required.

Therefore, and with the information provided from the operating entity, the pipes that most need to be replaced in terms of hydraulic capacity are determined as follows.

Decision factors: unit loss in load, velocity, roughness coefficient, significance index, zone.

- *Evaluation scenario 3. Cost*

As the piping deteriorates over years of use, the strength of the pipe decreases, increas-

ing its vulnerability to loads and presenting a higher risk of failure. The repair costs and consequences of failures in each line are different. Several factors are involved in the calculation of which failure represents the highest cost to an operating entity. The repair cost will be greater for pipes with larger diameters and will vary depending on the location of the piping. Consequences can be expected to be greater in vulnerable zones (areas near public buildings, hospitals, businesses, etc.) as well as for piping that is more difficult to isolate. That is, the repair would leave a large number of users without service when a failure occurs or during a repair, where the interruption in the service results in dissatisfied users and increases their costs, which will be reflected in complaints against the operating entity.

Repair costs can also vary according to the location of the piping. A repair in a recently paved street will damage the new payment and therefore result in a loss of money and dissatisfaction among users.

Given what has been mentioned above and the available information the pipes with the greatest need for replacement in terms of costs-benefits were determined based on the information below.

Decision factors: age, pressure, leak index, zone, pavement conditions, cost of repair.

Selection of the Methodology for the Multicriteria Decision

After reclassifying the decision factors mentioned for each evaluation scenario (Table 10), the raster calculator was used with the weighted linear function. In this case, the same weight was assigned to the value of each of the factors. The rehabilitation priority (RP) function was defined as follows:

Evaluation scenario 1

$$RP = \frac{\left(\begin{array}{l} \text{age} + \text{leak index} + \text{pressure} \\ + \text{length} + \text{roughness} + \text{zone} \\ + \text{repair cost} \end{array} \right)}{7}$$

Evaluation scenario 2

$$RP = \frac{\left(\begin{array}{l} \text{unit losses} + \text{velocity} \\ + \text{roughness} + \text{zone} + \text{repair price} \end{array} \right)}{5}$$

Evaluation scenario 3

$$RP = \frac{\left(\begin{array}{l} \text{age} + \text{leak index} + \text{pressure} \\ + \text{zone} + \text{pavement conditions} \\ + \text{repair cost} \end{array} \right)}{6}$$

The pipes with the highest rehabilitation priority value for each scenario shown in *ArcGis* are at the top of the rehabilitation list, that is, they were classified according to the values obtained from the raster calculation. The result was used for a final reclassification to determine which values resulting from the calculation had high, medium and low priorities.

Lastly, the resulting raster layer was converted into vector format, with which the pipes can be selected in relation to the raster result. To this end, the QUERY interface (selection by location) provided by GIS was used. With this tool, users can view the search and reduce it according to their own parameters to determine the pipes that are candidates for replacement, and display them in a list.

The list of pipes with the highest replacement priority was sorted based on the attribute of interest to the potable water network managements, for example, cost.

- *Evaluation scenario 4. Internal factors*

A new prioritization which only included the decision factors impacting hydraulic behavior was determined with existing operating information about the potable water network. The purpose of this was to prioritize the groups of piping presenting hydraulic deficiencies and directly impact the physical efficiency of the system.

Decision factors: unit loss in load, velocity, roughness coefficient, significance index.

Functioning was evaluated in a similar way as the evaluation scenarios presented above. After obtaining the results, changes to the *Pipilinet* hydraulic simulation model were made for a dynamic regime at peak hour (8 am) for pipes designated by the evaluation as high rehabilitation priority for this scenario.

After making these changes, the hydraulic functioning of the system was

Table 10. Reclassification of decision factors in raster format.

Factor/F	Decision factors	Reclassification	Criteria (priority)
F1	Vulnerability of zone	10	Zones under 50 m from a vulnerable point.
		5	Zones 51 to 100 meters.
		3	Zones 100 to 150 meters.
		2	Zones 150 to 250 meters.
		1	Zones over 250 meters.
F2	Material and diameter	10	Diameter under 3 inches.
		5	Diameter between 3 and 6 inches.
		9	Diameter over 6 inches.
F3	Roughness (mm)	10	Over 5 mm
		9	From 3 to 5 mm
		5	From 1 to 3 mm
		3	From 0.025 to 1 mm
		1	From 0.0015 to 0.025 mm
F4	Paved zone	10	Without pavement (0)
		9	Old pavement 2 (3)
		5	Old pavement (2)
		2	New pavement (1)
		1	Outside the street (1)
F5	Leak index	10	Over 20 reports
		8	Between 10 and 20 reports
		5	Between 5 and 10 reports
		3	Between 1 and 5 reports
		1	No reports
F6	Importance	10	Significance index larger than the mean
		5	Significance index smaller than the mean
F7	Repair cost	10	Smaller than \$130 000.00
		8	Between \$130 000.00 and \$260 000.00
		6	Between \$260 000.00 and \$380 000.00
		4	Between \$380 000 and \$500 000
		2	Over \$500 000
F8	Length	1 a 10	From 1 to 1 000 m long
F9	Velocity	10	Velocity over 5.0 m/s and under 0.3 m/s
		1	Velocity within range
F10	Unit loss in load	10	Losses in load from friction between sections that exceed 5 m/km (CNA)
		1	Losses within the range
F11	Pressure	10	Depends on type of analysis
F12	Age	10	Over 30 years of useful life
		8	15 to 30 years of useful life
		3	10 to 35 years of useful life
		2	5 to 10 years of useful life
		1	0 to 5 years of useful life

compared to that of the system before the changes were made. This was based on factors considered most significant to this purpose, such as velocity, pressure and unit loss in load.

Results and Discussion

The methodology presented was used to obtain and analyze information pertaining to the potable water distribution network for Providencia, Sonora. To perform the multicriteria evaluation in the GIS, the data had to first be collected and the hydraulic model of the Providencia network developed. This section deserves careful attention since the quality of the decisions largely depends on the quality of the data used.

The Providencia distribution system is located in an area of approximately 150 ha. It includes 107 nodes with an average network supply flow of 28.9 lps. There are 138 pipes, two supply sources (main and secondary) and a tank. The system operates with only one supply at a time depending on the availability and conditions of the sources. The water from the main supply source is delivered to the network and the tank. Table 9 presents the summary of the information about the distribution network.

Table 12 shows the summary of the results from the dynamic model analyzed at peak hour (8 am).

The decision factors were reclassified in raster format in *ArcGis* based on the priority criteria assigned by the distribution system administrators (see Table 10). Values near 0 were assigned to attributes with the lowest rehabilitation priority and the value 10 was assigned to attributes with the highest priority.

With the weighting criteria assigned to the factors, the raster calculator was used to generate a linear combination of the

criteria. Figures 7, 8, 9 and 10 present the scenario obtained.

The results show an average of 20 pipes identified as high rehabilitation priority for the four scenarios. Scenario 4 resulted in 20 pipes with a high priority. Table 11 shows a summary of the pipes designated as high rehabilitation priority. The replacement of these pipes was simulated in *Pipelinenet*. To this end, the new PVC roughness of the replaced piping was assumed to be as indicated by the manufacturer's tables, and the increase in demand in the consumption scenarios was eliminated (changes in flows assigned to nodes) because of leaks in the nodes that corresponded to pipes that had been replaced. The summary of the results of the final network (with changes) is presented in Table 12.

After making the changes to the model, the percentages of pipes complying with NWC specifications increased from 83 to 87% in the case of losses in unit load and 37 to 99% in the case of pressure. This increase is due to the immediate improvement of the modeling of the distribution system by optimizing the replacement of pipes based on the criteria established in evaluation scenario 4. The majority of the pipes replaced were old, with a high significance index for the network, high unit losses in load and a high roughness coefficient. The increase in pressure may reflect the replacement of pipes with probable leaks and lines that are important to the distribution network according to the significance index, which would significantly improve pressure.

Conclusions

The decisions made by administrators of potable water distribution systems are key to controlling operating entities' commercial, physical, hydraulic and energy efficiency, among other factors. The loss in potable water due to leaks is a

Table 11. Summary of tubes classified as high priority for rehabilitation, scenario 4.

Characteristic		Number of pipes	Length	% length
Diameter	<= 75 mm	14	952.2	57.60
	100 mm	3	476.8	28.90
	150 mm	3	223.6	13.50
	Total	20	1 652.6	100.00
Age	20	1	82.7	5.00
	30	19	1 569.9	95.0
	Total	20	1 652.6	100.00
Material	PVC	19	1 566.7	94.80
	AC	1	85.9	5.20
	Total	20	1 652.6	100.00
Community	Providencia	20	1 652.6	100.00
	Total	20	1652.6	100.00



Figure 7. Alternative scenario for evaluation 1. Probability of failure.

recurring problem in Mexico and different methodologies have been proposed to facilitate decision making in this area (Tzatchkov, Hansen, & Ramírez, 2010). The methodology proposed herein to

prioritize rehabilitation needs provides a practical tool which can be used as a basis for decisions about rehabilitating piping in a potable water system. This methodology enables prioritizing groups of pipes that



Figure 8. Alternative scenario for evaluation 2. Operating conditions.



Figure 9. Alternative scenario for evaluation 3. Cost.



Figure 10. Alternative scenario for evaluation 4. Internal factors.

Table 12. Summary of the results from the analysis of the Providencia network with a dynamic regime at 8 a.m. (hour with peak demand). Percentage of the total of 138 pipes and 108 nodes in the town of Providence, which meets the required velocity, unit loss in load and pressure indicated by the 2009 CNA manual.

Parameter	Initial network	Final network
Velocity	34%	36%
Losses in unit load	83%	87%
Pressure*	35%	99%

*For pressures, existing nodes in the network work taken into account; that is, junctions between piping.

need rehabilitation according to priority criteria established by operating entities.

The four scenarios proposed visually present the pipes classified as low, medium and high priority for rehabilitation, which completely depends on the decision factors and criteria considered. These criteria are supported by later investigations (Alonso-Guzmán, 2010; Alonso-Guzmán *et al.*, 2013; Francisque, Rodriguez, Sadiq, Miranda, & Proulx, 2009; Kleiner *et al.*, 2007;

Rostum, 2000), some of which are based on mathematics to prioritize pipes in the network, and some are related to hydraulic deterioration. Criteria is weighted using a heuristic model relying primarily on expert opinion.

The risk is the possibility of committing an error in the process of making decisions (Fallas, 2002). In this work, a complete exchange of decision factors with a medium risk was considered. This type of analysis

enables a weighted integration of all the factors that influence the prioritization of replacing pipes according to the evaluation scenario used. This provides the analyst the advantage of compensation among factors— a factor with low values can be compensated by the high values of other factors. The “weighted linear combination” method assumes the acceptance of a certain level of risk and offers better results than those provided by boolean intersection (Vega & Lou, 2003). Thus, pipes can be prioritized according to the different degrees to which they need to be replaced.

Geographic information systems facilitate the management, storage and filtering of information according to the needs presented when decisions have to be made (Malczewski, 2006). The methodology proposed can be used for any distribution network since it can manage the particular information that each operating entity considers necessary and is able to obtain, considering the large differences in the available data and in the amount of information from one water company to another.

Many factors are involved in decisions related to prioritizing the renovation of pipes. Therefore, all the factors involved in decision-making (as indicated by investigations and the experience of network administrators) should be included, to the extent possible. Thus, groups of pipes can be prioritized based on how urgently a technical intervention is needed. The quality of the decisions depends largely on the number of factors used and especially on the quality of the input data.

Ideally, the multicriteria evaluation would be applied by assigning weights to each criterion considered (Ozturk & Batuk, 2011). The influence of each decision variable is thereby evaluated based on the various degrees of importance. To this end,

the use of statistics is recommended as well as information from other investigations or methodologies— such as analytical hierarchy applied with heuristics or with statistically validated data— that can be obtained from data collection programs implemented by the operating entity itself.

The use of the multicriteria evaluation technique with GIS (weighted linear combination) reflects a risk of uncertainty which should be considered when making decisions. This risk can be decreased by applying different multicriteria evaluation techniques, such as ordered weighted averaging. This technique can reduce a large risk to a small risk while also performing different degrees of criteria exchange.

Acknowledgments

The authors would like to thank Robert Janke for help with the *Pipelinenet* software, in addition to Conacyt for support received during this project. The technical information required for the project was directly provided by the Organismo Operador de Agua Potable, Alcantarillado y Saneamiento de Cajeme (Cajeme Potable Water, Sewer and Treatment Operating Entity), who we especially thank for their availability, time and willingness.

References

- Alonso-Guzmán, C. D. (2010). *Modelo híbrido para la toma de decisiones en programas de rehabilitación de tuberías para sistemas de abastecimiento de agua: aplicación a la ciudad de Celaya, Gto. (México)*. Tesis doctoral. Valencia: Universidad Politécnica de Valencia.
- Alonso-Guzmán, C. D., Pérez-García, R., Izquierdo-Sebastian, J., & Herrera-Fernández, M. (2013). Factores de fiabilidad y eficiencia en la toma de decisiones para la rehabilitación de tuberías. *Ingeniería, investigación y tecnología*, 14, 489-498.
- Arulraj, G., & Rao, H. (1995). Concept of Significance Index for Maintenance and Design of Pipe Networks. *Journal of Hydraulic Engineering*, 121(11), 833-837, doi: doi:10.1061/(ASCE)0733-9429(1995)121:11(833)

- Ayuntamiento de Cajeme (2000). *Plan Municipal de Desarrollo 1997-2000*. Recuperado de <http://www.infocajeme.com/cajeme.php>.
- Bourguett, V., & Rodriguez, J. M. (2001). Evaluación económica de proyectos de reducción de pérdidas. En: *Reducción integral de pérdidas de agua potable* (Vol. 2, pp. 85-98). México, DF: Instituto Mexicano de Agua Potable.
- Castelán, E. (2001). *Water Management in the Mexico City Metropolitan Area: The hard Way to Learn*. Paper presented at the Proceedings from the Symposium Frontiers in Urban Water Management: Deadlock or Hope, Marseille, France.
- CEA (2004). *Programa estatal de mediano plazo, aprovechamiento sustentable del agua 2004-2009*. Recuperado de <http://www.bvsde.paho.org/bvsacd/cd27/sonara04.pdf>.
- CNA (2007). *Manual de agua potable, alcantarillado y saneamiento. Lineamientos técnicos para la elaboración de estudios y proyectos de agua potable y alcantarillado sanitario*. México, DF: Comisión Nacional del Agua.
- CNA (2008). *Programa de Modernización de Organismos Operadores de Agua (Promagua)*. Recuperado de http://www.cmic.org/comisiones/sectoriales/infraestructurahidraulica/varios/Ejecucion_de_proyectos/Promagua_lineamientos.pdf.
- CNA (2009). *Manual de agua potable, alcantarillado y saneamiento. Datos Básicos*. México, DF: Comisión Nacional del Agua.
- Eastman, J. R. (2006). IDRISI Andes Guide to GIS and image Processing. *Clark University, Worcester*, 87-131.
- Fallas, J. (2002). *Toma de decisiones y sistemas de información geográfica*. Programa Regional en Manejo de Vida Silvestre y Escuela Deficiencias Ambientales. Heredia, Costa Rica: Universidad Nacional.
- Francisque, A., Rodriguez, M., Sadiq, R., Miranda, L., & Proulx, F. (2009). Prioritizing Monitoring Locations in a Water Distribution Network: A Fuzzy Risk Approach. *Journal of Water Supply: Research and Technology, AQUA*, 58(7), 488-509.
- Garduño, H. (1994). *Uso eficiente del agua: un enfoque multidimensional*. Montevideo: Comisión Nacional del Agua, Instituto Mexicano de Tecnología del Agua, Programa Hidrológico Internacional UNESCO-ORCYT.
- INEGI (2005). *Conteo de población y vivienda 2005. Indicadores del Censo General de Población y Vivienda*. México, DF: INEGI.
- Kallis, G., & Coccossis, H. (2001). Sustainable Management of Water Supplies for Developed Urban Areas: Issues, Perspectives and a Vision. In I. Publishing (Ed.). *Frontiers in Urban Water Management: Deadlock or Hope* (Vol. 45, pp. 269-264). Paris: Technical Documents in Hydrology.
- Kleiner, Y., Rajani, B., & Wang, S. (2007). Consideration of Static and Dynamic Effects to Plan Water Main Renewal. *Middle East Water*, 1-13.
- Malczewski, J. (2006). GIS-Based Multicriteria Decision Analysis: A Survey of the Literature. *International Journal of Geographical Information Science*, 20(7), 703-726, doi: 10.1080/13658810600661508.
- Morais, D. C., & Almeida, A. T. (2006). Water Supply System Decision Making Using Multicriteria Analysis. *Water SA*, 32(2), 229-236.
- Ozturk, D., & Batuk, F. (2011). Implementation of GIS-Based Multicriteria Decision Analysis with VB in ArcGIS. *International Journal of Information Technology & Decision Making*, 10(6), 1023-1042.
- Rostum, J. (2000). *Statistical Modelling of Pipe Failures in Water Networks*. Doctoral thesis. Norwegian University of Science and Technology. Retrieved from <http://urn.kb.se/resolve?urn=urn:nbn:no:ntnu:diva-504>.
- Tortajada, C. (2006). Water Management in Mexico City Metropolitan Area. *Water Resources Development*, 22(2), 353-376.
- Tzatchkov, V., Hansen, M. P., & Ramírez, H. (2010). A Practical Approach for Prioritizing The Replacement of Water Pipes in Mexico City. *MRS Online Proceedings Library*, 1278/2010. XIX International Materials Research Congress, Cancún, México. <http://dx.doi.org/10.1557/PROC-1278-S07-5>.
- Vega, J. M., & Lou, M. A. M. (2003). *Métodos para la planificación de espacios naturales protegidos* (Vol. 2). Editorial CSIC-CSIC Press, España.
- Yamijala, S. (2007). *Statistical Estimation of Water Distribution System Pipe Break Risk*. Texas A&M University. Retrieved from <http://hdl.handle.net/1969.1/ETD-TAMU-1471>.
- Zeleny, M., & Cochrane, J. L. (1982). *Multiple Criteria Decision Making* (Vol. 25). New York: McGraw-Hill.

Institutional Address of the Authors

M.C. Vivian Verduzco

Instituto Tecnológico de Sonora
Departamento de Ciencias del Agua y Medio Ambiente
5 de Febrero 818 Sur, Centro
85000 Ciudad Obregón, Sonora, MÉXICO
Teléfono: +52 (644) 4109 000, extensión 2302
vivian.verduzco@gmail.com

Dr. Jaime Garatuzo

Instituto Tecnológico de Sonora
Dirección Académica de la División de Recursos Naturales
5 de Febrero 818 Sur, Centro
85000 Ciudad Obregón, Sonora, MÉXICO
Teléfono: +52 (644) 4109 000, extensión 2588
garatuzo1@gmail.com

M.I. Salvador Díaz

Instituto Tecnológico de Sonora
Departamento de Ciencias del Agua y Medio Ambiente
5 de Febrero 818 Sur, Centro
85000 Ciudad Obregón, Sonora, MÉXICO
Teléfono: +52 (644) 4109 000, extensión 2099
sdiaz@itson.edu.mx

Prioritization of Intervention Areas using a Morphometric Analysis and Vegetation Index

• Adolfo López-Pérez • Mario R. Martínez-Menes* •
• Demetrio S. Fernández-Reynoso •
Colegio de Postgraduados, México
*Corresponding Author

Abstract

López-Pérez, A., Martínez-Menes, M. R., & Fernández Reynoso, D. S. (January-February, 2015). Prioritization of Intervention Areas using a Morphometric Analysis and Vegetation Index. *Water Technology and Sciences* (in Spanish), 6(1), 121-137.

Morphometric characterizations and the Normalized Difference Vegetation Index (NDVI) can be used as a strategy for the environmental hydrological restoration of basins, since identifying the interrelation among the area, shape, topography, drainage system and changes in vegetation due to anthropogenic factors enables prioritizing the application of productive-conservation interventions in sub-basins. The purpose of this is to reduce the growth of drainage systems in regions with extreme meteorological events that cause landslides and flooding in lower portions of basins. The study was performed in the Huehuetan River Basin located in the Soconusco region of the state of Chiapas, Mexico. Its objective was to estimate the morphometric parameters (linear and shape) of 16 sub-basins, as well as the NDVI for the years 1993 and 2013, in order to prioritize changes in vegetation cover that affect the degradation of the soil in the sub-basin, for the purpose of hydrological restoration. The methodology enabled defining the order of intervention (water and soil conservation practices and sediment control works) in the sub-basins so as to reduce hydric erosion, the growth of the drainage system and the transport capacity of surface flow through hillsides and rivers.

Keywords: NDVI, watershed, conservation, LandSat, remote sensing.

Resumen

López-Pérez, A., Martínez-Menes, M. R., & Fernández Reynoso, D. S. (enero-febrero, 2015). Priorización de áreas de intervención mediante análisis morfométrico e índice de vegetación. *Tecnología y Ciencias del Agua*, 6(1), 121-137.

La caracterización morfométrica y el análisis del Índice de Vegetación de Diferencia Normalizada (NDVI) puede ser una estrategia en los programas de restauración hidrológica ambiental de cuencas, ya que la interrelación entre el área, forma, relieve, sistema de drenaje y los cambios de la cobertura vegetal causada por la alteración antropogénica permite hacer una priorización de subcuencas para su intervención con prácticas productivo-conservacionistas, a fin de reducir el crecimiento de los sistemas de drenaje en zonas con presencia de eventos meteorológicos extremos que causan deslaves y provocan inundaciones en las partes bajas de las cuencas. El estudio se realizó en la cuenca del río Huehuetán, ubicada en la región del Soconusco del estado de Chiapas, México, con el objetivo de estimar los parámetros morfométricos (lineales y de forma) de 16 subcuencas, así como el NDVI para los años 1993 y 2013, para priorizar los cambios en la cobertura vegetal que afectan la degradación del suelo de las subcuencas para la restauración hidrológica. La metodología permitió definir el orden de intervención de las subcuencas con prácticas de conservación del suelo, agua y obras de control de azolves, para reducir los procesos de erosión hídrica, el crecimiento del sistema de drenaje y la capacidad de transporte del flujo superficial en laderas y cauces.

Palabras clave: NDVI, cuenca, conservación, LandSat, sensores remotos.

Received: 20/01/14

Accepted: 25/07/14

Introduction

Various authors have studied hydrological processes associated with the morphometric characteristics of hydrographic basins, particularly in relation to extreme weather events caused by tropical storms and changes in land use (Delgado & Gaspari,

2010). The use of a morphometric analysis to study hydrological behavior has received much attention and been widely accepted by hydrologists and geomorphologists because of its ease in analyzing complex physical processes and precipitation-runoff relations (Javed, Khanday, & Rais, 2011; Mahadevaswamy *et al.*, 2011;

Srinivasa-Raju & Nagesh-Kumar, 2011; Sarma & Saikia, 2012). It is essential to integrate morphometric parameters with the hydrological characteristics of drainage areas in order to improve planning and formulate strategies that adequately conserve natural resources and facilitate management practices related to hydrological restoration (Srinivasa-Raju & Nagesh-Kumar, 2011).

A quantitative analysis of the morphometric parameters is useful to develop preliminary hydrological diagnostics in order to make approximate predictions based on the relationship of a basin's behavior to its geology and geomorphology, particularly to determine mass soil movement and growth in drainage systems (Esper-Angillieri, 2008). The hydrological response of a basin is related to its morphometric characteristics, such as size, shape, slope, density, number and length of channels, etc. Therefore, the morphometric analysis of a drainage area should be used as the first step towards understanding the dynamics of hydrological processes in basins (Kanth & Hassan, 2012).

Morphometric parameters have been reported as spatial distributions that enable comparing drainage units at different levels of intervention (basin, sub-basin, micro-basin or runoff unit). They provide preliminary findings about the characteristics of a territory based on a precise description of the geometry of surface shapes (Gaspari *et al.*, 2012). These parameters represent quantitative indices that can be used in hydrological studies of basins in order to identify distances and times involved in surface runoff concentrations corresponding to unusually large maximum floods caused by extreme weather events that generate floods and limit the productive and recreational activities of humans (Zucarelli, 2013).

They also are associated with the degree of soil saturation, which can cause mass landslides and increase the size of the drainage system (D'Odorico, Fagherazzi, & Rigon, 2005).

Horton (1945) indicated that drainage networks could be quantitatively studied based on a stream ordering model, which was later adapted by Strahler (1964). The morphometric parameters enable characterizing the intervention units and correlating them with other attributes of the basins to identify and evaluate hydrological, erosive and sediment production processes (Racca, 2010).

Meanwhile, spatial and temporal variations in the vegetation cover in drainage areas influence the response of soils to rainfall events of different magnitudes and intensities, generating changes in the drainage system in runoff areas. Therefore, vegetation indices obtained using remote sensors, such as the Normalized Difference Vegetation Index (NDVI), is useful to determine conditions related to vegetation cover and to evaluate the percentage change over time, since this is associated with erosion and sediment transport processes (Alatorre, Beguería, & Vicente-Serrano, 2010).

The NDVI helps to directly interpret the biophysical parameters of the vegetation and to identify the presence of vegetation on the surface as well as characterize its spatial and temporal distribution (Di *et al.*, 1994); Merg *et al.*, 2011). It also explains changes in vegetation cover (reforestation and deforestation) and their effect on surface runoff (Hibbert, 1971; Johnson, 1998; Andréassian, 2004).

The objective of the work herein is to analyze the relationship between morphometric parameters and the NDVI associated with the sub-basins in the Huehuetan River Basin, in the state of Chiapas, Mexico, in order to prioritize

them according to changes occurring in the drainage systems and risk of degradation caused by hydrological processes. The purpose of this is the environmental hydrological restoration of the basin to minimize flood risks and the growth of drainage systems.

Methodology

Location of the Study Area

The Huehuetan River basin is located in the southeast portion of the state of Chiapas. Its area is 317.51 km² from the upper portion to the Huehuetan hydrometric station located at the Arriaga-Tapachula highway, with geographic coordinates 15° 05' 56" north latitude and 92° 24' 02" west longitude, and an altitude of 30 m (Figure 1). The basin and sub-basins were automatically

delimited using the SWAT (Soil and Water Assessment Tool) model developed by the United States Department of Agriculture in collaboration with the University of Texas (Arnold, Williams, Nicks, & Sammons, 1990), with a digital elevations model (DEM) at a scale of 1:20 000 and level curves every 10 m. The scale of the DEM makes it possible to more precisely identify the drainage network pertaining to the 16 sub-basins.

Obtainment of Morphometric Information

The SWAT model was used to obtain area, perimeter, length of the main channel, mean slope of the sub-basin, minimum, mean and maximum elevation, difference in elevation, total number of channels and concentration time. These values were

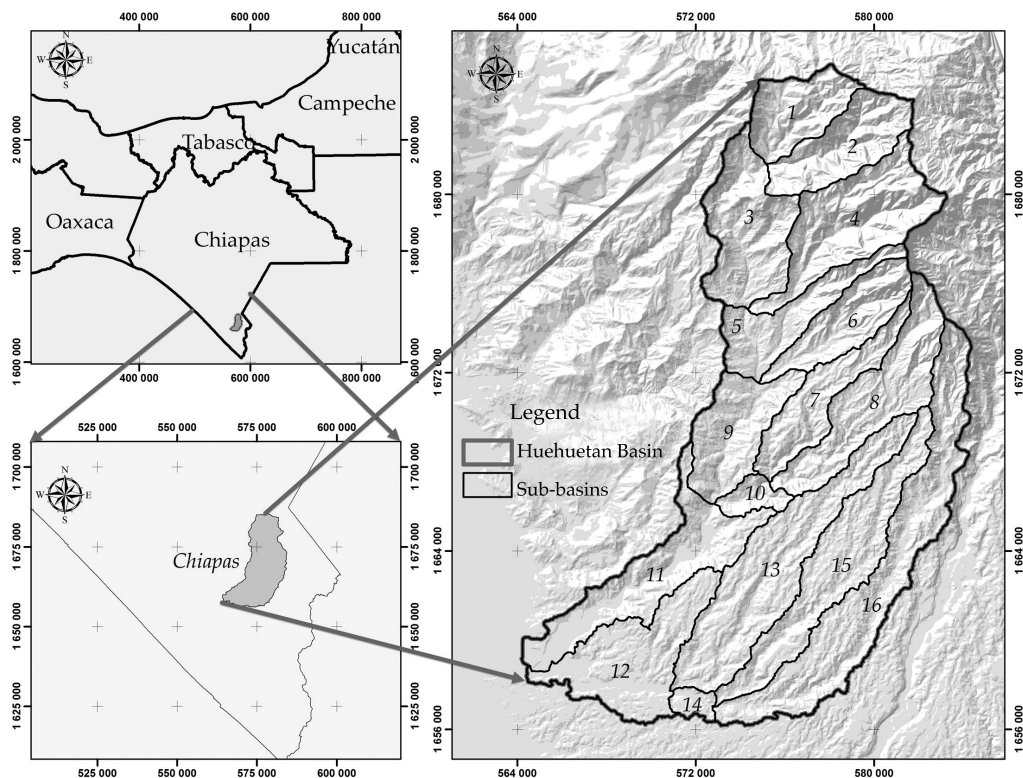


Figure 1. Location of the Huehuetan River basin and sub-basins.

Table 1. Formulas used to obtain the morphometric parameters of the sub-basins.

Parameter	Equation	Author	Year
Linear			
Drainage density (km/km ²)	$D_d = \frac{L_{tc}}{A}$	Horton	1945
Hydrographic density (rivers/km ²)	$D_h = \frac{L_u}{A}$	Horton	1945
Mean bifurcation ratio	R_{mb} = average of the bifurcation ratio for each of the orders	Strahler	1957
Drainage texture (rivers/km ¹)	$R_t = \frac{L_u}{P}$	Horton	1945
Length of surface flow (km)	$L_g = \frac{1}{2D_d}$	Horton	1945
Shape			
Elongation ratio	$R_e = \frac{2}{L_c} \times \left(\frac{A}{\pi}\right)^{0.5}$	Schumn	1956
Circularity ratio	$R_c = \frac{4\pi A}{P^2}$	Miller	1953
Compactness coefficient	$C_c = 0.2821 \frac{P}{A^{0.5}}$	Gravelius	1914
Forma factor	$R_f = \frac{A}{L_c^2}$	Horton	1932
Basin shape	$B_s = \frac{L_c^2}{A}$	Horton	1932

Donde A es el área (km²); P , el perímetro (km); L_c , la longitud del cauce principal (km); L_u , el número total de cauces (adim.), y N_u es el número de orden.

used to estimate the linear morphometric parameters (topography and drainage network) and the shape of the 16 sub-basins studied, with equations proposed by different investigations or studies (Table 1).

The linear and shape parameters are also known as evaluation parameters pertaining to the degree of soil degradation caused by drainage systems. These were analyzed using descriptive statistics (minimum, maximum, mean, standard deviation and variation coefficient) to identify the variability in each of the drainage areas for the purpose of prioritizing the sub-basins (Biswas, Sudhakar, & Desai, 1999).

Prioritizing sub-basins using a morphometric analysis is based on assigning ascending whole number values to each morphometric parameter

calculated according to the degree to which it affects the longitudinal and transversal growth of the drainage system. The linear parameters— bifurcation ratio (R_{bm}), drainage density (D_d), hydrographic density (D_h), drainage texture (R_t) and length of overland flow (L_g)— are directly related to the specific degradation of the intervention areas; that is, the higher these values the greater the degradation. Therefore, the value 1 was assigned to the highest value for each linear parameter, and a 2 to the next value in descending order, and so on. The shape parameters— elongation ratio (R_e), circularity ratio (R_c), compactness coefficient (C_c), form factor (R_f) and shape of the basin (B_s)— are inversely related to the specific degradation of the intervention area; that is, the lower the values the greater the

degradation. Therefore, a 1 was assigned to the lowest value of these parameters, and so on (Biswas *et al.*, 1999; Nooka-Ratnam *et al.*, 2005; Javed, Khanday, & Ahmed, 2009; Kanth & Hassan, 2012; Kiran & Srivastasa, 2012; Tamang, Dhakal, Shrestha, & Sharma, 2012; Tolessa & Rao, 2013).

Obtainment of the NDVI

The NDVI was obtained using LandSat 5 TM satellite images from July 13, 1993 and LandSat 8 OLI from July 20, 2013. Atmospheric correction was applied to both images to eliminate interference from atmospheric conditions and cloudiness. The NDVI values for both images were obtained using equation (1) (Hayes, 1985):

$$NDVI = \frac{IRC - R}{IRC + R} \quad (1)$$

Where NDVI is the Normalized Difference Vegetation Index, IRC and R correspond to the bands used for the calculation, which were 4 and 3 for the TM sensor and bands 5 and 4 for the OLI sensor, respectively.

The NDVI values for each sub-basin were grouped using reference values proposed by Merg *et al.* (2011) (Table 2).

Map algebra was used to obtain the variation in the NDVI for the different dates associated with the classification mentioned. The pixels were analyzed to determine the area of each type of vegetation (CW, WV, LV, MV and HV) for

Table 2. Classification of NDVI values.

Classification	Value
Clouds and water (CW)	< 0.01
Soil without vegetation (WV)	0.01 - 0.1
Light vegetation (LV)	0.1 - 0.2
Medium Vegetation (MV)	0.2 - 0.4
High Vegetation (HV)	> 0.4

each sub-basin. The percentage of change in area was calculated with equation (2):

$$PCS_n = \frac{((SNDVI_{2013}) - (SNDVI_{1993}))_n}{St_n} \times 100 \quad (2)$$

Where PCS_n is the percentage of change in surface area for each type of vegetation (%); sNDVI (2013, 1993) corresponds to the vegetation area present during the year evaluated (ha); St_n is the area of the sub-basin (ha) and n is the sub-basin number.

The prioritization of the sub-basins using the NDVI was performed based on the following criteria:

1. The areas corresponding to the classification of clouds and water were eliminated (CW).
2. The NDVI corresponding to the WV and LV directly impact the specific degradation, therefore higher values for this variable have a higher priority.
3. The NDVI of the MV and HV indirectly impact specific degradation, therefore lower values for this variable have more impact on specific degradation and therefore have a higher priority.

Prioritization of Intervention Areas

The morphometric parameters and the NDVI were classified according to the degree to which they affect the specific degradation of the soils. These values were averaged to obtain a compound parameter for morphometry (PC_m) and the NDVI (PC_{NDVI}). They were then classified from smallest to highest values according to the class intervals high, medium and low prioritization (Biswas *et al.*, 1999; Nooka-Ratnam *et al.*, 2005; Javed *et al.*, 2009; Kanth & Hassan, 2012; Kiran & Srivastasa, 2012; Tamang *et al.*, 2012; Tolessa & Rao, 2013). The class interval was obtained using PC_m, NDVI with equation (3), (4) and (5):

$$\text{Class int (high)} = \left[PC_{\min}, PC_{\min} + \left(\frac{PC_{\max} - PC_{\min}}{3} \right) \right] \quad (3)$$

$$\text{Class int (middle)} = \left[PC_{\min} + \left(\frac{PC_{\max} - PC_{\min}}{3} \right), PC_{\min} + 2 \times \left(\frac{PC_{\max} - PC_{\min}}{3} \right) \right] \quad (4)$$

$$\text{Class int (low)} = \left[PC_{\min} + 2 \times \left(\frac{PC_{\max} - PC_{\min}}{3} \right), PC_{\max} \right] \quad (5)$$

Where $PC_{\min, \max}$ corresponds to the limit values (lower and upper) of the compound parameters and “class int” (high, medium, low) are the three class intervals defined by the methodology.

An optimization scheme for multicriteria decision-making based on compound parameters and the relationships between

each one was used to prioritize drainage areas at different intervention levels (basin, sub-basin, micro-basin, runoff unit) (Figure 2).

Results and Discussion

Morphometric Analysis

Determining the order of the channels in the sub-basins is one of the first steps in a morphometric analysis based on the hierarchy proposed by Strahler (1964). The characteristics of the sub-basins are later used to estimate dimensional parameters and the expected values for the time of concentration of the runoff (Table 3).

In Table 3, P_{lc} is the slope of the main channel (%); P_{mc} is the mean slope of the sub-basin; $Alt_{\min, \max, \text{mean}}$ is the minimum, maximum and mean altitude (m), respectively; H is the difference in elevation (m); T_c is the time of concentration (h), and N_u is the order number of the sub-basin.

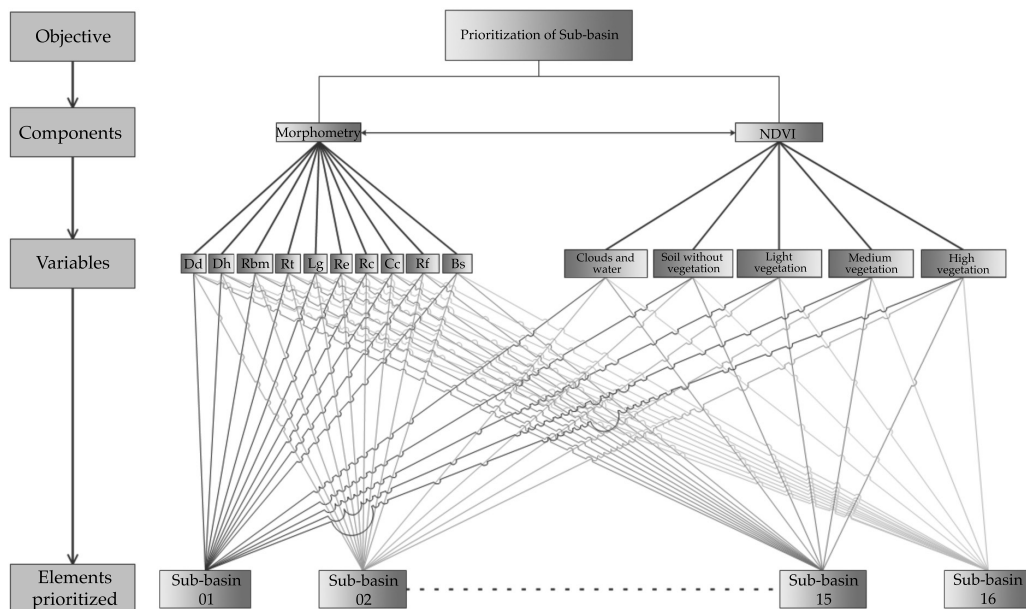


Figure 2. Methodology for the prioritization of drainage areas based on the morphometric analysis and NDVI.

Table 3. Dimensionless parameters corresponding to the sub-basins studied.

Sub-basin	A (km ²)	P (km)	L_c (km)	L_{tc} (km)	P_{lc} (%)	P_{mc} (%)	Alt_{min} (m)	Alt_{max} (m)	Alt_{med} (m)	H (m)	L_u	T_c (h)	N_u
1	12.99	20.70	6.45	70.61	18.57	57.60	1 322	2 520	2 019	1 198	293	0.53	V
2	16.22	24.76	7.98	75.57	17.16	68.28	1 321	2 690	1 980	1 369	292	0.65	V
3	22.47	30.58	8.96	133.56	18.74	51.12	660	2 339	1 200	1 679	558	0.68	V
4	25.92	37.40	12.66	145.28	15.80	66.95	660	2 660	1 745	2 000	634	0.95	V
5	13.99	32.00	10.35	83.28	20.48	43.87	510	2 630	960	2 120	325	0.74	V
6	14.24	26.40	9.53	76.02	21.09	57.64	510	2 520	1 205	2 010	291	0.68	IV
7	14.33	33.94	14.11	75.20	12.66	39.37	350	2 136	852	1 786	285	1.13	IV
8	23.36	39.62	15.56	125.53	13.36	43.14	350	2 430	1 014	2 080	470	1.19	V
9	16.84	26.34	8.99	83.94	7.12	32.34	210	850	529	640	308	0.99	IV
10	3.85	12.76	3.93	14.42	10.79	39.16	213	637	414	424	56	0.45	III
11	25.71	53.82	16.41	99.92	3.84	23.16	30	660	246	630	314	2.00	IV
12	24.41	42.00	14.97	106.70	2.81	16.17	30	450	174	420	391	2.11	V
13	33.90	52.80	22.19	154.58	4.28	25.90	100	1 050	469	950	568	2.42	V
14	2.40	9.22	2.06	10.80	5.92	17.18	100	222	155	122	45	0.34	III
15	26.98	53.44	21.50	140.67	4.83	26.41	131	1 170	549	1 039	590	2.26	IV
16	39.90	72.64	28.60	205.92	6.39	32.80	133	1 960	613	1 827	817	2.53	IV
Min.	2.40	9.22	2.06	10.80	2.81	16.17	30.00	222.00	155	122	45.00	0.34	
Max.	39.90	72.64	28.60	205.92	21.09	68.28	1 322	2 690	2 019	2 120	817.00	2.53	
\bar{x}	19.84	35.53	12.77	100.13	11.49	40.07	414.38	1 683	883	1 268	389.81	1.23	
σ	9.96	16.63	7.04	50.46	6.52	16.66	410.52	919.78	611	680	205.80	0.76	
CV	50.18	46.80	55.17	50.40	56.76	41.58	99.07	54.66	69.25	53.61	52.80	62.20	

The sub-basins are characterized by stream orders III, IV and V, the latter being dominant. The drainage areas range from 2.4 to 39.9 km², with a variation coefficient over 50% and perimeters over 10 km. The lengths of the main rivers range from 2 to 28 km and the total lengths of channels ranges from 10 to 205 km. The mean slopes of the main channels range from 3 to over 21% and the mean slopes of the sub-basins from 16 to 68%. These results indicate large differences in the characteristics of the sub-basins associated with the degradation of soils and surface runoff flowing into the main channel, which is magnified by the present of tropical storms which generate torrential flows and create the risk of flooding in lower portions of the basins. This coincides with reports by Villegas-Romero, Oropeza.Mota, Martínez-Ménes,

& Mejía-Sáenz (2009), who indicate that the flows increase as the drainage area increases and are affected by the spatial variation of the precipitations and the physiographic conditions.

The variation coefficient of the dimensional parameters is over 40, the slopes of the channels are less than the mean slopes and the elevations in the basin range from 30 to over 2000 m. When torrential rainfall occurs, these physiographic conditions generate areas where large amounts of runoff and sediment flow at high velocities to lower portions, causing flooding problems.

The morphometric parameters were divided into linear parameters (related to information about the channels) and shape parameters (related to the area and perimeter of the sub-basins). The

Table 4. Morphometric parameters corresponding to the sub-basins analyzed.

Sub-basin	Linear parameters					Shape parameters				
	D_d	D_h	R_{mb}	R_f	L_g	R_e	R_c	C_c	R_f	B_s
1	5.436	22.556	2.415	14.155	0.092	0.631	0.381	1.620	0.312	3.203
2	4.659	18.002	2.156	11.793	0.107	0.569	0.332	1.734	0.255	3.926
3	5.944	24.833	2.189	18.247	0.084	0.597	0.302	1.820	0.280	3.573
4	5.605	24.460	1.899	16.952	0.089	0.454	0.233	2.072	0.162	6.183
5	5.953	23.231	3.217	10.156	0.084	0.408	0.172	2.413	0.131	7.657
6	5.340	20.439	2.294	11.023	0.094	0.447	0.257	1.974	0.157	6.380
7	5.246	19.882	1.834	8.397	0.095	0.303	0.156	2.529	0.072	13.884
8	5.374	20.120	1.741	11.863	0.093	0.350	0.187	2.312	0.096	10.370
9	4.985	18.290	1.668	11.693	0.100	0.515	0.305	1.811	0.208	4.799
10	3.749	14.559	1.678	4.389	0.133	0.563	0.297	1.835	0.249	4.016
11	3.886	12.213	1.697	5.834	0.129	0.349	0.112	2.994	0.095	10.474
12	4.371	16.018	2.132	9.310	0.114	0.372	0.174	2.398	0.109	9.181
13	4.560	16.756	1.647	10.758	0.110	0.296	0.153	2.558	0.069	14.525
14	4.500	18.750	1.696	4.881	0.111	0.849	0.355	1.679	0.566	1.768
15	5.213	21.866	1.625	11.040	0.096	0.273	0.119	2.902	0.058	17.127
16	5.162	20.478	1.658	11.247	0.097	0.249	0.095	3.244	0.049	20.506
Min.	3.749	12.213	1.625	4.389	0.084	0.249	0.095	1.620	0.049	1.768
Max.	5.953	24.833	3.217	18.247	0.133	0.849	0.381	3.244	0.566	20.506
\bar{x}	4.999	19.528	1.972	10.734	0.102	0.452	0.227	2.244	0.179	8.598
σ	0.658	3.518	0.423	3.803	0.015	0.161	0.093	0.506	0.133	5.505
CV	13.17	18.02	21.48	35.43	14.31	35.69	40.91	22.55	74.27	64.02

linear parameters have smaller variation coefficients than the shape parameters (Table 4) and each has a different degree of influence on the degradation of the soils and surface flow on the hillsides and in the basins.

Drainage Density (D_d)

This parameter is associated with resistance to weathering, permeability of rocks in formation, climate and vegetation. The sub-basins have values between 3.75 and 5.95 km/km², with a variation coefficient of 13%, which indicates that they have good drainage and affect the capacity to produce a significant amount of surface flow, which agrees with a report by Nauyital (1994).

Hydrographic Density (D_h)

This indicates high values associated with impermeable materials with low infiltration capacity, scarce vegetation and steep topographic conditions (Kanth & Hassan, 2012; Kumar-Tamang, Dhakal, Shrestha, & Sharma, 2012). A variation of up to 12 channels/km² was found in the sub-basins of the Huehuetan River basin, which is explained by the variation coefficient estimated.

Mean bifurcation ratio (R_{bm})

This represents the average ratio of the number of streams of a given order number to the number of streams with the next highest order number (Horton, 1932). Strahler (1957) demonstrated that

the mean bifurcation ratio (R_{bm}) presents small ranges of variation for different regions or environments, except for those strongly influenced by geology. The higher the R_{bm} values the higher the degree of torrentiality in the drainage area, which is associated with different responses to floods, and more so when combined with morphometric characteristics, such as the compactness coefficient (Strahler, 1964). The R_{bm} is associated with the shape—the rounder the supply area the lower the bifurcation ratio and the higher the flood risk at the outlet (Gregory & Walling, 1973; Patton, 1988; Sala & Gay, 1981). The values of R_{bm} range from 1.63 to 3.22, where ten sub-basins have values under 2, six have values between 2 and 2.5 and only one was over 3.

Drainage Texture (R_t)

This is one of the most important parameters in geomorphology and indicates the difference between main channels and tributaries (Londhe, Nathawat, & Subudhi, 2010; Pareta & Pareta, 2011). It is affected by the lithology, infiltration capacity and topographic conditions (Pareta & Pareta, 2011). Smith (1950) established a classification of the drainage texture based on the following ranges: very thick (<2), thick (2 to 4), medium (4 to 6), fine (6 to 8) and very fine (>8). Sub-basins 10, 11 and 15 were found to belong to the medium class and the rest have a very fine texture. The R_t ranged from 4.39 to 18.25 channels/km¹, with a variation coefficient of 35.4%.

Length of Overland Flow (L_g)

Horton (1945) defined this parameter as the distance the water travels over the surface of the soil before concentrating in tributaries. This value is approximately equal to half of the reciprocal of the

drainage density and is inversely related to the average slope of the channel, and is synonymous with the length of the sheet flow over hillsides (Javed *et al.*, 2009; Ramaiah, Gopalakrishna, Srinivasa-Vittala, & Najeeb, 2012). The values of L_g in the sub-basins analyzed ranged from 0.084 to 0.133, indicating that the surface runoff length is shortest before entering first-order channels. This value influences the supply of water volumes to the main channel and the time of concentration of the flow.

Elongation Ratio (R_e)

This is the ratio of the diameter of a circle with the same area as the sub-basin to the length of the main channel. This parameter is very important to analyze the shape of the basin, particularly when trying to identify its hydrological behavior (Schumm, 1956; Tolessa & Rao, 2013). The values of the elongation ratio range from 0.6 to 1.0 for a wide variety of geologies and climates (Magesh, Jitheshlal, Chandrasekar, & Jini, 2013). Values between 0.6 and 0.8 are associated with mountainous topographies and steep slopes (Strahler, 1964). These values can be grouped into five categories: circular (> 0.9), oval (from 0.8 to 0.9), less elongated (from 0.7 to 0.8), elongated (0.5 to 0.7) and very elongated (< 0.5) (Pareta & Pareta, 2011). Ten sub-basins were found to be very elongated and number 15 is oval. These values are influenced by the geological and climate conditions of the region.

Circularity Ratio (R_c)

Miller (1953) defined this parameter as the ratio of the area of the sub-basin to the area of a circle with a circumference equal to the perimeter of the sub-basin (Magesh *et al.*, 2013). A circle has the value 1 and a

square 0.785. This parameter is influenced primarily by the lithological characteristics of a sub-basin (Sangita & Nagarajan, 2010; Magesh *et al.*, 2013), as well as by the length and hydrographic density, geological structures, land use, climate, topography and slope of the drainage area (Ramaniah *et al.*, 2012). Low, medium and high values of the circularity ratio are indicators of young, mature and old stages in the lifecycle of tributary areas, respectively. The extreme values in the sub-basins analyzed were between 0.095 and 0.381 for sub-basins 11 and 1.

Compactness Coefficient (C_c)

This is the ratio of the perimeter of the basin to the circumference of an area equal to the basin (Suresh, Sudhakar, Tiwari, & Chowdary, 2004; Javed *et al.*, 2011; Uniyal & Gupta, 2013). This parameter is independent of the size of the basin and depends only on the slope (Pareta & Pareta, 2011). A circular basin is more vulnerable to degradation from drainage since the time of concentration is shorter and maximum flow occurs over a short time period (Nooka-Ratnam *et al.*, 2005). Campos-Aranda (1998) divide C_c into three classes: class I (1.0-1.25, virtually round to oval-oblong), class II (1.26-1.50, oval-round to oval-oblong), class III (from 1.51 to > 2 , oval-oblong to rectangular oblong). The values of C_c ranged from 1.620 to 3.244, and therefore all the sub-basins fall into class III, indicating that the magnitude of the floods could increase at least at the outlets and the maximum runoff into the main channel could be very large. This parameter is an indicator of the occurrence of floods in towns near channels since the surface runoff reaches the main channel quickly (Maldonado de León, Palacios, Oropeza, Springall, & Fernández, 2001).

Form Factor

This is the ratio of the area of the basin to the square of its maximum or axial length (Horton, 1945; Pareta & Pareta, 2011; Chirala, Nooka-Ratnam, & Murali-Krishna, 2012; Jasrotia, Kumar, & Aasim, 2012; Kanth & Hassan, 2012; Tamang *et al.*, 2012; Tolessa & Rao, 2013). The latter is obtained by measuring the length of the main channel until reaching the furthest point in the drainage area (watershed); that is, the length of the longest route of a drop of water. The drainage areas with values near 0.7854 are circular and present maximum flows with short durations, while low values indicate elongated basins with smaller maximum flows and longer duration (Javed *et al.*, 2011; Londhe *et al.*, 2010; Tamang *et al.*, 2012). For the Huehuetan River's sub-basins, most tend to be elongated, since they are under 0.312, and only sub-basin 14 had a value of 0.566.

Shape of the Basin (B_s)

This is the ratio of the length of the main channel squared to the area of the basin (Horton, 1945). This parameter indicates the direct result of the evolution of a drainage system in a particular basin and must be analyzed taking into account the values of other parameters such as the form factor, circularity ratio and elongation ratio (Jawaharaj & Sakthivel, 2012). This parameter ranged from 1.768 to 20.506 for sub-basins 14 and 16, respectively, with a variation coefficient of 64%, exceeded only by the CV of the form factor (74.27%).

Prioritization of Intervention Areas (Sub-basins) based on the Morphometric Analysis

Based on the values of the morphometric parameters, an average value was

Table 5. Prioritization of sub-basins based on the morphometric analysis.

Sub-b	Linear parameters					Shape parameters					PC_m	NP_m	DP_m
	D_d	D_h	R_{mb}	R_t	L_g	R_e	R_c	C_c	R_f	B_s			
1	4	4	2	3	13	15	16	1	15	2	7.50	4	High
2	11	12	5	5	6	13	14	3	13	4	8.60	9	Medium
3	2	1	4	1	15	14	12	5	14	3	7.10	1	High
4	3	2	7	2	14	10	9	8	10	7	7.20	2	High
5	1	3	1	11	16	8	6	11	8	9	7.40	3	High
6	6	7	3	9	11	9	10	7	9	8	7.90	6	High
7	7	9	8	13	10	4	5	12	4	13	8.50	8	Medium
8	5	8	9	4	12	6	8	9	6	11	7.80	5	High
9	10	11	13	6	7	11	13	4	11	6	9.20	11	Medium
10	16	15	12	16	1	12	11	6	12	5	10.60	14	Low
11	15	16	10	14	2	5	2	15	5	12	9.60	12	Low
12	14	14	6	12	3	7	7	10	7	10	9.0	10	Medium
13	12	13	15	10	5	3	4	13	3	14	9.20	11	Medium
14	13	10	11	15	4	16	15	2	16	1	10.30	13	Low
15	8	5	16	8	9	2	3	14	2	15	8.20	7	High
16	9	6	14	7	8	1	1	16	1	15	7.80	5	High

obtained, called the compound parameter (PC_m), which enabled ordering the sub-basins by assigning prioritization level (NP_m) 1 to the smallest value of PC_m , which increases as the PC_m of the sub-basins increase. The degrees of prioritization (DP_m)— high, medium and low— were defined according to the range of the PC_m values (Table 5).

The degrees of priority (DP_m) are associated with the intervention order of the sub-basins. Eight sub-basins had a high priority, covering 56.64% of the total area of the basin, 5 had a medium priority (33.29%) and the rest had a low priority, covering only 10.07% of the total area. It is worth noting that the morphometric parameters corresponding to the upper basin are indicators of topography and shape conditions which influence the degree of degradation in the drainage areas.

Prioritization of Sub-basins based on the Change in Area Occupied by NDVI values

The NDVI values for each of the pixels were used to group zones with different NDVI values. The areas with different types of vegetation and their percentages (%) were defined based on the ranges of values presented in Table 2, with respect to the areas of each sub-basin for the years 1993 and 2013 (Tables 6 and 7).

The changes in the vegetation conditions over the years of reference indicate the degree to which the vegetation cover has been altered. The increases or reductions in the areas of each type of vegetation enable identifying the percentage difference in change (Table 8). The analysis of changes in NDVI area found that the high vegetation class had the greatest variation in vegetation cover, given that all percentage changes were negative, especially in the

Table 6. Area of the sub-basins according to the NDVI classification for the year 2013.

Sub-basin	Area with NDVI										Total area ha
	CW		WV		LV		MV		HV		
	ha	%	ha	%	ha	%	ha	%	ha	%	
1	0.00	0.00	8.46	0.65	86.40	6.66	316.62	24.42	885.33	68.27	1 296.81
2	0.00	0.00	5.04	0.31	87.21	5.38	526.50	32.47	1 002.87	61.84	1 621.62
3	0.00	0.00	0.36	0.02	16.74	0.74	172.80	7.68	2 061.54	91.57	2 251.44
4	0.00	0.00	20.25	0.78	148.14	5.72	620.19	23.93	1 802.61	69.57	2 591.19
5	0.00	0.00	0.45	0.03	29.61	2.08	92.43	6.49	1 301.31	91.40	1 423.80
6	0.00	0.00	0.00	0.00	32.76	2.30	145.80	10.24	1 244.88	87.46	1 423.44
7	0.00	0.00	0.36	0.03	2.52	0.18	117.63	8.21	1 312.83	91.59	1 433.34
8	0.00	0.00	0.09	0.00	21.06	0.90	133.02	5.70	2 180.70	93.40	2 334.87
9	0.09	0.01	1.26	0.08	5.94	0.36	47.25	2.85	1 602.36	96.71	1 656.90
10	0.00	0.00	0.09	0.02	0.18	0.05	9.27	2.38	379.62	97.55	389.16
11	2.43	0.10	18.54	0.73	60.66	2.38	250.65	9.83	2 217.33	86.97	2 549.61
12	0.27	0.01	3.69	0.16	6.57	0.28	176.22	7.50	2 163.78	92.05	2 350.53
13	0.00	0.00	0.18	0.01	18.81	0.53	143.37	4.06	3 368.43	95.40	3 530.79
14	0.00	0.00	0.18	0.06	2.88	0.89	43.83	13.52	277.38	85.54	324.27
15	0.00	0.00	0.00	0.00	3.69	0.14	117.09	4.32	2 591.91	95.55	2 712.69
16	0.00	0.00	0.00	0.00	1.71	0.04	144.72	3.57	3 904.20	96.39	4 050.63

Table 7. Area of the sub-basins according to the NDVI classification for the year 1993.

Sub-basin	Area with NDVI										Total area ha
	CW		WV		LV		MV		HV		
	ha	%	ha	%	ha	%	ha	%	ha	%	
1	0.00	0.00	0.00	0.00	0.00	0.00	4.77	0.37	1 292.04	99.63	1 296.81
2	0.00	0.00	0.09	0.01	0.72	0.04	18.54	1.14	1 602.27	98.81	1 621.62
3	0.09	0.00	0.09	0.00	0.27	0.01	19.71	0.88	2 231.28	99.10	2 251.44
4	0.00	0.00	0.09	0.00	0.63	0.02	16.83	0.65	2 573.64	99.32	2 591.19
5	0.00	0.00	0.36	0.03	0.90	0.06	10.08	0.71	1 412.46	99.20	1 423.80
6	0.00	0.00	0.27	0.02	3.33	0.23	39.87	2.80	1 379.97	96.95	1 423.44
7	0.00	0.00	0.63	0.04	3.24	0.23	11.25	0.78	1 418.22	98.95	1 433.34
8	6.21	0.27	14.94	0.64	18.54	0.79	50.13	2.15	2 245.05	96.15	2 334.87
9	0.00	0.00	0.09	0.01	0.36	0.02	5.94	0.36	1 650.51	99.61	1 656.90
10	0.00	0.00	0.00	0.00	0.00	0.00	0.27	0.07	388.89	99.93	389.16
11	0.00	0.00	2.07	0.08	14.94	0.59	135.63	5.32	2 396.97	94.01	2 549.61
12	0.00	0.00	0.00	0.00	4.32	0.18	93.69	3.99	2 252.52	95.83	2 350.53
13	0.00	0.00	0.27	0.01	0.99	0.03	25.83	0.73	3 503.70	99.23	3 530.79
14	0.00	0.00	0.45	0.14	3.60	1.11	48.69	15.02	271.53	83.74	324.27
15	0.00	0.00	0.72	0.03	1.98	0.07	13.59	0.50	2 696.40	99.40	2 712.69
16	10.44	0.26	33.21	0.82	27.09	0.67	61.11	1.51	3 918.78	96.74	4 050.63

Table 8. Percentage difference in area in sub-basins based on changes in the NDVI.

Sub-basin	Difference in change in area					Prioritization					PC_{NDVI}	NP_{NDVI}	DP_{NDVI}
	CW^* (%)	WV (%)	LV (%)	MV (%)	HV (%)	CW^*	WV	LV	MV	HV			
1	--	0.65	6.66	24.05	-31.36	--	2	1	15	2	5.00	1	High
2	--	0.31	5.33	31.32	-36.96	--	4	3	16	1	6.00	2	High
3	--	0.01	0.73	6.80	-7.54	--	8	7	11	6	8.00	6	Medium
4	--	0.78	5.69	23.29	-29.76	--	1	2	14	3	5.00	1	High
5	--	0.01	2.02	5.78	-7.81	--	9	5	10	5	7.25	4	High
6	--	-0.02	2.07	7.44	-9.49	--	11	4	13	4	8.00	6	Medium
7	--	-0.02	-0.05	7.42	-7.35	--	10	14	12	7	10.75	11	Low
8	--	-0.64	0.11	3.55	-2.76	--	14	10	7	13	11.00	12	Low
9	--	0.07	0.34	2.49	-2.91	--	6	9	4	12	7.75	5	Medium
10	--	0.02	0.05	2.31	-2.38	--	7	13	3	14	9.25	8	Medium
11	--	0.65	1.79	4.51	-7.05	--	3	6	9	8	6.50	3	High
12	--	0.16	0.10	3.51	-3.78	--	5	11	6	11	8.25	7	Medium
13	--	--	0.50	3.33	-3.83	--	16	8	5	10	9.75	9	Low
14	--	-0.08	-0.22	-1.50	1.80	--	13	15	1	16	11.25	13	Low
15	--	-0.03	0.06	3.82	-3.85	--	12	12	8	9	10.25	10	Low
16	--	-0.82	-0.63	2.06	-0.36	--	15	16	2	15	12.00	14	Low

*Area eliminated since it was not significant (see Tables 6 and 7).

sub-basins of the upper basin, which is associated with considerable deterioration in vegetation and with an increase in soil degradation processes.

The criteria described previously were considered to prioritize the change in vegetation cover in function of the NDVI. Values with higher percentage changes in cover were assigned the priority 1, and so on for each class. The compound parameter (PC_{NDVI}) was then obtained for each sub-basin by assigning the NP_{ndvi} value of 1 to the smallest PC_{NDVI} increasing this as the value of PC_{NDVI} increased. The degrees of prioritization (DP_{NDVI})— high, medium and low— were defined according to the range of PC_{NDVI} values (Table 8). Five sub-

basins that cover 29.69% of the basin were designated as high priority, another 5 medium priority (25.27% of the basin) and the remaining low priority (45.04%).

Prioritization of Intervention Areas (Sub-basins) Considering Both Components

The global compound parameter (PC_g) was obtained based on the compound parameters for each one of the components (PC_m and PC_{NDVI}), according to their prioritization by assigning ascending values in function of the PC_m and PC_{NDVI} obtained for each of the sub-basins. A global priority level NP_g of 1 was assigned to the lowest PC_g value. High, medium

Table 9. Final prioritization of the components analyzed (morphometry and NDVI).

Sub-basin	PC_m (morphometry)	PC_{NDVI} (% change in NDVI)	PC_g (components)	NP_g	DP_g
1	7.50	5.00	6.25	2	High
2	8.60	6.00	7.30	3	High
3	7.10	8.00	7.55	5	High
4	7.20	5.00	6.10	1	High
5	7.40	7.25	7.33	4	High
6	7.90	8.00	7.95	6	Medium
7	8.50	10.75	9.63	13	Low
8	7.80	11.00	9.40	11	Low
9	9.20	7.75	8.48	8	Medium
10	10.60	9.25	9.93	15	Low
11	9.60	6.50	8.05	7	Medium
12	9.00	8.25	8.63	9	Medium
13	9.20	9.75	9.48	12	Low
14	10.30	11.25	10.78	16	Low
15	8.20	10.25	9.23	10	Low
16	7.80	12.00	9.90	14	Low

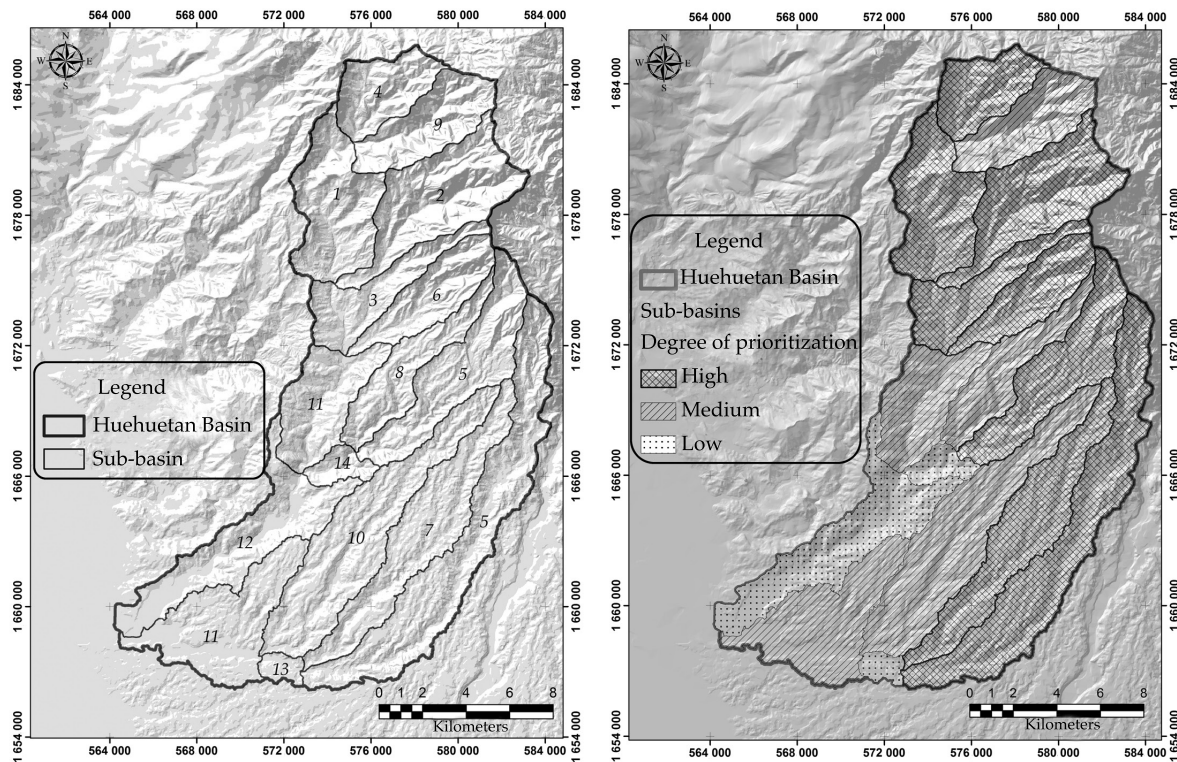


Figure 3. Global prioritization level (left) and degree of global prioritization (right) of the sub-basins in the Huehuetan River Basin.

and low global degree of priorities (DP_g) were defined for the sub-basins— that is, their global intervention levels based on the compound parameters (Table 9).

Thus, sub-basins 1 through 5 were defined as a high priority, which cover 29.20% of the basin, and sub-basin 4 had the highest priority. Four sub-basins were classified as medium priority, covering 25.89% of the basin. The remaining were low priority (44.91% of the basin) (Figure 3).

It is worth noting the importance of the methodology used to prioritize the intervention areas with multicriteria decision-making, which showed that the primary areas (sub-basins) needing interventions are in the upper basin and those needing less intervention are in the lower basin (Figure 3). This reflects the conditions that are prevalent in each of the sub-basins through the combination of the spatial analysis of data, hydrological behavior and the effect of temporal variations in vegetation cover on soil degradation processes and sediment transport.

In the upper and middle basins, the morphometric parameters and the temporal variation in the NDVI resulted in the same levels of prioritization, due to degradation. Meanwhile, in the lower basin the morphometric parameters defined sub-basins as having a high and medium priority and the temporal variation in the NDVI defined sub-basins as having a low priority. Therefore, in the global degree of prioritization, the NDVI has more impact when grouping the sub-basins into low priority.

Using a morphometric analysis combined with the changes in the multi-temporal vegetation index, associating linear and shape parameters can be associated. These are related to the hydrological variables involved in the

growth of drainage systems in sub-basins and changes in vegetation cover presenting a risk of degradation. Together, this makes it possible to define the intervention areas for hydrological restoration.

Conclusion

As a result of the prioritization of intervention areas based on morphometric parameters and changes in vegetation cover, 5 sub-basins were identified in the upper basin as having the highest priority for hydrological restoration, given the linear and shape parameters associated with the hydrological variables. This intervention is aimed at reducing the impact of unusually large maximum flows on the lower basin.

This methodology can be used to prioritize interventions at various levels— basin, sub-basin, micro-basin and runoff units— depending on the size of the project and its purpose. Nevertheless, it is particularly important to use a digital elevation model at a scale that enables obtaining more precise linear and shape morphometric parameters.

References

- Alatorre, L. C., Beguería, S., & Vicente-Serrano, S. M. (2010). Análisis de la evolución espacio-temporal del NDVI sobre las áreas vegetadas y zonas de riesgo de erosión en el Pirineo Central. *Pirineos. Revista de Ecología de Montaña*, 165, 7-27.
- Andréassian, V. (2004). Waters and Forests: From Historical Controversy to Scientific Debate. *Journal of Hydrology*, 291, 1-27.
- Arnold, J. G., Williams, J. R., Nicks, A. D., & Sammons, N. B. (1990). *SWRRB: A Basin Scale Simulation Model for Soil and Water Resources Management* (142 pp.). College Station, USA: Texas A & M University Press.
- Biswas, S., Sudhakar, S. And Desai, V. R. (1999). Prioritisation of Subwatersheds based on Morphometric Analysis of Drainage Basin: A Remote Sensing and GIS Approach. *Journal of the Indian Society of Remote Sensing*, 27(3), 155-166.

- Campos-Aranda, D. F. (1998). *Procesos del ciclo hidrológico* (pp. 22-23). Tercera reimpresión. San Luis Potosí, México: Facultad de Ingeniería, Universidad de San Luis Potosí, México.
- Chirala, U., Nooka-Ratnam, K., & Murali-Krishna, G. (2012). Correlation of Geomorphometric Parameters for the Hydrological Characterization of Meghadrigedda Watershed, Visakhapatnam, India – A GIS approach. *International Journal of Engineering Science and Technology*, 5(7), 3169-3183.
- D'odorico, P., Fagherazzi, S., & Rigon, R. (2005). Potential for Landsliding: Dependence on Hypsograph Characteristics. *Journal of Geophysical Research*, 110, 1-10.
- Di, L., Rundquist, D. C., & Han, L. (1994). Modeling Relationships between NDVI and Precipitation during Vegetative Growth Cycles. *International Journal of Remote Sensing*, 15, 2121-2136.
- Delgado, M. I., & Gaspari, F. J. (septiembre-diciembre 2010). Caracterización morfométrica geoespacial. Estudio de caso: arroyo Belisario, Argentina. *Tecnociencia Chihuahua*, 4(3), 154-163.
- Esper-Angillieri, Y. (2008). Morphometric Analysis of Colangüil River Basin and Flash Flood Hazard, San Juan, Argentina. *Environmental Geology*, 55, 107-111.
- Gaspari, F. J., Rodríguez-Vagaría, A. M., Senisterra, G. E., Denegri, G., Delgado, M. I., & Besteiro, S. (2012). Caracterización morfométrica de la cuenca del río Sauce Grande, Buenos Aires, Argentina (pp. 1-25). *Actas 7mo. Congreso de Medio Ambiente AUGM*, UNLP, Argentina.
- Gregory, K. J., & Walling, D. E. (1973). *Drainage Basin Form and Process: A Geomorphological Approach* (456 pp.). London: Edward Arnold.
- Hayes, L. (1985) The Current Use of TIROS-N Series for Meteorological Satellites for Land-Cover Studies. *International Journal of Remote Sensing*, 6(1), 35-45.
- Hibbert, A. R. (1971). Increases in Streamflow after Converting Chaparral to Grass. *Water Resources Research*, 7(1), 71-80.
- Horton, R. E. (1932). Drainage Basin Characteristics. *Trans. Am. Geophys. Unions*, 13, 350-361.
- Horton, R. E. (1945). Erosional Development of Streams and their Drainage Basins; Hydrophysical Approach to Quantitative Morphology. *Geological Society of America Bulletin*, 56, 275-370.
- Jasrotia, A. S., Kumar, A., & Aasim, M. (2012). Morphometric Analysis and Hydrogeomorphology for Delineating Groundwater Potential Zones of Western Doon Valley, Uttarakhand, India. *International Journal of Geomatics and Geosciences*, 2(4), 1078-1096.
- Javed, A., Khanday, M. Y., & Ahmed, R. (June, 2009). Prioritization of Sub-watersheds based on Morphometric and Land Use Analysis using Remote Sensing and GIS Techniques. *J. Indian Soc. Remote Sens.*, 37(2), 261-274.
- Javed, A., Khanday, M. Y., & Rais, S. (2011). Watershed Prioritization Using Morphometric and Land Use/Land Cover Parameters: A Remote Sensing and GIS Based Approach. *Journal Geological Society of India*, 78, 63-75.
- Jawaharaj, N., & R. Sakthivel (2012). Quantitative Morphometric Analysis and its Consequences: A case Study from Gomukhiriver Basin, Tamil Nadu. *Int. Journal of Advances in Remote Sensing and GIS*, 1(2), 154-159.
- Johnson, R. (1998). The Forest Cycle and Low River Flows: A Review of UK and International Studies. *Forest Ecology and Management*, 109, 1-7.
- Kanth, T. A., & Hassan, Z. U. (enero-abril, 2012). Morphometric Analysis and Prioritization of Watersheds for Soil and Water Resource Management in Wular Catchment Using Geo-Spatial Tools. *International Journal of Geology, Earth and Environmental Sciences*, 2(1), 30-41.
- Kiran, V. S. S., & Srivastava Y. K. (July, 2012). Check Dam Construction by Prioritization of Micro Watershed, using Morphometric Analysis as a Perspective of Remote Sensing and GIS for Simlapal Block, Bankura, W. B. *Bonfring International Journal of Industrial Engineering and Management Science*, 2(Special Issue 1), 20-31.
- Kumar-Tamang, D., Dhakal, D., Shrestha, D. G. And Sharma, N. P. (2012). Morphometric Analysis and Prioritization of Miniwatersheds in Rongli Watershed, Sikkim (India) Using Remote Sensing and GIS Techniques. *International Journal of Fundamental & Applied Sciences*, 1(2), 61-66.
- Londhe, S., Nathawat, M. S., & A. P. Subudhi (2010). Erosion Susceptibility Zoning and Prioritization of Mini-Watersheds Using Geomatics Approach. *International Journal of Geomatics and Geosciences*, 1(3), 511-528.
- Magesh, N. S., Jitheshlal, K. V., Chandrasekar, N., & Jini, K. V. (2013). Geographical Information System-Based Morphometric Analysis of Bharathapuzha River Basin, Kerala, India. *Appl. Water Sci.*, 3(2), 467-477.
- Mahadevaswamy, G., Nagaraju, D., Siddalingamurthy, S., Lakshamma, M., Subhan, L., Nagesh, P. C., & Rao, K. (2011). Morphometric Analysis of Nanjangud Taluk, Mysore District, Karnataka, India, using GIS Techniques. *International Journal of Geomatics and Geosciences*, 1(4), 721-734.
- Maldonado-De León, O. A., Palacios, O. L., Oropeza, J. L., Springall, R. G., & Fernández, D. S. (2001). Empleo del modelo SWRRB para generar alternativas de manejo en la cuenca de Iztapa, Guatemala. *Agrociencia* 35(2), 335-345.
- Merg, C., Petri, D., Bodoira, F., Nini, M., Fernández, M., Schmidt, F., Montalva, R., Guzmán, L., Rodríguez, K., Blanco, F., & Selzer, F. (2011). Mapas digitales regionales de lluvias, índice estandarizado de precipitación e índice verde. *Revista Pilquen, Sección Agronomía*, 13(11), 1-11.
- Miller, V. C. (1953). A Quantitative Geomorphic Study of Drainage Basin Characteristics in the Clinch Mountain

- Area (51 pp.). Technical report-3. New York: Department of Geology, Columbia University.
- Nauyital, M. D. (1994). Morphometric Analysis of a Drainage Basin using Aerial Photographs: A Case Study of Khairkuli Basin, District Dehradun, U. P. *J. Indian Soc. Remote Sensing*, 22(4), 251-261.
- Nooka-Ratnam, K., Srivastava, Y. K., Venkateshwara-Rao, V., Amminedu, E., & Murthy, K. S. R. (marzo, 2005). Check Dam Positioning by Prioritization of Micro-Watersheds using SYI Model and Morphometric Analysis – Remote Sensing and GIS Perspective. *J. Indian Soc. Remote Sensing*, 33(1), 25-38.
- Pareta, K., & Pareta, U. (2011). Quantitative Morphometric Analysis of a Watershed of Yamuna Basin, India using ASTER (DEM) Data and GIS. *International Journal of Geomatics and Geosciences*, 2(1), 248-269.
- Patton, T. L. (1988). *Drainage Basin Morphometry and Floods* (pp. 51-65). In: V. R. Baker, R. C. Kochel, & P. C. Patton (Eds.). Wiley, USA: Flood Geomorphology.
- Racca, J. M. G. (2010). Geomorfología de la cuenca del Arroyo del Medio. *Boletín del Instituto de Fisiografía y Geología*, 72-75, 13-42.
- Ramaiah, S. N., Gopalakrishna, G. S., Srinivasa-Vittala, S., & Najeeb, K. Md. (2012). Morphometric Analysis of Sub-Basins in and around Malur Taluk, Kolar District, Karnataka Using Remote Sensing and GIS Techniques. *Nature Environment and Pollution Technology*, 11(1), 89-94.
- Sala, M., & Gay, R. (1981). Algunos datos morfométricos de la cuenca del Isábena. *Notas de Geografía Física*, 4, 41-65.
- Sangita, M. S., & Nagarajan, R. (2010). Morphometric Analysis and Prioritization of Sub-Watersheds Using GIS and Remote Sensing Techniques: A Case Study of Odisha, India. *International Journal of Geomatics and Geosciences*, 1(3), 501-510.
- Sarma, S., & Saikia, T. (2012). Prioritization of Sub-Watersheds in Khanapara-Bornihat Area of Assam-Meghalaya (India) Based on Land Use and Slope Analysis Using Remote Sensing and GIS. *Journal of the Indian Society of Remote Sensing*, 40(3), 435-446.
- Schumm, S. A. (1956). Evolution of Drainage Systems and Slopes in Badlands at Perth Anboy, New Jersey. *Bulletin of the Geological Society of America*, 67, 597-646.
- Smith, K. G. (1950). Standards for Grading Texture of Erosional Topography. *American Journal Science*, 248, 655-668.
- Srinivasa-Raju, K., & Nagesh-Kumar, D. (2011). Classification of Microwatersheds Based on Morphological Characteristics. *Journal of Hydro-Environment Research*, 5, 101-109.
- Strahler, A. N. (1957). Quantitative Analysis of Watershed Geomorphology. *American Geophysical Union Transactions*, 38, 913-920.
- Strahler, A. N. (1964). Quantitative Geomorphology of Drainage Basin and Channel Networks (pp. 4-39/4-76). In V. T. Chow (Ed.), *Handbook of Applied Hydrology*. New York: McGraw Hill.
- Suresh, M., Sudhakar, S., Tiwari, K. N., & Chowdary, V. M. (2004). Prioritization of Watersheds Using Morphometric Parameters and Assessment of Surface Water Potential Using Remote Sensing. *Journal of Indian Society of Remote Sensing*, 32(3), 249-259.
- Tamang, D. K., Dhakal, D., Shresta, D. G., & Sharma, N. P. (2012). Morphometric Analysis and Prioritization of Miniwatersheds in Rongli Watershed, Sikkim (India) Using Remote Sensing and GIS Techniques. *International Journal of Fundamental and Applied Sciences*, 1(3), 61-66.
- Tolessa, G. A., & Rao, P. J. (February, 2013). Watershed Development Prioritization of Tandava River Basin, Andhra Pradesh, India – GIS Approach. *International Journal of Engineering Science Invention*, 2(2), 12-20.
- Uniyal, S., & Gupta, P. (2013). Prioritization Based on Morphometric Analysis of Bhilangana Watershed Using Spatial Technology. *International Journal of Remote Sensing and Geoscience*, 1(1), 49-52.
- Villegas-Romero, I., Oropeza-Mota, J. L., Martínez-Ménes, M., & Mejía-Sáenz, E. (2009). Trayectoria y relación lluvia-escorrentamiento causados por el huracán *Paulina* en la cuenca del río La Sabana, Guerrero México. *Agrociencia*, 43(4), 345-356.
- Zucarelli, G. V. (November-December, 2013). Identificación de eventos hídricos extremos en la cuenca del río Paraná. *Tecnología y Ciencias del Agua*, 4(5), 181-187.

Institutional Address of the Authors

M.C. Adolfo López-Pérez
Dr. Mario R. Martínez-Menes
Dr. Demetrio S. Fernández-Reynoso

Colegio de Postgraduados
Postgrado de Hidrociencias
km 36.5 carretera México-Texcoco
56230 Texcoco, Estado de México, MÉXICO
Teléfono: +52 (59) 5952 0200, extensiones 1213 y 1163
adolfohp@colpos.mx
mmario@colpos.mx
demetrio@colpos.mx



Overlook, Mazatlan, Sinaloa, Mexico.

Photo: Ricardo Espinosa Reza.

Numerical Hydrodynamic-Hydrological Modeling in Flood Zones Containing Infrastructure

• Israel E. Herrera-Díaz* •
Universidad de Guanajuato, México
*Corresponding Author

• Clemente Rodríguez-Cuevas •
Universidad Autónoma de San Luis Potosí, México

• Carlos Couder-Castañeda •
Instituto Politécnico Nacional, México

• José R. Gasca-Tirado •
Universidad de Guanajuato, México

Abstract

Herrera-Díaz, I. E., Rodríguez-Cuevas, C., Couder-Castañeda, C., & Gasca-Tirado, J. R. (January-February, 2015). Numerical Hydrodynamic-Hydrological Modeling in Flood Zones Containing Infrastructure. *Water Technology and Sciences* (in Spanish), 6(1), 139-152.

The computational numerical modeling of the surface hydrodynamics and hydrology of the study area is presented, where the construction of infrastructure to explore hydrocarbons is planned on the banks of the Grijalva River, Mexico. Meteorological information is analyzed to determine precipitation intensity, temperatures, evaporation and flows for the year 2014. Flood zones are estimated using programs developed in Fortran and Matlab to solve the Navier-Stokes-Reynolds equation for free surface flows. The intensity of precipitation was obtained with the Gumbel distribution with parameters estimated using probability weighted moments (PWM). Based on this, the magnitude of the flooding in the study area was obtained according to a numerical grid of the topography along with meteorological values such as initial and forcing conditions. Flows, velocities and the hydraulic functioning of mitigation works proposed to preserve the hydrological balance of the system were also obtained.

Keywords: Flood zones, hydrodynamic models, hydrological models, Grijalva River.

Resumen

Herrera-Díaz, I. E., Rodríguez-Cuevas, C., Couder-Castañeda, C., & Gasca-Tirado, J. R. (enero-febrero, 2015). Modelación numérica hidrodinámico-hidrológica en zonas de inundación con presencia de infraestructura. *Tecnología y Ciencias del Agua*, 6(1), 139-152.

Se presenta la modelación numérica computacional de la hidrodinámica superficial e hidrológica de la zona de estudio donde se pretende construir infraestructura para la exploración de hidrocarburos en las márgenes del río Grijalva, México; para ello se muestra el análisis de la información meteorológica, determinando los valores de intensidad de precipitación, temperaturas, evaporación y una estimación de los gastos, correspondiente al año 2014; las zonas de inundación se estimaron con el uso de programas desarrollados en Fortran y Matlab, que resuelven las ecuaciones de Navier-Stokes-Reynolds para flujos a superficie libre y la intensidad de precipitación con la distribución de Gumbel, con parámetros estimados mediante el método de Momentos Ponderados con Probabilidad (MPP), con los cuales, mediante una malla numérica de la topografía, en conjunto con los valores meteorológicos, como condiciones iniciales y forzantes, se determina la magnitud de la inundación del área de estudio, así como la obtención de gastos, velocidades y el funcionamiento hidráulico de las obras de mitigación propuestas para preservar el balance hidrológico del sistema.

Palabras clave: zonas de inundación, modelos hidrodinámicos, modelos hidrológicos, río Grijalva.

Received: 19/05/14
Accepted: 07/10/14

Introduction

The exploration of hydrocarbons in Mexico is one of the main tasks performed by the energy industry. Studies that provide accurate and timely information are crucial to making correct decisions by providing a current panorama about technical and socioeconomic factors that are of influence and converge in the same time and space.

Numerical computational modeling is one tool which has contributed to hydrological studies. It applies fluids dynamics (CFD) as an approach to study the fluids dynamics equation used to describe different physical phenomena related to the movement of fluids, such as those produced by compressible and non-compressible flows.

This work combines a hydrodynamic numerical model with a hydrological

numerical model to determine the hydrodynamic functioning of an area where the building of exploration and exploitation wells is proposed, and to evaluate the effect of the project's infrastructure (roads, accesses, bridges, etc.). The area is known to behave as a floodplain because of its topographical, hydraulic and geohydrological characteristics. Therefore, a secondary objective of this study is to analyze mitigation measures that prevent substantially altering the hydrodynamic balance of the area selected.

Location and Characteristics of the Study Area

The study site is located on the left banks of the Chilapa or Grijalva River in the state of Tabasco, Mexico (Figure 1). It is bounded by a polygon of channels in the upper and

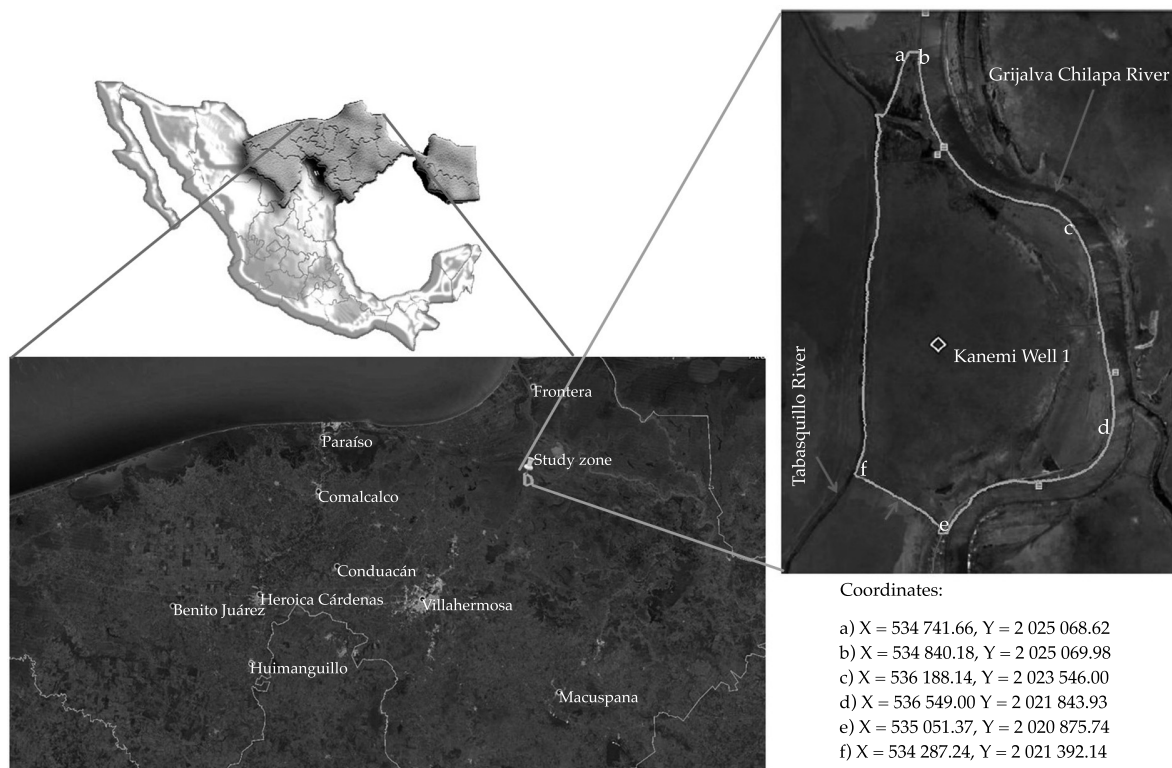


Figure 1. Location of the study zone (municipality of Centla, state of Tabasco, Mexico).

lower portions and the Tabasquillo River on the far left. A civil works structure is located in the center of the plains, which is part of the system and is the main focus of the study.

Figure 2 shows the proposed road leading to the proposed well structures. Since the road is new to the environment, the use of culverts or drainage ditches is being considered so that the hydrological flow of the system can function without substantially altering its original state. Their locations and dimensions are determined based on the magnitudes of calculated velocities and flows resulting from simulations, and should ensure that the hydrological flow is not interrupted and that it follows the natural channel in order to comply with NOM-022-SEMARNAT-2013.

From the hydraulic perspective, the overall morphology of the area is considered to be very constant over time. That is, the entire flood zone is continuously covered by vegetation and therefore the surface flow velocities are not significant enough to alter the morphology of the terrain. Therefore, this factor is considered a constant for simulation purposes.

To model surface flow for different return periods and rainfall intensities, precipitation data was collected from isohyet cards (SCT-DGST, 2013) corresponding to return periods and rainfall intensity and duration. The information was condensed and rainfalls lasting over 30 minutes were used with different return periods (Figures 3a and 3e).

A runoff coefficient between 15 and 25% was used since it presents medium and low permeability, given the average soil material and medium vegetation density throughout the environmental system.

Two study scenarios for one year were proposed—one for the dry season and one

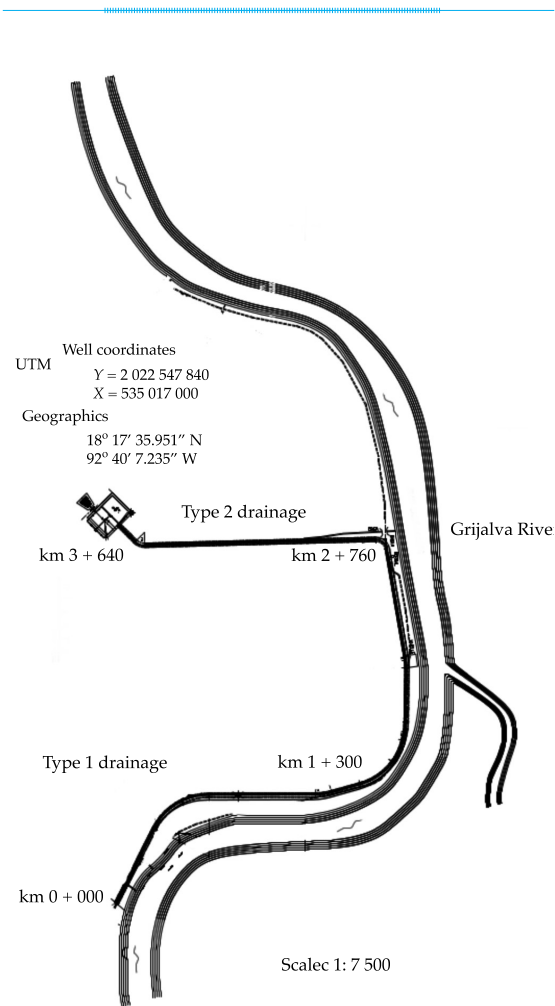


Figure 2. Map of proposed infrastructure inside the environmental system.

for the rainy season (Yin, Yu, Zhane, Wang, & Xu, 2013). The data for each scenario is presented in Tables 1 and 2.

The information obtained was used to estimate the flows in the Grijalva River for the year 2014 in order to perform 2D hydrodynamic flow simulations of flood routes during dry and rainy seasons, which was combined with a hydrological model (Mani, Chatterjee, & Kumar, 2014; Zhang, Long, Xie, Zhu, & Wang, 2007). Figure 4 shows the flows in the river.

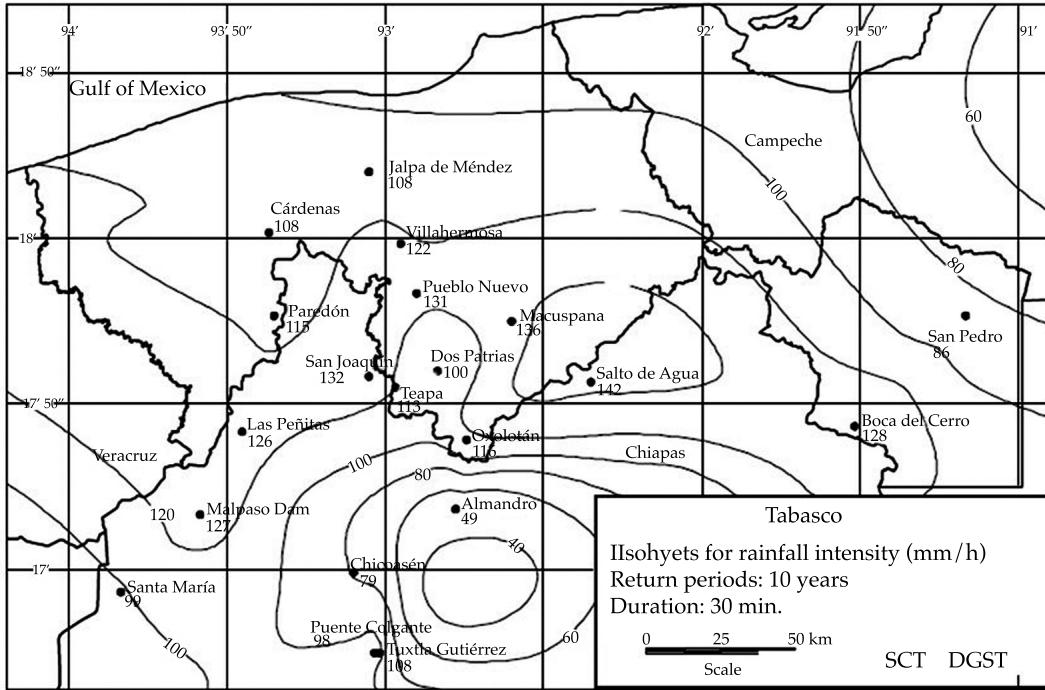


Figure 3a. Isohyets for rainfall intensity for a 10-year return period and 30 minute duration.

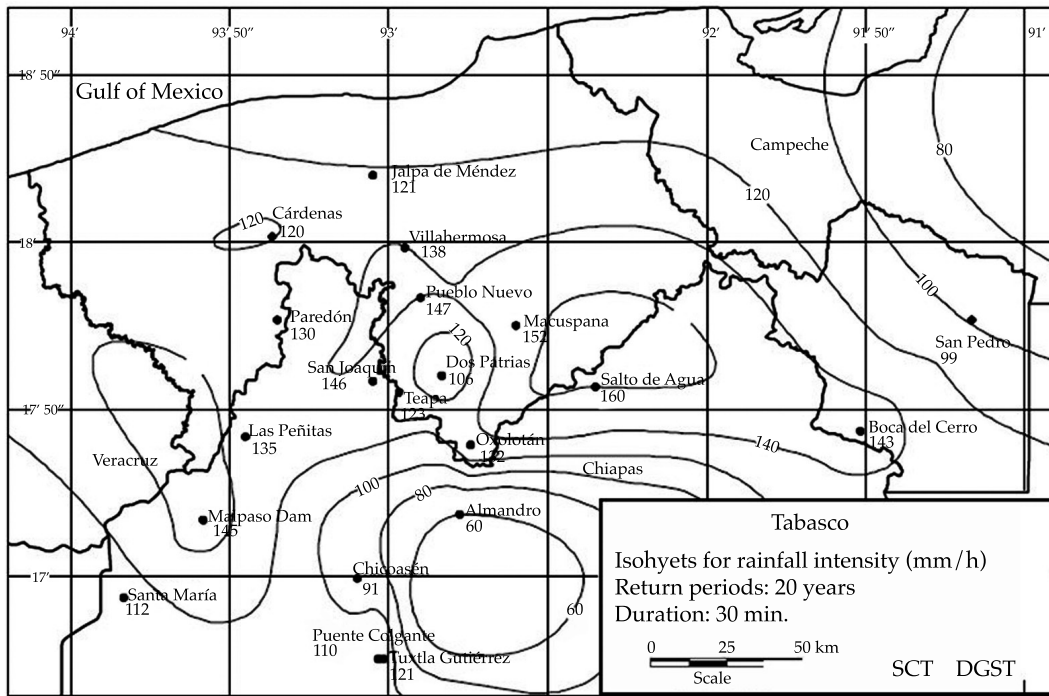


Figure 3a. Isohyets for rainfall intensity for a 20-year return period and 30 minute duration.

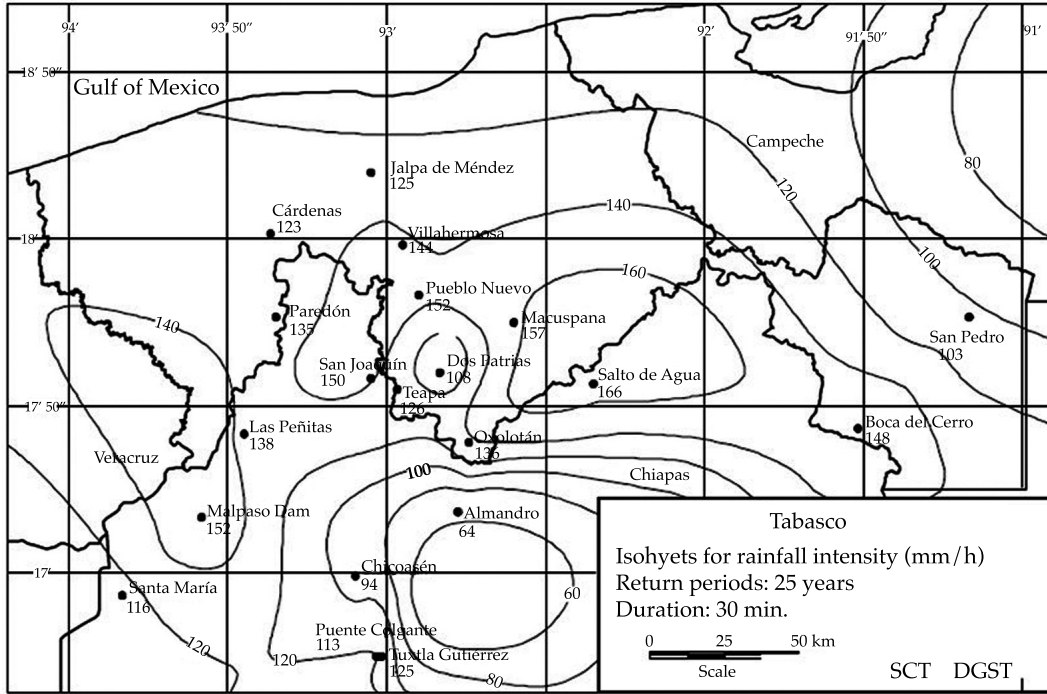


Figure 3c. Isohyets for rainfall intensity for a 25-year return period and 30 minute duration.

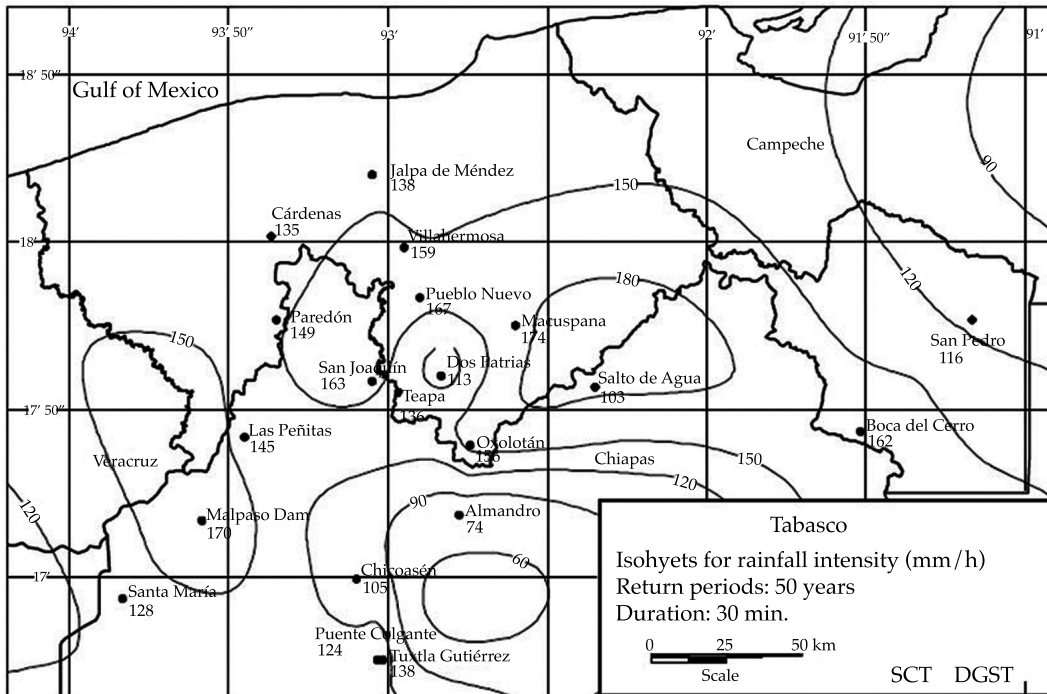


Figure 3d. Isohyets for rainfall intensity for a 50-year return period and 30 minute duration.

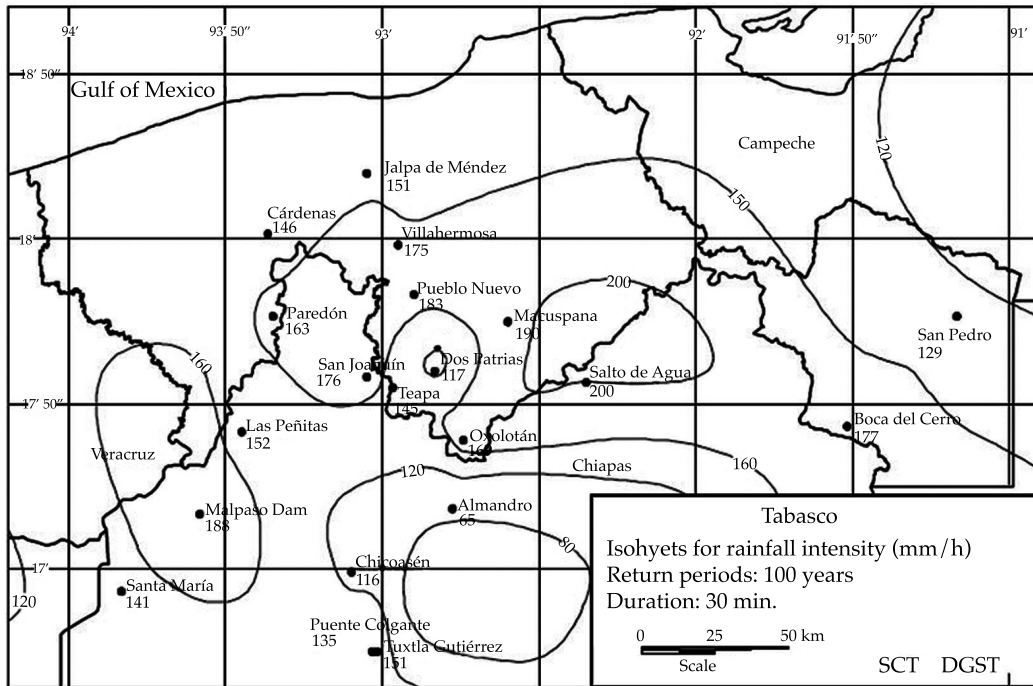


Figure 3e. Isohyets for rainfall intensity for a 100-year return period and 30 minute duration.

Table 1. Summary of values obtained from the data for input into the hydrodynamic model for the year 2014..

Season	Monthly mean precipitation	Monthly mean temperature	Monthly mean evaporation
Dry	156.79 mm	26.4 °C	148.66 mm
Rainy	206.15 mm	26.2 °C	117.33 mm

Table 2. Runoff and permeability of the environmental system.

Season	Vegetation density	Permeability of the soil	Runoff coefficient in the zone (%)
Dry	Medium-low	Medium	15 to 25
Rainy	Medium	Medium	Over 25

Methodology

The hydrodynamic model applied solves the simplified Navier-Stokes equations for free surface flows on Cartesian coordinates. Considering the hydrostatic pressure hypothesis and the Reynolds hypotheses (Broomans, 2003):

$$\begin{aligned}
 \frac{\partial u}{\partial t} + u \frac{\partial u}{\partial x} + v \frac{\partial u}{\partial y} + w \frac{\partial u}{\partial z} &= -g \frac{\partial \eta}{\partial x} + \text{div}(v_e \overline{\text{grad}}(u)), \\
 \frac{\partial v}{\partial t} + u \frac{\partial v}{\partial x} + v \frac{\partial v}{\partial y} + w \frac{\partial v}{\partial z} &= -g \frac{\partial \eta}{\partial x} + \text{div}(v_e \overline{\text{grad}}(v)), \\
 \frac{\partial \eta}{\partial t} &= -\frac{\partial}{\partial x} \left(\int_{-z_f}^n u dz \right) - \frac{\partial}{\partial y} \left(\int_{-z_f}^n v dz \right)
 \end{aligned} \tag{1}$$

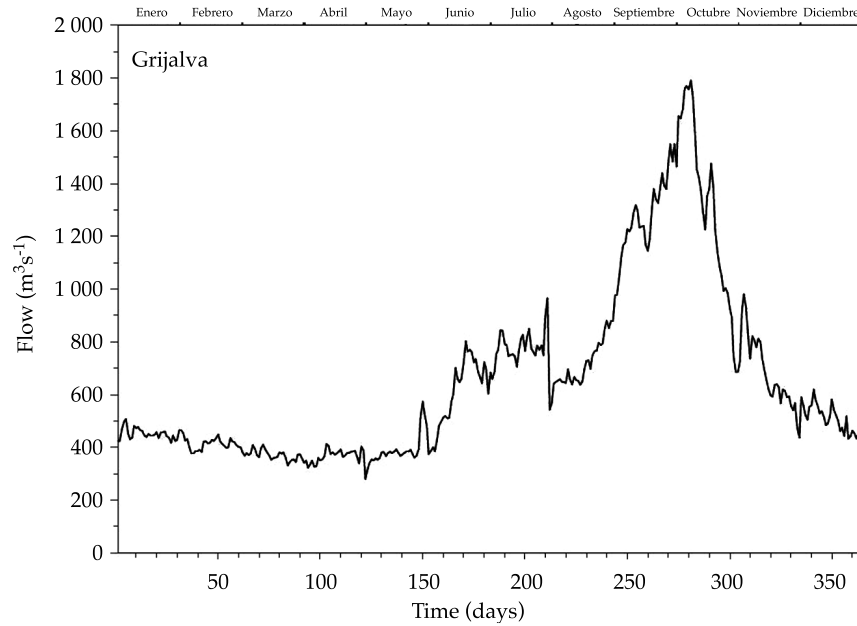


Figure 4. Estimation of flow in the Grijalva River for 365 days during the year 2014.

where v_e is the effective viscosity coefficient obtained by the sum of the turbulent and molecular viscosity coefficients, $v_e = v_t + v_m$. Stansby (2003) proposed the following model to solve for turbulent viscosity:

$$v_t = \left\{ \ell_h^4 \left[2 \left(\frac{\partial u}{\partial x} \right)^2 + 2 \left(\frac{\partial v}{\partial y} \right)^2 + \left(\frac{\partial v}{\partial x} + \frac{\partial u}{\partial y} \right)^2 \right] + \ell_v^4 \left[\left(\frac{\partial u}{\partial z} \right)^2 + \left(\frac{\partial v}{\partial z} \right)^2 \right] \right\}^{1/2} \quad (2)$$

donde la longitud vertical se define por where vertical length is defined by $\ell_v = K(z - z_b)$ for $(z - z_b)/\delta < \lambda/K$ y $\ell_v = \lambda\delta$ for $\lambda/K < (z - z_b)/\delta < 1$. K is the von-Karman constant which typically has a value of 0.41; $(z - z_b)$ is the distance from the bottom; δ is the thickness of the boundary layer and λ is a constant with a value of 0.09. The border conditions for the free surface and the bottom are represented by:

$$\begin{aligned} \tau_x^{\text{bottom}} &= v_e \left. \frac{\partial u}{\partial z} \right|_{\text{bottom}} = \frac{g\sqrt{u^2 + v^2}}{Cz^2} (u), \\ \tau_y^{\text{bottom}} &= v_e \left. \frac{\partial v}{\partial z} \right|_{\text{bottom}} = \frac{g\sqrt{u^2 + v^2}}{Cz^2} (v) \end{aligned} \quad (3)$$

where Cz is the Chezy friction coefficient. The velocity components take the values of the layer adjacent to the water-sediment interface, defined as:

$$\begin{aligned} \tau_x^{\text{sup}} &= v_e \left. \frac{\partial v}{\partial z} \right|_{\text{surface}} = -\frac{\rho_{\text{air}}}{\rho_{\text{water}}} a_{\text{wind}} \omega_x |\omega_x|, \\ \tau_y^{\text{sup}} &= v_e \left. \frac{\partial v}{\partial z} \right|_{\text{surface}} = -\frac{\rho_{\text{air}}}{\rho_{\text{water}}} a_{\text{wind}} \omega_y |\omega_y| \end{aligned} \quad (4)$$

where $\rho_{\text{air}} = 1.29 \text{ kg/m}^3$, ω_x and ω_y are the horizontal components of the wind velocity at x and y , respectively, at 10 m of altitude. The coefficient a_{air} (dimensionless) can be obtained using the equation by Flather (1976) (UNESCO, 1981) :

$$\begin{aligned}
 a_{\text{wind}} &= 0.565 \times 10^{-3} \text{ if } |\bar{\omega}| \leq 5 \frac{\text{m}}{\text{s}} \\
 a_{\text{wind}} &= (-0.12 + 0.137|\bar{\omega}|) 10^{-3} \text{ if } 5 \leq |\bar{\omega}| \leq 19.22 \text{ m/s} \\
 a_{\text{wind}} &= 2.513 \times 10^{-3} \text{ if } |\bar{\omega}| \geq 19.22 \text{ m/s}
 \end{aligned}
 \tag{5}$$

The threat of floods depends on the occurrence of the phenomenon and its intensity (Gurusamy & Jayaraman, 2012). Intensity is defined by the velocity and depth of water as well as the duration of the flood. Therefore, the definition of a flood threat in terms of potential damage (Zhou et al., 2014) takes into account the probability or frequency that a flood will occur as well as the levels or heights of the free water surface.

The principle behind the hydrological model proposed is the precipitation-runoff ratio. It incorporates the generation of stochastic convective rainfall (Gubarevat, 2011) in order to define specific threat scenarios for an evaluation of the risk of an associated flood. The Gumbel distribution is used with parameters estimated using the probability-weighted moments (PWM) method. This is considered to be the best fitted distribution for extreme precipitations for this case (Jean, Kim, & Kim, 2011):

$$P_m = \frac{\sum [P_i * A]}{\sum [A]}
 \tag{6}$$

$$I(t, T) = at^b
 \tag{7}$$

where P_m is the mean precipitation, A is the area bounded by the Thiessen polygons or isohyet curves; P_i is the precipitation measured at weather station “ i ” or average precipitation of two isohyet curves; I is the rainfall intensity in mm/h. The inverse of the return period is the probability of occurrence, that is, the probability that the storm intensity will occur in one year.

Parameters a , b , m , n are a function of the meteorological characteristics of the region. The accumulated hyetograph is described as:

$$H(t) = I(t, T) * t = at^b
 \tag{8}$$

And the associated instantaneous intensity as:

$$I(t) = \frac{dH(t)}{dt} = (b+1)at^b
 \tag{9}$$

To complete missing information from the rain gauge records, information from the National Weather Service was used (Patro, Chatterjee, Mohanty, Singh, & Raghuwanshi, 2009) based on the following correlation:

$$P = \frac{\sum [P_i / r_i^2]}{\sum [1_i / r_i^2]}
 \tag{10}$$

where P is the extrapolated precipitation, P_i is the precipitation from the existing stations in the area around the unknown precipitation and r_i is the distances between one station and the next.

Greenwood, Landwehr, Matalas and Wallis (1979) introduced the PWM as a robust estimation procedure and an alternative to methods of moments and the maximum likelihood method. The estimation of parameters using the PWM (Caeiro, Gomes, & Vandewalle, 2014) begins with the moments $M_{l,j,k}$:

$$M_{l,j,k} = E \left[X^l F^j (1-F)^k \right]
 \tag{11}$$

where j and k are non-negative whole numbers, the probability-weighted moment (l, j, k) is proportional to the n th moment with respect to the origin of $(j + 1)$ for a sample size $n = k + j + 1$.

The Gumbel distribution function is:

$$f(x) = \frac{1}{a} \exp \left\{ -\left(\frac{x-m}{a}\right) - \exp \left[-\left(\frac{x-m}{a}\right) \right] \right\} \quad (12)$$

where a and m are the parameters of the distribution and x is the magnitude of the extreme event.

According to Greenwood *et al.* (1979), the expression for the magnitude of the variable with return period T , based on this distribution, is:

$$X_T = m - a \ln \left[-\ln \left(1 - \frac{1}{T} \right) \right] \quad (13)$$

where:

$$m = M_0 - \varepsilon a \quad (14)$$

$$a = \frac{M_0 - 2M_1}{\ln(2)} \quad (15)$$

For $\varepsilon = 0.5772$ and where $M_k = M_{l,0,k}$ for non-negative whole number k :

$$M_k = \frac{1}{n} \sum_{i=1}^n x_i \binom{n-i}{k} \binom{n-1}{k} \quad (16)$$

where n is the number of historical data and x_i is the value of datum i , from higher to lower. For M_k :

$$M_0 = \frac{1}{n} \sum_{i=1}^n x_i \quad (17)$$

$$M_1 = \frac{1}{n} \sum_{i=1}^n x_i \frac{n-i}{n-1} \quad (18)$$

based on which the values of a and m are determined with equations (14) and (15).

Generation of Numerical Grids

Rectangular grids are generated using interpolated bathymetry for the study area, with spacings of 20 meters in both directions (Figure 5).

Results from the Simulation

The simulation stages consisted primarily of modeling two scenarios over the year—dry and rainy seasons. These seasons were chosen since they are most representative of the year. The initial conditions for each season are shown in Table 3.

Simulation of the Environmental System with Current Conditions (before the project)

The simulation of the surface hydrodynamics for the dry season scenarios with

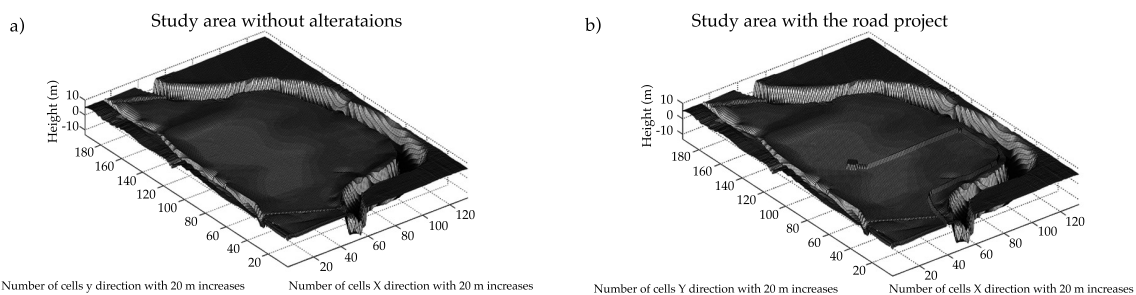


Figure 5. Numerical grid of the study area (left, natural state; right, with projected road).

Table 3. Summary of initial and forcing conditions for modeling the different stages and scenarios proposed.

Stage	Season	Precipitation (mm)	Temperature (°C)	Evaporation (mm)	Runoff (dimensionless)
Current condition and with project	Dry	45 to 156	26.4	148.66	0.020
	Rainy	160 to 206	26.2	117.33	0.037

Stage	Season	Permeability (%)	Vegetation density	Grijalva flow(m ³ /s)	Wind velocity, lagoon (m/s)
Current condition and with project	Dry	30.00	Medium-low	320 min 1 070 med	NE 4.1
	Rainy	20.00	Medium	1 900 max 3 050 max hist	E 7.3

precipitation heights resulted in 45, 80, 120 and 156 mm, where the rainy season presented heights of 160, 185, 197 and 206 mm in the environmental system as a whole. Rainfall duration lasted up to 2.5 continuous hours according to the records. Figure 6 shows the potential flood zones.

Eight percent of the total study area is potentially floodable with a precipitation height of 45 mm, and 86% with a precipitation height of 206 mm.

Simulation of the Environmental System with Project Structures

This simulation considers the construction of a road with drainage ditches and bridges, and/or culverts. These works have already been proposed and their locations have been strategically determined. The following results show the behavior of the road with its drainage and the flood zone in particular. With these mitigation measures in place, no alterations of the hydrological functioning of the environmental system are observed.

The results from the precipitation intensity scenarios for the flood zones (described in Figure 7) show that the free surface level resulting from rainfall and the overflow of the Tabasquillo River would not affect or cover the road.

The scenario representing the area previous to building the project indicates the same flood zones as well as some zones with an accumulation or damming of water. With the proposed road, the floodable zone percentage is 89%, that is, 3% more than for normal conditions before the project is built.

Hydrodynamic Analysis of Mitigation Measures (drainage ditches and culverts)

Since the road would be new, drains or drainage ditches would be needed to allow the free passage of hydrological flow through the study area. The project's proposal for the number, approximate dimensions and location of these works (Figure 2) are summarized below.

The hydraulic behavior was simulated for the two types of drainage systems described in Table 4, under precipitation height conditions of 45, 80, 120, 156, 160, 185, 197 and 206 mm. Figure 8 shows the results from the simulation with 206 mm for drainage type 2 (1.05 x 1.05 m), which is considered the least favorable situation and the one of most interest because of the possible velocities reached in the drainage ditch section. Flow through the culverts is simulated in order to review the following criteria:

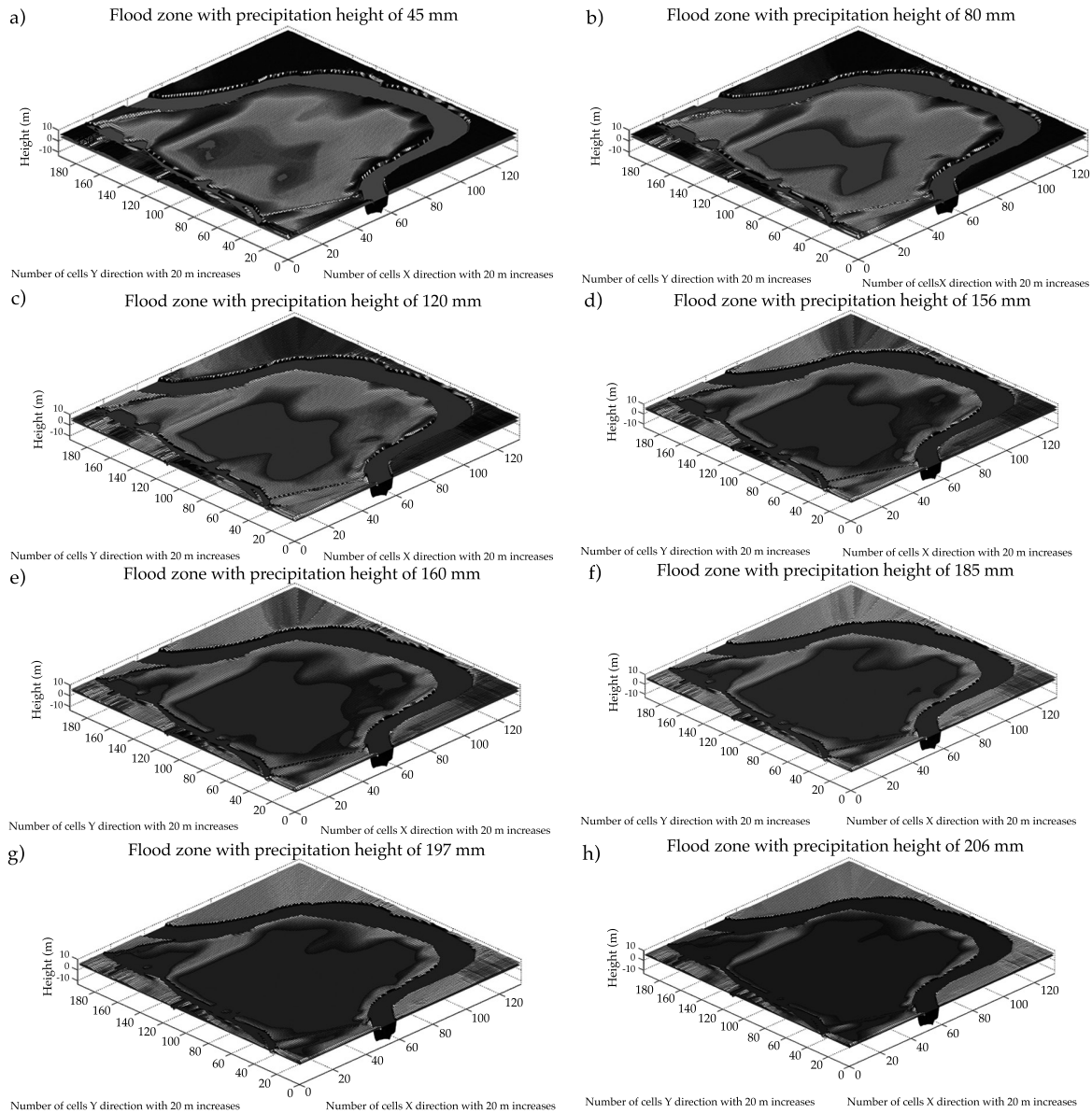


Figure 6. Potentially floodable zones before the project.

- The hydraulic area should ensure the hydraulic functioning for the most critical rainfall intensities, according to the records and the return times associated with the environmental system.
- The vegetation density at the site of each drainage ditch shall be designed to allow for a percentage growth in the

vegetation (obstruction of the hydraulic area from 65 to 70%), and therefore an area 15 to 20% larger than the design area is proposed.

The hydraulic behavior of the section of the drainage ditch shows an average velocity of 0.05 m/s, enough to allow the flow to pass, considering an effective

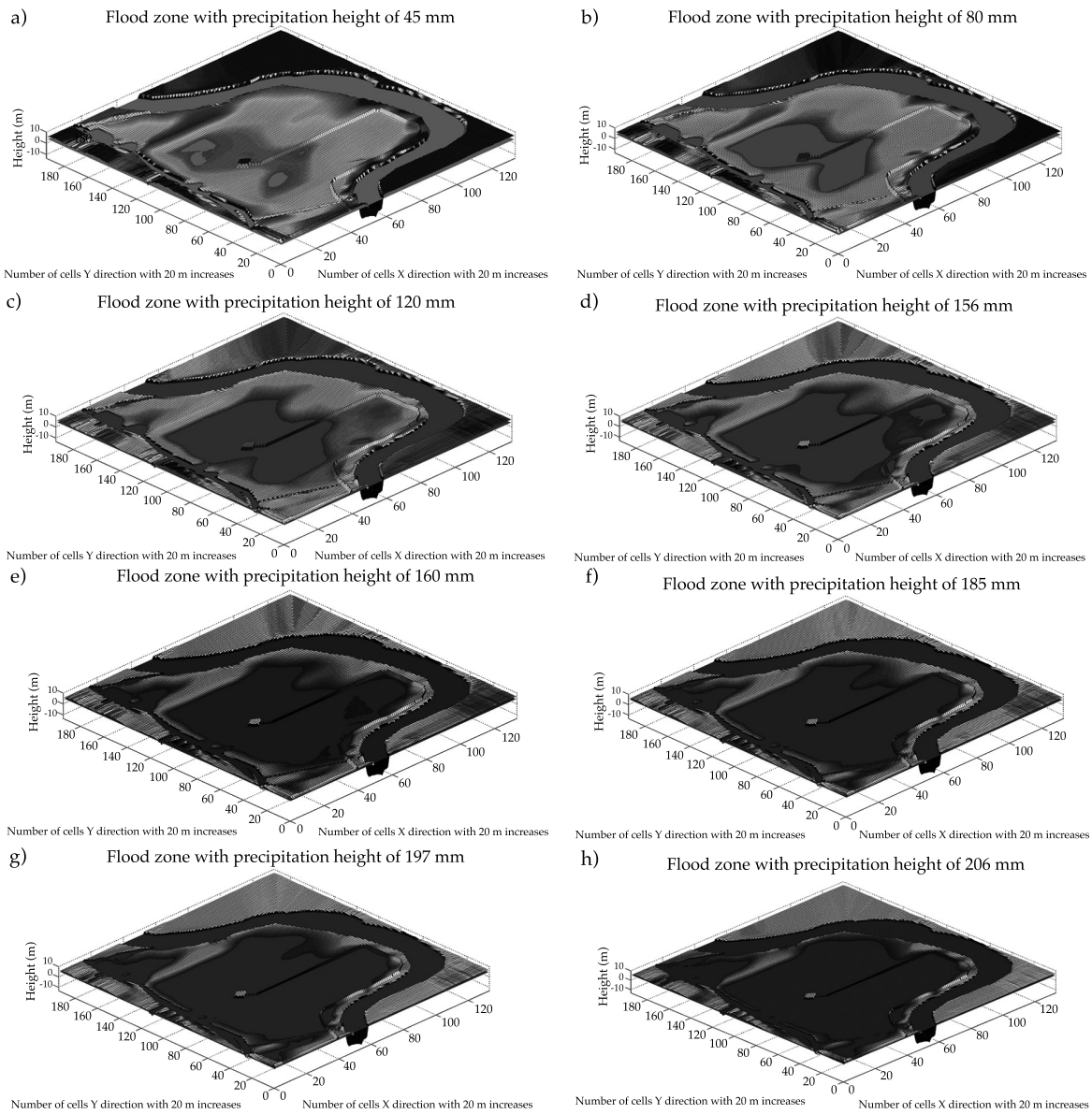


Figure 7. Potentially floodable zones, including road.

Table 4. Location and dimension of drainage in the road project.

Location kilometers	Number of drainage ditches	Dimensions of drainage (m)
0+000 to 1+300	5	0.91 x 0.91 (type 1)
2+760 to 3+640	4	1.05 x 1.05 (type 2)

hydraulic area of 35%. The obstruction of the remaining area is attributed to vegetation covering the section of the drainage ditch.

This condition is implemented in the simulation considering obstacles in the section similar to the vegetation conditions.

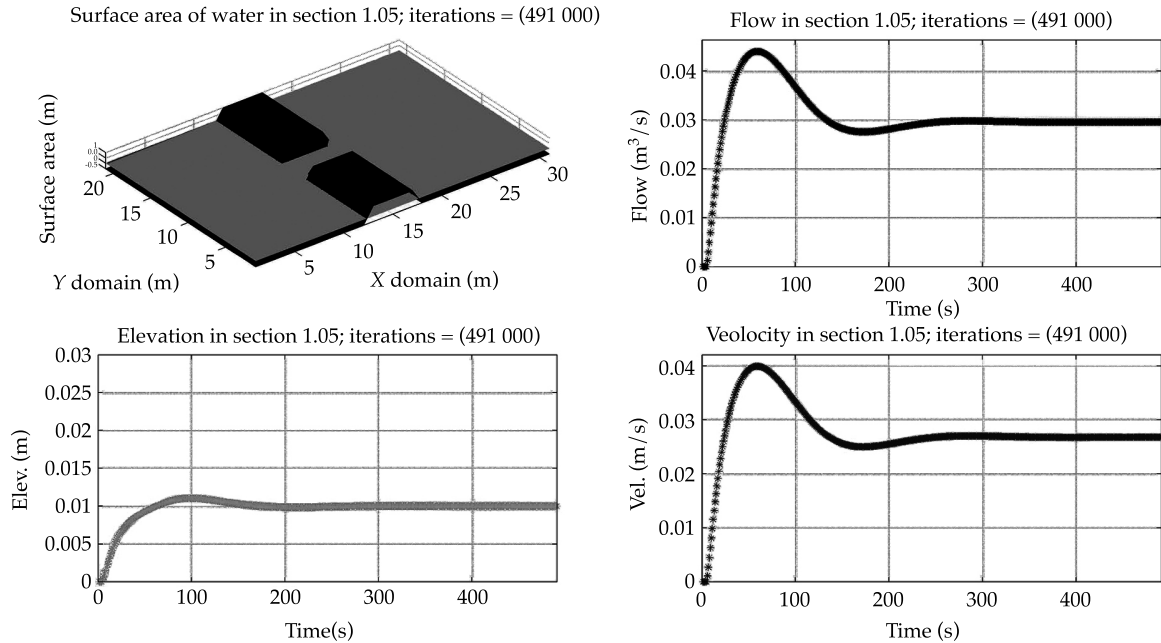


Figure 8. Hydraulic behavior of a 1.05 x 1.05 m drainage ditch with precipitation height of 206 mm.

The amplitude of the flood between minimum and maximum precipitation is 1.60 meters. This value was used to model the differences in surface levels with the two types of drainage ditches (0.91 and 1.05 m). Given these results, the magnitude of the velocity is estimated to be sufficient to generate circulation in the flood zone and minimize alterations to the study area, providing conditions similar to those present before the building of the project.

Conclusions

The results show that the Grijalva River does not present any evident effect on the surface. This is because the left bank of the river where the study area is located contains a dyke which protects from flooding by the river to some extent. Its height is approximately 3.7 meters and therefore the risk of flooding is minimized. Nevertheless, the Grijalva River does affect

the upper and lower channels, which with the help of the Tabasquillo River can flood the study area. The potential flood zones are considered to be at elevations of 0.5 to 3.5 meters, which covers approximately 80% of the environmental system. Well infrastructure is planned for these zones.

In terms of the possible location of the well, this would be in a low zone where runoff tends to accumulate, where the velocity of flow through the road's drainage system reaches 0.08 m/s under rainfall conditions, according to the model (average monthly precipitation intensity of 120 mm/h with a return period of 100 years and duration of 30 min). Therefore, the project does not substantially alter the intensity of the flow. In terms of the direction, since this is a low area, the direction is not altered since everything concentrates in the center.

The most important hydrological factor to be maintained is the passage of surface

flow. The drainage system enables this to function and only the vegetation needs to be monitored to prevent it from covering more than 65% of the proposed hydraulic area. This criterion was determined by observing the current conditions where the road's drainage will be located.

References

- Broomans, P. (2003). *Numerical Accuracy in Solutions of the Shallow-Water Equations* (120 pp.). Master Thesis. Delf: TU Delf & WL, Delf Hydraulics.
- Caeiro, F., Gomes, M. I., & Vandewalle, B. (March, 2014). Semi-Parametric Probability-Weighted Moments Estimation Revisited. *Methodology and Computing in Applied Probability Springer-Verlag*, 16(1), 1-29.
- Greenwood, J. A., Landwehr, J. M., Matalas, N. C., & Wallis, J. R. (1979). Definition and Relation to Parameters of Several Distribution Expressible In Inverse Form. *Water Resources Research*, 15(5), 1049-1054.
- Gubarevat, S. (December, 2011). Types of Probability Distributions in the Evaluation of Extreme Floods. *Water Resources Springer-Verlag*, 38(7), 962-971.
- Gurusamy, S., & Jayaraman, G. (December, 2012). Flood Inundation Simulation in River Basin Using a Shallow Water Model: Application to River Yamuna, Delhi region. *International Journal of Advances in Engineering Sciences and Applied Mathematics Springer-Verlag*, 4(4), 250-259.
- Jean, J. J., Kim, Y. O., & Kim, Y. (August, 2011). Expected probability Weighted Moment Estimator for Censored Flood Data. *Advances in Water Resources, Elsevier Sci. Ltd.*, 34(8), 933-945.
- Mani, P., Chatterjee, C., & Kumar, R. (January, 2014). Flood Hazard Assessment with Multiparameter Approach Derived from Coupled 1D and 2D Hydrodynamic Flow Model. *Natural Hazards Springer*, 70(2), 1553-1574.
- Patro, S., Chatterjee, C., Mohanty, S., Singh, R., & Raghuwanshi, N. S. (March, 2009). Flood Inundation Modeling Using Mike Flood and Remote Sensing Data. *Journal of the Indian Society of Remote Sensing Springer*, 37(1), 107-118.
- Stansby, P. (2003). A Mixing-Length Model for Shallow Turbulent Wakes. *Journal of Fluid Mechanics*, 495, 369-384. SCT-DGST (2013). *Cartas de isoyetas para el año 2013*. Secretaría de Comunicaciones y Transportes, Dirección Regional de Tabasco, México. Recuperado de <http://www.sct.gob.mx/carreteras/direccion-general-de-servicios-tecnicos/isoyetas/>.
- UNESCO (1981). Background Papers and Supporting Data on the International Equation of State of Seawater 1980. *UNESCO Technical Papers in Marine Science*, 38, 192.
- Yin, J., Yu, D., Zhane, Y., Wang, J., & Xu, S. (March, 2013). Multiple Scenario Analyses of Huangpu River Flooding Using a 1D/2D Coupled Flood Inundation Model. *Natural Hazards Springer*, 66(2), 577-589.
- Zhang, X., Long, W., Xie, H., Zhu, J., & Wang, J. (February, 2007). Numerical Simulation of Flood Inundation Processes by 2D Shallow Water Equations. *Frontiers of Architecture and Civil Engineering in China Springer*, 1(1), 107.
- Zhou, Z., Wang, X., Sun, R., Ao, X., Sun, X., & Song, M. (January, 2014). Study of the Comprehensive Risk Analysis of Dam-Break Flooding Based on the Numerical Simulation of Flood Routing. Part II: Model Application and Results. *Natural Hazards Springer*, 72(2), 675-700.

Institutional Address of the Authors

Dr. Israel E. Herrera-Díaz
Dr. José R. Gasca-Tirado

Universidad de Guanajuato
Depto. de Ingeniería Agroindustrial
Campus Celaya-Salvatierra, México
Av. Ing. Javier Barrios Sierra núm 201
Esq. Av. Baja California
38110 Ejido de Sta. María del Refugio, Celaya, Gto. MÉXICO
Teléfono: +52 (461) 5985 922, extensiones 1627 y 1628
eherrera@ugto.mx
jrgasca@ugto.mx

Dr. Clemente Rodríguez-Cuevas

Facultad de Ingeniería
Universidad Autónoma de San Luis Potosí
Av. Manuel Nava núm. 8, Zona Universitaria
78290 San Luis Potosí, San Luis Potosí, MÉXICO
Teléfono: +52 (444) 8262 330, extensión 2102
clemente.rodriguez@uaslp.mx

Dr. Carlos Couder-Castañeda

Instituto Politécnico Nacional
Centro de Desarrollo Aeroespacial
Belisario Domínguez núm. 22
06010 México, D.F., MÉXICO
Teléfono: +52 (55) 3436 3341
ccouder@ipn.mx

Characterization of Meteorological Droughts in the Central Argentina

• Leticia Vicario* • Carlos M. García • Ingrid Teich • Juan Carlos Bertoni •
 • Andrés Ravelo • Andrés Rodríguez •
Universidad Nacional de Córdoba, Argentina

*Corresponding Author

Abstract

Vicario, L., García, C. M., Teich, I., Bertoni, J. C., Ravelo, A., & Rodríguez, A. (January-February, 2015). Characterization of Meteorological Droughts in the Central Argentina. *Water Technology and Sciences* (in Spanish), 6(1), 153-165.

Varying degrees of droughts repeatedly affect several regions in Argentina. Given the agricultural-livestock character of central Argentina, the analysis and assessment of droughts in that region is economically and strategically important. This situation is even more relevant since some of the largest cities in the country are located in this area. The present work analyzes the spatial variability of the meteorological droughts in the study area using the standardized precipitation index (SPI) for sub-areas and the region, while also taking into account the influence of ENSO. To identify the sub-areas affected by hydrometeorological deficits, annual mean rainfall was analyzed in 15 locations in the study area. Because of its widespread spatial and temporal availability, this variable was adopted a priori as representative of the processes studied by the present work. Criteria and statistical techniques were applied to this variable and monthly rain gauge series were used from stations in the provinces of Córdoba, Santa Fe and Entre Ríos for the period 1980-2009. Three groups of stations with similar pluviometric behavior were identified, particularly behaviors related to intense droughts, thereby identifying spatial scales or sub-areas of influence corresponding to the hydrometeorological deficit.

Keywords: Central region of Argentina, meteorological droughts, multivariate analysis, SPI.

Resumen

Vicario, L., García, C. M., Teich, I., Bertoni, J. C., Ravelo, A., & Rodríguez, A. (enero-febrero, 2015). Caracterización de las sequías meteorológicas en la región central de la Argentina. *Tecnología y Ciencias del Agua*, 6(1), 153-165.

Los procesos de sequía de distintas intensidades afectan de manera recurrente varias regiones de la República Argentina. Dado el carácter agrícola-ganadero de la región central pampeana de ese país, el análisis y la evaluación de las sequías en dicha región adquiere gran relevancia en el plano económico y en el de la planificación estratégica, entre otros. Esta situación es aún más relevante si se menciona que en tal territorio se localizan algunas de las ciudades más importantes del país. En este trabajo se analiza la variabilidad espacial de las sequías-meteorológicas en la región de estudio mediante el índice estandarizado de precipitaciones (SPI) para subáreas y en el ámbito regional, teniendo en cuenta, además, la influencia del fenómeno climático ENSO. Para identificar subáreas de influencia de los fenómenos de déficit hidrometeorológico, se aplicaron criterios y técnicas estadísticas de análisis sobre la variable lluvia media anual (la cual se adopta a priori como representativa de los procesos que se estudian en este trabajo debido a su mayor disponibilidad espacial y temporal) de 15 localizaciones en la región de estudio. Se utilizaron series de datos pluviométricos mensuales de estaciones ubicadas en las provincias de Córdoba, Santa Fe y Entre Ríos, para el periodo 1980-2009. Se lograron identificar tres grupos de estaciones con comportamiento similar en lo que se refiere a los procesos pluviométricos y, en particular, aquellos relacionados con las sequías intensas, lo que permite identificar escalas espaciales o subáreas de influencia de los fenómenos de déficit hidrometeorológico.

Palabras clave: región central Argentina, sequías meteorológicas, análisis multivariado, SPI.

Received: 08/03/13

Accepted: 02/07/14

Introduction

The extreme hydrological process known as “droughts” refers to a scarcity of rainfall

(observed values below expected or mean values) in an area over a determined period of time. Every place on the planet will eventually undergo these processes,

including typically rainy areas (Dracup, Lee, & Paulson, 1980). These phenomena can be detected using information related to several variables. For example, Wilhite and Glantz (1985) have defined four categories of droughts. The first is meteorological, which is based on climate data and expresses the difference in precipitation with respect to the average value for a determined period of time. The second is agricultural droughts, which occurs when there is not enough moisture in the soil to enable a particular crop to develop normally during any of its growth phases. The third is hydrological, which is a deficiency in the flow or volume of surface water or groundwater (rivers, lakes, watersheds, etc.). And the fourth is socioeconomic droughts, which are produced when water availability decreases to the point of causing economic or personal damages to the population in a zone affected by rainfall scarcity.

When a drought period begins, the agricultural sector is generally the first to be affected because of its high dependence on the amount of moisture in the soil. Nevertheless, an agricultural drought period in a region is the consequence of a previous meteorological drought period which, in turn, may also be a precursor to the occurrence of a hydrological drought period, depending on the amount of time and one or more characteristics.

While droughts are an inevitable occurrence, they are still not very predictable because of the chaotic behavior of meteorological processes (Kim, Valdés, & Aparicio, 2002). Therefore, statistical tools are used to characterize them. In particular, to statistically characterize and describe droughts, their main variables are considered, such as the probability of occurrence, duration and intensity.

Droughts need to be studied and

analyzed in order to better understand their parameters, the specific thresholds of these processes according to hydroclimatic region (Mishra & Singh, 2010). Dry periods (with droughts) need to be analyzed to plan and manage water resources in areas where a good deal of economic activity depends on the use of water (Ortiz-Gómez, Barragán-Barrios, & Alvarado-Medellin, 2010). Given the amount of agriculture and livestock activities in Argentina's central Pampean region and their importance to the area's economy, it is crucial to analyze droughts that can cause significant economic losses in agriculture and livestock in that area (Ravelo, 2009). The effects of droughts are particularly seen in the province of Cordoba, where they have caused the hydric conditions of the soil in the south to quickly deteriorate, negatively affecting the crops (Ravelo, Planchuelo, Zanvettor, Barbeito, & Marraco, 2008).

Droughts in the plains region (such as the region included in the study area) have not been widely studied, in part because there are few rain gauge stations and they are not distributed in a very wide area (Ovalles, Cortez, Rodríguez, Rey, & Cabrera-Bisbal, 2007). To support reliable studies of droughts in a study area with few hydrometeorological and hydrological records, Vicario (2008) recommends the implementation of a hydrometeorological network to create a complete database. Even when information is scarce, the regional analysis of available land stations is important, such as the one developed by the present work, in order to identify hydrometeorologically homogeneous areas and optimize existing information, thereby minimizing the uncertainty in the results.

The analysis of the results from a regional drought analysis should consider that while drought processes are chaotic and

are statistically analyzed, climate processes occur on different temporal scales which could affect the probabilities of occurrence and intensity. Scarce precipitation in a study area may be associated with the climatological phenomenon known as ENSO (El Niño-Southern Oscillation), which is the result of a cycle of heating and cooling of the ocean surface in the central and eastern Pacific. During certain periods, unusual cooling occurs in this region, even though it is near the equator. This is due to northeasterly winds, the rise of cold water on the coast of Peru and a cold ocean current traveling along the coast of Chile. When this cooling is more intense than normal, it is known as La Niña, which causes extreme climatic effects in different macro-regions of the planet, such as periods of drought in South America and intense rainfalls associated with floods in eastern Australia. Meanwhile, when the cooling decreases considerably, the phenomenon is known as El Niño and causes effects opposite to those just mentioned. Therefore, analyzing periods of drought in central Argentina and their relationships with the ENSO (La Niña and El Niño) cycle is of interest, in order to make an initial prediction of the possible occurrence of periods of drought.

The overall purpose of the present work is to study the spatial variability of precipitation and droughts in central Argentina. Since rainfall is the primary component of precipitation in the study area both terms will be used interchangeably. To fulfill the overall purpose, the following specific objectives were developed: (1) identify hydrometeorologically homogeneous regions using a regional analysis; (2) characterize meteorological droughts in the regions identified; (3) analyze relationships between the periods of drought observed and the ENSO phenomenon.

Materials and Methods

Information Used

The study is based on monthly rainfall data recorded from 1980 to 2009, collected from surface hydrometeorological stations in the central Pampean region of Argentina. The data were recorded by the Argentine National Weather Service (NWS) and are available through the Agriculture and Livestock Integrated Information System (Sistema Integrado de Información Agropecuaria (SIIA, sitio web: <http://www.sii.gov.ar/>). Stations with data for the study period and with no more than 5% of missing data were included. The missing data for each month were completed with the historical average values corresponding to the station analyzed in order to minimize the effect of this discontinuity on the mean of the series and the drought index to be calculated later. Fifteen rain gauge stations were selected (Table 1), 7 of which were located in the province of Córdoba, Argentina (in the localities of Córdoba, Laboulaye, Marcos Juárez, Pilar, Río Cuarto, Villa Dolores and Villa María de Río Seco), 5 in the province of Santa Fe (in the localities of Ceres, El Trébol, Rosario, Sauce Viejo and Venado Tuerto) and 3 in the province of Entre Ríos (in the localities of Gualaguaychú, Paraná and Concordia). Since the study period includes 30 years, a series of 360 rainfall values were used for each station, corresponding to 12 months over the 30 years included in the study period.

Regional Analysis: Identification of Hydrometeorologically Homogeneous Zones

In order to perform a regional drought analysis, sub-groups of rain gauge stations were defined that characterized regions

Table 1. Rain gauge stations selected in the central region of Argentina.

Station	Province	Latitude (°S)	Longitude (°O)	Altitude (masl)
Córdoba (CBA)	Córdoba	31.19	64.10	474
Laboulaye (LAB)		34.08	63.20	137
Marcos Juárez (MJ)		32.42	62.10	114
Pilar (PI)		31.40	63.50	338
Río Cuarto (RC)		33.07	64.10	421
Villa Dolores (VDOL)		31.57	65.10	569
Villa María de Río Seco (VMRS)		29.54	63.40	341
Ceres (CE)	Santa Fe	29.53	61.60	88
El Trébol (TR)		32.30	61.40	96
Rosario (ROS)		32.55	60.50	25
Sauce Viejo (SV)		31.42	60.50	18
Venado Tuerto (VT)		33.40	61.60	112
Gualeguaychú (GUAL)	Entre Ríos	33.00	58.40	21
Paraná (PAR)		31.47	60.30	78
Concordia (CON)		31.18	58.00	38

with homogenous hydrometeorological characteristics. To this end, two complementary methodologies were implemented: a) based on the similarity of the physical characteristics of the locations where the stations were installed (Pierrehumbert, 1977) and b) based on the similarity in the behavior of the annual rainfall data series (with a multivariate statistical analysis). The former methodology identifies groups according to criteria defined by Pierrehumbert (1977), which establishes that the data from a rain gauge station can be presumed to be representative of other sites if the following conditions are met:

- Terrain within a 5 km radius of the location of each station is similar.
- Sites are located in the same hydrological watershed.
- Difference in topographical level between sites is less than 200 m.

- Sites are not more than 150 km from each other.
- The difference in annual mean rainfall between sites is under 100 mm, when the annual mean is less than 1 000mm.
- The difference in annual mean rainfall is less than 10% in zones with more moisture.

To implement the second methodology, annual mean rainfall series were created for each station and a principal components analysis (PCA) was performed. Using this technique, the relationships between multidimensional observations can be explored by ordering them on planes that are optimal for ordering the observations and analyzing interdependencies. Essentially, with the PCA, components are successively extracted from a matrix of similarities (or distances) among observations calculated using multiple variables. Those components are used as axes to

graphically represent the objects. In the ordering, each study unit is placed on one or more axes so their relative position reflects the similarities and/or distances among them (Gabriel, 1971). In the present work, the PCA was performed with a 15 x 30 matrix corresponding to 15 rain gauge stations (observations) and 30 annual rainfall values for the study period (variables). The graphical spread of the rain gauge stations ordered by the PCA was analyzed.

In addition, to identify groups of stations, a cluster analysis was performed using the 30 annual rainfall values for the study period as variables. This technique enables associating the observations from a set with a determined number of groups according to the distance or similarity among observations. The present work used Euclid's distance (d) because it is a simple model and it is recommended for cases with homogeneous variables that are measured using the same units. The average link method (Sokal & Michener, 1958) was used since it is one of the simplest methods and has provided efficient results in numerous cases. With two clusters, this method consists of averaging all the distances between object pairs where each one belongs to the cluster of the other pair. The results can be represented with a graph, called a dendrograph, showing different clustering stages. Both analyses were performed with *Infostat* (Di Rienzo et al., 2011).

Analysis of Meteorological Droughts

After identifying the sub-areas with homogenous rain gauge measurements to evaluate the behavior of droughts by observing the inter-annual variability of the process, the standardized precipitation index (SPI) (McKee, Doesken, & Kliest, 1993) was calculated for each temporal series and then averaged at the sub-area level. This index was used because it is currently the index that most adequately synthesizes the characteristics of a drought as a natural phenomenon. It is based on the principle that, as part of the hydrological cycle, rainfall defines whether there is an abundance or deficit of water in relation to the mean conditions corresponding to the scale or period studied (Velasco & Aparicio, 2004). This index considers the probabilities of the occurrence of rainfall for a given period and is calculated by fitting a historical monthly rainfall series to a probabilistic gamma distribution function, which is the distribution function that best fits the rainfall variable (Thom, 1966; Young, 1992). Using the SPI index, droughts can be measured at different temporal scales depending on the objective of the study. In this case, a temporal scale of 12 months was considered appropriate for the calculation of the SPI in order to observe and characterize the multi-annual

Table 2. Dimensionless values corresponding to the standardized precipitation index (SPI) and characteristics of the associated periods.

Index	Category
> 2	Extremely wet
1.99 to 1.50	Very wet
1.49 to 1.00	Moderately wet
0.99 to -0.99	Normal
-1.00 to -1.49	Moderately dry
-1.50 to -1.99	Severely dry
< -2.00	Extremely dry

behavior of meteorological droughts at a monthly level, with various stations in a wide region and over a long period of time (30 years). Drought conditions (when there is a deficit) are considered to exist when the value of the index is equal to or less than -1. McKee *et al.* (1993) defined the SPI values and the characteristics of the periods associated with these values, which are presented in Table 2.

In addition, in order to observe the variability in the SPI drought index and adequately represent its trend, moving averages were calculated with constant intervals of 12 monthly periods.

To analyze the relationship between the drought periods observed and the ENSO phenomenon, two statistical methods were used before graphing— the Correlation Coefficient for the Average Monthly Regional SPI Values (calculated based on the respective SPI indices for all the stations in the study area) and the Historical Ocean Temperature Index (representative of the different ENSO phases for the time period of the present study). The correlation coefficient between two random variables X and Y is the quotient of the covariance of (X, Y) divided by the product of the typical deviations of each one of the variables. This measures the strength of the linear relations between two data series, where the higher the absolute value of the correlation the stronger the linear relationship between the two variables, and vice versa. The limits of the coefficient are: a, which indicates a total dependence of the two variables, called direct relationship; 0, no linear relation exists; and -1 indicates total dependency between the two variables, called inverse relationship. Based on these thresholds, the middle values of the coefficient are measured.

Results and Discussion

Regional Analysis: identification of homogeneous hydrometeorological regions

According to the criteria by Pierrehumbert (1977), the Villa Dolores station cannot be grouped with any of the stations selected for this work because it does not meet the condition related to the difference in topographic level or the difference in annual rain gauge measurements. This is explained by this station's location in the mountainous region. The Concordia station is likewise not representative of any subgroup, since precipitation at that station is considerably different than the other study stations. The remaining physical characteristics suggested by Pierrehumbert (1977) were evaluated to complement the multivariate statistical analysis of mean annual rainfall in order to validate the clustering of stations. Figure 1 shows the ordering of the rain gauge stations in central Argentina as defined by the first two principal components obtained with the PCA, based on annual rainfall data between 1980 and 2009. The different colors correspond to stations located in different provinces. The first two axes obtained with the principal components analysis explain 75.1% of the variability in mean annual rain gauge measurements observed among the stations. The first axis (CP1) is the most important for showing the variability among observations, since it explains 67% of the total variability. This axis is associated with higher mean annual precipitation values, particularly for the years 2002 and 2009. That is, high CP1 values indicate higher annual precipitation for the study period, in particular between 2002 and 2009. As shown in Figure 1, the

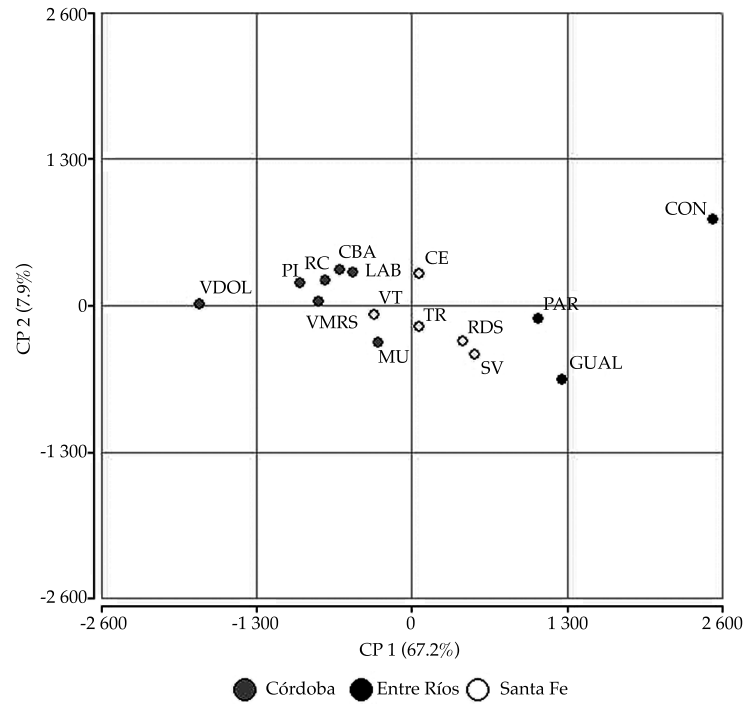


Figure 1. Ordering of rain gauge stations in central Argentina on the graph defined by the first two principal components obtained with the PCA based on annual rainfall data from 1980-2009. Different shades of gray correspond to stations located in different provinces.

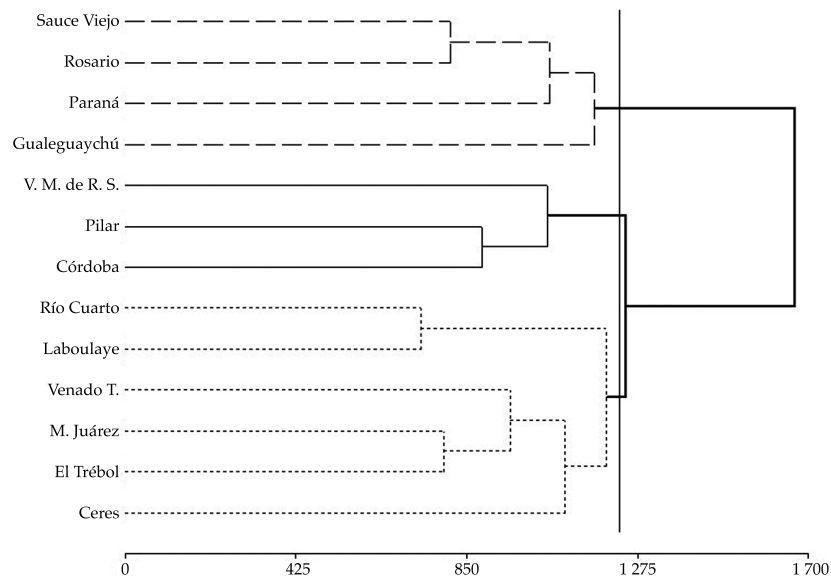


Figure 2. Dendrograph obtained using a clusters analysis (Euclidean distance and average link) based on annual rainfall data from 1980-2009 for the 13 stations analyzed. The vertical gray line indicates the distance separating the three groups obtained. The dashed lined indicates the rain gauge stations in group 1, the solid line the stations in group 2 and the dotted line those in group 3.

mean annual rainfall at the stations in the Cordoba province is lower than that in Entre Ríos, and in some cases is similar to the behavior of the Santa Fe stations. Figure 1 also shows that the rain gauge characteristics for Villa Dolores and the Concordia stations are most different than the rest of the cases in the group, which agrees with the results obtained with the Pierrehumbert (1977) criteria. Therefore, both stations were eliminated from later analyses.

The optimal number of regions or homogeneous sub-areas is three, given the number of stations and their physical and rain gauge characteristics. The cluster analysis identified the following three groups: group 1, stations Sauce Viejo, Rosario, Paraná and Gualeguaychú; group 2, stations Villa María de Río Seco, Pilar and Córdoba; group 3, stations Río Cuarto, Laboulaye, Venado Tuerto, Marco

Juárez, Trébol and Ceres. Figure 2 shows the dendrograph obtained by the cluster analysis and Figure 3 the location of the study region in Argentina, identifying the stations in each group or sub-area.

Analysis of Meteorological Droughts

After grouping the representative stations in each sub-area, meteorological droughts were studied jointly for each of the three groups defined. The stations in each one of the groups were found to present similar behavior in terms of the occurrence of periods of droughts.

All the stations in group 1 (Sauce Viejo, Rosario, Paraná and Gualeguaychú) presented periods of severe and/or extreme droughts in 1989 and 2008-2009. In addition, two extreme events were recorded at the Rosario stations in the year 1983 and at Parana in 1997. In group 2 (Villa

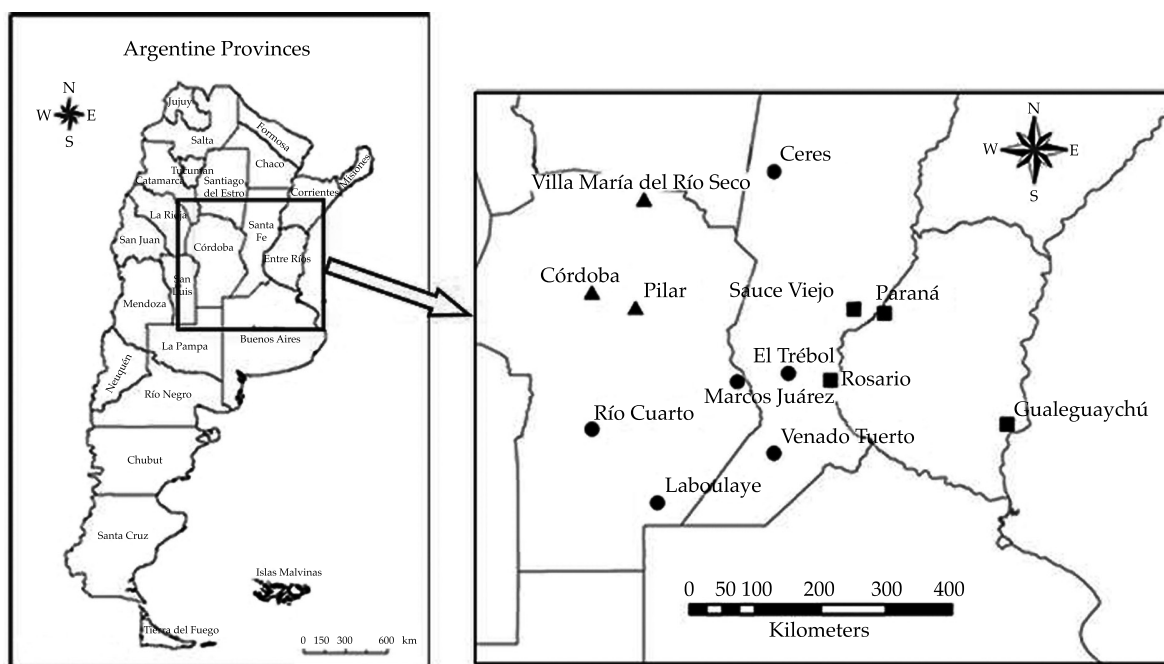


Figure 3. Location of the provinces in Argentina that are included in the study area. From west to east: Córdoba, Santa Fe and Entre Ríos; the enlargement shows the location of the stations corresponding to each group: group 1, square; group 2, triangle; group 3, circle.

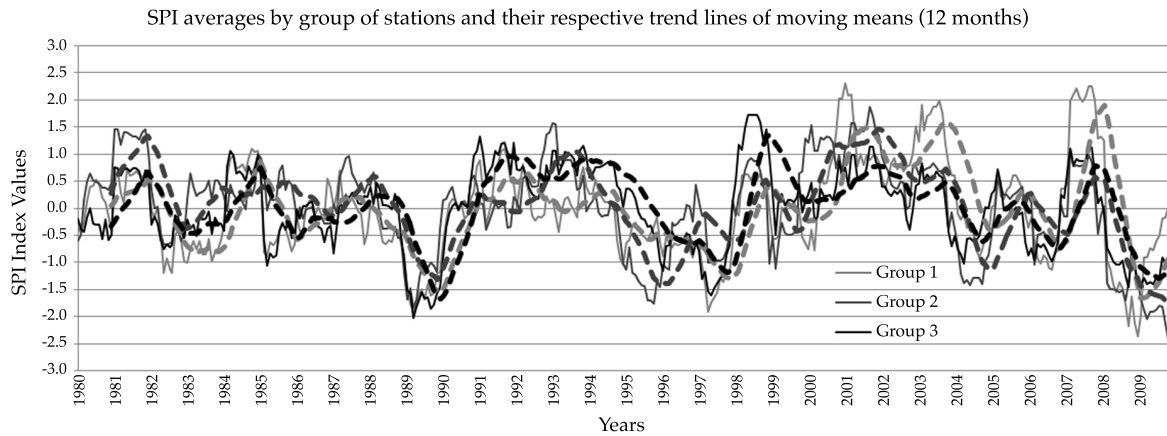


Figure 4. Graph of average SPI index values for each group of stations and their respective trend lines obtained based on a 12-month moving mean (dotted lines). Group 1, light gray; Group 2, gray; and Group 3, black.

María de Río Seco, Pilar and Córdoba), severe and/or extreme droughts were observed from 1988-1990 and 2008-2009 in all the cases, as well as from 1994-1996 and 2003-2004, with the exception of the Córdoba station which presented moderate to severe droughts. Group 3 (Río Cuarto, Laboulaye, Venado Tuerto, Marcos Juárez, El Trébol and Ceres) presented periods with severe and/or extreme droughts around the years 1989 and 2008-2009 at all the stations, as was the case in the rest of the study area. Droughts with different intensities were registered in some of the stations in the group from 1996 to 2006. Figure 4 shows the average values of the SPI index for each group of stations. It is worth mentioning that the three groups of rain gauge stations in the study area registered

severe or extreme droughts around the years 1989, 1995/1997 and 2008, indicating a significant hydrometeorological deficit (drought) in the region during the second half of the decade.

Meanwhile, according to the average SPI index for each group of stations, the intensity of moisture cycles was found to be greatest in the region as of the year 1998, approximately. To more clearly identify this situation, trend lines were graphed based on a 12-month moving mean for the data series corresponding to the average SPI index for each group of stations, also shown in Figure 4. Groups 1 and 3 were observed to behave similarly as of approximately the year 1997. From 1998 to the end of the series, the trends for the three groups were similar in terms of the

Table 3. Descriptive statistics of average standardized precipitation index SPI values for each group of stations (1980-2009).

Variable	<i>n</i>	Mean	SD	Var (<i>n</i>)
Group 1	360	-0.02	0.90	0.80
Group 2	360	0.01	0.87	0.75
Group 3	360	-0.0004	0.77	0.59

Table 4. Descriptive statistics of average standardized precipitation index SPI values for each group of stations (1980-1997 and 1998-2009).

Periods	Variable	<i>n</i>	Mean	SD	Var (<i>n</i>)
1980-1997	Group 1	204	-0.17	0.64	0.41
	Group 2	204	0.05	0.73	0.54
	Group 3	204	0.02	0.72	0.51
1998-2009	Group 1	156	0.17	1.12	1.24
	Group 2	156	-0.04	1.02	1.02
	Group 3	156	-0.03	0.83	0.68

occurrence of normal or dry cycles, while group 1 presented more intense wet cycles than the other groups. Based on this trends analysis, a descriptive statistical analysis was performed with average SPI values for each group, first with the complete series and then dividing the series into two ¾ 1980 to 1997 and 1998 to 2009. The results are presented in Tables 3 and 4, respectively.

During the first period analyzed (1980-1997), the characteristic values of group 2 were found to be higher than those of groups 1 and 3. Meanwhile, as of 1998 the mean value for group 1 was higher and positive for this first period while the rest of the groups presented more intense wet cycles, or more months when rainfall was recorded by the stations in the groups.

Analysis of the Relationship Between Observed Meteorological Droughts and ENSO

Figure 5 shows the Historical Ocean Temperature Index (NOAA, 2012) for the period 1982-2012, which indicates the occurrence of El Niño events (index values higher than zero) or La Niña events (index values under zero) if the temperature differences with respect to their normal value are over or under zero, respectively. Comparing this figure to Figure 4, it can be seen that during the study period the years with intense droughts registered at the three groups of stations representative

of the study area coincide with the occurrence of La Niña. Nevertheless, during the study period corresponding to the present work, other periods of La Niña occurred, such as the years 1984-1986 and 1999-2001, as well as other lesser events which did not considerably affect the intensity of droughts. Based on this, the correlation coefficient was determined for the Complete Series of Monthly Regional Average SPI Values versus the Historical Ocean Temperature Index. A complete lack of correlation between these indices is observed in this case, since the value of the coefficient is roughly zero. Meanwhile, when correlating only periods defined by the Historical Ocean Temperature Index, such as La Niña, with the respective SPI values for the same period, the coefficient increases to 0.14. Nevertheless, this is not considered to be an acceptable value to indicate a direct relationship between the occurrence of La Niña and the occurrence of meteorological droughts in the region. This indicates that even though La Niña is a fundamental cause of rainfall scarcity in central Argentina, identifying the factors involved and their interactions in order to determine the characteristics of periods of drought is complex. For example, Cicero (2005) reports that ENSO has different affects on the various regions in Argentina. In central Argentina and on the coast, El Niño can cause a decrease in precipitation in some cases and La Niña

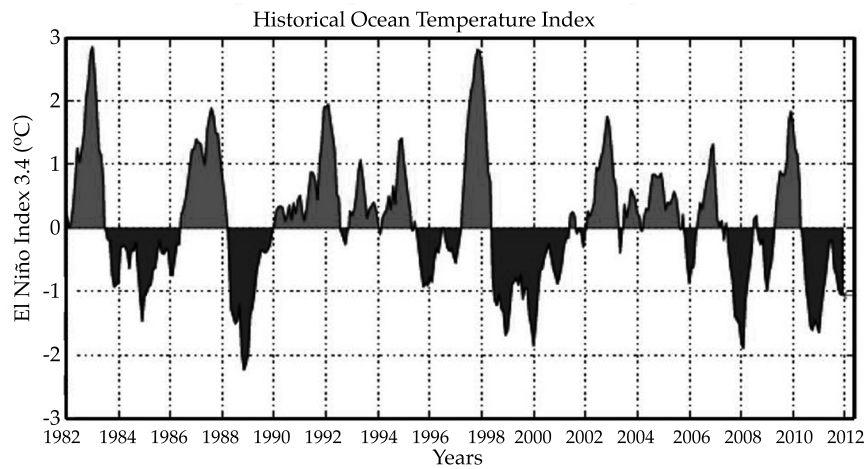


Figure 5. Historical Ocean Temperature Index (1982-2009). Index values under and over zero indicate conditions associated with La Niña or El Niño, respectively. Source: National Oceanic and Atmospheric Administration (NOAA), Earth System Research Laboratory (ESRL, 2012).

can generate above normal rainfalls in other cases. Meanwhile, Coronel and Sacchi (2006) observed that in a locality in southern Santa Fe, dry and wet events can occur along with El Niño, La Niña or neutral situations, implying the need to locally analyze the relationships between precipitation and large-scale atmospheric anomalies.

Conclusions

This work analyzes the spatial variability of meteorological droughts in the central region of Argentina (a large region where plains are predominant). Rain gauge processes associated with groups of stations or locations were identified as having similar behaviors, particularly in terms of intense droughts. This enables identifying spatial scales or sub-areas of influence related to hydrometeorological deficits.

A classification criteria was implemented to group the stations, and complemented by an analysis of the physical characteristics of the sites containing rain gauge sta-

tions, as well as by a multivariate statistical analysis of annual mean rainfall at each location. First, the Villa Dolores (province of Córdoba) and Concordia (Entre Ríos) stations were discarded as non-representative of the region since they did not show sufficient similarities with the rest of the stations in the region. In the end, three statistically homogenous sub-areas (groups) were determined according to their rain gauge behavior. The stations representative of each group are: group 1, Sauce Viejo, Rosario, Paraná and Gualeguaychú; group 2, Villa María de Río Seco, Pilar and Córdoba; group 3, Río Cuarto, Laboulaye, Venado Tuerto, Marco Juárez, Trébol and Ceres.

Based on the SPI index (12months) as a reference, the stations belonging to each of the groups were shown to have similar behaviors in terms of periods of droughts.

Specifically, for the three groups, periods of severe and/or extreme droughts were observed around the years 1989 and 2008-2009 at all the stations, in addition to specific periods of intense droughts at some of the stations in the late 1990s. This would indicate the possibility of a regional

hydrometeorological deficit around the second half of each decade. In addition, periods of moisture were observed to be more intense in the eastern portion of the study area in the late 1990s.

When analyzing the evolution of the Historical Ocean Temperature Index for the years with a deficit, two La Niña periods were found to have occurred. Nevertheless, other cycles of La Niña occurred during the study period which did not considerably affect droughts in the region. When applying the correlation coefficient, no relationship was observed between monthly average SPI values for the study region and the Historical Ocean Temperature Index. Meanwhile, when only correlating La Niña periods with the respective SPI values, the coefficient increased slightly, but is not considered an acceptable value for defining any type of direct relationship between periods of La Niña and the occurrence of meteorological droughts in the region. This indicates that although La Niña could cause rainfall scarcity in central Argentina, determining the characteristics of periods of droughts is complex.

References

- Cicero, A. R. (2005). *Evaluación agrometeorológica de indicadores de sequía en la provincia de Mendoza*. Tesis de Magíster en Ciencias Agropecuarias. Mención Agrometeorología. Córdoba, Argentina: Escuela para Graduados, Facultad de Ciencias Agropecuarias, Universidad Nacional de Córdoba.
- Coronel, A., & Sacchi, O. (2006). Climatología de eventos secos y húmedos en el sur santafesino. *Revista de Investigaciones de la Facultad de Ciencias Agrarias de la Universidad Nacional de Rosario*, 9, 15-24.
- Di Rienzo, J. A., Casanoves, F., Balzarini, M. G., Gonzalez, L., Tablada, M., & Robledo, C. W. (2011). *InfoStat versión 2011*. Córdoba, Argentina: Grupo InfoStat, FCA, Universidad Nacional de Córdoba, Argentina. Recuperado de <http://www.infostat.com.ar>
- Dracup, J. A., Lee, K. S., & Paulson, E. G. Jr. (1980). On the Definitions of Drought. *WRR*, 16(2), 297-302.
- ESRL-NOAA (2012). Earth System Research Laboratory, National Oceanic and Atmospheric Administration (NOAA). Recuperado de <http://www.esrl.noaa.gov/>.
- Gabriel, K. R. (1971). Biplot Display of Multivariate Matrices with Application to Principal Components Analysis. *Biometrika*, 58, 453-467.
- Kim, T., Valdés, J. B., & Aparicio, J. (September, 2002). Frequency and Spatial Characteristics of Droughts in the Conchos River Basin, México. *Water International*, 27(3), 420-430.
- McKee, T. B., Doesken, N. J., & Kliest, J. (1993). The Relationship of Drought Frequency and Duration to Time Scales (pp. 179-184). In *Proceedings of the 8th Conference of Applied Climatology*, 17-22 January, Anaheim, CA. American Meteorological Society, Boston.
- Mishra, A. K., & Singh, V. P. (2010). A Review of Drought Concepts. *Journal of Hydrology*, 391, 202-216.
- Ortiz-Gómez, R., Barragán-Barrios, M. C., & Alvarado-Medellin, P. (noviembre, 2010). *Evaluación de la sequía meteorológica a escala regional en la cuenca Lerma Chapala*. XXIV Congreso Latinoamericano de Hidráulica, Punta del Este, Uruguay.
- Ovalles, F., Cortez, A., Rodríguez, M., Rey, J., & Cabrera-Bisbal, E. (2007). *Variación geográfica del impacto del cambio climático en el sector agrícola en Venezuela*. I Congreso Venezolano de Agrometeorología y V Reunión Latinoamericana de Agrometeorología. Maracay, Venezuela.
- Pierrehumbert, C. L. (1977). Rainfall Intensity-Frequency-Duration Estimation. Chapter 2. In *Australian Rainfall and Runoff*. Canberra, Australy: The Institution of Engineers.
- Ravelo, A. C. (2009). *Monitoreo y evaluación de las sequías en Argentina*. Seminario Internacional sobre Sequías y Gestión del Riesgo Climático. Chile: CAZALAC.
- Ravelo, A. C., Planchuelo, A., Zanvettor, R., Barbeito, A., & Marraco, G. (2008). Monitoreo, evaluación e impacto de la sequía en la provincia de Córdoba. *Boletín Agroclimático de la Provincia de Córdoba*. Periodo septiembre, 5 pp.
- Sokal, R. R., & Michener, C. D. (1958). A Statistical Methods for Evaluating Systematic Relationships. *University of Kansas Science Bulletin*, 38, 1409-1438.
- Thom, H. (1966). *Some Methods of Climatological Analysis* (53 pp.). WMO Technical Note Number 81. Geneva, Switzerland: Secretariat of the World Meteorological Organization.
- Velasco, I., & Aparicio, J. (julio-septiembre, 2004). Evaluación de índices de sequía en las cuencas de afluentes del río Bravo/Grande. *Ingeniería Hidráulica en México*, 19(3), 37-53.
- Vicario, L. (2008). *Evaluación de las sequías hidro-meteorológicas en la cuenca del dique San Roque, Córdoba*. Tesis de maestría. Córdoba, Argentina: FCEfyN, Universidad Nacional de Córdoba.
- Wilhite, D. A., & Glantz, M. H. (1985). Understanding the Drought Phenomenon: The Role of Definitions. *Water International*, 10, 111-120.
- Young, K. C. (1992). A Three-Way Model for Interpolating for Monthly Precipitation Values. *Monthly Weather Review*, 120, 2561-2569.

Institutional Address of the Authors

M.I. Leticia Vicario

Facultad de Ciencias Exactas, Físicas y Naturales
Centro de Estudios y Tecnología del Agua
Universidad Nacional de Córdoba
Av. Filloy s/n, Ciudad Universitaria
Cba., Rep. Argentina
Teléfono y fax: +54 (0351) 4334 446
lvicariotm@gmail.com

Dr. Carlos M. García

Consejo Nacional de Investigaciones Científicas y Técnicas
(Conicet)
Facultad de Ciencias Exactas, Físicas y Naturales
Universidad Nacional de Córdoba
Av. Filloy s/n, Ciudad Universitaria
Cba., República Argentina
Teléfono y fax: +54 (0351) 4334 446
cgarcia2mjc@gmail.com

Dra. Ingrid Teich

Consejo Nacional de Investigaciones Científicas y Técnicas
(Conicet)
Estadística y Biometría
Facultad de Ciencias Agropecuarias
Universidad Nacional de Córdoba
Av. Filloy s/n, Ciudad Universitaria
Cba., República Argentina
Teléfono y fax: +54 (0351) 4334 103
ingridteich@gmail.com

Dr. Juan Carlos Bertoni

Facultad de Ciencias Exactas, Físicas y Naturales
Universidad Nacional de Córdoba
Av. Filloy s/n, Ciudad Universitaria
Cba., República Argentina
Teléfono y fax: +54 (0351) 5353 800
jcbertoni@gmail.com

Dr. Andrés Ravelo

Facultad de Ciencias Agropecuarias
Universidad Nacional de Córdoba
Av. Filloy s/n, Ciudad Universitaria
Cba., República Argentina
Teléfono y fax: +54 (0351) 4334 103
ravelo1@crean.agro.uncor.edu

Dr. Andrés Rodríguez

Consejo Nacional de Investigaciones Científicas y Técnicas
(Conicet)
Facultad de Ciencias Exactas, Físicas y Naturales
Universidad Nacional de Córdoba
Av. Filloy s/n, Ciudad Universitaria
Cba., República Argentina
Teléfono y fax: +54 (0351) 4334 446
arodrig@efn.uncor.edu



Conservation Works, Patzcuaro, Michoacan, Mexico.

Photo: Roberto Menéndez

Water Usage in Northern Sinaloa: Allocating the Resource to Consumers

• Jesús Torres-Sombra •
Universidad Autónoma de Sinaloa, México

• José Alberto García-Salazar* •
Colegio de Postgraduados, México

*Corresponding Author

Abstract

Torres-Sombra, J., & García-Salazar, J. A (January-February, 2015). Water Usage in Northern Sinaloa: Allocating the Resource to Consumers. *Water Technology and Sciences* (in Spanish), 6(1), 167-174.

Population growth and an increase in agricultural, livestock, industrial and commercial activities in northern Sinaloa have increased the demand for water. To determine the allocation of water to consumers, a spatial and intertemporal equilibrium model was validated for 2010, which includes demand functions and fixed supply. The results indicate that when water is scarce demand should decrease in the sector with the lowest value-in-use, such as agriculture, and should not change in sectors with a high value, such as the residential sector. A 10% reduction in the availability of water stored in dams would decrease consumption in Irrigation Districts 075 and 076 by 271 and 54 hm³ with respect to values from 2010, respectively, while consumption would not change significantly for livestock, residential, industrial and commercial activities. To decrease water consumption in the districts, the price needs to increase 82.7 and 70.0%, respectively.

Keywords: Agriculture sector, livestock, residential, commercial and industrial, water price, spatial equilibrium and intertemporal model.

Resumen

Torres-Sombra, J., & García-Salazar, J. A (enero-febrero, 2015). *Uso del agua en el norte de Sinaloa: ¿a cuál consumidor asignar el recurso?* *Tecnología y Ciencias del Agua*, 6(1), 167-174.

El crecimiento de la población y de la actividad agrícola, pecuaria, industrial y comercial en el norte de Sinaloa ha generado un aumento en la demanda de agua. Para determinar la asignación de agua entre los consumidores se validó un modelo de equilibrio espacial e intertemporal para 2010, que considera funciones de demanda y una oferta fija. Los resultados indican que ante una situación de escasez, la demanda del agua debe disminuir en el sector con menor valor de uso, como la agricultura, y no sufrir cambios en sectores con alto valor, como el sector residencial. Una reducción de 10% en la disponibilidad del recurso captado en las presas bajaría el consumo en los Distritos de Riego 075 y 076 en 271 y 54 hm³, respectivamente, respecto a los valores observados en 2010, en tanto que en los sectores pecuario, residencial, industrial y comercial, el consumo no sufriría cambios significativos. Para disminuir el consumo de agua en los distritos se requiere un aumento en el precio de 82.7 y 70.0%, respectivamente.

Palabras clave: sectores agrícola, pecuario, residencial, comercial e industrial, precio del agua, modelo de equilibrio espacial e intertemporal.

Received: 19/04/13

Accepted: 07/08/14

Introduction

Competition for water stored in dams in northern Sinaloa has been heightened by the expansion of agricultural boundaries, the introduction of crops with high water

requirements and growth in livestock, demographics and commerce and industry, as well as the effects of climate change. This region is composed of the municipalities of Ahome, EL Fuerte and Choix.

The annual mean water extracted from the dams in the Fuerte River basin for irrigation modules in Irrigation Districts 075 and 076 (IR075 and IR076) falls short of demand by 61 hm³ (Conagua-DR075, 2011; Conagua-DR076, 2011).

The state's agriculture is important to the country, producing 8 million tons of food annually, part of which comes from the northern part of the state which contains 37.2% of the total irrigation area. In 2010, the Sinaloa's GDP for the primary sector represented 6.6% of the national GDP (INEGI, 2011c). The largest consumer of water in the region is the agricultural sector, whose demand is generated by the planting of 233 and 80 thousand ha located in ID075 and ID076, in the El Fuerte and El Carrizo Valleys. From 1990 to 2010, the water demanded by this sector represented 98.4% of the total. In the livestock sector, cattle and swine represented the largest demand. Between 1990 and 2010, cattle inventories ranged from 195 to 200 thousand heads and in 2010 swine livestock reached 204 thousand heads (INEGI-BIE, 2011).

Demand by the residential sector includes water consumed by the population for use in preparing foods, personal hygiene, cleaning and washing clothes and dishes. Demand by this sector was 41 hm³ annually between 1990 and 2010, representing 1.2% of the total (JAPAMA, 2010; JAPAF, 2010; JAPACH, 2010; Conagua, 2011; INEGI, 2011a; INEGI, 2011b). Most of the industry-related water demand comes from Ahome, where 98% of the 1 655 industries in the region are located. Between 1990 and 2010, industrial water demand represented 0.029% of the total (Canacintra, 2011; JAPAMA, 2010; JAPAF, 2010; JAPACH, 2010). Water demand by the commercial sector is driven by cooling and cleaning in 6 828 establishments. From

1990 to 2010, the demand was 2.21 hm³, or 0.107% of the total (JAPAMA, 2010).

Demand in this region is supplied by water stored in the following dams: 1) Josefa Ortiz de Domínguez-El Sabino, 2) Miguel Hidalgo and Costilla-El Mahone, and 3) Luis Donaldo Colosio-Huites. Competition for water results in the need to find alternatives that more efficiently allocate water resources. Growth in the GDP and in the population will increase water demanded by consumers and a decrease in the supply will heighten conflicts. The above situation leads to the question: How should water be distributed among consumers? From an economical perspective, the distribution of the resource will depend on its use value. Consumption in sectors having a higher use value will not decrease as much as in those with a lower use value.

Dinar and Mody (2004), García, Guzmán and Fortis (2006), Guzmán *et al.* (2006), and García and Mora (2008) indicate that price can be used as a tool to increase efficiency in water usage. There is evidence of a negative relationship between prices and the amount of water demanded. Arbués and Villanúa (2006), Guzmán *et al.* (2006) and Torres-Sombra (2012) estimated a negative price elasticity for water demand in consumer sectors in Zaragoza, España, Comarca Lagunera and northern Sinaloa, Mexico. Therefore, water consumption can be reduced by increasing the price.

The objective was to analyze the distribution of water among consumers under scarcity conditions and to determine the price increase that will result in reducing consumption. Given a contraction in the supply of water, demand will decrease more in sectors with a lower use value, such as the agricultural sector, and less in sectors with a higher use value such as the residential sector.

Materials and Methods

A spatial and temporal equilibrium model was used which included water consumption by sector— agriculture (ID075 and ID076), livestock, industry and the commercial and residential sectors in northern Sinaloa. Assuming t periods of time ($t = 1, 2, 3, \dots, T = 12$), s dams ($s = 1, 2, \dots, S = 3$), m irrigation modules in ID075 ($m = 1, 2, 3, \dots, M = 13$), n irrigation modules in ID076 ($n = 1, 2, 3, \dots, N = 9$); g livestock regions ($g = 1, 2, \dots, G = 3$); r residential regions ($r = 1, 2, \dots, R = 3$); c commercial regions ($c = 1, 2, \dots, C = 3$) and f industrial regions ($f = 1, \dots, F = 2$). The model is:

$$\begin{aligned} \text{MaxSNV} = & \sum_{t=1}^T \sum_{m=1}^M \left[\theta_{mt} y_{mt} + \frac{1}{2} \omega_{mt} y_{mt}^2 \right] \\ & + \sum_{t=1}^T \sum_{n=1}^N \left[\theta_{nt} y_{nt} + \frac{1}{2} \omega_{nt} y_{nt}^2 \right] + \sum_{t=1}^T \sum_{g=1}^G \left[\theta_{gt} y_{gt} + \frac{1}{2} \omega_{gt} y_{gt}^2 \right] \\ & + \sum_{t=1}^T \sum_{r=1}^R \left[\theta_{rt} y_{rt} + \frac{1}{2} \omega_{rt} y_{rt}^2 \right] + \sum_{t=1}^T \sum_{c=1}^C \left[\theta_{ct} y_{ct} + \frac{1}{2} \omega_{ct} y_{ct}^2 \right] \\ & + \sum_{t=1}^T \sum_{f=1}^F \left[\theta_{ft} y_{ft} + \frac{1}{2} \omega_{ft} y_{ft}^2 \right] - \sum_{t=1}^T \sum_{s=1}^S [p_{st} x_{st}] \\ & - \sum_{t=1}^T \sum_{s=1}^S \sum_{m=1}^M [p_{smt} x_{smt}] - \sum_{t=1}^T \sum_{s=1}^S \sum_{n=1}^N [p_{snt} x_{snt}] \\ & - \sum_{t=1}^T \sum_{s=1}^S \sum_{g=1}^G [p_{sgt} x_{sgt}] - \sum_{t=1}^T \sum_{s=1}^S \sum_{r=1}^R [p_{srt} x_{srt}] \\ & - \sum_{t=1}^T \sum_{s=1}^S \sum_{c=1}^C [p_{sct} x_{sct}] - \sum_{t=1}^T \sum_{s=1}^S \sum_{f=1}^F [p_{sft} x_{sft}] \\ & - \sum_{t=1}^T \sum_{s=1}^S [ca_{st,t+1} x_{st,t+1}] \end{aligned} \quad (1)$$

Subject to:

$$\begin{aligned} x_{st} + x_{st-1,t} - x_{st,t+1} \geq & \left[\sum_{m=1}^M x_{smt} + \sum_{n=1}^N x_{snt} \right] \\ & + \left[\sum_{g=1}^G x_{sgt} + \sum_{r=1}^R x_{srt} + \sum_{c=1}^C x_{sct} + \sum_{f=1}^F x_{sft} \right] \end{aligned} \quad (2)$$

$$\sum_{s=1}^S x_{smt} \geq (1 + \alpha + \beta + \gamma) y_{mt} \quad (3)$$

$$\sum_{s=1}^S x_{snt} \geq (1 + \alpha + \beta + \gamma) y_{nt} \quad (4)$$

$$\sum_{s=1}^S x_{sgt} \geq (1 + \beta + \gamma) y_{gt} \quad (5)$$

$$\sum_{s=1}^S x_{srt} \geq (1 + \beta + \gamma) y_{rt} \quad (6)$$

$$\sum_{s=1}^S x_{sct} \geq (1 + \beta + \gamma) y_{ct} \quad (7)$$

$$\sum_{s=1}^S x_{sft} \geq (1 + \beta + \gamma) y_{ft} \quad (8)$$

$$\sum_{s=1}^S x_{st,t+1} \geq VSH_t \quad (9)$$

$$x_{1mt} = 0 \quad (10)$$

$$x_{2nt} = 0 \quad (11)$$

$$x_{13t} = 0 \quad (12)$$

$$y_{mt}, y_{nt}, \dots, x_{sft} \geq 0 \quad (13)$$

where for month t , θ_{mt} , θ_{nt} , θ_{gt} , θ_{rt} , θ_{ct} and θ_{ft} is the ordinate of the water demand function for sectors m , n , g , r , c and f ; and y_{ft} is the amount of water consumed by m , n , g , r , c and f ; ω_{mt} , ω_{nt} , ω_{gt} , ω_{rt} , ω_{ct} and ω_{ft} is the slope of the demand function for m , n , g , r , c and f ; p_{st} is the price of water at the outlet of s ; x_{smt} , x_{snt} , x_{sgt} , x_{srt} , x_{sct} and x_{sft} is the volume of water sent from s to m , n , g , r , c and f ; $p_{st,t+1}$ is the cost of storage in s for t with $t + 1$; $x_{st,t+1}$ is the storage volume of water in s for t with $t + 1$; α is the inefficiency index corresponding

to use in a parcel; β is the inefficiency index corresponding to conduction; γ is the inefficiency index corresponding to evaporation; VSH is the volume required to store the water in dams to cover human consumption over two consecutive years; $s = 1$ = Josefa Ortiz de Domínguez dam; $s = 2$ = Miguel Hidalgo and Costilla dam; $s = 3$ = Luis Donaldo Colosio dan; $r = 1$ = Ahome; $r = 2$ = El Fuerte; $r = 3$ = Choix.

The objective function of the model (equation (1)) maximizes the Social Net Value (SNV), which is equal to the area below the demand curve minus the cost of water at the dam outlet, the cost of conductions and the cost of storage in the dam. The objective function is subject to 12 restrictions. Restriction 2 indicates how water is distributed from each dam to the consumers. Restrictions 3 to 8 indicate how to supply water for consumption among the six consumer sectors. Restriction 9 indicates that the amount of water stored (in the three dams) for t with $t + 1$ should be equal to or larger than the storage volume required in the dams to cover human consumption for two consecutive years. This period is considered to comply with the norms established by Conagua, which recommend storing enough water in dams to meet the needs for human ingestion for at least two consecutive years (Conagua- DR075, 2011; Conagua-DR076, 2011). Restrictions 10 and 11 indicate that water cannot be sent from the Josefa Ortiz and Miguel Hidalgo dams to modules in ID075 and ID076. Restriction 12 that water cannot be sent from the Josefa Ortiz de Dominguez dam to residential sector Choix. Restriction 13 indicates conditions of no-negativity.

Based on Francois and Reinert (1997), the calibration of the model consisted of calculating the parameters, intercepts and slopes of the water demand functions such that the model replicates the observed values of water price and amount of demand

in the base year. The intercept and slopes of the demand functions were obtained for each sector based on Kawaguchi, Suzuki and Kaiser (1997), according to the amount consumed and the price of the water observed in 2010, as well as the price elasticity for water demand estimated by Torres-Sombra (2012) for northern Sinaloa. The model was validated by calculating the percentage difference between the observed values corresponding to the amount demanded and water price in 2010 (using intercepts and slopes of the demand function for the calculation) versus the base model's estimate of these values. To analyze distribution under conditions of water scarcity, reductions of 10 and 20% in the supply were applied.

Monthly water consumption in each module was obtained from progress reports sent by irrigation programs to each district. The price of water in each module was determined by dividing the irrigation districts' total operating costs by the volume of water delivered to the control point. The information related to water price, monthly consumption per module, stored volume, cost of storage, length of channels and efficiency indices was obtained from Conagua-DR075 (2011) and Conagua-DR076 (2011).

Water consumption by the livestock sector was obtained based on Guzmán *et al.* (2006) by multiplying the number of heads of livestock by the annual mean consumption per capita. The price used was the mean value of the amounts charged by the livestock associations when transporting water to the watering holes during the planting season. The data to calculate the demand functions corresponding to the residential, commercial and industrial sectors were obtained from the operating entities' operating reports and financial statements (JAPAMA, 2010; JAPAF, 2010; JAPACH, 2010). Monthly consumption was obtained for each sector by dividing

the income from the monthly sale of water by the official charges approved by the Sinaloa congress and published in the Official State Journal (*Diario Oficial del Estado*) (Sinaloa State Government, 2011).

Distribution costs were calculated according to the difference between the price paid by the end consumers and extractions costs. This difference was considered to reflect all the costs involved in supply. For the all the sectors, the prices were spatially different, with lower prices for locations closer to dams and higher prices for points further away. This information was provided by JAPAMA (2010), JAPAF (2010), JAPACH (2010), Conagua-DR075 (2011) and Conagua-DR076 (2011).

The monthly cost of storage was determined by dividing the cost of storage corresponding to ID075 and ID076 by 12. These data were obtained from the irrigation districts' annual budgets and the annual water rates for irrigation in each module.

The model was solved using MINOS, written in GAMS (*General Algebraic Modeling System*) programming language.

Results and Discussion

Table 1 presents the observed and estimated values corresponding to water demand and

price. The estimated values are very close to the observed values, with a difference of -0.5% in the price of water in ID075, which indicates an underestimate; and difference of zero for the rest. The difference between observed and estimated consumption is greater. The model underestimated consumption in ID076 by -2.2%, and overestimated this variable in the rest of the sectors. In the agricultural sector (ID075), the difference is +0.1%; in the livestock sector +2.1%, in the residential sector +6.9%; in the industrial sector +7.7%; and in the commercial sector +0.8% (Table 1). Since the model satisfactorily replicated water consumption and price, it was used to model the scenarios.

With a 10% decrease in the supply, the demand for water would be reduced by 324 hm³, with the greatest decreases in ID075 and ID076— 10.5 and 8.7%, respectively. The contraction in the residential sector would be -0.2% and no changes would occur in the rest of the sectors. With a reduction of 20% in the availability of water, demand would decrease by 21.0 and 17.5% in ID075 and ID076, respectively. These results indicate that water consumption decreases more in sectors with a lower use value such as agriculture, and less in sectors with a higher use value, such as the residential sector. Decreases in demand

Table 1. Validation of the water model in northern Sinaloa, 2010.

Sector	Consumption			%	Price			%
	Observed	Estimated	Difference		Observed	Estimated	Difference	
	hm ³				\$/m ³			
ID 075	2 577 148	2 580 850	3 702	0.1	0.111	0.110	0.00	-0.5
ID 076	629 696	616 303	-13 393	-2.2	0.130	0.130	0.00	0.0
Livestock	5 514	5 631	117	2.1	12.000	12.005	0.01	0.0
Residential	36 995	39 738	2 743	6.9	3.607	3.608	0.00	0.0
Industrial	619	671	52	7.7	15.86	15.860	0.00	0.0
Commercial	2 422	2 440	19	0.8	12.000	12.000	0.00	0.0
Total	3 252 395	3 245 634	-6 761	-0.2				

can be achieved by making water use more efficient, for example, by changing technology to reduce the irrigation water depth.

Based on data from Conagua-DR075 (2011) and Conagua-DR076 (2011), the greatest loss in water occurs in the agriculture sector, where an annual inefficiency of 30% in the use of water has been observed for a crop pattern composed primarily of white corn, sorghum, beans, wheat and tomato. These crops occupied 87% of the total surface area in 2010, the majority of which was white corn. Efforts to decrease inefficiency have been focused on investing in irrigation technology and planting policies.

To decrease demand in the agricultural sector, an increase of 82.7% in the price of water is needed in ID 075 and 70.0% in ID 076. Since the volume of water extracted for livestock, residential, industrial and commercial sectors is nearly constant, the

effect on rates by reducing extractions would be virtually null. A reduction of 20% in the extraction of water provided to the agricultural sector would require a price increase of 165.5 and 139.2 Mexican pesos per m³ in ID075 and ID076 (Table 2).

An increase in the price of water to 0.201 and 0.221 pesos per m³ for ID075 and ID076 would cover the operating costs of the entities that manage the resource and would have an effect on its efficient use. Because of the currently low price of water, an increase would not have a significant effect on the production cost of corn. A water conservation policy requires efficient conduction systems and the measurement of volumes consumed by parcels, which does not exist. Increases in the price of water is recommended to support investments in technology, given that it can produce a 10 to 50% savings in the resource (He, Wallace, & Doukkali, 2005). Avoiding effects on crop yields

Table 2. Allocation of water among consumers and prices increases in response to scarcity of the resource.

Sector	Consumption			%	Price			%
	Base model	Scenario	Difference		Base model	Scenario	Difference	
	hm ³				\$/m ³			
10% decrease in availability								
ID 075	2 580 850	2 310 215	-270 635	-10.5	0.110	0.201	0.091	82.7
ID 076	616 303	562 464	-53 839	-8.7	0.130	0.221	0.091	70.0
Livestock	5 631	5 629	-3	0.0	12.005	12.095	0.090	0.6
Residential	39 738	39 651	-87	-0.2	3.608	3.696	0.088	2.4
Industrial	671	671.1	0	0.0	15.860	15.951	0.091	0.8
Commercial	2 440.37	2 440	-0.099	0.0	12.000	12.091	0.091	0.8
Total	3 245 634	2 921 070	-324 563	-10.0				
20% decrease in availability								
ID 075	2 580 850	2 039 581	-541 269	-21.0	0.110	0.292	0.182	165.5
ID 076	616 303	508 625	-107 678	-17.5	0.130	0.311	0.181	139.2
Livestock	5 631	5 626	-6	-0.1	12.005	12.186	0.181	1.5
Residential	39 738	39 564	-173	-0.4	3.608	3.789	0.181	5.0
Industrial	671	671	-1	-0.1	15.860	16.041	0.181	1.1
Commercial	2 440	2 440	-0.199	-0.008	12.000	12.181	0.181	1.5
Total	3 245 634	2 596 507	-649 127	-20.0				

should be considered when determining price increases to control demand.

Conclusions

A contraction in water demand in northern Sinaloa requires a decrease in demand in the sectors where the use value of the resource is lower, such as agriculture. A decrease in water consumption could be achieved by lowering demand in the agricultural sector, since this sector consumes the most water and is sensitive to price changes. Increases in the price of water could provide an incentive for producers to more efficiently use the resource. Therefore, any distortions in the fees charged for the use of water should be eliminated. A more efficient use of the resource would enable expanding agricultural boundaries since the decrease in requirements per unit of surface area would make it possible to plant more hectares using the same amount of water.

References

- Arbués, F., & Villanúa I. (December, 2006). Potential for Pricing Policies in Water Resource Management: Estimation of Urban Residential Water Demand in Zaragoza, Spain. *Urban Studies*, 43(1), 2421-2442.
- Canacintra (2011). *Número de industrias instaladas en el municipio de Ahome, Sinaloa*. Los Mochis, México: Gerencia Regional de Canacintra.
- Conagua (2011). *Consumo anual de agua por sector y municipios de Sinaloa durante el periodo 1990-2010*. Culiacán, México: Organismo de Cuenca Pacífico Norte.
- Conagua-DR075 (2011). *Estadísticas de riego y agrícolas*. Los Mochis, México: Gerencias de Operación, Conservación y Estadística del Distrito de Riego 075, Cuencas Pacífico Norte.
- Conagua-DR076 (2011). *Estadísticas de riego y agrícolas*. Villa Gustavo Ordaz, Sinaloa, Gerencia de Operación, Conservación y Estadística del Distrito de Riego 076, Cuencas Pacífico Norte.
- Dinar, A., & Mody, J. (2004). Irrigation Water Management Policies: Allocation and Pricing Principles and Implementation Experience. *Natural Resources Forum* 28. Agadir, Marruecos: United Nations.
- Francois, J. F., & Reinert, K. A. (1997). *Applied Methods for Trade Policy Analysis* (560 pp.). Cambridge: Cambridge University Press.
- García, J. A., & Mora, J. S. (mayo-agosto, 2008). Tarifas y consumo de agua en el sector residencial de la Comarca Lagunera, México. *Región y Sociedad*, 20(42), 119-132.
- García, J. A., Guzmán, E., & Fortis, M. (marzo-abril, 2006). Demanda y distribución del agua en la Comarca Lagunera, México. *Agrociencia*, 40(2), 269-276.
- Gobierno del Estado de Sinaloa (varias fechas, 2011). Publicaciones de tarifas para consumo de agua por parte de las juntas de agua potable y alcantarillado municipales para el periodo 1990-2010. *Diario Oficial del Estado de Sinaloa*.
- Guzmán, E., García, J. A., Mora, J. S. Fortis, M., Valdivia, R., & Portillo, M. (noviembre-diciembre, 2006). La demanda de agua en la Comarca Lagunera, México. *Agrociencia*, 40(2), 793-803.
- He, L., Wallace, T., Doukkali, R., & Siam, G. (July, 2005). *Strategic Policy Option to Improve Irrigation Water Allocation Efficiency: Analysis on Egypt and Morocco* (pp. 24-27). American Agricultural Economics Association Annual Meeting, Providence, Rhode Island.
- INEGI (2011a). *Censo General de Población y Vivienda 2010* [en línea]. Aguascalientes, México. Citado el 4 febrero. Recuperado de <http://www.inegi.org.mx/est/contenidos/Proyectos/ccpv>.
- INEGI (2011b). *Conteo de Población y Vivienda 2005* [en línea]. Aguascalientes, México. Citado el 4 de febrero. Recuperado de <http://www.inegi.org.mx/est/contenidos/Proyectos/ccpv>.
- INEGI (2011c). *Valores del PIB nacional y entidad federativa* [en línea]. Aguascalientes, México. Citado el 4 de febrero. Recuperado de <http://www.inegi.org.mx/est/contenidos/Proyectos/ccpv>.
- INEGI-BIE (2011). *Número de cabezas de ganado en el norte de Sinaloa, número de personas empleadas y económicamente activas, nivel de empleo en Sinaloa, producto interno bruto nacional y estatal en el periodo 1990-2010* [en línea]. Aguascalientes, México. Citado el 3 de febrero. Recuperado de <http://dgcnesyp.inegi.org.mx/cgi-win/bdieinti.exe/SER208477>
- JAPACH (2010). *Estados financieros y reportes de operación*. Choix, México: Gerencia de Operación, Junta de Agua Potable y Alcantarillado de Choix.
- JAPAF (2010). *Estados financieros y reportes de operación*. El Fuerte, México: Gerencia de Operación, Junta de Agua Potable y Alcantarillado de El Fuerte.
- JAPAMA (2010). *Estados financieros y reportes de operación*. Los Mochis, México: Gerencia de Informática, Contabilidad y Operación, Junta de Agua Potable y Alcantarillado del Municipio de Ahome.
- Kawaguchi, T., Suzuki, N., & Kaiser, H. M. (August, 1997). A Spatial Equilibrium Model for Imperfectly Competitive Milk Markets. *American Journal of Agricultural Economics*, 79(3), 851-859.

Torres-Sombra, J. (2012). *Demanda y distribución de agua en el norte de Sinaloa* (139 pp.). Tesis doctoral. Posgrado en Socioeconomía, Estadística e Informática-Economía. Montecillo, México: Colegio de Postgraduados.

Institutional Address of the Authors

Dr. Jesús Torres-Sombra

Universidad Autónoma de Sinaloa
Calle Universidad s/n, Ciudad Universitaria
82017 Mazatlán, Sinaloa, MÉXICO
Teléfono: +52 (669) 9812 100, extensión 113
jesussombra@uas.edu.mx

Dr. José Alberto García-Salazar

Colegio de Postgraduados
Km 36.5 Carretera México-Texcoco
56230. Montecillo, Texcoco, Estado de México, MÉXICO
Teléfono: +52 (595) 9520 200, extensión 1836
jsalazar@colpos.mx

Application of the *ArcHydro* Data Model to Calculate Surface Water Availability

• María de los Ángeles Suárez-Medina* •
Instituto Mexicano de Tecnología del Agua

*Corresponding Author

• Carlos Patiño-Gómez •
Universidad de Las Américas, Puebla, México

• Jaime Velázquez-Álvarez • Jaime Rivera-Benites • Ernesto Aguilar-Garduño •
Instituto Mexicano de Tecnología del Agua

• Guillermo Bautista •
Comisión Nacional del Agua, México

• Citlalli Astudillo-Enríquez •
Instituto Tecnológico de Zacatepec, México

Abstract

Suárez-Medina, M. A., Patiño-Gómez, C., Velázquez-Álvarez, J., Rivera-Benites, J., Aguilar-Garduño, E., Bautista, G., & Astudillo-Enríquez, C. (January-February, 2015). Application of the ArcHydro Data Model to Calculate Surface Water Availability. *Water Technology and Sciences* (in Spanish), 6(1), 175-181.

The concept of geographic databases is currently being used to integrate spatial data and time series corresponding to water resources in a region. Geographic information systems (GIS), which are based on this concept, not only integrate both types of information into one database but also determine relationships among the information. The present study presents a GIS tool to estimate surface water availability based on the continuity equation, as established by Official Mexican Norm 011-CNA-2000 "Conservation of Water Resources – Establishment of Specifications and the Method to Determine National Annual Mean Availability of Water," published in the Official Journal of the Federation, April 17, 2002. Therefore, a geographic database of the ArcHydro data model needs to be generated, which applies mathematic models and stores information about the water resources, monitoring points and historical data in a hydrological basin. The advantages are the centralization of information and reducing the inconveniences involved in using different formats.

Keywords: availability, Arc Hydro, geodatabase, GIS, watershed, hydrological región.

Resumen

Suárez-Medina, M. A., Patiño-Gómez, C., Velázquez-Álvarez, J., Rivera-Benites, J., Aguilar-Garduño, E., Bautista, G., & Astudillo-Enríquez, C. (enero-febrero, 2015). Aplicación del modelo de datos ArcHydro en el cálculo de disponibilidad de agua superficial. *Tecnología y Ciencias del Agua*, 6(1), 175-181.

Actualmente, el concepto de base de datos geográfica está siendo utilizado para integrar datos espaciales y series de tiempo de los recursos hídricos de una región. Los sistemas de información geográfica (SIG) basados en este concepto permiten no sólo integrar ambos tipos de información en una base de datos sino que establecen relaciones entre la misma información. Aquí se presenta una herramienta dentro de un SIG para estimar la disponibilidad de agua superficial expresada con base en la ecuación de continuidad, conforme lo establece la Norma Oficial Mexicana NOM-011-CNA-2000 "Conservación del recurso agua – Que establece las especificaciones y el método para determinar la disponibilidad media anual de las aguas nacionales", publicada en el Diario Oficial de la Federación el 17 de abril de 2002. Para ello es necesario implementar una base de datos geográfica del modelo de datos ArcHydro, que aplique los modelos matemáticos y almacene la información asociada con los recursos hídricos en cuencas hidrológicas, puntos de monitoreo y sus correspondientes datos históricos. Las ventajas es que centraliza la información y se reducen los inconvenientes que se presentan al utilizar diversos formatos.

Palabras clave: disponibilidad, ArcHydro, geodatabase, SIG, cuenca, región hidrológica.

Received: 20/06/11

Accepted: 30/06/14

Introduction

Knowing the amount and quality of water in a region is a priority for making decisions about its distribution, a task which can be difficult when there is little or no information. Mexico is composed of 37 hydrological regions which, in turn, are divided into 731 basins. The availability of surface water is calculated using the continuity equation. Historical series and additional data required to calculate the availability of surface water are extensive, making it complicated to store, organize and manage this information in a logical and flexible structure. The *ArcHydro* data model provides a suitable solution to this problem by enabling the integration of geographic data associated with water resources in a region into a geographic database. A tool contained in a GIS application is presented herein which calculates the availability of surface water in a basin in Balsas Hydrological Region 18 based on the values of the variables in a database having an *ArcHydro* structure.

Objective

The objective of the present work is to develop a computational tool to calculate the availability of surface water using a geographic database with a *ArcHydro* structure, for a hydrological region in Mexico.

Methodology

This section describes 1) the methodology described in NOM-011-CNA-2000 and developed by Conagua (NOM-011-CNA-2000) to calculate the availability of surface water in a basin; 2) the general form of the *ArcHydro* data model and implementation of the geographic database using this model, and 3) the computing

tool developed to automatically calculate the availability of surface water.

Availability of Surface Water

According to Official Mexican Norm NOM-011-CNA-2000, "Conservation of water resources," to calculate the availability of surface water in an interconnected basin system, the following three steps are recommended: a) estimation of the runoff downstream, b) distribution of demands upstream and c) estimation of availability.

a) Estimation of runoff downstream

The calculation for runoff downstream uses the continuity equation expressed as:

$$\frac{dV}{dt} = E - S \quad (1)$$

The change in the volume is equal to the inflows minus outflows for a specific time interval t . The time interval is annual and the units are expressed in cubic hectometers.

Using the surface as the plane of reference, equation (1) is transformed into:

$$Ab = (Cp + Ar + Im + R) - (Ev + Ex + Uc + \Delta V) \quad (2)$$

Where Ab is the runoff downstream; ΔV is the change in storage on the surface; Cp is the natural or "virgin" runoff in the same basin; Ar is runoff upstream; Im importation from external basins; R the returns; Ev evaporation in water bodies and in areas without vegetation; Ex is exports to external basins and Uc is consumptive and non-consumptive uses.

The variables that are measured *in situ* are: change in volume (ΔV), consumptive and non-consumptive uses (Uc), imports (Im) and exports (Ex). Others are measured indirectly, such as evaporation (Ev), runoff

upstream (Ar) and returns (R). In cases in which measurements at control points (Ab) are not available, Cp is calculated using indirect methods according to established norms.

Equation (2) is applied successively to the partial basins in the system analyzed, from upstream to downstream. It is worth mentioning that when estimating availability, the mean supply is taken into account, represented by annual average virgin runoff. For the rest of the variables, the year corresponding to the analysis is used.

b) Distribution of Upstream Demand and Determination of Reserved and Available Volumes

Apparently, all the runoff that flows downstream in a basin could be used entirely within the basin. Nevertheless, a fraction of this runoff is used downstream to partially satisfy demand. This occurs because volumes extracted from a main channel in a middle basin are satisfied by runoff from upstream, runoff in the same basin, returns from different sources located in the basin and by importations, if any. Thus, except for the upper-most basin, the basins depend to a greater or lesser degree on volumes they receive from those located upstream. To determine this, a traditional analysis is needed from upstream to downstream and in the opposite direction, which will be performed by proportionally distributing the water requirements to the components of the water supply in each basin in order to obtain reserved volumes corresponding to each one of the components.

In this regard, it is useful to define the reserved runoff downstream from a basin x , R_{xy} , as the fraction of surface runoff that exits the basin, and contributes to satisfying extractions taken by basin y downstream.

Similarly, the reserved runoff in the same basin x , R_{xx} , is the fraction of runoff in a basin that contributes to satisfying the extractions within the same basin x . It is worth mentioning that the volumes reserved downstream, R_{xy} , are reserved at the outlet of basin x and can be used in basin y or in others located further downstream. In this sense, it could also be said that R_{xy} is the reserved volume at the outlet of basin x .

c) Estimation of availability

The volume available at the outlet of each one of the basins, D_{xy} , is calculated by subtracting the reserved volume from the runoff downstream:

$$D_{xy} = Ab_x - R_{xy}$$

Where D_{xy} is the available volume at the outlet of the basin x ; Ab_x is the runoff downstream and R_{xy} is the reserved runoff at the outlet of basin x . Similarly, the available volume in the same basin, D_{xx} , is calculated by subtracting the reserved volume in the same basin from the virgin runoff in the same basin, that is:

$$D_{xx} = Cp_x - R_{xx}$$

where D_{xx} is the available volume in the same basin corresponding to basin x ; Cp_x is runoff in the same basin and R_{xx} is the reserved volume in the same basin.

The reserved volumes are used either in the basin and/or in another basin downstream. There are two considerations in relation to this: 1) when basin y is furthest downstream, the total flow at its outlet does not have any committed volumes to be reserved downstream; 2) when basin y is furthest upstream, its total inflows are generated in the same basin, as long as there are no importations that

represent a reserved volume considered as downstream from the basin that exports said volume.

The returns (R) in a basin and importations from another basin (Im), if any, should be included as part of the supply that satisfies the volumes committed in the same basin x and part of the basins y downstream.

Database with the ArcHydro Structure

ArcHydro is a data model that proposes a standard structure using a geographic database to store information associated with water resources for a determined area (Maidment, 2002). It uses a vector model and other geographic data models to store information about objects on the land surface that are related to water. The information associated with water resources is primarily composed of two parts:

1. Geospatial information. This refers to land surface features related to the resource and is stored in a vector or matrix format.
2. Time series. These are historical data resulting from measuring variables or parameters associated with the resource in a specific place and period of time.

This model is used to solve problems and improve the quality of the data used. The geographic database (*geodatabase*) represents the pillar of a hydrological information system, which can be defined as a computing system. The layers included in the database containing an *ArcHydro* structure are: water bodies, hydrometric and weather stations, water quality stations, and surface wells/reservoirs and discharges registered by the Public Water Rights Registry. The descriptions

of the weather and hydrometric and water quality stations as well as the Repda wells/reservoirs were provided by Conagua (2005). The database was created for Balsas Hydrological Region 18, which was composed of 12 exorheic and three endorheic basins. The scale of the vector information was 1:50 000 and was generated by INEGI. The Lambert projection coordinate system was used with parameters proposed by INEGI for Mexico and ITRF92 datum. As a first step, the current lines were reviewed and edited to verify that they were completely connected, had no cycles and were in the designated flow direction (Figure 1). Then, the watersheds of each of the basins were delimited using a DEM at a scale of 1:50 000. To this end, control points at the outlet of each open basin and virtual points for each closed basin were defined. The control points corresponded to hydrometric stations and points at the outlets of dams. The geographic coordinates of these points were determined with a GPS for better precision. Each basin was processed separately, after which the results from each one were joined by applying a regionalization process (Patiño, McKinney, & Maidment, 2007) to obtain the complete hydrological regions. The data from the hydrometric, weather and water quality stations in the area were integrated into one table. These data were stored with the *Class Monitoring Point Feature* in the *geodatabase*. Fields were added to store characteristics related to the coordinates and to further describe the stations. Procedures were also performed to transform the time series of the hydrometry, climatology and storage data into a format containing four columns defined by *ArcHydro*. And an additional dimension was included to indicate the source of the data. The climatological and hydrometric data were taken from *Clicom* and *Bandas* systems, respectively (Bandas,

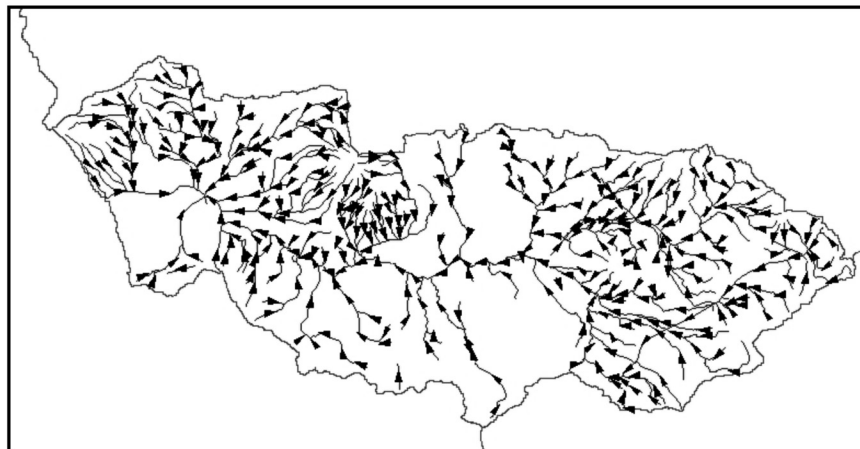


Figure 1. Hydrological network modeled as a geometric network.

2002). Mean daily flows, daily precipitation, evaporation and temperature values were included.

User Interface to Calculate Availability of Surface Water

This part of the work involved developing a computational tool consisting of a user interface and routines connected to the *ArcHydro* database in order to calculate availability and show the results graphically. The program was developed using *Visual Basic for Applications* with *ArcGIS* software, version 9.2. The *ArcHydro* data model requires the level *ArcEditor* or *ArcInfo*.

The computational tool is used to calculate runoff downstream based on the upper basins and then in reverse order. This tool is included in the *ArcGIS*'s *ArcMap* application project (.mxd file).

The project contains the geographic layers needed to calculate water availability and consult the information related to the locality, such as states, municipalities, hydrography and weather stations. Layers are added if required. The calculation

options are available to the user on the project's toolbar (Figure 2).

The system interacts with the *ArcGIS* application through the map and with VBA through user-friendly interfaces to obtain and store the data in the database. A graphic interface shows the user options to calculate availability, enabling the user to select the sub-basin and year desired. Then, using a SQL search of the *VARIABLEANUAL* table contained in the *ArcHydro* database, the data for the year selected by the user is obtained: downstream (*Ab*), exportation (*Ex*), importation (*Im*), returns (*Re*), consumptive uses (*Uc*). These are stored in the general table *DATOANUAL*, which stores the variables needed to calculate water availability. The averages of the variables— same basin (*Cp*), standard deviation (*Dv*) and evaporation (*Ev*)— are also stored in the *DATOANUAL* table in the *ArcHydro* database for the period ending with the year indicated by the user. Missing variables are then calculated using the results from the *DATOANUAL* table.

The data stored in the *ArcHydro* database are daily while each of the consultations are annual. The system will use data from

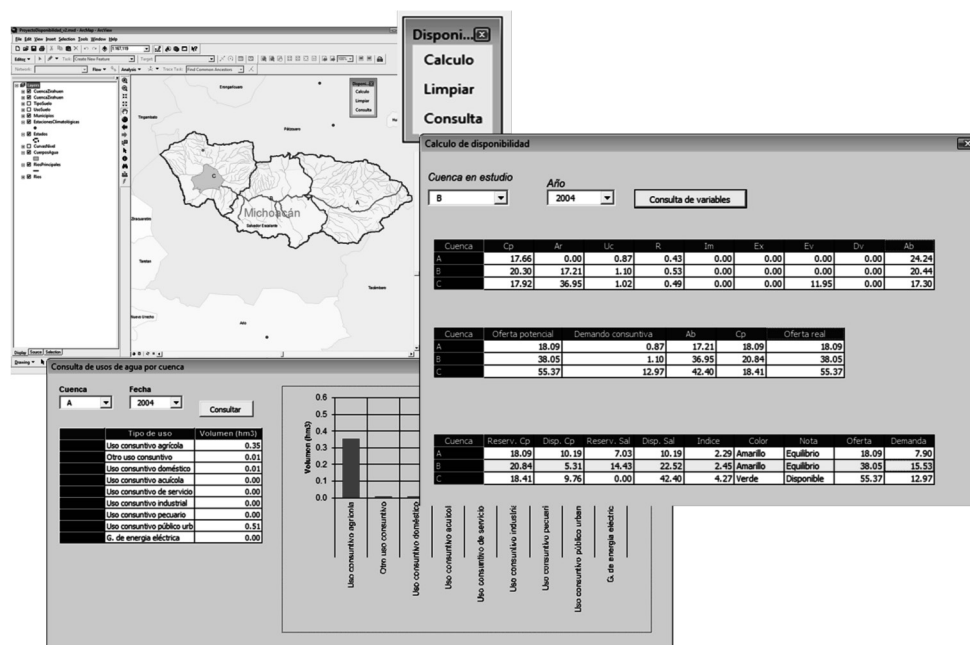


Figure 2. Results from the calculation of availability.

the DATOANUAL table to determine the water availability in the region selected using the corresponding formulas.

Finally, the system shows the results in a tabular format through a graphic interface. These results are stored in the *ArcHydro* database for future consultations (Figure 2).

Conclusions

The *ArcHydro* model enables integrating all the information needed to calculate availability in one single geographic database, as well as the results from the calculation. The structure is standard, flexible and adaptable to calculation requirements. The database stores the metadata of each layer such that the user knows the characteristics of the information and therefore the quality of the data. The user interface facilitates and automates the calculation and serves as a useful tool to

make decisions involving water resources management. Even after the project has been completed, the model can be adjusted to include information desired by the user and additional information can be added. The results from the availability of surface water for the Balsas are published in the Conagua webpage.

References

- Bandas (2002). *Banco Nacional de Datos de Aguas Superficiales*. Jiutepec, México: Instituto Mexicano de Tecnología del Agua.
- Conagua (2005). *Estimación de la disponibilidad de agua superficial en cuencas*. México, DF: Comisión Nacional del Agua.
- Maidment, D. R. (2002). *ArcHydro GIS for Water Resources*. Redlands, USA: ESRI Press.
- Patiño, C., McKinney, D., & Maidment, D. (September/October, 2007). Sharing Water Resources Data in the Bi-National Rio Grande/Bravo basin. *Journal of Water Resources Planning and Management*. American Society of Civil Engineers, 133(5), 416-426.

Institutional Address of the Authors

M.I. María de los Ángeles Suárez-Medina
M.C. Jaime Velázquez-Álvarez
M.I. Jaime Rivera-Benites
M.I. Ernesto Aguilar-Garduño

Instituto Mexicano de Tecnología del Agua
Coordinación de Hidrología
Subcoordinación de Planeación Hídrica
Paseo Cuauhnáhuac 8532, colonia Progreso
62550 Jiutepec, Morelos, México
Teléfono: + 52(777) 3293 600, extensiones 257, 531, 374, 478
Fax: + 52 (777) 3293 685
msuarez@tlaloc.imta.mx
jaimevel@tlaloc.imta.mx
jrivera@tlaloc.imta.mx
eaguilar@tlaloc.imta.mx

Dr. Carlos Patiño-Gómez

Universidad de Las Américas, Puebla, México
Sta. Catarina Mártir
72810 Cholula, Puebla, México
Teléfono: +52 (222) 229 2000
carlos.patino@udlap.mx

Ing. José Guillermo Bautista Bárcenas

Comisión Nacional del Agua, México
Insurgentes Sur número 2416, noveno piso, ala sur, Colonia
Copilco El Bajo, Delegación Coyoacán
04340 México, D.F., MÉXICO
Teléfono: +(52) (55) 5174 4000, extensión 1317
Guillermo.bautista@conagua.gob.mx

M.T.I. Citlalli Astudillo-Enríquez

Consortio Empresarial ADPER, S.A. de C.V.
Manuel Ávila Camacho 1903 int 600 A
Ciudad Satélite
53100 Naucalpan de Juárez, MÉXICO
Teléfono: +52 (777) 2199 545
xitlae@gmail.com



Sumidero Canyon, Chiapas, Mexico.

Photo: Ricardo Espinosa Reza.

Comparison of PPD, SPI and RDI Indices to Classify Droughts: Zacatecas Weather Station, Mexico

• Daniel Francisco Campos-Aranda •

Profesor jubilado de la Universidad Autónoma de San Luis Potosí, México

*Corresponding Author

Abstract

Campos-Aranda, D. F. (January-February, 2015). Comparison of PPD, SPI and RDI Indices to Classify Droughts: Zacatecas Weather Station, Mexico. *Water Technology and Sciences* (in Spanish), 6(1), 183-193.

Meteorological droughts are common and recurring events in a climate system and can occur in any region with varying degrees of severity, duration and geographic coverage. Its principal characteristic is a decrease in rainfall from normal or average levels. Therefore, the various procedures available to detect and monitor droughts are generally based on available monthly precipitation records. The present work presents the operating procedures for three methods used to classify droughts by severity (light, moderate, severe and extreme). These methods include the probabilistic precipitation deficit (PPD), standardized precipitation index (SPI) and the reconnaissance of drought index (RDI), which also includes monthly potential evapotranspiration. These indices are applied to the available monthly rainfall registry from the Zacatecas weather station located in the capital of the state of Zacatecas, Mexico. It contains 83 years of records from January 1930 to December 2012. The results are described and conclusions are presented, which suggest the joint application of these indices to complement and /or verify the classification of droughts obtained.

Keywords: Mixed Gamma distribution, monthly potential evapotranspiration, statistical tests of homogeneity, probabilistic models LP3, GEV and GLO, standard error of fit, severity and duration of droughts.

Resumen

Campos-Aranda, D. F. (enero-febrero, 2015). Contraste de los índices DPP, SPI y RDI para clasificación de sequías, en la estación climatológica Zacatecas, México. *Tecnología y Ciencias del Agua*, 6(1), 183-193.

Las sequías meteorológicas son eventos comunes y recurrentes del sistema climático, que pueden acontecer en cualquier zona, pero con características diferentes en severidad, duración y extensión en cada región. Su característica fundamental es una disminución en la lluvia en relación con sus valores normales o promedio. Debido a ello, los variados procedimientos disponibles para su detección y seguimiento se basan, por lo general, en los registros disponibles de precipitación mensual. En este trabajo se exponen los procedimientos operativos de tres métodos que permiten clasificar las sequías según su severidad en ligeras, moderadas, severas y extremas. Tales métodos son los siguientes: el déficit probabilístico de precipitación (DPP), el índice estandarizado de precipitación (SPI) y el índice de reconocimiento de sequías (RDI), el cual, además, utiliza la evapotranspiración potencial mensual. Se aplican tales índices al registro disponible de lluvia mensual en la estación climatológica Zacatecas, ubicada en la capital del estado del mismo nombre, en México, con 83 años, de enero de 1930 a diciembre de 2012. Se describen los resultados y se formulan las conclusiones, las cuales sugieren la aplicación conjunta de tales índices, para complementar y/o ratificar la clasificación de sequías obtenida.

Palabras clave: distribución Gamma Mixta, evapotranspiración potencial mensual, pruebas estadísticas de homogeneidad, modelos probabilísticos LP3, GVE y LOG, error estándar de ajuste, severidad y duración de sequías.

Received: 02/12/13

Accepted: 04/05/14

Introduction

Droughts are natural and recurring phenomena associated with a rainfall deficit over a large geographic area for a

significant period of months or years. This general definition implies that droughts are regional and characterized by three dimensions: severity or intensity, duration and extension. For a particular locality, the

most important aspect involving droughts is their intensity, that is, how much the decreased rainfall differs from normal conditions (Tsakiris & Vangelis, 2005). In addition, it has recently been established that a preventive approach should be used to minimize the damaging effects of droughts, which requires an effective system to detect and monitor droughts (Cacciamani, Morgillo, Marchesi, & Pavan, 2007; Campos-Aranda, 2013).

The *objective* of this work is to present a detailed description of the operating procedures for three indices which use available monthly precipitation records to define the severity of droughts for a specific period (months) and occurring in a particular place. The probabilistic precipitation deficit (PPD) and the standardized precipitation index (SPI) perform probabilistic processing of monthly rainfall data, but in different ways. Meanwhile, the reconnaissance drought index (RDI) relates the precipitation that has occurred with potential evapotranspiration. In the present study, the three indices are applied with available precipitation records from the Zacatecas weather station, located in the city of Zacatecas, which is the capital of the state of Zacatecas, Mexico. The records contain 83 years, from January 1930 to December 2012. It is concluded that the results from the three indices complement and verify each other.

Description of Operating Procedures

Campos-Aranda (2014) have presented a detailed description of the operating procedures for each of the indices— PPD, SPI and RDI. Therefore, the following sections will only briefly outline their proposal and present their equations.

Probabilistic Precipitation Deficit (PPD)

This index was proposed in the mid 1990s in England and has been recently applied in Mexico. It involves the probabilistic processing of annual sums solely composed of negative differences between monthly and mean precipitation. Logically, the annual sums (DA^i) for each year i take into account duration and period, in months, of the drought under analysis. Droughts are classified based on the predictions obtained, as shown in Table 1.

Since the predictions sought correspond to short return periods (< 50 years), they are very consistent. Therefore, to obtain the limits that define the magnitude of a drought, the fitting of only three probabilistic models that have been used as a rule is recommended, which are the Log-Pearson Type III (LP3), General Extreme Values (GEV) and the Generalized Logistic (LOG). Their fit parameters are obtained using methods that have been universally proven and those resulting in the smallest standard error of fit are adopted (Kite, 1977).

Table 1. Classification of droughts according to expanded criteria by Mawdsley, Petts and Walker, 1994.

Classification of droughts	Return period (years)	Probability of non-exceedance $P(X < x)$
Slight (SD)	2 to 5	0.50 to 0.80
Moderate (MD)	5 to 20	0.80 to 0.95
Severe (SD)	20 to 50	0.95 to 0.98
Extreme (ED)	> 50	> 0.98

Standardized Precipitation Index (SPI)

This index was proposed in the early 1990s (McKee, Doesken, & Kleist, 1993) and may be the most universally used index to detect and monitor meteorological droughts. As with the PPD, it only uses monthly precipitation, but with very different processing. Once the *duration of drought in months (DDM)* is defined, all the possible sequences of that duration are obtained from the records using moving sums. For example, for the seasonal drought with $DDM = 4$, the first sequence will be the sum of the first to the fourth month, the second sequence the sum of the second to the fifth month, and so on. The number of sequences or data (ND) to process will be:

$$ND = 12 \cdot NY - DDM + 1 \quad (1)$$

where NY is the number of years in the available records, which usually begin in January and end in December. Next, the two-parameter gamma distribution is fitted to the ND series that was defined, whose probability density function is:

$$g(x) = \frac{1}{\beta^\lambda \cdot \Gamma(\lambda)} x^{\lambda-1} \cdot e^{-x/\beta} \quad \text{for } x > 0 \quad (2)$$

where $\lambda > 0$ is the form parameter, $\beta > 0$ is the scale, $x > 0$ accumulated precipitation in DDM and $\Gamma(\cdot)$ the *factorial* function or gamma function from which the distribution gets its name, originally known as Pearson Type III. To estimate the two fit parameters, the maximum likelihood method is used, which is quite precise. These expressions are (Thom, 1971; Haan, 1977):

$$\lambda = \frac{1 + \sqrt{1 + 4A/3}}{4A} \quad (3)$$

$$\beta = \frac{\bar{x}}{\lambda} \quad (4)$$

where A is an auxiliary variable defined as:

$$A = \ln(\bar{x}) - \frac{\sum_{i=1}^{n'} \ln(x_i)}{n'} \quad (5)$$

in which n' is the number of non-null data (x_i) whose arithmetic mean is \bar{x} . The estimation of the form parameter using equation (3) requires a correction by subtracting the $\Delta\lambda$ term when the result is less than 5.60, that is:

$$\Delta\lambda = a_0 + a_1 \cdot \lambda + a_2 \cdot \lambda^2 + a_3 \cdot \lambda^3 + a_4 \cdot \lambda^4 + a_5 \cdot \lambda^5 \quad (6)$$

$$\begin{aligned} a_0 &= 0.04701236 & a_1 &= -0.0742802 \\ a_2 &= 0.05139812 & a_3 &= -0.0177746 \\ a_4 &= 0.002974521 & a_5 &= -0.0001899932 \end{aligned}$$

The mixed gamma distribution considers the probability of null values (q) in the ND series generated and no null values in $p = 1 - q$ when the probability of non-exceedance is evaluated for a value x . This expression is:

$$H(x) = q + p \cdot G(x) \quad (7)$$

when $x = 0$, $H(0) = q$. If m is the number of zeros in the series processed, the value q will be calculated by m/ND and therefore $n' = ND - m$. When the series does not have null values, q will equal zero, the value of p will be 1 and $H(x) = G(x)$.

To calculate the probability of non-exceedance, $G(x)$, relative to a value x , the Pearson Type III model is converted to the chi-squared model (INSERTAR SIMBOLO) with v degrees of freedom, whose variable equivalence is (Haan, 1977; Bobée & Ashkar, 1991; Rao & Hamed, 2000):

$$\chi^2 = 2 \cdot x / \beta \tag{8}$$

$$v = 2 \cdot \lambda \tag{9}$$

The series is expanded to evaluate the probability of non-exceedance for distribution χ^2 with a value v ; that is (Zelen & Severo, 1965):

$$G(x) = P(\chi^2 | v) = \tag{10}$$

$$\left(\frac{\chi^2}{2}\right)^{v/2} \frac{e^{-\chi^2/2}}{\Gamma\left(\frac{v+2}{2}\right)} \left[1 + \sum_{r=1}^{\infty} \frac{\chi^{2r}}{(v+2) \cdot (v+4) \cdot \dots \cdot (v+2r)}\right]$$

The gamma factorial function is calculated with the Stirling formula (Davis, 1965), which is:

$$\Gamma(\alpha) \cong e^{-\alpha} \cdot \alpha^{\alpha-1/2} \cdot \sqrt{2\pi} \tag{11}$$

$$\cdot \left(1 + \frac{1}{12 \cdot \alpha} + \frac{1}{288 \cdot \alpha^2} - \frac{139}{51840 \cdot \alpha^3} - \frac{571}{2488320 \cdot \alpha^4} + \dots\right)$$

Lastly, as indicated by Edwards and McKee (1997), a logical number approximation presented by Zelen and Severo (1965) is used to convert the accumulated probability, $H(x)$, into the standardized normal variable Z with a mean of zero and unit variance, which defines the SPI index:

$$Z = SPI = -\left(t - \frac{b_0 + b_1 \cdot t + b_2 \cdot t^2}{1 + c_1 \cdot t + c_2 \cdot t^2 + c_3 \cdot t^3}\right) \tag{12}$$

for $0 < H(x) < 0.50$

$$Z = SPI = +\left(t - \frac{b_0 + b_1 \cdot t + b_2 \cdot t^2}{1 + c_1 \cdot t + c_2 \cdot t^2 + c_3 \cdot t^3}\right) \tag{13}$$

for $0.50 < H(x) < 1$

where:

$$t = \sqrt{\ln\left[\frac{1}{(H(x))^2}\right]} \quad \text{for } 0 < H(x) < 0.50 \tag{14}$$

$$t = \sqrt{\ln\left[\frac{1}{(1-H(x))^2}\right]} \quad \text{for } 0.50 < H(x) < 1 \tag{15}$$

$$b_0 = 2.515517 \quad b_1 = 0.802853 \quad b_2 = 0.010328$$

$$c_1 = 1.432788 \quad c_2 = 0.189269 \quad c_3 = 0.001308$$

The wetness and dryness levels are defined in Table 2 (Cacciamani *et al.*, 2007; Tsakiris, Tigkas, Vangelis, & Pangalou, 2007). Details about the procedure can be found in Velasco (2002).

Reconnaissance Drought Index (DRI)

This was recently proposed and the theoretical background and detailed description of its advantages can be found in Tsakiris and Vangelis (2005). Its general expression is (Tsakiris *et al.*, 2007):

$$\delta_k^i = \frac{\sum_{j=1}^k P_j^i}{\sum_{j=1}^k ETP_j^i} \tag{16}$$

where i is the year ranging from 1 to NY ; k is the number of months used to calculate

Table 2. Classification of Rainy and Dry Periods according to the SPI Index.

SPI value	Designation
> 2.00	Extreme rainfall
1.50 to 1.999	Severe rainfall
1.00 to 1.499	Moderate rainfall
0 to 0.999	Slight rainfall
0 to -0.999	Slight drought (SD)
-1.00 to -1.499	Moderate drought (MD)
-1.50 to -1.999	Severe drought (SD)
-2.00 or less	Extreme drought (ED)

the RDI, P_j^i and ETP_j^i the precipitation and potential evapotranspiration for month j in year i . This index attempts to account for the highest temperatures occurring during periods of drought, resulting in higher evaporative demand. Therefore, the RDI will likely be more sensitive than the previous two indices which are exclusively based on monthly precipitation. The RDI is generally calculated for the growth season of crops (3 or 6 months) and for each year ($k = 12$). The normalized and standardized RDI index are (Tsakiris *et al.*, 2007):

$$RDI_N^i = \frac{\delta_k^i}{\bar{\delta}_k} - 1 \quad (17)$$

$$RDI_{ST}^i = \frac{y_i - \bar{y}}{S_y} \quad (18)$$

where $\bar{\delta}_k$ is the arithmetic mean of the annual NY values and y_i are the natural logs of δ_k^i , whose mean and standard deviation are \bar{y} and S_y . The above standardization considers that δ_k^i follows a Log-Normal distribution. Since RDI_{ST}^i behaves the same as the SPI index, Table 2 also is used specifically to designate wet and dry years.

To estimate monthly ETP , the first Hargreaves-Samani empirical formula was used, proposed in the early 1980s, which calculates the daily mean ETP in millimeters solely based on the mean temperature (Tt), expressed in Fahrenheit, and the daily mean incident solar radiation corresponding to the depth of water evaporated (Ri'), expressed in millimeters. This equation is (Hargreaves & Samani, 1982):

$$ETP = 0.0075 \cdot Ri' \cdot Tt \quad (19)$$

Incident solar radiation (Ri) can be calculated with the Angstrom formula when data are available for actual daylight

hours, or duration of sunshine (Campos-Aranda, 2005), or with the available maps of Mexico (Almanza & López, 1975; Hernández, Tejeda, & Reyes, 1991), reported in Langleys/day (ly/d). That is, cal/cm²/day. To convert depth of water evaporated, the following formula is used:

$$Ri' = 10 \cdot Ri / Hv \quad (20)$$

where Hv is the latent heat of evaporation or the energy required to evaporate 1 g or 1 cm³ of water. This is estimated with the following expression, where the mean monthly temperature (T) is measured in °C:

$$Hv = 595.9 - 0.55 \cdot Tt \quad (21)$$

In Mexico, equation (19) and two other empirical formulas have been compared to the modified Penman method, finding that the latter better reproduces estimations of monthly ETP (Campos-Aranda, 2005).

Description of the Numerical Application

Monthly Rain Gauge Records Processed

The geographic coordinates of the Zacatecas weather station, located in the capital of the state (also called Zacatecas), Mexico, are at 22° 45' N latitude and 102° 34' W longitude, at an altitude of 2 485 masl. The monthly rainfall records (mm) are in Excel format at the Local Zacatecas Department of the National Water Commission (Conagua, Spanish acronym). They begin in January 1953 and end in December 2012, with missing data for April 1986 and several months between 2010 to 2012. The monthly mean was adopted for the missing data from April 1986, and the other data were considered to be the same as the rainfall measured at the Guadalupe weather station during the same months,

Table 3. Annual estimations associated with the PPD, SPI and RDI indices and droughts identified at the Zacatecas weather stations, Zacatecas, Mexico.

1	2	3	4	5	6	7	8	9	10	11
Year	Annual precipitation (mm)	DA ⁱ	TD _{PPD}	H(x)	SPI ₁₂	TD _{SPI}	ETP ⁱ	RDI ₁₂	RDI _{ST}	TD _{RDI}
1930	630.9	137.5	SL	0.869	1.123	-	1 379.7	0.457	1.094	-
1931	429.9	147.4	SL	0.415	-0.215	SL	1 366.0	0.315	-0.077	SL
1932	350.7	161.8	SL	0.197	-0.851	SL	1 408.4	0.249	-0.811	SL
1933	598.8	73.7	-	0.823	0.927	-	1 410.9	0.424	0.861	-
1934	769.3	34.5	-	0.974	1.950	-	1 382.1	0.557	1.711	-
1935	893.4	69.4	-	0.993	2.449	-	1 380.6	0.647	2.183	-
1936	441.2	117.0	-	0.448	-0.130	SL	1 408.7	0.313	-0.092	SL
1937	400.4	131.5	-	0.329	-0.442	SL	1 428.1	0.280	-0.439	SL
1938	475.6	136.7	SL	0.547	0.118	-	1 413.0	0.337	0.134	-
1939	587.8	42.7	-	0.805	0.859	-	1 400.2	0.420	0.826	-
1940	516.4	75.2	-	0.655	0.398	-	1 404.6	0.368	0.410	-
1941	672.4	33.3	-	0.915	1.371	-	1 403.9	0.479	1.240	-
1942	540.0	76.9	-	0.710	0.554	-	1 401.9	0.385	0.557	-
1943	371.9	184.7	SL	0.251	-0.672	SL	1 402.8	0.265	-0.615	SL
1944	483.5	126.8	-	0.569	0.173	-	1 397.5	0.346	0.220	-
1945	375.8	155.6	SL	0.261	-0.640	SL	1 443.0	0.260	-0.671	SL
1946	350.9	136.9	SL	0.198	-0.850	SL	1 430.9	0.245	-0.859	SL
1947	387.5	203.1	SM	0.293	-0.545	SL	1 417.6	0.273	-0.519	SL
1948	485.7	69.9	-	0.575	0.188	-	1 433.1	0.339	0.155	-
1949	347.7	189.4	SL	0.190	-0.877	SL	1 428.4	0.243	-0.883	SL
1950	396.7	119.6	-	0.319	-0.471	SL	1 437.8	0.276	-0.490	SL
1951	437.6	151.7	SL	0.438	-0.157	SL	1 425.4	0.307	-0.155	SL
1952	364.8	188.5	SL	0.232	-0.731	SL	1 406.6	0.259	-0.684	SL
1953	441.7	122.2	-	0.450	-0.127	SL	1 398.5	0.316	-0.066	SL
1954	284.2	190.9	SM	0.071	-1.467	SM	1 422.2	0.200	-1.501	SS
1955	584.7	101.2	-	0.799	0.839	-	1 406.9	0.416	0.795	-
1956	389.7	183.1	SL	0.299	-0.527	SL	1 411.5	0.276	-0.488	SL
1957	252.1	264.6	SS	0.036	-1.800	SS	1 435.2	0.176	-1.906	SS
1958	682.7	63.9	-	0.924	1.432	-	1 403.1	0.487	1.289	-
1959	481.5	135.7	SL	0.563	0.159	-	1 403.7	0.343	0.193	-
1960	321.8	240.4	SM	0.134	-1.108	SM	1 430.1	0.225	-1.129	SM
1961	334.7	155.9	SL	0.161	-0.992	SL	1 436.2	0.233	-1.019	SM
1962	309.4	215.1	SM	0.111	-1.223	SM	1 446.0	0.214	-1.287	SM
1963	326.3	184.9	SL	0.143	-1.067	SM	1 439.6	0.227	-1.106	SM
1964	447.7	125.4	-	0.467	-0.082	SL	1 403.5	0.319	-0.035	SL
1965	510.9	153.6	SL	0.641	0.361	-	1 397.4	0.366	0.393	-
1966	514.3	85.6	-	0.650	0.384	-	1 386.0	0.371	0.439	-
1967	590.9	101.8	-	0.810	0.878	-	1 393.7	0.424	0.857	-
1968	635.1	111.6	-	0.875	1.148	-	1 356.4	0.468	1.169	-
1969	169.3	313.7	SE	0.002	-2.825	SE	1 378.5	0.123	-3.028	SE
1970	549.4	107.1	-	0.731	0.615	-	1 379.9	0.398	0.660	-
1971	764.3	134.1	SL	0.972	1.919	-	1 390.9	0.550	1.670	-
1972	414.4	102.5	-	0.370	-0.333	SL	1 411.1	0.294	-0.294	SL
1973	521.7	157.7	SL	0.668	0.433	-	1 392.1	0.375	0.470	-
1974	415.9	133.1	-	0.374	-0.321	L	1 396.9	0.298	-0.251	SL

Table 3. (continuation) Annual estimations associated with the PPD, SPI and RDI indices and droughts identified at the Zacatecas weather stations, Zacatecas, Mexico.

1	2	3	4	5	6	7	8	9	10	11
Year	Annual precipitation (mm)	DA^i	TD_{PPD}	$H(x)$	SPI_{12}	TD_{SPI}	ETP^i	RDI_{12}	RDI_{ST}	TD_{RDI}
1975	367.6	164.6	SL	0.239	-0.708	SL	1 397.6	0.263	-0.640	SL
1976	570.0	150.7	SL	0.773	0.747	-	1 365.9	0.417	0.808	-
1977	405.7	142.9	SL	0.344	-0.400	SL	1 386.5	0.293	-0.305	SL
1978	278.3	194.7	SM	0.064	-1.526	SS	1 388.2	0.200	-1.491	SM
1979	300.1	237.5	SM	0.095	-1.311	SM	1 399.2	0.214	-1.279	SM
1980	377.0	178.4	SL	0.264	-0.630	SL	1 400.4	0.269	-0.567	SL
1981	588.5	41.8	-	0.806	0.863	-	1 385.8	0.425	0.862	-
1982	299.6	254.8	SS	0.094	-1.316	SM	1 430.7	0.209	-1.354	SM
1983	533.0	92.6	-	0.694	0.508	-	1 366.3	0.390	0.596	-
1984	560.1	52.8	-	0.753	0.684	-	1 383.7	0.405	0.712	-
1985	542.0	126.2	-	0.715	0.567	-	1 334.9	0.406	0.722	-
1986	511.3	119.6	-	0.642	0.364	-	1 359.3	0.376	0.482	-
1987	632.6	115.3	-	0.871	1.133	-	1 346.6	0.470	1.179	-
1988	489.7	86.2	-	0.586	0.216	-	1 358.1	0.361	0.349	-
1989	412.8	148.9	SL	0.365	-0.345	SL	1 383.5	0.298	-0.244	SL
1990	721.4	54.4	-	0.952	1.660	-	1 370.2	0.526	1.536	-
1991	669.6	149.2	SL	0.912	1.354	-	1 384.4	0.484	1.270	-
1992	537.1	183.3	SL	0.704	0.535	-	1 363.9	0.394	0.626	-
1993	468.3	54.6	-	0.526	0.066	-	1 386.8	0.338	0.144	-
1994	554.1	81.4	-	0.741	0.645	-	1 416.3	0.391	0.605	-
1995	342.8	173.7	SL	0.179	-0.920	SL	1 410.1	0.243	-0.887	SL
1996	568.8	84.6	-	0.770	0.739	-	1 396.2	0.407	0.732	-
1997	354.0	195.3	SM	0.205	-0.823	SL	1 364.4	0.259	-0.683	SL
1998	473.0	147.9	SL	0.540	0.099	-	1 427.8	0.331	0.084	-
1999	343.5	181.8	SL	0.180	-0.914	SL	1 417.3	0.242	-0.896	SL
2000	339.0	220.4	SM	0.170	-0.954	SL	1 419.0	0.239	-0.941	SL
2001	481.9	142.4	SL	0.564	0.162	-	1 394.6	0.346	0.216	-
2002	693.3	19.0	-	0.932	1.494	-	1 403.9	0.494	1.336	-
2003	559.9	77.2	-	0.753	0.683	-	1 404.9	0.399	0.663	-
2004	718.3	62.7	-	0.950	1.642	-	1 407.9	0.510	1.438	-
2005	358.7	206.3	SM	0.217	-0.783	SL	1 441.0	0.249	-0.812	SL
2006	520.3	66.0	-	0.664	0.424	-	1 453.9	0.358	0.326	-
2007	408.8	167.7	SL	0.353	-0.376	SL	1 419.3	0.288	-0.355	SL
2008	591.3	132.6	-	0.811	0.881	-	1 401.7	0.422	0.842	-
2009	502.9	67.4	-	0.621	0.307	-	1 430.7	0.352	0.270	-
2010	493.0	213.0	SM	0.595	0.239	-	1 390.2	0.355	0.297	-
2011	179.5	293.4	SE	0.004	-2.682	SE	1 384.1	0.130	-2.857	SE
2012	255.0	229.8	SM	0.039	-1.768	SS	1 361.2	0.187	-1.704	SS

Legend:

- DA^i sum of annual deficiencies in rainfall for year i .
 TD_{PPD} type of drought according to the probabilistic precipitation deficit.
 $H(x)$ probability of non-exceedance of a value x (equation (7)).
 SPI_{12} standardized precipitation index with 12-month duration.
 TD_{SPI} type of drought according to the standardized precipitation index.
 ETP^i potential evapotranspiration potential for year i .
 RDI_{12} Reconnaissance Drought Index with 12-month duration.
 RDI_{ST} Standardized Reconnaissance Drought index.
 TD_{RDI} Type of droughts according to the Reconnaissance Drought Index.

which is approximately 6 km in a straight line from the Zacatecas station and is located in the same geographic sub-region. This was considered acceptable because of the similarity in annual data between the registries. According to historical information from Conagua, the Zacatecas weather station has operated continuously and has not changed location, therefore these records can be considered reliable.

Issue 3 of the *Weather Bulletin (Boletín Climatológico)* (SARH, 1980) for Hydrological Region No. 37 (El Salado) contains monthly rainfall records corresponding to the Zacatecas station from January 1930 to December 1978. Therefore, the period from January 1930 to December 1952, which has no missing data, was taken from this *Bulletin* and thus a registry with 83 years was generated. The 12 average monthly values from the resulting registry are 15.8, 9.3, 4.4, 7.4, 17.3, 78.5, 100.6, 98.5, 83.1, 34.5, 12.6, and 10.9, whose sum is 472.9 mm, which corresponds to the annual mean precipitation. The second column of Table 3 shows the annual rainfall values for the period 1930 to 2012. These range from 169.3 mm in the year 1969 to 893.4 mm in the year 1935.

Verification of the Homogeneity of the Annual Registry

The annual precipitation registry was used to analyze the statistical quality of the data, searching for deterministic components using two general tests (Sequences and Helmert) and six specific tests—persistence

(Anderson & Sneyers), trends (Kendall and Spearman), variability (Bartlett) and changes in the mean (Cramer). Most of these tests can be found in WMO (1971) and Machiwal and Jha (2012). The registry only showed persistence in the Anderson test, with a first-order serial correlation coefficient of 0.181 and a critical coefficient of 0.168. Nevertheless, the general tests do not detect lack of homogeneity. Therefore, the monthly registry generated was considered to be suitable for statistical and probabilistic processing.

Results from the PPD

The monthly average rainfall from the registry generated was used to obtain the annual sums of the rainfall deficits for a DDM = 12. These are listed in column 3 of Table 3, without the minus sign. The probabilistic processing of the series of 83 DA^i values resulted in the predictions shown in Table 4, which correspond to the LP3 (Bobée & Ashkar, 1991), GEV (Stedinger, Vogel, & Foufoula-Georgiou, 1993) and LOG (Hosking & Wallis, 1997) distributions with the least standard error of fit (*SEF*).

The limits found with the GEV distribution were adopted and the designations indicated in column 4 of Table 3 were defined for each year with droughts ($DA^i > 133.9$ mm).

Results from the SPI Index

For a DDM = 12, an ND = 985 was obtained. The fit of the mixed gamma distribution

Table 4. The value ranges of DA^i that define the types of drought, in millimeter.

Designation of drought	LP3 <i>SEF</i> = 6.5 mm	GEV <i>SEF</i> = 5.6 mm	LOG <i>SEF</i> = 6.3 mm
Slight (SD)	133.7 to 192.3	133.9 to 190.1	134.6 to 185.2
Moderate (MD)	192.3 to 246.5	190.1 to 247.8	185.2 to 247.3
Severe (SD)	246.5 to 270.7	247.8 to 277.2	247.3 to 287.9
Extreme (ED)	> 270.7	> 277.2	> 287.9

resulted in a form parameter (λ) of 11.11265 and a scale (β) of 42.6922, with $q = 0$. The estimations of the probability of non-exceedance $H(x)$ for each annual rainfall value x are shown in column 5 of Table 3 and column 6 shows the respective SPI indices. Figure 1 presents the SPI index values (shown as bars). Lastly, column 7 presents the designation of drought when $SPI < 0$, according to Table 2. These calculations were performed with equations (3) through (15). To apply equation (10), an algorithm was developed which evaluates the expansion of the series until the last term is less than 10^{-7} .

Estimation of the monthly and annual ETP

First, the monthly mean temperature (Tt) registry was generated in the same way as the precipitation registry. Since few values were missing they were considered to be the same as the monthly averages. Next, the 12 Ri values were obtained from the Alamanza and Lopez (1975) maps, corresponding to the city of Zacatecas. These were: 411, 477, 565, 645, 661, 528, 521, 498, 447, 412, 405 and 353 ly/d. The above values were compared to the magnitudes obtained with the global solar irradiation maps (daily mean) reported by Hernández *et al.* (1991). Agreement was found in the magnitude and behavior over the course of a year.

To estimate each monthly ETP value, first the Hv is obtained with the respective Tt (equation (21)), then equation (20) is applied with the monthly value corresponding to Ri to obtain Ri' . The Tt is multiplied by 1.8 and 32 is added. These last two amounts are used in equation (19) and the result is multiplied by the number of days in the month. The 12 monthly values are added and the ETP^i is obtained, which is shown in column 8 of Table 3.

Results from the RDI Index

The results from applying equation (16) are shown by year in column 9 of Table 3. The natural logarithms of the above values define these two statistical parameters, $\bar{y} = -1.131497$ and $S_y = 0.318919$ based on which the standardized RDI values are obtained. These are shown in column 10 of Table 3. The last column of this table presents the designation of droughts based on the RDI_{ST} index and Table 2. Figure 1 shows the values of the RDI_{ST} index (shown with dots).

Overall Analysis of the Results

According to the results presented in Table 3, the PPD index detected 43 years with droughts, and the SPI and RDI detected 39 years. The results from the three indices do not reflect a total or complete correspondence, though much more agreement exists between the classifications by the SPI and RDI. Only the years 1954, 1961 and 1978 do not coincide—the RDI index detected more severe droughts in 1954 and 1961 and the opposite occurred in 1978. The similarity among the results from the SPI and RDI indices is shown in Figure 1, where the greatest differences between the two can be seen in years with rainfall.

Though the anomalies shown in the PPD index for the years 1930, 1965, 1971 and 1991 reflect years with abundant rainfall they are classified as a slight drought. This occurred because the index detected anomalous behavior over the course of a year. For example, in 1930 rainfall was 53.0 in August and 21.8mm in September, with mean values of 98.5 and 83.1 mm, resulting in a deficit of 106.8 mm only for those two months. In 1971, no rainfall was recorded during the first four months and 16.0 mm was recorded in July, resulting in a deficit of 84.6 mm. Nevertheless, this year is

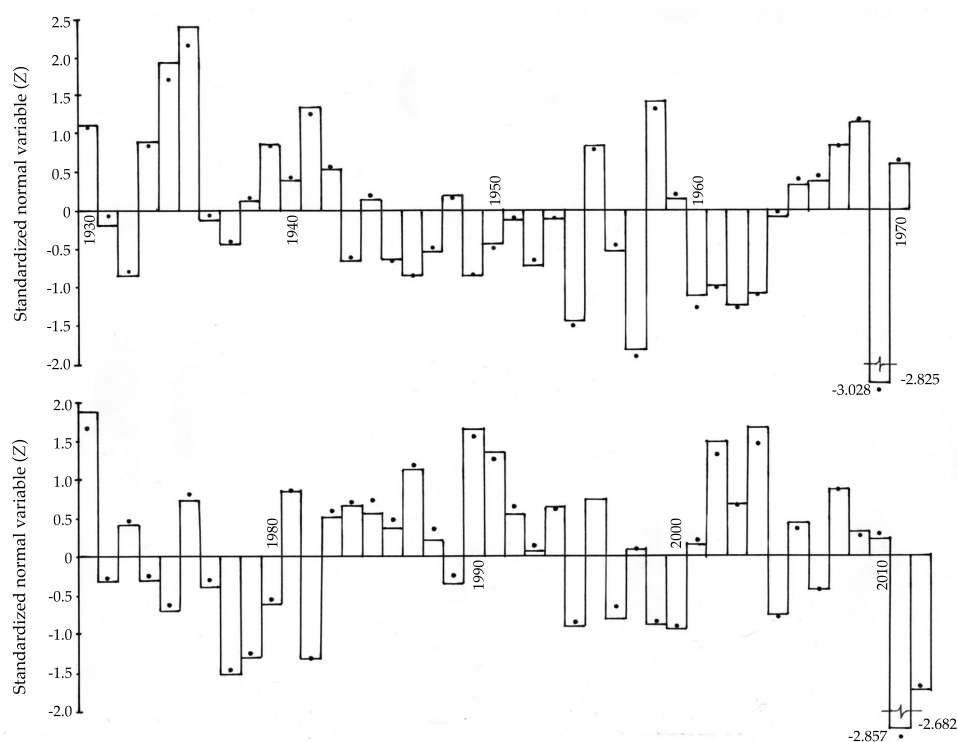


Figure 1. Comparison of results from the annual SPI (barras) and RDIST (dots) indices for the Zacatecas Weather Stations, Mexico.

indicated as severe rainfall according to the SPI and RDI indices. In August of 1991, only 37.4 mm of rainfall occurred and the year began with no rainfall and ended with very little magnitudes. Logically, when droughts with durations of 3 and 6 months are studied or detected, the results from the PPD index will likely coincide with those from the SPI and RDI indices.

With regard to the periods of droughts, 1943 to 1953 was identified as slight drought, and 1954 to 1964 as severe or moderate. The year 1969 was designated as extreme drought but was isolated. The years 1972 to 1982 were designated as another period of alternating slight and moderate droughts. Another period of intermittent slight droughts began in 1995 and may have ended in 2012 with two extraordinary, one extreme and another severe drought (see Table 3).

Conclusions

Overall, the results from the three indices compared in the present study show excellent agreement for most of the years in which droughts were detected, as well as for their severity. Considerable similarity was found between the SPI and RDI in the classification of droughts, with only subtle differences for just three years (1954, 1961 and 1978) of the 39 designated as droughts.

The results presented in Table 3 show that the PPD index detects more years with droughts (43) given that it reflects anomalies in their distribution over the course of a year. Therefore, slight droughts were designated for years with abundant rainfall (1930, 1971 and 1991).

Considering the level of agreement among the three indices presented herein, their joint application is recommended

since their classifications of years with droughts can be considered to complement and/or verify each other.

References

- Almanza, R., & López, S. (1975). *Radiación solar global en la república mexicana mediante datos de insolación* (20 pp.). Series del Instituto de Ingeniería, núm. 357. México, DF: Universidad Nacional Autónoma de México.
- Bobée, B., & Ashkar, F. (1991). Log-Pearson Type 3 Distribution LP (α , λ , m). Chapter 7. (pp. 76-120). In *The Gamma Family and Derived Distributions Applied in Hydrology*. Littleton, USA: Water Resources Publications.
- Campos-Aranda, D. F. (2005). Estimación empírica de la ETP en la república mexicana. *Ingeniería Hidráulica en México*, 20(3), 99-110.
- Campos-Aranda, D. F. (julio-septiembre, 2013). Consideraciones generales relativas a la aplicación de acciones para mitigación de Sequías. *Revista digital Tláloc*, 60.
- Campos-Aranda, D. F. (2014). Comparación de tres métodos estadísticos para detección y monitoreo de Sequías meteorológicas. *Agrociencia*, 48(5), 463-476.
- Cacciamani, C., Morgillo, A., Marchesi, S., & Pavan, V. (2007). Monitoring and Forecasting Drought on a Regional Scale: Emilia-Romagna Region. Chapter 2. (pp. 29-48). In G. Rossi, T. Vega, & B. Bonaccorso (Eds.). *Methods and Tools for Drought Analysis and Management*. Dordrecht, The Netherlands: Springer.
- Davis, P. J. (1965). Gamma Function and Related Functions. Chapter 6. (pp. 253-293). In M. Abramowitz, & I. Stegun (Eds.). *Handbook of Mathematical Functions*. New York: Dover Publications.
- Edwards, D. C., & McKee, T. B. (1997). *Characteristic of 20th Century Drought in the United States at Multiple Timescales* (155 pp.). Climatology Report No. 97-2. Fort Collins, USA: Colorado State University.
- Haan, C. T. (1977). Some Continuous Probability Distributions. Chapter 6. (pp. 97-127). In *Statistical Methods in Hydrology*. Ames, USA: The Iowa State University Press.
- Hargreaves, G. H., & Samani, Z. A. (1982). Estimating Potential Evapotranspiration. *Journal of the Irrigation and Drainage Division*, 108(IR3), 225-230.
- Hernández H., E., Tejeda M., A., & Reyes T., S. (1991). *Atlas solar de la república mexicana* (155 pp.). Textos Universitarios. Xalapa, México: Universidad Veracruzana y Universidad de Colima.
- Hosking, J. R. M., & Wallis, J. R. (1997). L-Moments for Some Specific Distributions. Appendix (pp. 191-209). In *Regional Frequency Analysis. An Approach Based on L-Moments*. Cambridge: Cambridge University Press.
- Kite, G. W. (1977). Comparison of Frequency Distributions. Chapter 12 (pp. 156-168). In *Frequency and Risk Analysis in Hydrology*. Fort Collins, USA: Water Resources Publications.
- Machiwal, D., & Jha, M. K. (2012). *Hydrologic Time Series Analysis: Theory and Practice* (303 pp.). Dordrecht, The Netherlands: Springer.
- Mawdsley, J., Petts, G., & Walker, S. (1994). *Assessment of Drought Severity* (41 pp.). Occasional Paper No. 3. London: British Hydrological Society.
- McKee, T. B., Doesken, N. J., & Kleist, J. (1993). The Relationship of Drought Frequency and Duration to Times Scales (pp. 179-184). 8th. Conference on Applied Climatology, Anaheim, California, USA.
- Rao, A. R., & Hamed, K. H. (2000). The Gamma Family. Chapter 6 (pp. 127-206). In *Flood Frequency Analysis*. Boca Raton, USA: CRC Press.
- SARH (1980). *Boletín Climatológico No. 3. Región Hidrológica No. 37. El Salado*. México, DF: Subsecretaría de Planeación, Secretaría de Agricultura y Recursos Hidráulicos.
- Stedinger, J. R., Vogel, R. M., & Foufoula-Georgiou, E. (1993). Frequency Analysis of Extreme Events. Chapter 18. (pp. 18.1-18.66). In D. R. Maidment (Ed.). *Handbook of Hydrology*. New York: McGraw-Hill, Inc.
- Thom, H. C. S. (1971). *Some Methods of Climatological Analysis* (53 pp.). Technical Note No. 81. Geneva: World Meteorological Organization.
- Tsakiris, G., & Vangelis, H. (2005). Establishing a Drought Index Incorporating Evapotranspiration. *European Water*, 9, 3-11.
- Tsakiris, G., Tigkas, D., Vangelis, H., & Pangalou, D. (2007). Regional Drought Identification and Assessment. Case Study in Crete. Chapter 9 (pp. 169-191). In G. Rossi, T. Vega, & B. Bonaccorso (Eds.). *Methods and Tools for Drought Analysis and Management*. Dordrecht, The Netherlands: Springer.
- Velasco, I. (2002). Detalle teórico metodológico del SPI. Anexo 26 (pp. 188-195). En *Plan de preparación para afrontar sequías en un distrito de riego*. Tesis doctoral. Facultad de Ingeniería de la Universidad Nacional Autónoma de México, Campus Morelos.
- WMO (1971). Annexed III: Standard Tests of Significance to be Recommended in Routine Analysis of Climatic Fluctuations (pp. 58-71). In *Climatic Change*. Technical Note No. 79, WMO-No. 195. Geneva: World Meteorological Organization, Secretariat of the WMO.
- Zelen, M., & Severo, N. C. (1965). Probability Functions. Chapter 26 (pp. 925-995). In M. Abramowitz, & I. Stegun (Eds.). *Handbook of Mathematical Functions*. New York: Dover Publications.

Corresponding author

Dr. Daniel Francisco Campos Aranda

Profesor jubilado de la Universidad Autónoma de San Luis Potosí
Genaro Codina 240, Colonia Jardines del Estadio
78280 San Luis Potosí, San Luis Potosí, MÉXICO
campos_aranda@hotmail.com



Media Luna Lagoon, San Luis Potosi, Mexico.

Photo: David Vinicio Carrera Villacrés.

DISCUSSION

Technical notes and technical articles are open to discussion according to the following guidelines:

- The discussion will be written in the third person.
- The writer of the discussion shall use the term “commentator” when referring to oneself and the term “author” when referring to the one responsible for the technical note or article.
- The discussion shall be sent within 12 months of the last day of the quarter in which the a technical article or note was published.
- The length of the discussion may be extended by written request from the commentator.
- The discussion is to be presented according to the Guide for Collaborators published in this journal (omitting data referring to the length and abstract). In addition, the bibliographical citation of the technical notes or articles to which the discussion refers shall be included.
- The maximum length of the discussion is 4 journal pages (approximately 10 cuartillas, including figures and tables).
- The figures and tables presented by the commentator shall be progressively marked with Roman numbers and when citing those generated by the author the original numeration should be respected.
- The editors will suppress data that does not pertain to the subject of the discussion.
- The discussion will be rejected if it contains topics addressed by other sources, promotes personal interests, is carelessly prepared, raises controversy involving already established facts, is purely speculative or falls outside the purpose of the journal.
- The discussion will be published along with commentaries from the author or authors to which it refers.
- The discussion will be directed by the editor in chief.



Sunrise from the Mazatlan-Tepic Roadway, Mexico.

Photo: Ricardo Espinosa Reza.

GUIDE FOR COLLABORATORS

The journal *Water Technology and Sciences* invites specialists to collaborate with original, unpublished technical articles or notes **related to water, resulting from investigations and provide original contributions**, based on the disciplines of hydrology, hydraulics, water management, water and energy, water quality, and physical, biological and chemical sciences as well as political and social sciences, among other disciplines, according to the guidelines stated below.

PREPARATION OF THE ARTICLE

FORMAT

FONT: Palatino throughout the entire document (body of text, tables and figures).

FONT SIZE: Use 8, 9, 10 and 20 points, according to the following table:

8 POINTS (PALATINO)	9 POINTS (PALATINO)
<ul style="list-style-type: none">• Tables.• Figures.• Acknowledgements.	<ul style="list-style-type: none">• Name of authors.• Institution of authors.• Abstract.• <i>Abstract</i> and <i>keywords</i>.• Institutional address of the authors.
10 POINTS (PALATINO)	20 POINTS CAPITAL LETTERS (PALATINO)
<ul style="list-style-type: none">• Body of the text.• Title of the work in Spanish.	<ul style="list-style-type: none">• Title of the work in English.

LINE SPACING: double-spaced.

PAGE NUMBERS: all pages shall be numbered.

LENGTH

Technical article: 30 pages (numbered), including figures and tables.

Technical note: 10 pages (numbered), including figures and tables.

CONTENS

TITLE

The article shall present significant contributions to scientific and technological knowledge pertaining to the specialty. It shall be based on finished works or those that have completed a development cycle. It shall show results from a series of experiences over 1 year or more of investigations and be supported by an adequate bibliographical review. **The basic structure of the text shall contain an introduction, the development and the conclusions.** The classic layout is preferable: abstract, introduction, methodology, results, discussion, conclusion and references.

TITLE

The title, **written in Spanish and English**, shall be informative and not exceed 12 words.

ABSTRACT

The abstract, **written in Spanish and English**, shall be concise and provide a broad overview of the investigation (objective, method, results and conclusions) without exceeding 250 words.

KEY WORDS

Eight words or key phrases (maximum) shall be provided **in Spanish and English** that facilitate the identification of the information.

FOOTNOTES

Not admitted. The information is to be incorporated into the text.

ACKNOWLEDGEMENTS

To be included after the text and before the references.

TABLES

- One page for each table.
- A list of all the tables cited shall be presented after the references.

FIGURES

- One page for each figure.
- All the names of the figures shall be included after the tables.
- They should be high-resolution (300 dpi).

Note: When the article is approved by the publication, the author shall send each figure in JPG format with high-resolution (300 dpi).

REFERENCES

- The entire bibliography must be referenced in the main body of the text.
- In the case of addressing scientific and technological topics that are common domain, works that denote the knowledge of the authors about the state-of-art shall be cited.
- Avoid self-citations to the extent possible
- APA format shall be used as a basis.

Some examples of references in APA format are:

Complete Books

Last name, A. A. (Year). Title of work. city published: Publisher.

Last name, A. A. (Year). Title of work. Consulted at <http://www.xxxxx>

Last name, A. A. (Year). Title of work. doi:xxxxx

Last name, A. A. (Ed.). (year).City published: Publisher.

Book Chapters

Last Name, A. A., & Last Name, B. B. (Year). Title of chapter or entry. In A. Last Name, B. Last Name & C. Last Name (Eds.), Title of book (pp. xxx-xxx). Place: Publisher.
 Last Name, A. A., & Last Name, B. B. (Year). Title of chapter or entry. In A. Last Name, B. Last Name & C. Last Name (Eds.), Title of book (pp. xxx-xxx). Consulted at <http://www.xxxxxxx>

Newspaper Article or Note Consulted Online

Last Name, A. A., & Last Name, B. B. (Year). Title of article. Title of publication, issue (number), pp. Consulted at <http://www.xxxxxxx>

That is: Last Name, A. A., & Last Name, B. B. (Year). Title of article. Title of publication, 1(2), 5-17, pp. Consulted at <http://www.xxxxxxx>

Printed Newspaper Article or Note

Last Name, A. A., & Last Name, B. B. (Year). Article Title. Title of publication, 8(1), 73-82.

Newspaper Article Publication with DOI

Last Name, A. A., & Last Name, B. B. (Year). Article Title. Title of publication, 8(1), 73-82, doi:xxxxxx

Conferences or Symposiums

Collaborator, A. A., Collaborator, B. B., Collaborator, C. C., & Collaborator, D. D. (Month, year). Title of collaboration. In E. E. President (Presidency), Title of symposium. Symposium held at the conference by Name of Organization, Place.

Citations within the body of the text

Type of citation	First appearance in text	Subsequent appearances	Format in parenthesis, first citation in text	Format in parenthesis, subsequent citing in text
Work by one author	Last name (Year)	Last name (Year)	(Last name, year)	(Last name, year)
Work by two authors	Last name and Last name (Year)	Last name and Last name (Year)	(Last name & Last name, Year)	(Last name & Last name, Year)
Work by three authors	Last name, Last name and Last name (Year)	Last name <i>et al.</i> (Year)	(Last name, Last name, & Last name, year)	(Last name of first author <i>et al.</i> , year)
Work by four authors	Last name, Last name, Last name and Last name (Year)	Last name <i>et al.</i> (Year)	(Last name, Last name, Last name, & Last name, year)	(Last name of first author <i>et al.</i> , year)
Work by five authors	Last name, Last name, Last name, Last name and Last name (Year)	Last name <i>et al.</i> (Year)	(Last name, Last name, Last name, Last name, & Last name, year)	(Last name of first author <i>et al.</i> , 2008)
Work by six or more authors	Last name of first author <i>et al.</i> (Year)	Last name of first author <i>et al.</i> (Year)	(Last name of first author <i>et al.</i> , Year)	(Last name of first author <i>et al.</i> , year)
Groups (easily identified with abbreviations) such as authors	Complete name of institution (Acronym, year)	Acronym (Year)	(Complete name of institution [acronym], year)	(Institution, year)
Groups (without abbreviations) such as authors	Complete name of institution (year)	Complete name of institution (year)	(Complete name of institution, year)	

LANGUAGE

Spanish or English

SEPARATION OF NUMBERS AND USE OF DECIMAL POINTS

In *Tecnología and Ciencias del Agua*, the separation between thousands is denoted with a blank space. A decimal point is used to separate whole numbers from fractions. In this regard, refer to Diccionario panhispánico de dudas, edited by the Real Academia Espyearla and the Asociación de Academias de la Lengua Espyearla, in 2005, with respect to numeric expressions: **“the Anglo-Saxon use of the period is accepted, normal in some Hispano-American countries...: $\pi = 3.1416$.”**

DELIVERY OF ARTICLE

Send the article in *Word* with the name of the authors and institutional address to revista.tyca@gmail.com, with copy to Elizabeth Peña Montiel, elipena@tlaloc.imta.mx.

GENERAL INFORMATION

The review process will begin once the material is received, during which time the manuscript could be rejected. If the text is suitable for review, having fulfilled the Editorial Policy and the Editorial Committee having determined so, it will proceed to the review stage.

Depending on the review process, the text may be accepted without changes, with minor changes, with extensive changes or rejected.

Once a work is published, the main author has the right to two journals and ten offprints free of charge.

In there are any questions, please write to Helena Rivas López, hhrivas@tlaloc.imta.mx or Elizabeth Peña Montiel, elipena@tlaloc.imta.mx

Editorial Policy

Mission

Disseminate scientific and technical knowledge and advances related to water through the publication of previously unpublished articles and technical notes that provide original contributions.

Our Principles

- Impartiality
- Objectivity
- Honesty

Our Values

- Knowledge
- Experience
- Thematic expertise

Contents

Interdisciplinary, composed of previously unpublished articles and technical notes related to water, that result from research and provide original scientific and technological contributions or innovations, developed based on the fields of knowledge of diverse disciplines.

Topics Covered

Interdisciplinary, related to water, with priority topics in the following knowledge areas:

- Water and energy
- Water quality
- Physical, biological and chemical sciences
- Hydro-agricultural sciences
- Political and social sciences
- Scientific and technological development and innovation
- Water management
- Hydrology
- Hydraulics

Type of Contributions

Technical article: scientific document that addresses and communicates, for the first time, results from a successful investigation or innovation, whose contributions provide and increase current knowledge about the topic of water.

Technical note: text that addresses advances in the field of hydraulic engineering and professional practices in the field of water, while not necessarily making an original contribution in every case it must be a previously unpublished work.

Some of the articles submitted to the review process can result in being published as notes and vice versa. This will occur through a proposal and process of mutual agreement between the authors and the editor responsible for the topic. The article and the note have nearly the same structure (abstract, introduction, methodology, results, discussion, conclusion, references).

Review Process

The journal is governed by a rigorous review process which establishes that each article be analyzed separately by three reviewers who recommend its acceptance, acceptance with minor changes, acceptance with extensive changes, rejection or acceptance as a technical note with the required changes.

At least one of three reviewers will be sought from a foreign institution.

The reviewers may not belong to the same institution as the authors proposing the article for publication.

When the decisions are opposing or inconsistent, the involvement of other reviewers or the members of the Editorial Committee may be requested.

On occasion, the approval of an article will be decided by two reviewers in addition to the opinion of the editor of the corresponding topic or, the editor in chief.

A rejected article will not be accepted for a new review process.

The review process will be performed in such a way that neither the authors nor the reviewers know the names of the other party.

The review process is performed by high-level specialists and experts who are national and internationally renowned in their professional fields and have the ability to reliably evaluate, in a timely manner, the quality as well as the originality of contributions, in addition to the degree of scientific and technological innovation in the topic under which it is submitted for possible publication.

This participation is considered a professional contribution and will be performed as a courtesy.

The reviews have a "Guide for the Reviewer" provided by the journal's Editorial Department.

Final Ruling

The ruling resulting from the review process is not subject to appeal.

Authors

Works are published from authors of any nationality who present their contributions in Spanish; nevertheless, we all accept works in Spanish or English.

Responsibility of the Authors

Submitting a proposal for the publication of an article commits the author not to simultaneously submit it for consideration by other publications. In the event an article has been submitted to another media for eventual publication, the author agrees to do so with the knowledge of the Editorial Department, which will suspend the review process and inform the Editorial Committee of the decision by the authors.

Collaborators whose articles have been accepted will formally cede the copyright to *Tecnología y Ciencias del Agua*.

The authors are responsible for the contents of the articles.

The author is responsible for the quality of the Spanish used. If the writing is deficient the work will be rejected. *Water Technology and Sciences* will only be responsible for the editorial management.

The author commits to making the changes indicated by the editor of the topic in the time frame established by the editor. In the event these indications are not met, the article will be removed from the review process and be classified as rejected.

The author shall be attentive to resolving the questions and proposals presented by the editors and the editorial coordinator.

Each author shall approve the final printed proofs of their texts.

It is suggested that authors consult the "Guide for Collaborators."

Readers

Academics, investigators, specialists and professionals interested in the analysis, investigation and search for knowledge and solutions to problems related to water.

Reception of Articles

The reception of articles and notes is ongoing.

Time period

Bimonthly, appearing in the second month of the period.

Subscription and Distribution

The journal is distributed through paid and courtesy subscriptions.

Open Access

Water Technology and Sciences, previously *Hydraulic Engineering in Mexico*, provides a digital version of all the material published since 1985.

Special editions and issues

Water Technology and Sciences will publish special numbers independently or in collaboration with other journals, professional associations or editorial houses with renowned prestige and related to water resources.

In addition, it will publish articles by invitation, acknowledging the professional advances of prominent investigators.

In both cases, the quality of the technical contents and scientific contributions will be reviewed.

Water Technology and Sciences is registered in the following national and international indices and abstracts:

• Thomson Reuters Science Citation Index® (ISI) • Expanded Thomson Reuters Research Alert® (ISI) • Índice de revistas mexicanas de investigación científica y tecnológica del Consejo Nacional de Ciencia y Tecnología (Conacyt) (2013-2018) • Sistema de Información Científica Redalyc (Red de Revistas Científicas de América Latina y El Caribe, España y Portugal), Universidad Autónoma del Estado de México • EBSCO (Fuente Académica Premier NISC; Geosystems, como Marine, Oceanographic and Freshwater Resources) • ProQuest (Cambridge Scientific Abstracts) • Elsevier (Fluid Abstracts; Process Engineering; Fluid Abstracts; Civil Engineering) • CAB Abstracts, CAB International • Latindex (Sistema Regional de Información en Línea para Revistas Científicas de América Latina, el Caribe, España y Portugal), Universidad Nacional Autónoma de México • Periódica (Índice de Revistas Latinoamericanas en Ciencias), Universidad Nacional Autónoma de México • Catálogo Hela (Hemeroteca Latinoamericana), Universidad Nacional Autónoma de México • Actualidad Iberoamericana, CIT-III, Instituto Iberoamericano de Información en Ciencia y Tecnología.

Other Sources

The journal can also be found archived in Google scholar.



Technical articles

Flow Caused by Dam Breaks: Numerical Modeling Analysis
 Ignacio Sabat
 Oscar Link
 Bernd Ettmer

Forensic Analysis of Floods: A Methodological Guide
 Aldo I. Ramírez
 L. Alejandra Herrera-Lozano

Growth Kinetics and Nutrient Uptake of Microalgae in Urban Wastewaters with Different Treatment Levels
 César Carlos García-Gozalbes
 Zouhayr Arbib
 José Antonio Perales-Vargas-Machuca

Improvements in the Hydraulic Efficiency of Weirs with Free Outfalls in Dams
 Mauro Iñiguez-Covarrubias
 Waldo Ojeda-Bustamante
 Carlos Díaz-Delgado

Development of the Balsas Hydrological Region by Modifying Prohibitions
 Juan Carlos Valencia-Vargas

Prioritization of Needs to Replace Piping Using GIS and Multicriteria Evaluation
 Vivian Verduzco
 Jaime Garatuza
 Salvador Díaz

Prioritization of Intervention Areas using a Morphometric Analysis and Vegetation Index
 Adolfo López-Pérez
 Mario R. Martínez-Menes
 Demetrio S. Fernández-Reynoso

Numerical Hydrodynamic-Hydrological Modeling in Flood Zones Containing Infrastructure
 Israel E. Herrera-Díaz
 Clemente Rodríguez-Cuevas
 Carlos Couder-Castañeda
 José R. Gasca-Tirado

Technical notes

Characterization of Meteorological Droughts in the Central Argentina
 Leticia Vicario
 Carlos M. García
 Ingrid Teich
 Juan Carlos Bertoni
 Andrés Ravelo
 Andrés Rodríguez

Water Usage in Northern Sinaloa: Allocating the Resource to Consumers
 Jesús Torres-Sombra
 José Alberto García-Salazar

Application of the ArcHydro Data Model to Calculate Surface Water Availability
 María de los Ángeles Suárez-Medina
 Carlos Patiño-Gómez
 Jaime Velázquez-Álvarez
 Jaime Rivera-Benites
 Ernesto Aguilar-Garduño
 Guillermo Bautista
 Citlalli Astudillo-Enríquez

Comparison of PPD, SPI and RDI Indices to Classify Droughts: Zacatecas Weather Station, Mexico
 Daniel Francisco Campos-Aranda

Discussion
 Contributor's guide

Artículos técnicos

Flujo inducido por el rompimiento de una presa: análisis mediante modelación numérica
 Ignacio Sabat
 Oscar Link
 Bernd Ettmer

Análisis forense de inundaciones: una guía metodológica
 Aldo I. Ramírez
 L. Alejandra Herrera-Lozano

Cinéticas de crecimiento y consumo de nutrientes de microalgas en aguas residuales urbanas con diferentes niveles de tratamiento
 César Carlos García-Gozalbes
 Zouhayr Arbib
 José Antonio Perales-Vargas-Machuca

Mejoras de eficiencia hidráulica en vertederos con canal de descarga libre en presas: propuesta metodológica
 Mauro Iñiguez-Covarrubias
 Waldo Ojeda-Bustamante
 Carlos Díaz-Delgado

Desarrollo de la región hidrológica del Balsas mediante la modificación de su veda
 Juan Carlos Valencia-Vargas

Priorización de necesidades de reemplazo de tuberías usando SIG y evaluación multicriterio
 Vivian Verduzco
 Jaime Garatuza
 Salvador Díaz

Priorización de áreas de intervención mediante análisis morfométrico e índice de vegetación
 Adolfo López-Pérez
 Mario R. Martínez-Menes
 Demetrio S. Fernández-Reynoso

Modelación numérica hidrodinámico-hidrológica en zonas de inundación con presencia de infraestructura
 Israel E. Herrera-Díaz
 Clemente Rodríguez-Cuevas
 Carlos Couder-Castañeda
 José R. Gasca-Tirado

Notas técnicas

Caracterización de las sequías meteorológicas en la región central de la Argentina
 Leticia Vicario
 Carlos M. García
 Ingrid Teich
 Juan Carlos Bertoni
 Andrés Ravelo
 Andrés Rodríguez

Uso del agua en el norte de Sinaloa: ¿a cuál consumidor asignar el recurso?
 Jesús Torres-Sombra
 José Alberto García-Salazar

Aplicación del modelo de datos ArcHydro en el cálculo de disponibilidad de agua superficial
 María de los Ángeles Suárez-Medina
 Carlos Patiño-Gómez
 Jaime Velázquez-Álvarez
 Jaime Rivera-Benites
 Ernesto Aguilar-Garduño
 Guillermo Bautista
 Citlalli Astudillo-Enríquez

Contraste de los índices DPP, SPI y RDI para clasificación de sequías, en la estación climatológica Zacatecas, México
 Daniel Francisco Campos-Aranda

Discusión
Guía para colaboradores